

Floating Cruise Terminal in Exposed Sea at Curaçao

Feasibility Study on the Dynamic Behaviour and Resulting Downtime

X. Groenenberg

MASTER OF SCIENCE THESIS

Floating Cruise Terminal in Exposed Sea at Curaçao

Feasibility Study on the Dynamic Behaviour and Resulting Operational Downtime

To obtain the degree of Master of Science in Civil Engineering at the Delft University of Technology

Xavier Groenenberg

Delft, 2016



Hydraulic Engineering Department
Delft University of Technology



Ports & Waterways
Witteveen + Bos



Cover image:

Port of Willemstad, Curaçao.

Retrieved from: http://www.curports.com/wp-content/uploads/2014/09/BEA_9911-0011.jpg,
Curacao Port Authority, [Downloaded: February 2015].

Title page image:

Willemstad with a departing cruise ship on the background, Curaçao.

Retrieved from: <http://cdn.c.photoshelter.com/img-get/I0000egI0WOScwZI/s/850/850/CUR-03-16-07-cs.jpg>,
B. Harrington, [Downloaded: November 2014].



Published through the Delft University of Technology Institutional Repository, based on Open Access.

This MSc. Thesis is the authors own work, based on personal study and research. All material and sources used in its preparation, whether they be books, articles, reports, lecture notes, and any other kind of document, electronic or personal communication have been acknowledged.

© X. Groenenberg, 2016

All rights reserved. Reproduction or translation of any part of this work in any form by print, photo copy or any other means, without the prior permission of either the author, members of the graduation committee or Witteveen + Bos is prohibited.

DELFT UNIVERSITY OF TECHNOLOGY
DEPARTMENT OF
Civil Engineering and Geosciences

In cooperation with

WITTEVEEN + BOS
Ports & Waterways

January 13, 2016

COMMITTEE MASTER THESIS

Prof. Ir. T. Vellinga Chairman	Delft University of Technology Hydraulic Engineering , Section: Ports & Waterways
Prof. Dr. Ir. R.H.M. Huijsmans	Delft University of Technology Maritime & Transport Technology, Section: Ship Hydromechanics & Structures
Ir. P. Quist	Delft University of Technology Hydraulic Engineering, Section: Ports & Waterways
Ir. M. Fousert	Witteveen + Bos Deltas, Coasts & Rivers, Section: Ports & Waterways

GRADUATE STUDENT

X. Groenenberg B.Sc.
Foulkeslaan 49
2625PZ, Delft
Tel. 0615476010
Student number: 1387502

Hydraulic Engineering Department
Delft University of Technology



Ports & Waterways
Witteveen + Bos



“ *The pessimist complains about the wind;
The optimist expects it to change;
The realist adjusts the sails.* ”

William A. Ward

ABSTRACT

Curaçao is a tropical island in the Caribbean Sea, which lies North of Venezuela. The island is a popular destination for tourists, because of the tropical climate with little rainfall, the colourful architecture and beautiful landscapes. A very comfortable way of visiting this island is by cruise ship. The number of cruise ships calling to port at Willemstad increases every year. This growth will continue to increase in the upcoming years, because of the increasing popularity of cruise holidays, and the ambition of the government to increase the number of annual cruise tourists from 600.000 to 1 million by the year 2020. A new berth will need to be realised to be able to facilitate this increasing number of port calls at Willemstad.

Two main aspects make it interesting to realise a floating cruise terminal: on the one hand, there is a steep drop of the ocean bed floor just offshore of the southern coast near Willemstad. On the other hand, the island of Curaçao lies just south of the hurricane belt. This does not immediately mean that there is a hurricane going over the island every year, but it definitely feels the effect of hurricanes in the form of high wind speeds and large wave heights. A bottom-founded permanent pier will have to be able to withstand all storms so it will not break down. A floating terminal on the other hand will only need to withstand wave conditions to that extent that it still will be used by cruise ships. If the conditions get too severe, the floating structure can then simply be moved into a more sheltered area, to protect it from large waves.

The main objective of this study is to determine whether a floating terminal could be a suitable and feasible solution for the realisation of a new berthing location for the cruise ships of the future. This feasibility study is based on the amount of downtime of a terminal due to excessive motions because of wave loading. Therefore, this study focuses on the hydrodynamic responses of such floating terminals.

To be able to carry out this study, local wave data are required, which are not available. Therefore, the local climate is approximated with the wave model SWAN. This is done by simulating the propagation of offshore deep water waves into the shallow water of the intended project location, just west of the current Megapier Cruise Terminal. Wave scenarios are defined from deep water wave data. Two types of scenarios are taken into account: swell-wave scenarios and wind-wave scenarios. From the simulations carried out with SWAN, it seems that hardly any swell-wave energy reaches the project location because of a shadow effect of the island. Also the amount of wind wave energy is much lower. Because of the low sensitivity found for different wave parameters the number of scenarios is reduced from in total 16 to three wind wave scenarios and four swell wave scenarios. These seven scenarios are used as input for the hydrodynamic assessment.

The hydrodynamic assessment consists of simulations carried out in the frequency domain, using the Ansys AQWA Suite. Considered are vertical and lateral accelerations, roll and pitch motions. Motion criteria for these motions are compared with the simulation results from AQWA. The following aspects have been studied to determine their influence on the amount of downtime: the presence of a cruise vessel, wave angles, swell and wind wave scenarios and two floating terminal variants: Model A (30x30m) and Model B (80x30m). Regarding the motion criteria, both the *Cruise Liner* criteria and the less strict *Transit Passenger* criteria from Nordforsk have been used to determine downtimes.

From this study, it is concluded that all mentioned aspects do have a notable influence on the amount of downtime of a floating terminal. For both terminal models and all wave angles, heave accelerations are the limiting factor, with and without a cruise vessel next to the terminal. Still, the presence of a cruise vessel does lower motion responses. Applying the less strict *Transit Passenger* Criteria leads to lower downtimes, but the operability remains limited.

For these two specific floating terminals studied, the realisation is only feasible in a specific case: Model B with a cruise vessel leads to the lowest downtime: at most 0.1% for swell wave scenarios, and at most 4.2% for the wind-wave scenarios. This holds for an alignment angle of 45° relative to the dominant wave angle, when the *Transit Passenger* criteria are used.

The main recommendation is to optimize both the mooring configuration and the dimensions and hull of the floating structure in an additional study. This may lead to reduction of heave accelerations, which in turn can greatly improve the potential of this concept.

PREFACE

This thesis presents a study on the dynamic response of a floating structure with the function of cruise terminal. This study is carried out in order to obtain the degree of Master of Science in Civil Engineering at the Delft University of Technology. This work is established under the supervision of the Hydraulic Engineering Department of Delft University of Technology and in close cooperation with the PMC Ports & Waterways of Witteveen + Bos.

The approach, used methods and final results of the feasibility study are described in this report. The final product consists of approximations of down-time values, determined from dynamic responses, for different scenarios and structures. These results are a basis for further research into the feasibility of the application of floating cruise terminals in deeper and exposed seas.

A quick overview of the structure of this thesis and used approach method can be found in Chapter 1. Readers particularly interested in the determination of local wave climates with the use of the software SWAN are referred to Chapter 4. The calculation of the hydrodynamic behaviour and motion responses is discussed in Chapter 7. Chapter 8 elaborates on the downtime assessment, comparing the model results with motion criteria, forms the core of this feasibility study on the motion dynamics of floating cruise terminals.

References to the bibliography are split up into reference groups. Each reference either does or does not contain a prefix letter. The references starting with a number refer to the first reference group namely *Book References*. The prefix letter refers to the first letter of the reference group name. For example: a reference starting with a *W* refers to the reference group *Websites*.

ACKNOWLEDGEMENTS

This study has been a challenging and adventurous task with the almost usual and never avoidable setbacks. It could not have been completed without the participation and support of numerous people. These people and their contributions of any kind are greatly appreciated and gratefully acknowledged.

Most of all I would like to express my deep gratitude to all the members of my graduation committee for their spent time and great support. Despite their full agendas, they could not have helped me more with their knowledge and useful comments. I would like to thank chairman Prof. Ir. Tiedo Vellinga for his guidance and supervision during this research. Dr. Ir. R.H.M. Huijsmans deserves my great gratitude for introducing and guiding me in the beautiful specialism of ship hydromechanics. I further would like to acknowledge Ir. P. Quist for his part in reaching this final goal with great suggestions and sharp comments.

I owe a special debt of gratitude to the company Witteveen + Bos, in particular Ir. Menno Fousert, for providing me with this opportunity to work at such a renowned company. Menno spent a lot of time reading and thinking along as much as he could to help me improve this study. His creative way of thinking out of the box often resulted in new ideas and helped me increase my motivation. The contribution in providing the facilities and knowledge available at this company has greatly helped in reaching this final result. Although not a part of the graduation committee, I also owe Ir. Daniël Dusseljee my gratitude for his great guidance and support with the software SWAN.

In addition, I would like to express my gratitude and appreciation to my family and friends for their endless support and interest during my time as a student. Special thanks go to Wouter van Duijn, Sven Suijkens, Gerben Jan Vos and Laurine Eikelboom.

Xavier Groenberg
Delft, January 2016

CONTENTS

Abstract	vii
Preface	ix
List of Symbols	xviii
1 Introduction	1
1.1 Background Information	1
1.1.1 Curaçao, a Cruise Destination With an Ambition.	1
1.1.2 Description of the Concept.	1
1.1.3 Motivation for Research	1
1.2 Scope and Research Objectives	2
1.2.1 Problem Definition	2
1.2.2 Research Objective	2
1.2.3 Research Questions	2
1.3 Approach	2
2 Analyses of the Location and Situation	7
2.1 The Cruise Industry	7
2.1.1 History of the Cruise Industry	7
2.1.2 Cruise Ships and Their Size	7
2.1.3 Market Size and Growth	9
2.2 Environmental and Boundary conditions.	11
2.2.1 Location and Topography	11
2.2.2 Description of the Port of Willemstad	11
2.2.3 Local Climate	12
2.2.4 Wave Climate Near the Shore of Willemstad	12
2.2.5 Wind.	14
2.2.6 Bathymetry	14
2.2.7 Tides and Currents.	15
2.3 Conclusion.	15
3 Design Requirements for the Concept	17
3.1 Design Cruise Ship	17
3.2 Structural Requirements	17
3.2.1 Type of Structure.	17
3.2.2 Station Keeping	17
3.3 Functional Requirements.	18
3.3.1 Number and Orientation of Berths	18
3.3.2 Downtime of the Floating Terminal	18
3.3.3 Accessibility between the Floating Terminal and the shore	18
3.3.4 Terminal Facilities	18
3.3.5 Movable and Multifunctional.	18
3.4 Nautical Requirements	19
3.4.1 Minimal Water Depth	19
3.4.2 Vessel Approach Conditions and Tug Support	19
3.4.3 Wind Restrictions	19

3.5	Requirements Regarding Hydraulic Aspects	19
3.5.1	Tides and Currents	20
3.5.2	Wave Conditions	20
3.5.3	Motions and Dynamic Response	20
4	Modelling the Local Wave Climate	21
4.1	Approach	21
4.2	The SWAN Wave Model	22
4.2.1	Theory Used in SWAN	22
4.2.2	Physics	22
4.2.3	Limitations and Not Considered Effects	22
4.3	Description and Set-Up of SWAN Wave Model	23
4.3.1	Wave- and wind input and data output locations	23
4.3.2	Computational Grid	23
4.3.3	Bathymetry	24
4.3.4	Boundary- and Initial Conditions	25
4.4	Simulation of Different Wave Conditions	26
4.4.1	Determination of Key Scenarios	26
4.4.2	Initialisation of the Wave Model: Example Scenario W2A	26
4.5	SWAN Model Results	27
4.5.1	Observed Effects From Calculation Results	28
4.5.2	Wave- Height & Period	29
4.5.3	Local Wave Energy: Variance Density Spectra	30
4.5.4	Influence of Output Location on Calculated Local Wave Climate	30
4.6	Conclusion	31
5	Floating Structures in General	33
5.1	Advantages and disadvantages	33
5.1.1	Advantages	33
5.1.2	Disadvantages	33
5.2	Structure Types and Applications	33
5.3	Dynamics and motion limits	34
5.3.1	Definitions	34
5.3.2	Dynamics in irregular waves	34
5.3.3	Stability of Floating Structures	37
5.3.4	Motion and safety limits for ships	38
6	General Design Considerations	39
6.1	Introduction	39
6.2	General Description and Characteristics	39
6.2.1	Structural Description	39
6.2.2	Main Particulars of Two Structural Variants	39
6.2.3	Station Keeping: Anchorage	39
6.2.4	Hydrostatic Properties	40
6.3	Terminal Location and Alignment	40
6.3.1	Location of the Floating Terminal	40
6.3.2	Berth Arrangement and Alignment	41
6.3.3	Connection to the Shore	41
6.3.4	Station Keeping of the Floating Components	42
6.3.5	Plan View Impression and Cross Section Sketch	42
7	Hydrodynamic Assessment of Variants	45
7.1	Approach	45
7.2	The Ansys AQWA Model	45
7.2.1	Programs in the Ansys AQWA Suite	45
7.2.2	Limitations and not considered effects	46

7.3	Set-up of Hydrodynamic Analysis System	46
7.3.1	Geometric Models of the Variants	46
7.3.2	Anchorage and Connections	47
7.3.3	Mesh	47
7.3.4	Model Domain and Ocean Environment	48
7.4	AQWA Simulations	49
7.4.1	Sign Convention & Data Extraction Points	49
7.4.2	Varied Parameters	49
7.4.3	Analytical Approximation of Hydrostatic and Hydrodynamic Properties	50
7.5	AQWA Results	50
7.5.1	Natural Frequencies	50
7.5.2	Free Floating RAO's	52
7.5.3	RAO's	54
7.5.4	Response Spectra	56
7.5.5	Root Mean Squared Values of the Response Spectra	59
7.6	Remarks	59
7.7	Conclusion	60
8	Downtime Assessment	63
8.1	Approach	63
8.2	Downtimes of the Floating Terminals	64
8.3	Conclusions	64
9	Conclusions and Recommendations	67
9.1	Conclusions	67
9.2	Recommendations	69
	Bibliography	71
	Book References	71
	Websites	71
	Datasets	72
	Software Packages	72
	Figures	72
	List of Figures	73
	List of Tables	75
	Appendices	76
A	Introduction on Physics of Waves	79
A.1	Description of Waves	79
A.1.1	Observing Waves	79
A.1.2	Measurement of Sea-state	79
A.2	Linear Wave Theory	79
A.2.1	Propagating Harmonic Waves, Derived from Linear Wave Theory	82
A.2.2	Describing Irregular Waves	82
A.3	Wave Transformation	84
A.3.1	Wave Reflection	84
A.3.2	Diffraction	84
B	Wave and Wind Data	85
B.1	Deep Sea Wave Data	85
B.1.1	General Information About the Dataset	85

B.2	Wind Data	86
B.2.1	General Information About the Dataset	86
B.2.2	Wind Scatter Diagram	86
B.1.2	Wind Sea Wave Data	87
B.1.3	Swell Wave Data	88
C	SWAN Model Set-Up	93
C.1	Set-up of Model Domain with Boundaries	93
C.2	The Importance and Influence of Wind on the Wave Model	94
C.3	Overview of Defined Scenarios	94
C.3.1	Swell Wave Scenarios Visualised in Scatter Diagrams	94
C.3.2	Wind Sea Wave Scenarios Visualised in Scatter Diagrams	96
C.4	SWAN Command File	97
D	SWAN Model Results	99
D.1	Parameter Comparison Between Initial Scenarios and Simulated Local Wave Climate Results	99
D.2	Plots of Scenario Results	101
D.2.1	Significant Wave Height	102
D.2.2	Peak Wave Period	106
D.2.3	Direction of Wave Propagation	110
D.3	Local Swell- and Wind Wave Spectra	114
D.3.1	Propagation of Wave Energy	114
D.3.2	Variance Density Spectra for the Swell and Wind Sea Scenarios	114
E	Analytic Approximation of Hydrodynamic Properties	117
E.1	Equations of Motion	117
E.2	Equation of Motion in Multiple Degrees of Freedom	117
E.3	Overview of General Parameters	119
E.4	Hydrostatic Terms: Heave, Roll and Pitch	119
E.5	Hydrostatic Terms: Surge and Sway	120
E.5.1	Geometry and Parameter Definition	120
E.5.2	Parametric Relations	120
E.5.3	Restoring Force Coefficient	120
E.6	Overview of Calculated Hydrostatic Values	121
E.7	Undamped Natural Frequency Without Hydrodynamic Mass	121
E.8	Hydrodynamic Terms	122
E.8.1	Added Mass For the Surge and Sway Motion	122
E.8.2	Added Mass for the Heave Motion	122
E.8.3	Added Mass Moment of Inertia for the Roll and Pitch Motion	122
E.8.4	Overview of Calculated Values	123
E.9	Conclusion	123
F	AQWA Model Set-Up	125
F.1	Conventions for Signs and Directions	125
F.1.1	Axes System	125
F.1.2	Wave Direction	125
F.2	Set-Up of and Input for the Ansys AQWA Programs	125
F.2.1	Mesh and Geometry Details	125
F.2.2	Anchorage & Connections	126
F.3	AQWA Command Files	129
F.3.1	AQWA-LINE	129
F.3.2	AQWA-LIBRIUM	130
F.3.3	AQWA-FER	131
G	AQWA Simulation Results	133

G.1	Hydrostatic & Hydrodynamic Properties	133
G.2	Free Floating RAO's and RAO's	134
G.3	Response Spectra.	136
G.3.1	Model A	136
G.3.2	Model B	138
G.3.3	Model C+A.	140
G.3.4	Model C+B.	142
G.4	RMS values.	144
H	Seakeeping Criteria by Nordforsk	147

LIST OF SYMBOLS

Acronyms

CLIA	Cruise Lines International Association	
CoB	Centre of Buoyancy	
CoG	Centre of gravity	[-]
DUT	Delft University of Technology	
ECMWF	European Centre for Medium-Range Weather Forecast	
GT	Gross Tonnage	[-]
LOA	Length Over All	[m]
M	Metacentre	
MSL	Mean Sea Level	[m]
RAO	Response Amplitude Operator, also called <i>Transfer Function</i>	
RMS	Root Mean Square	
SWAN	Simulating Waves Nearshore	

Greek Symbols

α_i	Phase angle of regular wave	[rad]
ϵ	Phase angle	[rad]
ω	Radian frequency	[rad/s]
ϕ	Velocity potential function	[-]
ϕ_f	Roll of a floating structure about the x-axis	[°]
ψ_f	Yaw of a floating structure about the z-axis	[°]
ρ	Mass density of fluid	[kg/m ³]
σ_θ	Directional spreading of waves	[°]
θ_f	Pitch of a floating structure about the y-axis	[°]
θ_{wind}	Wind direction at 10 metres above ground level/ sea surface	[°]
θ_w	Wave direction	[°]
ζ_a	Wave amplitude	[m]

Roman Symbols

$\dot{R}_{\dot{z}}$	Acceleration RAO of a translational motion indicated by the subscript	[1/s ²]
\dot{R}_z	Velocity RAO of a translational motion indicated by the subscript	[1/s]
\dot{R}_z	Response amplitude operator of a translational motion indicated by the subscript	[-]
\overline{BG}	Distance between C.o.G. and C.o.B	[m]
\overline{BM}	Distance between Metacentre and Centre of Buoyancy	[m]
\overline{GM}	Metacentric height	[m]
\overline{KB}	Distance between the bottom of the structure to the <i>CoB</i>	[m]
C	Reflection coefficient	[-]
E_e	Energy density spectrum	[js/m ²]
E_{var}	Variance density spectrum	[m ² s]
F	Force	[N]
f_i	Wave frequency of individual regular wave	[s ⁻¹]
g	Gravitational acceleration	[m/s ²]
H_i	Incoming wave height	[m]
H_{rms}	Root-mean-squared wave height	[m]
H_r	Reflected wave height	[m]
H_s	Significant wave height	[m]
k	Wave number	[rad/m]
L	Wave length	[m]

N	Number of frequencies	[-]
p	Pressure	[N/m ²]
P_E	Probability of Exceedance	[-]
S_r	Response Spectrum for displacements	[m ² s]
S_r	Response Spectrum for rotations	[deg ² /s]
T	Wave period	[s]
t	Time	[s]
T_p	Peak wave period	[s]
T_r	Wave record duration	[s]
u	Velocity	[m/s]
x, y, z	Indication of direction in a 3-dimensional reference frame	[-]
x_f	Surge motion: displacements in the x-direction	[m]
y_f	Sway motion: displacements in the y-direction	[m]
z_f	Heave motion: displacements in the z-direction	[m]
d	Water depth	[m]
D_d	Draught of floating structure	[m]
D_h	Height of floating structure	[m]
I_{xx}	Mass Moment of Inertia about the x-axis	[m ⁴]
I_{yy}	Mass Moment of Inertia about the y-axis	[m ⁴]
L_f	Length of floating structure	[m]
m_f	Mass of floating structure	[t]
M_H	Restoring heeling moment about the principal axes per degree of rotation	[Nm]
$u_{10,wind}$	Wind velocity at 10 metres above ground level/ sea surface	[m/s]
V_w	Water Displacement	[m ³]
W_f	Width of floating structure	[m]
z_a	Heave amplitude	[m]

INTRODUCTION

This chapter introduces the thesis topic: '*The feasibility of a floating cruise terminal in exposed sea*'. Section 1.1 gives background information on the island Curaçao as a cruise destination and describes both the scope and the concept. Section 1.2 presents the objectives and research questions followed up with the used approach for this thesis in §1.3.

1.1. BACKGROUND INFORMATION

1.1.1. CURAÇAO, A CRUISE DESTINATION WITH AN AMBITION

Curaçao is the largest of the ABC islands (i.e. Aruba, Bonaire and Curaçao), all located on the southern side of the Caribbean Sea. The islands are a popular holiday destination for people all around the world. Many people that visit Curaçao do this during a cruise holiday. The cruise industry is therefore an important source of income for the island.

The size of newly build ships increase. The same holds for cruise ships. Because of this development, Curaçao finished the construction of the Megapier Cruise Terminal [W1] at Willemstad in 1999 to provide a new berth for large ships. At that time no cruise ship was too big to visit the port of Willemstad with this new mooring location.

Nowadays there are more and more ships that cannot call the port due to either their size or because of occupied berths. In addition, the government of Curaçao has set the goal to increase the number of cruise tourists from an annual 600.000 to one million by the year 2020 [W2]. These developments lead to the need of additional mooring facilities, which are sufficiently large to accommodate the (cruise) ships of the future and able to realise the government's ambition.

The ocean bed floor runs very steep close to the shore, which makes a fixed construction expensive. Therefore the concept of a floating terminal is proposed, which is described in the next section.

1.1.2. DESCRIPTION OF THE CONCEPT

Witteveen + Bos, a consultancy and engineering company, proposed the conceptual idea of a floating cruise terminal, which is movable. A floating concept is proposed because of the steepness of the ocean bed floor close to the coasts of Curaçao. The movable aspect is suggested because the ABC islands lie on the southern edge of the hurricane belt. This way, when a storm is coming, the floating structure can be moved to a more sheltered area, like for example in the nearby St Anna Bay. Because of this possibility, the structure will not have to withstand extreme weather conditions. This study will therefore focus on operational conditions outside the hurricane season. Storm conditions will not be taken into account in the hydrodynamic study, because in these cases, the terminal will not be used. The definition of storm conditions as used in this study is presented in §4.3.1.

1.1.3. MOTIVATION FOR RESEARCH

For this study, it is interesting to know whether this concept could be a solution for this situation, given the local conditions. The application of floating terminals is not uncommon, but in general only applied in sheltered and inland waters. In exposed seas, waves are higher and the wave spectrum consists not only of wind waves, but also swell waves are present. Floating structures will move due to the present wave conditions. These movements should remain within limits for the structure to be usable as a cruise terminal, because people of all ages will set foot on this terminal when their cruise ship calls to the port of Curaçao.

The main objective regarding the dynamics of a floating cruise terminal is to keep the motion response low in all kinds of weather conditions. The amount of response of the floating structure is an important parameter for the determination of downtime of the terminal. This is the time period in which the floating terminal

cannot fulfil its function. The allowable downtime is therefore a decisive criterion for the feasibility of the floating terminal concept.

The concept of a floating cruise terminal is an interesting alternative for the island of Curaçao. But it is important to know whether such a terminal will not suffer too much downtime due to the local wave climate. In the case of large motion responses, it is of interest to look into ways to influence and limit this response. This study focuses on the effect of different wave angles and dimensions of the floating structures. In case of positive results, Curaçao might not be the only island that could benefit from this concept.

1.2. SCOPE AND RESEARCH OBJECTIVES

The problem definition and research objectives are formulated below. After that, the research questions are formulated.

1.2.1. PROBLEM DEFINITION

The problem is defined as follows:

The current mooring facilities at the capital of the island Curaçao, Willemstad, are not capable of accommodating modern large cruise ships. In addition, the government has set the goal to accommodate one million cruise passengers by the year 2020. Therefore, a new berth is required to prevent large queues and guarantee the ready availability of adequate berth capacity. Local weather and bathymetric conditions form a challenge for a financial viable solution.

1.2.2. RESEARCH OBJECTIVE

The objective is defined as followed:

Provide insight in the suitability and feasibility of a floating structure to be utilised as cruise terminal at an exposed area near the shore of Willemstad, Curaçao, by means of a numerical analysis. The motion response of a conceptual floating structure due to wave loads should be quantified. These motions should meet criteria to limit downtime. This will be done by making a dynamic response and downtime analysis for two variants of a conceptual floating structure.

1.2.3. RESEARCH QUESTIONS

From the above formulated problem definition and research objective the main research question of this study is formulated:

Given the local wave climate, is a conceptual floating structure suited as a solution for the realisation of a new mooring location for large, modern and future ships?

This main research question is divided into five sub questions:

1. What is the local wave climate at the project location near the St Anna Bay?
2. What is the influence of different wave conditions on the downtime?
3. Does the shape and size of the floating structure have any significant influence on the motion response and downtime?
4. What is the influence of a cruise ship located next to the floating structure?
5. Will the conceptual floating structures be able to fulfil its function as a cruise terminal often enough i.e. does the motion response remain often enough within limits to prevent large downtimes?

1.3. APPROACH

The approach to determine the answers on the above research questions is described in an outline. This outline indicates where in the chapters of this thesis an attempt is made to answer the different research questions.

OUTLINE OF THE THESIS

In general, this thesis consists of four consecutive, main parts and a concluding chapter which formulates the answer on the main research question:

- Chapter 2: an analysis of the actual situation and available data;
- Chapter 4: a simulation of the local wave conditions near the port of Willemstad with the use of deep sea wave data. This part treats sub-research question 1;
- Chapter 6 and 7: the determination of the dynamic behaviour of different structural concepts of a floating terminal for different wave conditions and structural models;
- Chapter 8: the downtime as a result of the determined dynamic behaviour for different structural models, local wave condition scenarios and wave angles. This part answers the sub-research questions 2, 3, 4 and 5.

These four parts are completed with additional chapters to further elaborate on the design requirements (Chapter 3) and floating terminals in general (Chapter 5).

For the sake of clarity, the outline of this thesis is presented in one summarising overview. It shows the studied research questions and most important results for each main part of this thesis. It is in fact the whole thesis in a nutshell, to quickly find information of interest for the reader.

See attachment file OUTLINE.PDF The final version of this page will be printed on A3.

CHAPTER 2

ANALYSES OF THE LOCATION AND SITUATION

To be able to answer the research questions, information and data is harvested with multiple analyses. Background information on the history, development and growth of the cruise industry is presented in §2.1 to get a better understanding of the current situation and the actual problem. The location, including topography and port infrastructure, and environmental conditions, i.e. wave-, wind- and bathymetry data, are studied in §2.2. This information is used to formulate boundary conditions for the local wave climate simulation and the hydrodynamic assessment.

2.1. THE CRUISE INDUSTRY

2.1.1. HISTORY OF THE CRUISE INDUSTRY

Centuries ago, ships sailed on the oceans for long periods. Exploring was the main reason to set out on these dangerous voyages. When the largest part of the world had been discovered and in most cases colonised, exploring became less important. Transportation of cargo became the main reason for ocean-going vessels to set out on the long voyages.

A new kind of ship was introduced by the 1930's: the steamship. These steamships reduced the time to cross the Atlantic Ocean remarkably [1]. This made it for ordinary people more interesting to set foot on ocean-going ships and cross the Atlantic Sea to America or Europe. As a result, shipping lines started to point their attention more to the well-being of their passengers and this is where a new industry started to take shape.

In 1900 the German company Hamburg-America Line finished the construction of the first vessel exclusively build for luxury cruising: Prinzessin Victoria Luise [W3] (See figure 2.1). From that moment on, a battle for the passengers started between the ocean-liners by increasing the luxury and comfort on the vessels. The most famous example of an early luxurious ocean liner is the Titanic, sinking on its maiden voyage in 1912 with more than 1500 fatalities [W4].

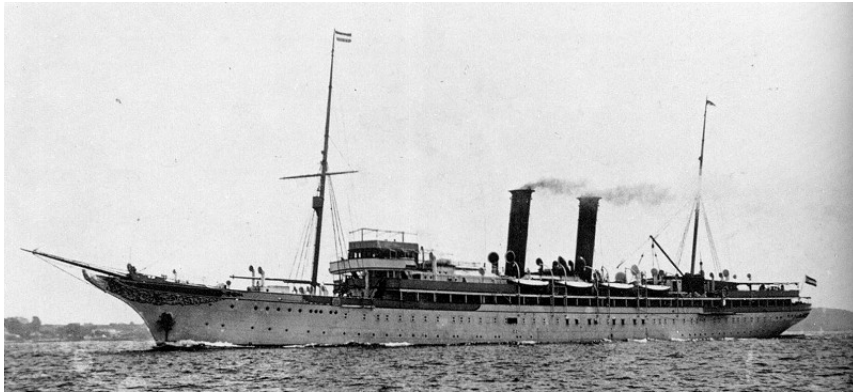


Figure 2.1: A picture from the first purpose-built cruise ship "Prinzessin Victoria Luise" [W3].

In the 1960's it became more interesting for passengers to book a flight with a jet plane instead of an ocean-liner. This new development in aviation and transportation meant the loss of many passengers in the market of ocean-liners. Their market took a tremendous hit between the 1960's and 1980's, and the remaining companies sought new opportunities in luxury cruising services [W3]. This search for new opportunities has led to cruise ships that we nowadays often call floating cities.

2.1.2. CRUISE SHIPS AND THEIR SIZE

There has always been the tendency to make the next ship bigger than the last one. The same goes for cruise ships. The above mentioned ship "Prinzessin Victoria Luise", launched in 1900, had already a length over all

(LOA) of 124 m. The passenger liner Titanic, launched twelve years later, was at that moment the largest ship in the world with a LOA of 269 m [W3].

With the start of modern luxury cruising in the 1980's, ships grew not only longer but moreover they became much higher and wider. This way, it became possible to carry more passengers and provide more space for amenities.

THE DEFINITION OF SHIP SIZE

To compare the size of ships, there are the obvious parameters like length, beam and draught. Those properties are straightforward and tell a lot about the extremes in length scale.

Another measurement is the *displacement tonnage*, defined as the amount of weight of water being displaced by a floating ship. This is directly derived from Archimedes' principle about buoyancy.

The measure currently used to indicate and compare the size of ships is Gross Tonnage (GT), adopted by the International Maritime Organisation [2] in 1969. It is a unit-less index obtained by measuring the ships internal volume in cubic metres (m^3) multiplied by a multiplier.

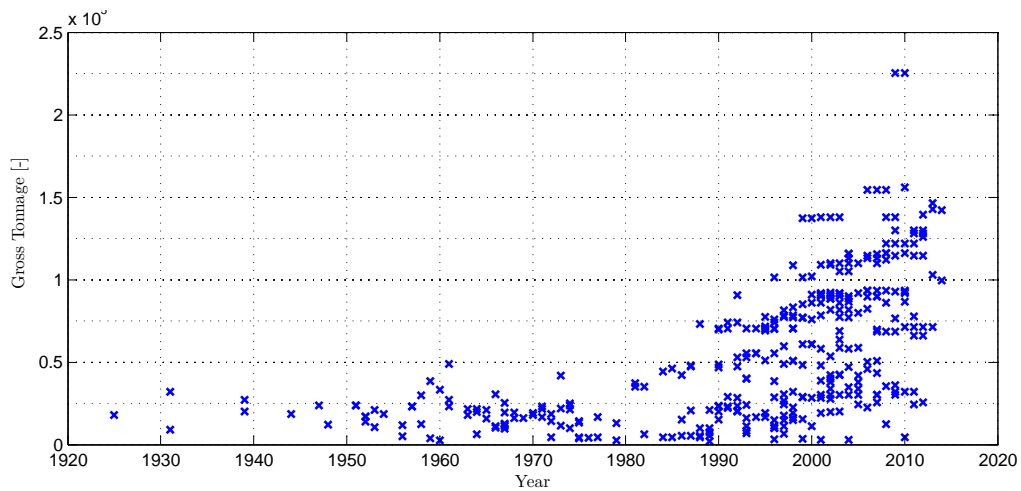


Figure 2.2: Scatter plot showing the increase of gross tonnage of passenger vessels in time [W5].

In Figure 2.2 a scatter graph shows the size of cruise ships in gross tonnage with their respective building years from the year 1910 to 2014. It gives a good idea of the growth of cruise ships in time. From the figure it can be seen that around the 1990's the ship size starts to increase almost exponentially. This is a result of the increasing popularity of destinations in the Caribbean Sea, because of its good weather throughout the year and the large investments in port facilities for the islands to be able to facilitate cruise ships.

THE LARGEST CRUISE SHIP IN THE WORLD

Since 2009, the cruise line 'Royal Caribbean International' owns the largest cruise ship in the world, called 'Oasis of The Seas'. Table 2.1 shows a comparison between this ship and the Titanic.

Table 2.1: Comparison of properties between the Titanic and Oasis of the Seas.

Property		Titanic [3]	Oasis of The Seas [W6]
Year of construction	-	1912	2009
Gross Tonnage	-	46.328	225.282
Length o.a.	m	269	362
Beam o.a.	m	28	65
Draught (loaded)	m	10.5	9.3
Passenger capacity	-	3547	6296
Max. Speed	knots	24	26

Although dimensions like length, beam and height continue to grow with every newly built cruise ship, the draft of the current mega cruises hardly increases. The largest drafts of these current mega cruise ships is around 9.2 m, like the Oasis of the Seas [W6]. The increase of the required draft is intentionally limited by

cruise liners, because too large drafts may limit the accessibility of cruise ships to current or future ports of call. Port authorities are not in all cases able to increase the water depth because of environmental restrictions.

2.1.3. MARKET SIZE AND GROWTH

The cruise market is an interesting market. It is very dynamic and steered by the feedback given by its passengers. The more people that take a cruise, the more experiences with cruise ships are spread. As long as the cruise liners do a good job, this can have a very positive snowball effect on the market as a whole.

Just like in Figure 2.2, exponential growth of the cruise industry can be deduced from Figure 2.3. This confirms the increasing popularity of cruise tourism. The growth strategy of cruise line companies consist of e.g. increasing ship capacity and diversity, more destinations and more local ports [W7]. Worldwide the cruise industry is estimated at \$37.1 billion, with a total of 21.6 million passengers carried in 2013.

The Caribbean is the most popular destination in the world for cruise tourists. According to capacity data published by Cruise Lines International Association (CLIA), the cruise industry had 42.8 million bed days deployed throughout the Caribbean, including the Bahamas, in 2011 accounting for nearly 40% of the industry's global bed day capacity [W8].

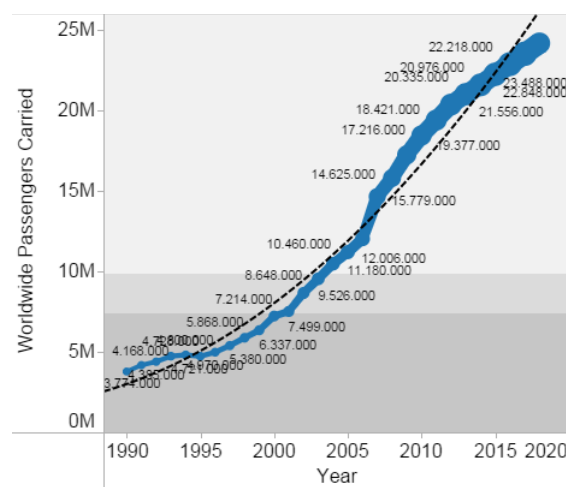


Figure 2.3: The growth of worldwide passengers carried by cruise liners [W7].

The growth of passengers to destinations has all kinds of positive influences on the actual destinations. Cruise tourism is a very big source of income for ports and small sized economies. For example, about 20% of the economic growth of Costa Rica in 2008 is caused by tourism [4]. The cruise passengers take around 17% of the total number of stayover tourists and have therefore a relevant impact on the total economy of Costa Rica.

When income from the cruise industry is injected again into port facilities, cruise terminals, shopping centres and maintenance of streets and buildings, this strengthens the previously mentioned snowball effect as cruise passengers have an even better positive experience from their visit.



Figure 2.4: Geographic map of the Caribbean Sea. The ABC Islands can be found on the southern side of this sea. The island of Curaçao is further zoomed in, showing additional geographical information. The map of Curaçao indicates the locations of important ports with letters in correspondence with Table 2.2. Source: [F1].

2.2. ENVIRONMENTAL AND BOUNDARY CONDITIONS

2.2.1. LOCATION AND TOPOGRAPHY

The tropical island of Curaçao is the largest of the ABC islands, with an area of 444 km². Aruba (193 km²) lies to the west of Curaçao and Bonaire (288 km²) to the east. They are located on the southern side of the Caribbean Sea, around 1300 km North of the equator. Figure 2.4 shows the geographical location of the island group. The orange circle in the figure indicates the location of the ABC-Islands.

The capital of Curaçao is Willemstad, which is built around the 60.75 ha inner bay Schottegat. The historic centre of the capital is one of the main attractions of the island because of the typical colours and architecture of the historic buildings.

2.2.2. DESCRIPTION OF THE PORT OF WILLEMSTAD

All the ports of Curaçao are in natural bays which provide shelter. In total there are five bays with varying levels of service. The ports of Curaçao are listed in Table 2.2. The letters in the first column correspond with the letters in Figure 2.4 indicating the locations of these ports. Only the first one, Port of Willemstad, is treated in more detail as it is the largest and most important port for tourism. Large parts of this section are based on the Curaçao Port Authority Directory [5].

Table 2.2: Ports of Curaçao and their maximum particulars [5]. Dashed values are either unknown or unlimited.

Port		LOA	Draft	Height	Beam
		[m]	[m]	[m]	[m]
A	Willemstad - Schottegat/ St Anna Bay	280 ¹	13.7 ²	<55 ³	42.6
B	Bullen Bay	-	28.7	-	-
C	Caracas Bay	320	13.7	-	-
D	Fuik Bay	109.7	7.3	-	44.8
E	St Michiel's Bay (SMB)	-	-	-	-

ST ANNA BAY & SCHOTTEGAT

The port of Willemstad covers the St Anna Bay and the Schottegat. The Schottegat is a natural basin in the capital Willemstad. This port has a wide range of facilities, which attracts tankers, cruise ships, container-, general cargo and Ro-Ro vessels. The port also houses repair and bunkering services with its numerous wharfs. Except for a mooring dolphin with two mooring buoys in the south west area of Schottegat Bay there are no further anchorage areas at the port of Willemstad to accommodate large ships.



Figure 2.5: The port of Willemstad: Megapier and St Anna Bay with occupied berths [F2].

¹Even longer vessels (LOA:378 m) have been piloted into the harbour of Willemstad.

²Ships with a draft larger than 12.8 m can only be allowed in consultation with the Port Authority.

³In order to access the Schottegat and the St Anna Bay beyond the Queen Juliana Bridge.

Access to the Schottegat is restricted to ships with limited dimensions. These dimensions are given in Table 2.2. The restrictions follow from the dimensions of the St Anna Bay, which is the entrance channel to the Schottegat. This channel is height restricted because of the Queen Juliana Bridge, which is a 55 m high fixed bridge. Ships with a larger height have to moor before the bridge (two larger berths with a depth varying from 9.4 m to 11.0 m) or at the Megapier.

THE MEGAPIER CRUISE FACILITY

The Megapier Cruise Facility lies 200 m to the west of the entrance of the St Anna Bay. It extends approximately 100 m into the sea. This pier was built in 1997 as a concrete T-shaped pier capable of accommodating mega-cruise ships and other types of ships up to 200.000 GT. Thanks to underground pipelines it is also possible for ships to bunker fuel and water.



Figure 2.6: The Megapier Cruise Facility, with the terminal in the lower left corner and a cruise ship moored at the Megapier [F2].

The length of the pier is 150 m and the draft directly in front of it is 15 m. The deck has an open space area of 2508 m², with a cruise terminal area of 8361 m³ directly accessible from the pier. The construction consists of a concrete deck, supported by piles. Two separate piled mooring dolphins are located on each end of the pier. Cruise ships mooring at the Megapier are piloted, which is obligated by the Curaçao Port Authority for every ship over 50 GT. Work boats of the boatman assist with the mooring procedure as the two mooring dolphins can not be reached from the Megapier.

2.2.3. LOCAL CLIMATE

The island group lies on the southern edge of the Atlantic Hurricane Belt in the Caribbean Sea. Chances of getting hit by a hurricane are very small, but tropical storms do occur. Still, the islands are affected by active hurricanes with strong winds, heavy rainfall and rough sea states. More information can be found in §2.2.5.

Curaçao has a tropical climate with dominant trade winds continuously blowing from the north-east. The average wind speed is 7 m/s [D1]. The annual mean temperature is around 27 °C with a difference of 3 °C between mean summer and mean winter temperatures [6]. A low amount of precipitation falls there with an annual mean of 560 mm. These mild conditions make the island a popular holiday destination for tourists all year long.

2.2.4. WAVE CLIMATE NEAR THE SHORE OF WILLEMSTAD

As there is no accurate wave data of the wave climate near the southern shore of Curaçao, this has to be estimated by means of simulations. To estimate the local wave climate, deep water offshore wave data is required. This deep water wave data is obtained from BMT ARGOS [D2], which is a company specialised in metocean consultancy and weather forecasting. Their database contains 20 years of wave measurements and model results. From Curaçao, remote wave data from this database is used for this study, implying that there is no influence of the presence of the island of Curaçao on the deep water wave data.

This section presents scatter diagrams which are simplified for the sake of clarity. Values in these diagrams between zero and fifty have been left out, as these wave conditions occur rarely, and therefore it is assumed that these will not have a significant influence on the downtime. The complete scatter diagrams which are not simplified can be found in §B.1. This appendix also presents further details on the source of the wave data and the wave data themselves.

BMT ARGUSS WAVE DATA - SWELL AND WIND SEA WAVES AT DEEP WATER

The service of BMT ARGUSS that distributes wave and wind data is called *waveclimate* [D2]. It collects this data by means of both buoy measurements and satellite observations, which are stored in their database. This database contains data on the total sea state, also separated in both wind waves and swell waves.

For this study, the available wave and wind data of the past 20 years was downloaded from their database, originating from their wave model. To extract the time series, choices are made which are summarised in Table 2.3.

Table 2.3: Details about the data set used for this study, containing swell and wind wave data [D2].

Dataset	From 1-1-1992 0:00	Until 31-12-2012 21:00
Time steps	[hours]	3
Grid Cell Centre Coordinates	[°N; °E]	(12.5; -68.75)
Size of Cell	[km]	200×200
No. of Data Records		61368

The data of this time series are used to determine the local wave climate on the project location. The time series contains a large number of wave records, each containing values based upon a time period of three hours. To make this bulk of data more comprehensible, scatter diagrams are made from the time series, which can be found in Table 2.4 and 2.5. A scatter diagram shows characteristic wave data values, which are grouped and arranged in a table. The number in each cell of this table indicates the amount of occurrences in the time series. The significant wave height (H_s in metres) lies between the two values in the left and right blue columns with a peak wave period (T_p in seconds) as listed at the blue top and bottom rows of the table. For the sake of clarity, all observations with less than 50 occurrences have been left out of this diagram.

Table 2.4: Wave climate scatter diagram of wind waves of the past 20 years at deep water, North of Curaçao. The data are obtained from BMT ARGUSS [D2].

		Wave Peak Period [s]											#		%					
		3.2	3.6	3.9	4.3	4.7	5.2	5.7	6.3	6.9	7.6	8.4					9.2	10.2	11.2	
Significant Wave Height [m]	0 - 0.3	326	195	96	-	-	-	-	-	-	-	-	-	-	-	-	-	0 - 0.3	617	1.1
	0.3 - 0.6	1060	1480	1220	756	359	128	-	-	-	-	-	-	-	-	-	-	0.3 - 0.6	5003	8.6
	0.6 - 0.9	-	377	1412	3302	3042	1586	516	110	-	-	-	-	-	-	-	-	0.6 - 0.9	10345	17.9
	0.9 - 1.2	-	-	64	785	3513	5372	3106	774	165	62	-	-	-	-	-	-	0.9 - 1.2	13841	23.9
	1.2 - 1.5	-	-	-	-	414	3421	5177	2694	574	122	-	-	-	-	-	-	1.2 - 1.5	12402	21.4
	1.5 - 1.8	-	-	-	-	-	320	3110	3726	1210	172	-	-	-	-	-	-	1.5 - 1.8	8538	14.7
	1.8 - 2.1	-	-	-	-	-	-	316	2486	1589	332	-	-	-	-	-	-	1.8 - 2.1	4723	8.2
	2.1 - 2.4	-	-	-	-	-	-	-	349	1179	366	-	-	-	-	-	-	2.1 - 2.4	1894	3.3
	2.4 - 2.7	-	-	-	-	-	-	-	-	240	208	-	-	-	-	-	-	2.4 - 2.7	448	0.8
	2.7 - 3.0	-	-	-	-	-	-	-	-	-	75	-	-	-	-	-	-	2.7 - 3.0	75	0.1
		3.2	3.6	3.9	4.3	4.7	5.2	5.7	6.3	6.9	7.6	8.4	9.2	10.2	11.2			57886		
#		1386	2052	2792	4843	7328	10827	12225	10139	4957	1337	0	0	0	0			57886		
%		2.4	3.5	4.8	8.4	12.7	18.7	21.1	17.5	8.6	2.3	0.0	0.0	0.0	0.0			100		

Table 2.5: Wave Climate Scatter Diagram of swell waves of the past 20 years at deep water, North of Curaçao. The data are obtained from BMT ARGUSS [D2].

		Wave Peak Period [s]															#		%			
		4.7	5.2	5.7	6.3	6.9	7.6	8.4	9.2	10.2	11.2	12.3	13.5	14.9	16.3	18.0					19.8	21.8
Significant Wave Height [m]	0 - 0.3	-	-	94	183	267	624	1041	1468	1751	1975	1863	1076	497	149	-	-	-	0 - 0.3	10988	18.4	
	0.3 - 0.6	89	224	510	845	1303	2440	2702	1862	1339	930	768	517	191	-	-	-	-	0.3 - 0.6	13720	23.0	
	0.6 - 0.9	174	447	1182	2158	2207	2664	2485	1642	1045	831	566	350	159	-	-	-	-	0.6 - 0.9	15910	26.7	
	0.9 - 1.2	-	173	690	1690	2343	1933	1427	965	655	488	401	191	83	-	-	-	-	0.9 - 1.2	11039	18.5	
	1.2 - 1.5	-	-	121	516	1191	1295	828	483	372	238	179	107	59	-	-	-	-	1.2 - 1.5	5389	9.0	
	1.5 - 1.8	-	-	-	62	324	563	435	242	173	84	-	-	-	-	-	-	-	1.5 - 1.8	1883	3.2	
	1.8 - 2.1	-	-	-	-	153	215	123	52	-	-	-	-	-	-	-	-	-	1.8 - 2.1	543	0.9	
2.1 - 2.4	-	-	-	-	-	64	62	-	-	-	-	-	-	-	-	-	-	2.1 - 2.4	126	0.2		
		4.7	5.2	5.7	6.3	6.9	7.6	8.4	9.2	10.2	11.2	12.3	13.5	14.9	16.3	18.0	19.8	21.8			59598	
#		263	844	2597	5454	7635	9672	9197	6847	5387	4546	3777	2241	989	149	0	0	0			59598	
%		0.4	1.4	4.4	9.2	12.8	16.2	15.4	11.5	9.0	7.6	6.3	3.8	1.7	0.3	0.0	0.0	0.0			100	

The time series of BMT ARGUSS gives data on both swell and wind waves of the past 20 years. Swell waves are long, smooth waves which are generated in a storm far away from the actual location, with wave periods within the range that may lead to resonance phenomena on larger floating structures and ships. Wind waves are short, irregular and locally generated waves by the presence of wind. As the influence of short wind waves on larger floating structures is less significant, it is of importance to have information on the presence of swell. Swell

waves have a larger wave period and therefore have a higher potential of leading to large dynamic responses.

2.2.5. WIND

Wind data close to Curaçao are obtained from the European Centre for Medium-Range Weather Forecasts (ECMWF) [D1]. It is an independent intergovernmental organisation supported by 34 states. They are specialized in global numerical weather forecast, including severe weather prediction. This includes wind storms and floods. Although these severe weather conditions are not of interest for this study, information is given about these conditions nonetheless. For more detailed information on the used data set, reference is made to §B.2.

This section presents information on the prevailing wind direction and speeds, based on this data set from ECMWF. Also the occurrence of hurricanes and extreme winds is discussed, because it is a reason to study the concept of realising a floating terminal.

WIND DIRECTION

As Curaçao lies near the equator, reasonably strong trade winds blow almost permanently. These trade winds blow predominantly from the East. As Figure 2.7 shows, wind from other directions hardly occur. The wind speed is mostly between 7 m/s and 9 m/s. The distribution on the long term wind speeds near Curaçao is shown in Figure 2.8.

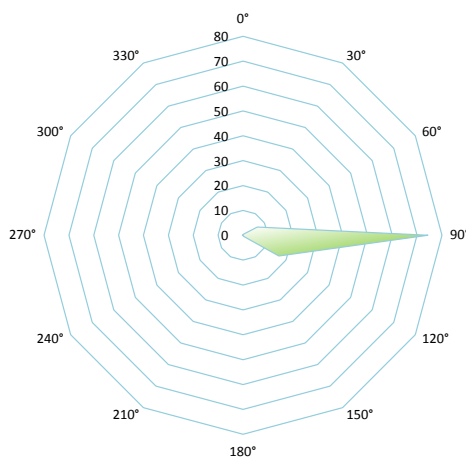


Figure 2.7: The windrose visualises the occurrence of winds as a function of the wind direction. Source: [D1].

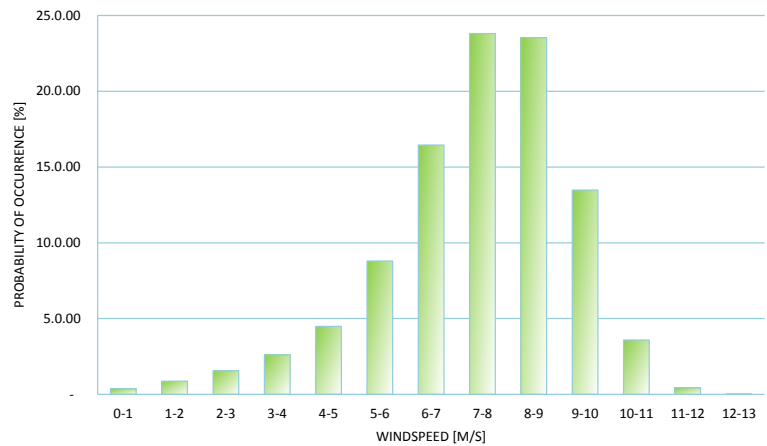


Figure 2.8: The long term distribution of the wind speeds near Curaçao. Source: [D1].

HURRICANES AND EXTREME WINDS

Curaçao lies in the south of the hurricane belt. The hurricane season is from mid-August till mid-November. In the Caribbean Sea there are on average 8-11 tropical storms of which 5-7 develop into hurricanes every year.

On average, a tropical storm passes every 4-5 years within this distance of the island. The figure below shows the path of hurricanes that have passed the island within 200 km in the last 60 years [W9]. Although it seems that Curaçao does not suffer a lot from hurricanes each year, it definitely feels the effect from hurricanes much further away from the island in the form of high waves and wind speeds.

Climate change may well lead to an increase of extreme wind speeds and storms. An increase in the amount of storms and hurricanes will damage the cruise market of the Caribbean Sea for sure. It is therefore an aspect that should be kept in mind which further supports the suggestion of using a floating structure as cruise terminal, instead of a bottom-founded jetty structure.

2.2.6. BATHYMETRY

The foreshore of Curaçao is typically very steep. This can be confirmed by looking at nautical maps from C-Map [S1]. These maps are used for navigation and therefore are very accurate to guarantee the indicated water depths. Figure 2.10 shows the local bathymetry near the port of Willemstad, including the Megapier Cruise Terminal. It shows the mentioned steep profile of the ocean bed floor very close to the shore.

Data about the offshore and deep water bathymetry is obtained from the GEBCO'08 Database. This is the data set used for the numerical computations in Chapter 4. More detailed information on the GEBCO'08 data set can be found in §4.3.3, including a plot of the depth contours using this data set in Figure 4.2.

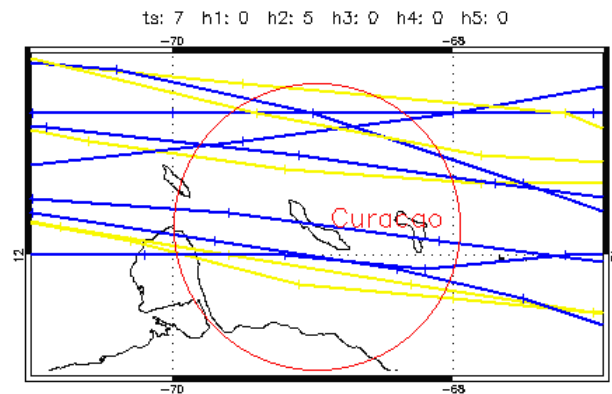


Figure 2.9: Storm tracks of all storms with a category of tropical storm or worse from 1851 - 2010. Blue lines are tropical storms (ts) and yellow lines are hurricanes class h2. The red circle indicates the 200 km radius from the island. Source: [F3].

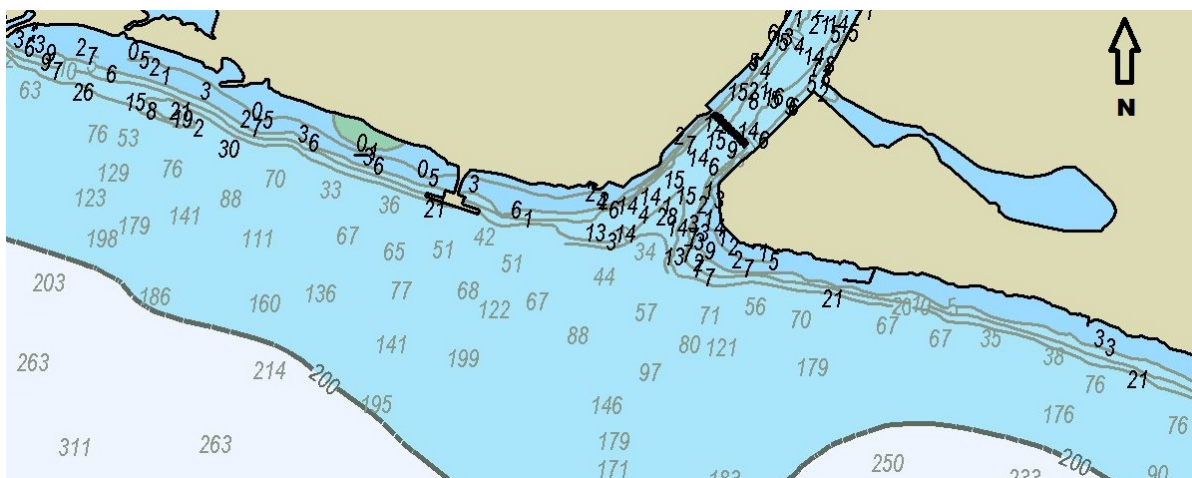


Figure 2.10: Nautical chart from C-Map of the area near port of Willemstad. Scale: 1:15000. Source: [S1].

2.2.7. TIDES AND CURRENTS

Tidal rise normally is in the order of 0.30 m. Current speeds near the shore are negligible, with a regular velocity of 0.2 m/s. Peak velocities can be up to 1.3 m/s further into the ocean along the South-West Coast [5].

2.3. CONCLUSION

Analyses have been carried out to determine the current situation and environmental conditions. From the analyses, a number of conclusions can be drawn, which are presented by section:

CRUISE INDUSTRY

A clear growth is visible in the global cruise industry. Not only in the absolute amount of passengers carried world wide, but this is also clearly visible in the growth of the actual size of cruise ships. The gross tonnage of passenger ships has grown almost exponentially to as much as 225000 (Oasis of the Seas, owned by Royal Caribbean International).

Present cruise ships start to reach the limits of maximum practical size. If the growth in length and draught of these ships is not limited, an increasing number of ports will not be able to accommodate future cruise ships, because of local limitations.

The number of cruise tourists visiting the island of Curaçao increases every year. The ambition of the government to increase the number of cruise tourists from an annual 600.000 to one million by the year 2020 requires expansion of the current port facilities because of two reasons:

- There are not enough berths to handle the future amount of calls to the port of Willemstad not able to berth the current largest cruise ships;
- Local conditions limit the maximum size of cruise ships that can be berthed at the port of Willemstad.

ENVIRONMENTAL CONDITIONS

The analysis on the environment of Curaçao confirmed the steep profile of the ocean bed floor. This makes future port expansions with bottom-founded constructions cost sensitive. Wind waves are generally present because of the reasonably strong trade winds from the East. The north side is the unprotected and rough side with respect to wave and wind attack. The southern side is more or less protected by the island itself.

Tropical storms do occur in this area. Even hurricanes are a potential threat because of the islands location in the hurricane belt.

For the simulation of the local wave climate near Willemstad, data from BMT ARGOS is used. Wind Data is obtained from ECMWF. The bathymetry of the ocean bed is acquired from GEBCO'08 and nautical charts.

DESIGN REQUIREMENTS FOR THE CONCEPT

Requirements are established to be fulfilled by the structural variants of a floating terminal. Boundaries and the scope of the study are stated. The governing design cruise ship that is taken into account is discussed in §3.1. Conceptual floating structures are designed. These are used as input for the hydrodynamic assessment. Structural requirements and considerations are presented in §3.2, followed by functional requirements in §3.3. Additionally, §3.4 treats nautical aspects that influence the site location. Hydraulic requirements, describing dynamic and motion limits and criteria, are presented in §3.5.

3.1. DESIGN CRUISE SHIP

The idea of a new cruise terminal started because of a lack of berths to facilitate the growth in cruise tourism as discussed in §1.1.1. To be ready for the future, the realisation of a mooring location surpassing the performance of the current Megapier Cruise Terminal is desired.

From the analyses in §2.1 it follows that the cruise industry is growing, including the size of cruise ships. The current Megapier Cruise facility may accommodate vessels up to 200.000 GT. The current largest cruise ships (Oasis-Class cruise ships, owned by Royal Caribbean International [W6]) are therefore too large. New ships of this class, with similar dimensions are scheduled to be launched by Royal Caribbean International in the upcoming years. Therefore, the design cruise ship will be one of the Oasis-Class from Royal Caribbean International. The parameters of this design ship are presented in Table 3.1

Table 3.1: Main Particulars of the Design Cruise Ship: Oasis Class Ships from Royal Caribbean International. Source: [W10].

Design Vessel:	Oasis Class	
Gross tonnage	-	227.000
Length o.a.	m	362
Beam	m	47
Max. Breadth	m	66
Draught (loaded)	m	9.2

The benefit of this concept is that ships like the design cruise ship and even larger are able to moor at the facility. For this study, only the design cruise ship, which is the largest at the time of writing, is taken into account for the determination of the influence on the dynamic response.

3.2. STRUCTURAL REQUIREMENTS

3.2.1. TYPE OF STRUCTURE

The studied concept describes a floating terminal, because the feasibility of this type of terminal is interesting. The current Megapier, a fixed structure, has already been realised. This study therefore focuses on the feasibility of a floating terminal as an alternative for the realisation of a new mooring location for the largest cruise ships at present and in the future.

The motion response is studied for floating structures with a single pontoon hull type. Swell wave loads are expected to be low enough to be able to apply this type of hull. The size and weight of such a structure is deemed sufficient to keep motion responses because of wind sea waves low enough for the function of a terminal. Further details on the type of structure can be found in §5.2.

3.2.2. STATION KEEPING

Because of the steep slope of the ocean bed floor and the large water depths, not all station keeping systems are an attractive or feasible solution. Because of this, the solution needs to be economical and environmentally friendly. Also the requirement that the structure should be movable needs to be taken into account.

The station keeping system to be applied for this concept are anchor blocks and catenaries. The latter should be detachable and remain afloat with a buoy to be able to recover and re-attach the catenaries to the floating terminal.

3.3. FUNCTIONAL REQUIREMENTS

3.3.1. NUMBER AND ORIENTATION OF BERTHS

The cruise terminal has to provide berth for at least one design cruise ship. The possibility to provide a berth on each side of the floating terminal will not be part of this study.

There is only one requirement regarding the orientation of the berth. This is that an ideal orientation is to be used for the floating terminal to keep downtimes low. The most ideal orientation will follow from the dynamic analysis. The alignment angle relative to the shoreline will be chosen in such a way that it leads to the lowest downtimes i.e. motion responses. This is discussed in §8.2.

3.3.2. DOWNTIME OF THE FLOATING TERMINAL

The downtime of this concept for multiple variants and wave conditions will be evaluated in Chapter 8. From this assessment it will follow whether the concept of a floating terminal will be feasible. In order to obtain the reputation of a reliable berth, the intention is to limit the yearly downtime to 10% of the time, based upon the recommendation of Thorensen [7].

STORM CONDITIONS

Storm-like conditions, whereby cruise ships will skip port, are not taken into account with this downtime percentage, because in these situations the floating terminal will not be used as such. The definition of these storm-like conditions, which are out of scope, is presented in §3.4.3. This means that the floating terminal must be able to function 90% of the time with local waves up to 1.2 m while maintaining a low enough motion response for any person to remain safe and on their feet.

3.3.3. ACCESSIBILITY BETWEEN THE FLOATING TERMINAL AND THE SHORE

Cruise ships carry many passengers. When a cruise ship arrives at a port, passengers want to disembark and go sightseeing. The number of passengers may range from dozens to even a few thousands within about an hour. This requires a proper connection to the shore, able to process such large quantities within a limited timespan. The location of this connection is indicated in Figure 3.1.

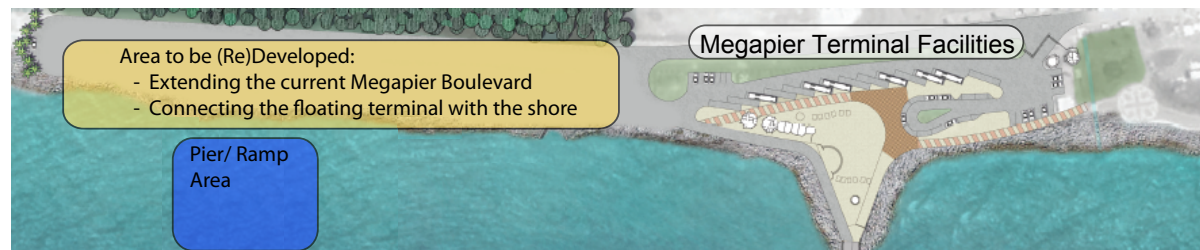


Figure 3.1: Sketch of the areas to be developed to realise the non-floating part of the new cruise terminal. Source original image: [F2]

3.3.4. TERMINAL FACILITIES

Because of the small distance between the project location and the Megapier Cruise Terminal, all current facilities of the Megapier will be used and expanded where necessary. Also the already existing boulevard will need to be extended to the location where the transfer bridge connects with the shore, to provide a warm welcome for all the cruise passengers disembarking from the floating terminal. Further details on the shore facilities fall out of the scope of this study and will not further be taken into account. Figure 3.1 shows an indication of the area that needs to be developed in order to realise additional shore facilities and an extension of the current boulevard.

3.3.5. MOVABLE AND MULTIFUNCTIONAL

Because storm conditions occur occasionally, the concept should take this into account. To reduce production cost and because of the fact that cruise ships skip port in the case of storm conditions, it is suggested to make

the floating structure movable. During longer downtime periods, it is interesting to study the possibilities of other applications for the floating terminal during extreme weather in an additional research.

It is required that the structure fits through the St Anna Bay, thereby limiting the dimensions of the structure. Placing the structure in the St Anna Bay or in the Schottegat provides the required shelter for more extreme weather conditions, and at the same time makes it usable for other applications during these weather conditions.

3.4. NAUTICAL REQUIREMENTS

Nautical requirements are defined as the aspects of the cruise terminal that make safe mooring of the design vessel possible.

3.4.1. MINIMAL WATER DEPTH

The current Megapier Cruise Terminal is the only berth at Willemstad for ships with a draft of more than 13.6 m, because of the limited depth of the St Anna Bay, with a maximum draught of 15 m. The port of Willemstad is not able to provide berth for ships with a draught larger than 15 metres. Those ships will need to moor in one of the other ports/bays that Curaçao has.

For cruise ships in particular, there is no real necessity to increase the maximum draught of the new berth. The maximum draught of these ships has not yet exceeded 10 m. It is not likely to increase significantly because of the consequences it has on the general accessibility of ports.

It is suggested to locate the terminal at a water depth of around 20 m. Because of the steep ocean floor this does not increase the distance to the shore significantly. Tidal windows will not be necessary and sufficient keel clearance will be available at all times for all ships calling at the port of Willemstad. Because of the concept of a floating terminal, this increase in minimal water depth does not have a significant influence on the cost, compared to a bottom founded and permanent jetty like the current Megapier Cruise Terminal.

3.4.2. VESSEL APPROACH CONDITIONS AND TUG SUPPORT

Cruise vessels call at the port of Willemstad so that tourists can visit the well known highlights of Curaçao. Whenever there are poor weather conditions, cruise ships will skip to a port with better weather conditions. Poor weather conditions mean in this case storm-like conditions and worse, with high wind speeds and waves. Prior to these situations, the floating terminal will be towed to the Schottegat, where it lies sheltered from high waves.

Large ships mooring at the Megapier are assisted by working boats of the boatmen. These working boats help for example with placing the mooring lines, and assist in case there are strong winds. To be able to function properly, the weather conditions should be not too severe. Waves with a significant wave height of 1.5 m lead to a reduced efficiency of tugboats [7]. As mentioned above in §3.3.2 and further discussed in §4.3.1, the significant wave height for scenario *W3C* is 1.2 m. This leads to no additional limitations and restrictions with respect to assisting tugboats or working boats.

3.4.3. WIND RESTRICTIONS

According to Thorensen [7], cruise ship motion should be limited for wind speeds up to 18 m/s. This is an upper limit to ensure that gangways and transfer bridges remain operationally safe. According to the wind data from ECMWF (see Appendix B.2.2) the normal averaged wind conditions do not exceed velocities of 13 m/s. Because cruise ships will skip a port in case of storm conditions, these extreme conditions do not pose additional restrictions on the wind speeds. For this study, the service limit state is 11.8 m/s blowing predominantly from the East. The wave conditions at even larger wind speeds are not studied, because the main focus of this study lies on the influence of local wave conditions for defined scenarios, determined from deep sea wave data.

3.5. REQUIREMENTS REGARDING HYDRAULIC ASPECTS

The feasibility also depends on the hydraulic aspects near the project location. The dynamic response of the floating structure depends for example on the properties of the structure, but also on the height and period of waves. Limitations and requirements are quantified here to ensure safe mooring and disembarking of passengers. From the latter, safety criteria follow for the sake of tourists of all ages.

3.5.1. TIDES AND CURRENTS

From the analyses, it follows that the tidal range is in the order of 0.60 m. As the considered concept is a floating structure, the tide does not have a direct influence on the structure itself, as it will move along with the tide. The effect on the wave height due to fluctuating water depths is assumed negligible due to the large water depth at the intended project location. Therefore, tidal influences are not considered in this study. This assumption is checked in §4.5.4.

For currents it is known that velocities may attain up to 1.3 m/s along the South-West coast. These speeds are reached only for very short periods further from the shore. In general, the current speeds are in the order of 0.2 m/s and therefore not taken into account in the study of the dynamic behaviour.

3.5.2. WAVE CONDITIONS

Because of the limitations regarding tug assistance, the floating structure will be required to still fulfill its function as a floating terminal with a maximum significant wave height of 1.5 m. If the motion response for waves up to 1.5 m exceed the safety limits, this will result in downtime. In this case, whereby the motion response limits the maximum allowable wave height, the requirement regarding the downtime will be leading.

3.5.3. MOTIONS AND DYNAMIC RESPONSE

Nordforsk [8] and PIANC [9] both determined motion criteria for ships and floating structures. The motion criteria from Nordforsk [8], which can be found in Table 3.2, are defined in terms of Root Mean Squared (RMS) accelerations and roll angles. Taking into account the diversity of passengers on a cruise ships, the limiting criteria for both *Cruise Liners* and *Transit Passengers* are used to determine the downtime. These criteria will be leading for this study on the feasibility of a floating cruise terminal as they are more strict than the displacement based criteria from PIANC. The latter will therefore not be used in this study, but for the sake of completeness they are presented in §5.3.4, which is an introduction on floating structures.

As the floating structure will fulfil the function of a cruise terminal, motions of the structure should remain limited to guarantee safe operation. Passengers of all ages will make use of the cruise terminal. The intended concept therefore imposes a very restricting factor regarding the allowable wave and weather conditions. Tourists should feel safe and comfortable during the process of embarking or disembarking the cruise ship.

The *Transit Passengers* criteria from Nordforsk are also taken into account, because the *Cruise Liner* criteria are very strict. The latter are defined to guarantee a comfortable journey on a cruise ships at all times (sleeping, eating, etc.). The cruise terminal will be the connecting element between the shore and the moored cruise ship. Cruise tourists are therefore not likely to remain on the terminal very long. The less strict *Transit Passengers* criteria are therefore also studied, to determine the influence of less strict criteria on the downtime of the terminal.

Considering the PIANC criteria, displacements cannot be neglected at later design stages, because probably use will be made of a ramp to connect the floating terminal with the shore. If displacements become very large, this may well lead to problems when tourists want to make use of the ramp. But as stated before, the PIANC guidelines will be left out of the scope of this study. These criteria may be studied in an additional study.

Table 3.2: Seakeeping performance for human effectiveness - Limiting criteria with regard to accelerations (vertical and lateral) and roll motions [8].

Description	RMS Vertical Acceleration	RMS Lateral Acceleration	RMS Roll Motion
Light Manual Work	0.20 g	0.10 g	6.0°
Heavy Manual Work	0.15 g	0.07 g	4.0°
Intellectual Work	0.10 g	0.05 g	3.0°
Transit Passengers	0.05 g	0.04 g	2.5°
Cruise Liner	0.02 g	0.03 g	2.0°

MODELLING THE LOCAL WAVE CLIMATE

It takes a number of steps to simulate the local wave climate with the use of deep-sea wave data. The determination of local wave climate conditions is an important intermediate step in the process to carry out a hydrodynamic assessment for floating structures near the shore of Willemstad.

In §4.1 the approach of modelling the local wave climate is presented. Section 4.2 introduces the SWAN wave model, including limitations and not considered effects. An explanation on the set-up of the SWAN-models is given in §4.3. Simulations are run for different wave scenarios to obtain wave data at the local output location. Section 4.4 treats both this and the determination of key scenarios. These key scenarios will be used as input for the hydrodynamic assessment later on in this study. The final Section 4.5 discusses the results from all the simulations. Findings are summarised and remarks on the entire modelling process are stated in §4.6.

4.1. APPROACH

The floating cruise terminal will be situated near the shore on the southern side of Curaçao. There is no shelter from waves nor wind apart from the island itself. Local wave data are needed to be able to study the behaviour of such a terminal on this particular location. As there are no near-shore wave data available, this data will be obtained by means of simulation using a wave model. In order to run such a simulation, four things need to be prepared. These are shown in table 4.1, together with the services or products used.

Table 4.1: Preparation steps for the simulation of local wave data, indicating data sources and software.

#	Description	Source of data/ Software
1:	Deep-water wave data close by	BMT Argoss [D2]
2:	Bathymetry data of the location	GEBCO 08 Database [D3]
3:	Wind Data	ECMWF [D1]
4:	Wave model	SWAN [10]

1: DEEP WATER WAVE DATA

BMT ARGROSS is specialised in metocean consultancy and weather forecasting. The company uses satellite observations and numerical models for the prediction and observation of wave conditions with a collection of data of up to 30 years. Their models cover large parts of the world's oceans with numerical grid cells. The nearest deep water grid point is used for this study. Appendix B.1 contains additional and more detailed information on this data. Close attention should be paid to the fact that this data source does not incorporate storm and other short extreme weather conditions.

2: LOCAL BATHYMETRY

GEBCO provides global bathymetry data of oceans. Ship soundings and satellite data are used and combined to create a 30 arc-second grid data set (roughly 926×905 metres grid cells). Between sounding points the data are interpolated, using gravity data from satellites to increase accuracy. For the bathymetry of the area of interest, these data are used and visualised in Figure 4.2.

3: WIND DATA

The European Centre for Medium-Range Weather Forecasts(ECMWF) is an independent intergovernmental organisation. The organisation is both a research institute and a numerical weather prediction service. Use is made of their service to obtain general wind data near the project location. A wind scatter diagram is created from this data, which can be found in Appendix B.2. This diagram shows the wind speed in relation to the wind direction and the amount of occurrences.

4: WAVE MODEL

The deep water wave data are put into a wave model which results in a simulated local wave climate. The model used for the near-shore wave transformation is called SWAN (Simulating Waves Near shore). SWAN is a shallow water wave model and is a free open source computer model. The program is used to obtain realistic estimates of wave parameters, and is an important tool for scientists and engineers. Further information on this model is given in §4.2.

The input, containing the local bathymetry, deep-water wave data, wind-parameters etcetera, results in an output after running the model. The output data obtained from the simulation will then be used to model the dynamics of a floating structure at the output location.

4.2. THE SWAN WAVE MODEL

4.2.1. THEORY USED IN SWAN

The software *Simulating WAves Nearshore* (SWAN) [S2] is a third-generation numerical wave model that computes random, short-crested wind-generated waves in coastal regions and inland waters. The model uses *Linear Wave Theory* to describe waves using a three dimensional spectral density function. It is able to describe the evolution of wave spectra by solving the spectral action balance equation. In addition, it can also incorporate additional wave physics, like for example wave-induced set-up, triad wave-wave interactions and quadruplet wave-wave interactions in the approximations. SWAN is able to produce 2-d maps of wave heights or other parameters over the whole model domain. This area is bound by a user set-up input model with initial- and boundary conditions and bathymetric data.

The software is continuously developed by Delft University of Technology. The version used in this study is V41.01.

4.2.2. PHYSICS

SWAN is able to include physical processes in the calculation. They can add or withdraw wave energy to or from the wave field. To increase accuracy it is important to include any processes that are (assumed) relevant for the actual situation. Without going too much in detail (further details on the physical processes simulated by SWAN can be found in the Scientific/Technical documentation of SWAN [11]) these processes include:

- Wind input;
- Whitecapping of waves;
- Bottom friction;
- Depth-induced wave breaking;
- Dissipation due to vegetation;
- obstacle transmission;
- Nonlinear wave-wave interactions;
- wave-induced set-up.

4.2.3. LIMITATIONS AND NOT CONSIDERED EFFECTS

An important limitation is the use of a phase-decoupled approach to avoid considerable computing effort for the computation of diffraction.

Another limitation is related to the fact that SWAN does not include wave generated currents, because of, for example, wave-induced set-up. The software uses an approximation method with the condition that it is applied on an open ocean with unlimited supply of water from outside the domain. This is the case in this study. It is assumed that the absence of wave generated currents does not have a significant influence on this specific study and has therefore not been taken into account in this study.

To limit the scope of this study, the following effects are not considered:

- Tidal influence: changes in water level due to the tide are very limited. It is also regarded as so slow, that it does not have any significant influence on the dynamic response of the floating terminal;
- Long-shore currents: From the analysis it follows that long shore currents close near the shore are low with speeds in the order of 0.20 m/s. This effect has therefore not been taken into account in the determination of the wave climate and dynamic analysis of the floating cruise terminal. Still, this may definitely not be neglected in the further development of this conceptual terminal;

- Dissipation due to vegetation;
- Storm Conditions. This topic is further elaborated in §4.3.1.

4.3. DESCRIPTION AND SET-UP OF SWAN WAVE MODEL

Before a simulation can be run, a model needs to be set up. This includes defining all the required input and model parameters:

- Wave- and wind input and data output locations;
- Applied computational grid;
- Bathymetry;
- Boundary- and initial conditions.

These items are all subsequently discussed below. For the full input file i.e. the command file used for the simulation, reference is made to Appendix C.

4.3.1. WAVE- AND WIND INPUT AND DATA OUTPUT LOCATIONS

Data from both BMT ARGOS and ECMWF is a.o. calculated from satellite observations and defined at a grid point of their model. This grid point is given by a geographical location. The wind and wave data at these grid points are representative for the entire grid cell.

LIMITATIONS TO THE WAVE DATA: WEATHER CONDITIONS THAT ARE OUT OF SCOPE

The wave data obtained from BMT ARGOS do not include (short) extreme weather conditions, also meaning that they do not contain information on tropical storms or worse. The extremes at deep water in the used data are: $H_{s,max} = 3.75$ m and $u_{10,max} = 15.7$ m/s which is equivalent to *near gale* conditions (7 on the Beaufort Scale). In §4.4 wave scenarios are defined from the obtained data. The most extreme scenarios chosen to be studied lie close to these *near gale* weather conditions. Therefore, for this study the very important following assumption is made:

Weather conditions exceeding the most extreme scenario W3C defined in §4.4.1 are considered storm conditions. In case of worse weather conditions the assumption is made that cruise ships with the port of Willemstad as destination will skip port and sail on to the next destination with calmer weather conditions.

This assumption or limitation leads to downtime for the port of Willemstad. But this downtime follows from weather conditions and the choice of - necessity for - cruise ships to skip port. This is unrelated to the stability and dynamic behaviour of the floating concept, also leading to downtime on all cruise berths in the port of Willemstad. This down time is therefore not taken into account in the study on the feasibility of this floating concept.

DATA OUTPUT LOCATION

For this study it is necessary to get SWAN output data at only one particular area. The area of interest for the concept floating cruise terminal is indicated with a geographical coordinate. From here on, this project location is defined as location 'CT2' with the following coordinates: (12.1025N; -68.9450E). It is assumed that the wave conditions in the direct area, with a minimal water depth of 15 metres, of these coordinates do not change significantly.

4.3.2. COMPUTATIONAL GRID

To be able to run waves through a model, the space in the model needs to be defined. This is done by boundaries and boundary conditions. Within this model space a computational grid defines how many calculation points are used by the model. The higher the resolution of this grid, the better the accuracy of the results. The consequence is a larger computation time.

The defined computational grid with the output location is visualised in Figure 4.1. The grid contains 400 meshes in both x- and y-direction, this means 401×401 grid points spread over a distance of 1° (= ± 60 M ≈ 60·1852 m) in both South-North and West-East direction.

4.3.3. BATHYMETRY

The GEBCO'08 Database is used as input for the bathymetry of the offshore modelled area. This grid is extracted using the software *DelftDashboard* [S3]. A model domain is defined as a square with longitudinal boundaries at $-69.5^{\circ}E$ and $-68.5^{\circ}E$ and lateral boundaries at $11.75^{\circ}N$ and $12.75^{\circ}N$ divided into 401×401 grid points. Grid points that are not exactly known from measurements are interpolated with the aid of satellite derived gravity data. Figure 4.2 shows a plot of this data set within the model boundaries.

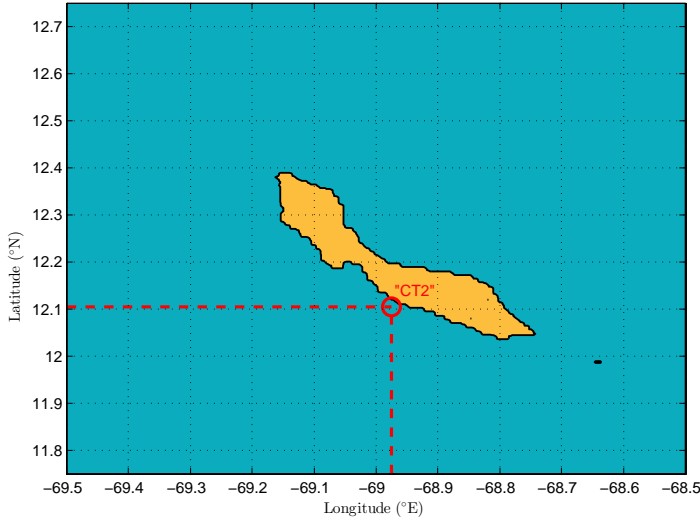


Figure 4.1: Defined model boundaries for the computational grid. The red circle indicates the model output location of SWAN results.

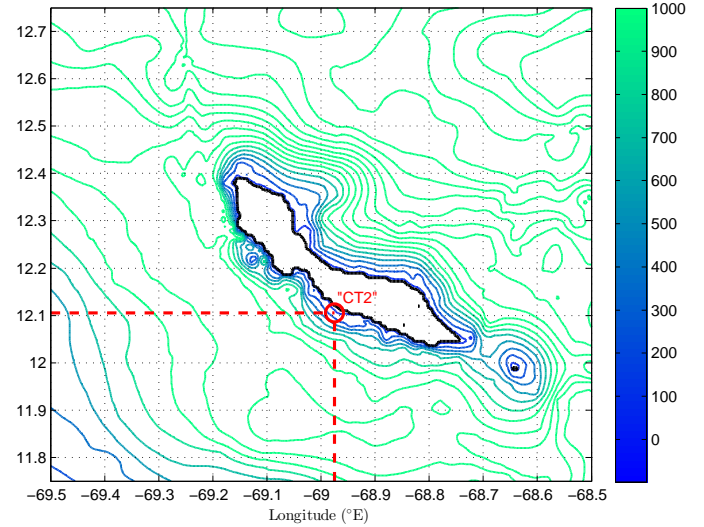


Figure 4.2: Plot showing the depth contours extracted from the GEBCO'08 Database and the project location indicated in red. The water depths are shown in metres.

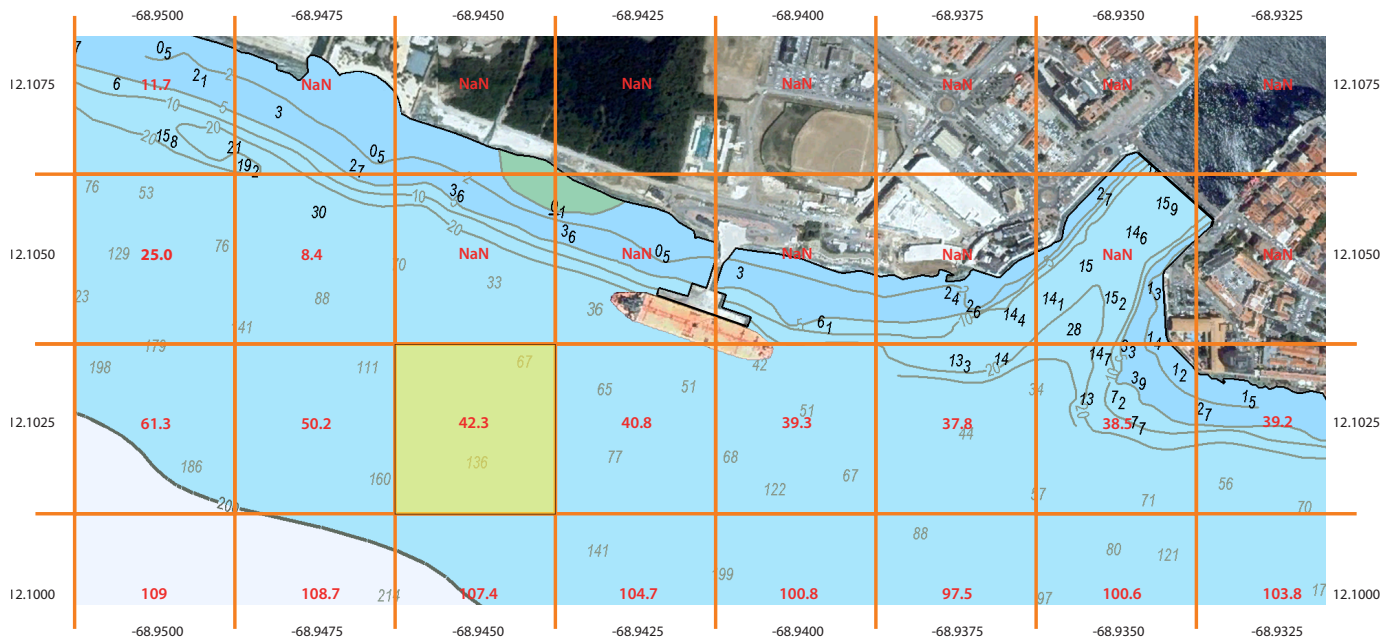


Figure 4.3: Project area with the water depths and geographical coordinates shown for all grid cells. The yellow highlighted cell represents the SWAN model output location. Satellite image source: [F4]. Source of nautical chart: [S1]

GEBCO'08 is a relatively rough data source, used for larger models. As long as the depths near the project location remain relatively large (order: tens of metres), model results like the significant wave height are not influenced very much (H_s in the order of centimetres). As the project location studied for this thesis has in any case a larger depth than 15 metres, the GEBCO'08 data set will suffice to model the local wave climate.

The GEBCO'08 data visualised in Figure 4.2 give an idea about the depth contours in the entire model domain. It gives a rough indication of the water depths around the island. This information is combined in Figure 4.3. It shows the depths as given by GEBCO'08 for each grid cell, with the corresponding geographical

coordinates on the edges of the image. The yellow highlighted cell represents the output location for the SWAN model. Parameters like the *variance density spectra* will be determined for this location. On the background, a nautical map shows more accurate depth information, which is used by ships. This chart is obtained from the chart room of Delft University of Technology (DUT) using the software *TheMap® 10VR 3d* with *Jeppesen C-Map Max charts* from 2011 [S1].

4.3.4. BOUNDARY- AND INITIAL CONDITIONS

Boundary- and initial conditions are required as input for the computations. The boundary conditions are user imposed and contain for example wave properties that propagate into the model. This input is in this case defined as a wave spectrum. The boundary wave spectrum is defined as a JONSWAP-spectrum and is imposed only on the eastern and northern boundaries, as the majority of all the deep-water waves come from an angle between 55° and 85°. This can be confirmed by looking at Table 4.3. The significant wave height H_s , peak period T_p , wave direction θ_w and the directional spreading of waves σ_θ are the required input parameters for SWAN to define the boundary waves. The directional spreading is for this study assumed to be 30° for wind waves and 15° for swell waves [12].

In the SWAN-command file, additional start-up commands set values for general model parameters. These parameters and the chosen values can be found in Table 4.2.

Table 4.2: General parameters values to start-up the SWAN Wave Model.

Parameter	Value
ρ	[kg/m ³] 1.025
g	[m/s ²] 9.81
MSL	[m] 0

Table 4.3 shows the wave scatter diagram for the deep sea wave climate obtained from BMT ARGOS. This wave scatter diagram is used to determine the boundary wave conditions for different scenarios. This is further elaborated in §4.4. This particular table is cleaned up, to shows only the most relevant wave heights and directions; all cells with less than 50 occurrences have been removed from this scatter to remain comprehensible. The full tables can be found in Appendix B.1.

From Table 4.3 one can see that at deep water most occurring wind waves have a significant wave height of 0.9-1.2 metres and come from an angle of 80°.

Table 4.3: Deep water wind wave scatter diagram: Wave height vs. wave direction. Waves with less than 50 occurrences are left out of this scatter diagram. Source: [D2].

		Wave Direction [deg]												#	%				
		0	10	20	30	40	50	60	70	80	90	100	110			120			
Significant Wave Height [m]	0 - 0.3	-	-	50	97	111	180	254	421	486	314	169	67	-	0	-	0.3	2149	3.6
	0.3 - 0.6	-	-	-	-	103	205	504	1064	1697	1114	427	131	-	0.3	-	0.6	5245	8.8
	0.6 - 0.9	-	-	-	-	-	240	732	2166	4265	2247	532	115	-	0.6	-	0.9	10297	17.3
	0.9 - 1.2	-	-	-	-	-	225	827	2963	6744	2749	232	-	-	0.9	-	1.2	13740	23.1
	1.2 - 1.5	-	-	-	-	-	139	682	2570	6641	2234	116	-	-	1.2	-	1.5	12382	20.8
	1.5 - 1.8	-	-	-	-	-	74	446	1834	4690	1482	-	-	-	1.5	-	1.8	8526	14.3
	1.8 - 2.1	-	-	-	-	-	-	179	1035	2671	823	-	-	-	1.8	-	2.1	4708	7.9
	2.1 - 2.4	-	-	-	-	-	-	70	436	1108	296	-	-	-	2.1	-	2.4	1910	3.2
	2.4 - 2.7	-	-	-	-	-	-	-	103	292	65	-	-	-	2.4	-	2.7	460	0.8
2.7 - 3.0	-	-	-	-	-	-	-	-	56	-	-	-	-	2.7	-	3.0	56	0.1	
		0	10	20	30	40	50	60	70	80	90	100	110	120			59473		
#		0	0	50	97	214	1063	3694	12592	28650	11324	1476	313	0			59473		
%		0	0	0	0	0	2	6	21	48	19	2	1	0			100		

In all cases, the wind speed and direction are linked with the wave parameters of each scenario: The wind direction is chosen the same as the direction of the boundary waves. Regarding the wind speed: larger waves require a higher wind speed to be generated and maintained. Therefore, the wind speed is chosen such that the wave height does not decrease significantly until it has reached the island of Curaçao. Further explanation on this is given in §4.4.2.

4.4. SIMULATION OF DIFFERENT WAVE CONDITIONS

4.4.1. DETERMINATION OF KEY SCENARIOS

Due to limited resources, it is chosen to not simulate each and every cell in the wave scatter diagrams. Alternatively, several key scenarios are defined, which represent larger parts of the wave scatter diagrams. This way, the amount of runs is reduced, without large losses of accuracy. To transform the deep-water wave data to the project location near shore, specific sets of wave parameters are chosen for each scenario. Each of these scenarios are then imposed on the boundaries of the model.

Defining key scenarios is done by using the wave data sets from BMT ARGOSS (see Appendix B.1). Every three hours the total-, wind-sea and swell significant wave height is calculated. The corresponding zero-crossing-, mean-, and peak period is also given in this appendix, among with the wave direction and wind speed and direction. Wave scatter diagrams like Figure 4.3 are created from this data, to be better comprehensible.

From the data of BMT ARGOSS, scenarios with different wave parameters are chosen that are or could be of significance for the determination of the dynamic behaviour of the floating cruise terminal. The scenarios are chosen in such a way that the influence of the parameters wave- direction, height and period can be evaluated. The difference between parameter values are such that it is large enough to show its effect on the results, but still occurs often enough to be of importance on the possible downtime. In addition, extreme scenarios are also defined, which don't occur very often. These scenarios are also taken into account to get an idea about the robustness of different solution. The scenarios that are used as boundary conditions for the SWAN-model are given below. Running each scenario gives the modelled output of the wave conditions near the project area, which is required for the study in the dynamic behaviour.

Table 4.4: Different scenarios for boundary wave conditions run in SWAN model. These are determined from the wave scatter diagrams in Appendix B.1. The probability of exceedance P_E concerns the significant wave height of the scenarios.

Wind sea waves								Swell waves							
#	H_s [m]	T_p [s]	θ_w [°]	σ_θ [°]	u_{10} [m/s]	θ_{wind} [°]	P_E [%]	#	H_s [m]	T_p [s]	θ_w [°]	σ_θ [°]	u_{10} [m/s]	θ_{wind} [°]	P_E [%]
W1A	0.6	5.2	80	30	5.8	80	70.3	S1A	0.3	8.4	70	15	4.9	70	
								S1B	0.3	11.2	70	15	5.2	70	58.6
								S1C	0.3	16.3	70	15	5.6	70	
W2A	1.2	5.2	80	30	7.7	80		S2A	0.9	8.4	70	15	6.6	70	
W2B	1.2	6.9	80	30	7.4	80		S2B	0.9	8.4	50	15	6.6	50	13.6
W2D	1.2	5.2	70	30	7.8	70	26.4	S2C	0.9	8.4	80	15	6.6	80	
W2E	1.2	5.2	90	30	7.8	90		S2E	0.9	11.2	70	15	6.6	70	
W3A	1.8	6.3	80	30	9.5	80	4.2	S3A	1.5	11.2	70	15	7.5	70	1.4
W3C	2.7	6.9	80	30	11.7	80	0.1	S3C	2.1	8.4	70	15	9.2	70	0.1

The chosen parameters for each scenario are visualised in the wave scatter diagrams. The scatter diagrams of wind sea waves showing the representative parameters can be found in the Figures 4.5 and 4.7. With the determined general parameters and key scenarios, the next step is to put all the data into the SWAN model and run it. This is treated in the next section.

The same figures but for swell waves can be found in Appendix B.1. The scatter diagrams with the scenarios indicated help visualise the coverage area of the scenarios. From the scatter diagrams it is also possible to determine the return period and probability of exceedance for waves regarding the significant wave height. This is used together with the model results of Chapter 7 for the determination of the downtime period in Chapter 8.

4.4.2. INITIALISATION OF THE WAVE MODEL: EXAMPLE SCENARIO W2A

The requirements mentioned at the beginning of §4.3 have been fulfilled. SWAN requires a command file to run, which has discussed and set-up in §4.3. This file contains all important commands, parameters and paths to other data files. After completing the command-file (see Appendix C.4), SWAN can be used to model scenarios. This section presents plots, results and data for one particular scenario, which is scenario W2A, to demonstrate additional steps and the model results. The results of all scenarios can be found in Appendix D.

The Figures 4.4 and 4.5 show the output results of the model. Table 4.4 shows the parameter values belonging

Table 4.5: Wind sea wave scatter diagram showing the wave parameters that each wave scenario represents. Source: [D2].

Table 4.6: Legend of Table 4.5 and 4.7.

		Wave Direction [deg]											#	%			
		0	10	20	30	40	50	60	70	80	90	100			110	120	
Significant Wave Height [m]	0 - 0.3	-	-	50	97	111	180	254	421	486	314	169	67	-	0 - 0.3	2149	3.6
	0.3 - 0.6	-	-	-	-	103	205	504	1064	1697	1114	427	131	-	0.3 - 0.6	5245	8.8
	0.6 - 0.9	-	-	-	-	-	240	732	2166	4265	2247	532	115	-	0.6 - 0.9	10297	17.3
	0.9 - 1.2	-	-	-	-	-	225	827	2963	6744	2749	232	-	-	0.9 - 1.2	13740	23.1
	1.2 - 1.5	-	-	-	-	-	139	682	2570	6641	2234	116	-	-	1.2 - 1.5	12382	20.8
	1.5 - 1.8	-	-	-	-	-	74	446	1834	4690	1482	-	-	-	1.5 - 1.8	8526	14.3
	1.8 - 2.1	-	-	-	-	-	-	179	1035	2671	823	-	-	-	1.8 - 2.1	4708	7.9
	2.1 - 2.4	-	-	-	-	-	-	70	436	1108	296	-	-	-	2.1 - 2.4	1910	3.2
	2.4 - 2.7	-	-	-	-	-	-	-	103	292	65	-	-	-	2.4 - 2.7	460	0.8
2.7 - 3.0	-	-	-	-	-	-	-	-	56	-	-	-	-	2.7 - 3.0	56	0.1	
		0	10	20	30	40	50	60	70	80	90	100	110	120	#	%	
#		0	0	50	97	214	1063	3694	12592	28650	11324	1476	313	0	59473		
%		0	0	0	0	0	2	6	21	48	19	2	1	0	100		

Not Considered	Scenario W1A	Scenario W2A	Scenario W2D	Scenario W2E	Scenario W3A	Scenario W3C
----------------	--------------	--------------	--------------	--------------	--------------	--------------

Table 4.7: Wind sea wave scatter diagram showing the covered area with respect to the peak wave period of the different scenarios. Source: [D2].

		Wave Peak Period [s]									#	%	
		3.2	3.6	3.9	4.3	4.7	5.2	5.7	6.3	6.9			7.6
Significant Wave Height [m]	0 - 0.3	326	195	96	-	-	-	-	-	-	-	617	1.1
	0.3 - 0.6	1060	1480	1220	756	359	128	-	-	-	-	5003	8.6
	0.6 - 0.9	-	377	1412	3302	3042	1586	516	110	-	-	10345	17.9
	0.9 - 1.2	-	-	64	785	3513	5372	3106	774	165	62	13841	23.9
	1.2 - 1.5	-	-	-	-	414	3421	5177	2694	574	122	12402	21.4
	1.5 - 1.8	-	-	-	-	-	320	3110	3726	1210	172	8538	14.7
	1.8 - 2.1	-	-	-	-	-	-	316	2486	1589	332	4723	8.2
	2.1 - 2.4	-	-	-	-	-	-	-	349	1179	366	1894	3.3
	2.4 - 2.7	-	-	-	-	-	-	-	-	240	208	448	0.8
2.7 - 3.0	-	-	-	-	-	-	-	-	-	75	75	0.1	
		3.2	3.6	3.9	4.3	4.7	5.2	5.7	6.3	6.9	7.6	#	%
#		1386	2052	2792	4843	7328	10827	12225	10139	4957	1337	57886	
%		2.4	3.5	4.8	8.4	12.7	18.7	21.1	17.5	8.6	2.3	100	

to scenario W2A which are imposed as boundary wave conditions on the northern and eastern boundary.

As SWAN is based on wind-generated surface gravity waves, wind is a very important part of the simulation. It is the main source of energy for waves inside the model domain. Without any wind, the boundary waves would decay while propagating into the domain. Therefore, to not lose the wave properties set on the chosen boundaries, wind has to be added to the model. The influence of wind on the wave model is shown in Appendix C.2. This is done by running the model a first time without wind, and a second run with wind enabled. The result of the simulation of scenario W2A with wind included is shown in Figure 4.4.

Therefore, before the actual simulation is run, a preliminary run is executed, to determine the wind speed at which the boundary wave properties in deep-water are maintained the best. The values of the wind speed for all scenarios are listed in Table 4.4. As expected, the required wind speed increases for higher significant waves.

The corresponding wind speed for this example (scenario W2A) is found to be 7.7m/s with the same direction as the boundary waves. This can be confirmed by looking at Figure 4.4: the waves at the eastern boundary initially remain roughly the same while travelling into the domain. This means that the amount of wave energy (imposed via the wave parameters) at the boundaries is maintained while propagating through deep water within the model domain. This is important, because as wind is an input of energy for waves, the amount of wind should match the energy level of the waves posed on the boundaries. Otherwise, much wave energy would dissipate while propagating as there is no energy source to maintain the imposed wave parameters.

4.5. SWAN MODEL RESULTS

The significant wave height, wave peak period, wave direction and wave spectra are calculated at the output location for different scenarios. The output of SWAN is a file containing a Matlab table with all the parameters

asked for in the SWAN command file. With use of the software Matlab [S4], graphs are plotted using this Matlab table file. Of interest are the local wave conditions at the foreshore of Willemstad (location CT2). Important parameters that describe these conditions are the significant wave height H_s (Fig. 4.4), peak wave period T_p (Fig. 4.5), wave direction θ (Fig. 4.4) and the wave spectrum (Fig 4.6) at the project location.

Again, all plots and results presented in this section belong to the scenario W2A, unless indicated otherwise. The variance density spectra in Figure 4.6 of Scenario W2A is indicated with the green line. For the results and plots of all other scenarios, reference is made to Appendix D.

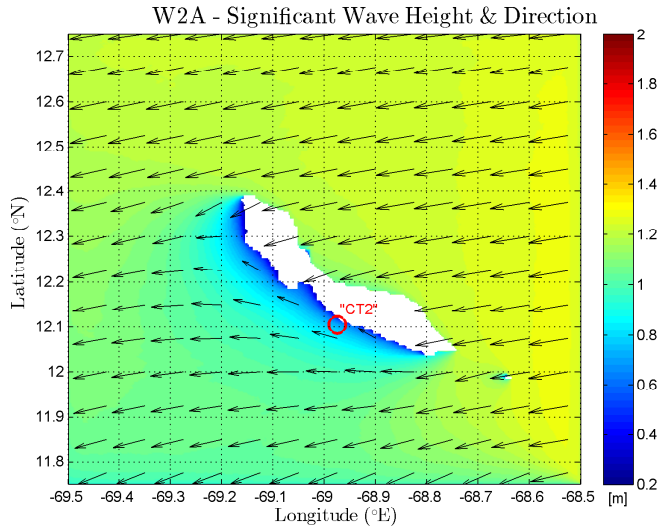


Figure 4.4: Scenario W2A: Plot showing both wave directions and significant wave heights H_s as calculated by the SWAN Model, including stationary winds: wind speed: 7.7 m - s, wind direction: 80°.

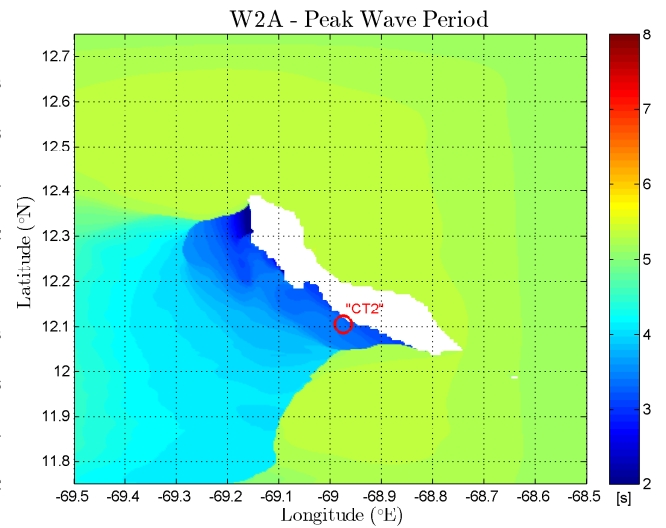


Figure 4.5: Scenario W2A: Plot showing the results for the peak wave period T_p .

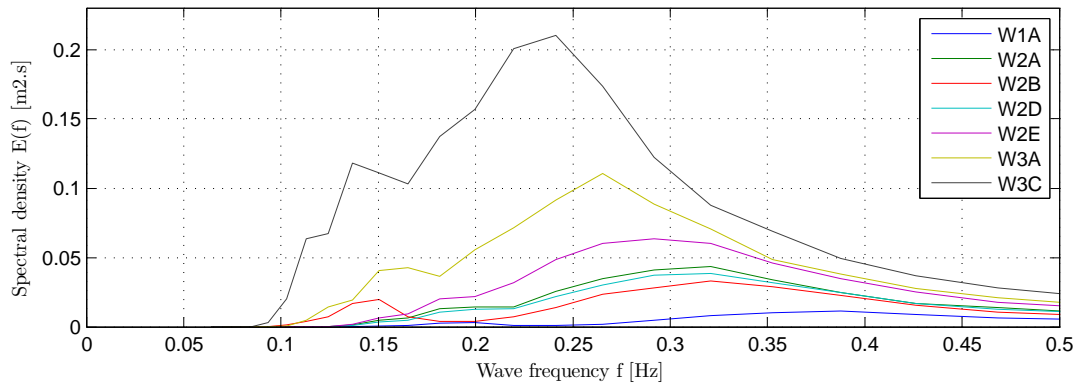


Figure 4.6: The variance density spectra plotted against the wave frequency in the case of wind waves at location CT2.

First, any observed effects are discussed to be able to better understand the results. This way it is also easier to verify whether the output is physically plausible and correct. Then the calculated wave- height and period are presented followed by the wave spectrum indicating what happens with the wave energy and how this energy is distributed over the frequency. This gives a good picture of the local wave climate.

4.5.1. OBSERVED EFFECTS FROM CALCULATION RESULTS

The previous section showed the importance of wind in the model. Plotting additional parameters like the peak wave- period and direction help identifying any occurring effects. At first glance Figure 4.4 shows a reduced significant wave height on the south side of the island. This is caused by the shadow effect which occurs because of the island blocking the waves. This is also visible in Figure 4.5. It shows the sharp transition of the peak wave period from deep water waves to the locally generated wind-waves. From the same plot it is clear that the waves bend around the island. This is shown more clearly in Figure 4.4 where the wave angle increases from 80° to approximately 160°.

4.5.2. WAVE- HEIGHT & PERIOD

After running all the scenarios, the calculated significant wave heights and peak periods are placed in two tables. Table 4.8 shows the output results for the case of wind sea waves. The same table for swell waves can be found in Appendix D.2. The difference between the local wave results and the initial deep water wave parameters is of importance. From both tables it can be observed what happens with a boundary wave of a particular scenario that propagates to location CT2. In all scenarios, the significant wave height of the wind waves decreases. The local peak period does not show large mutual differences but does decrease in comparison with the boundary waves. The values at the local output location do not differ very much mutually, despite the larger differences at deep water.

Table 4.8: Difference between imposed boundary wind waves and the waves at the project location CT2.

#	Wind sea waves								
	Input			CT2			Δ		
	H_s [m]	T_p [s]	θ [°]	H_s [m]	T_p [s]	θ [°]	H_s [m]	T_p [s]	θ [°]
W1A	0.60	5.2	80.0	0.62	5.2	76.8	+0.00	+0.0	-3.2
W2A	1.20	5.2	80.0	0.61	3.2	129.3	-0.59	-2.0	+49.3
W2B	1.20	6.9	80.0	0.56	3.1	127.4	-0.64	-3.8	+47.4
W2D	1.20	5.2	70.0	0.59	3.2	127.3	-0.61	-2.0	+57.3
W2E	1.20	5.2	90.0	0.71	3.5	133.3	-0.49	-1.7	+43.3
W3A	1.80	6.3	80.0	0.84	3.7	130.1	-0.94	-2.6	+50.1
W3C	2.70	6.9	80.0	1.20	4.4	132.0	-1.50	-2.5	+52.0

SHADOW EFFECT

Both Figure 4.4 and 4.5 show lower values on the southern side of the island. Clearly a shadow effect is visible because of the island blocking direct propagation of waves. Waves do reach the southern shores of the island, but are remarkably smaller and shorter due to a.o. diffraction and dissipation. The sharp edge of the peak wave period in Figure 4.5 is explained by the fact that at a certain point the amount of locally generated wind wave energy becomes larger than the original boundary wave energy. The period of these locally generated wind waves is in the order of 2 - 4 seconds, visualised as a blue shadow in this figure.

The process of reaching this sudden change in peak wave period goes very smooth: the original amount of boundary wave energy decreases while propagating, especially when waves extend beyond the islands of Curaçao. There the wave energy starts to diffract, which results in a further decrease of wave energy. As the original boundary waves propagate further there comes a point where the locally generated wave energy becomes larger. This is shown by a clear edge in this figure.

If a plot would be made of the mean wave period, there would not show such a clear edge, because the mean wave period shifts smoothly along the path of the propagating waves.

WAVE ANGLE

The waves bend around the islands tip because of diffraction and refraction. This leads to changes in the original wave direction and spreading of wave energy. When the deep water waves approach the shore, the wave crests turn towards the depth contours as it starts to 'feel' the sea bottom. At the output location there is only little difference between the local wave angles: for the case of the wind sea waves the mutual difference is limited to approx. 5°. The first scenario shows an angle of 76.8°, which is explained by the fact that for this scenario the locally generated wave energy is already higher than the wave energy from the original boundary waves.

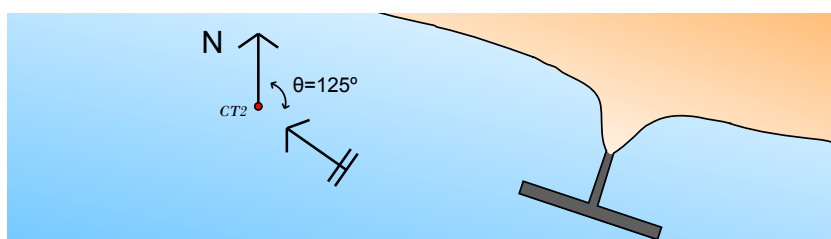


Figure 4.7: The dominant wave angle at CT2 is considered to be 125° relative to the North.

The calculated wave angles for wind waves lie between the 127° and 133° , except for scenario *W1A*. In the case of swell waves, the incoming wave angles lie between the 112° and 127° . The dominant incoming wave direction at location *CT2* is estimated by an angle of 125° relative to the North.

4.5.3. LOCAL WAVE ENERGY: VARIANCE DENSITY SPECTRA

Besides the significant wave- height, period and direction, use is also made of the variance density spectrum. This parameter shows how the variance of the sea-surface is distributed over the wave period, rewritten in terms of wave frequency.

A graph with a very flat and horizontal line means that waves with all kinds of periods occur about an equal amount of time. When there is a peak in a wave spectrum graph, this means that waves with a particular wave frequency occur more often. The wave energy distribution for both swell and wind wave scenarios are determined, as this is necessary to model the dynamics of floating structures. Figure 4.8 shows this spectral density distribution for the scenarios with swell waves. The one for wind waves, other resulting plots and further details can be found in Appendix D.2.

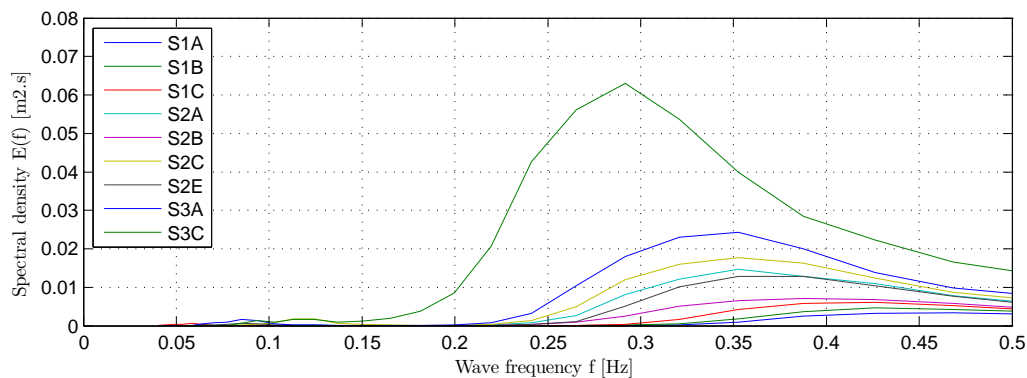


Figure 4.8: Wave spectrum of swell waves at location *CT2*.

As can be seen from Figure 4.8 there are two peaks in the wave spectra of all scenarios: between the frequencies 0.05 Hz and 0.1 Hz and between the frequencies 0.25 Hz and 0.45 Hz. This first frequency band originates from the boundary swell waves, while the second frequency band belongs to wind waves. Immediately visible is the large difference in wave energy between these two types of waves: Swell wave energy is hardly present at *CT2* in comparison with the amount of wind wave energy.

4.5.4. INFLUENCE OF OUTPUT LOCATION ON CALCULATED LOCAL WAVE CLIMATE

The output location used in the SWAN-model, *CT2*, is chosen because its location benefits from the nearby Megapier Cruise Terminal. The facilities can be shared and integrated into one large terminal area. But perhaps a slightly shifted project location leads to much more ideal hydraulic conditions. To check this, the sensitivity of the output location on the wave parameters is investigated. A low sensitivity will result in little variance in the wave parameter values. The sensitivity of the following parameters is checked: H_s , T_p , θ_{wave} . Looking at Figure 4.3, the yellow shaded cell is *CT2*. The cell to the right or East is checked. The wave parameter values of the cell North-West of the yellow shaded cell is also checked. For an overview and comparison of the values, see Table 4.9.

Table 4.9: Wave parameter sensitivity for three different wave data output locations. The water depth at each location is indicated with d in metres.

Output Location	d [m]	H_s [m]	T_p [s]	θ_w [$^\circ$]
<i>CT2</i>	42.3	0.6	3.2	139
North-West of <i>CT2</i>	8.4	0.4	3.2	129
East of <i>CT2</i>	40.8	0.6	3.2	130

From the table above can be concluded that the maximum difference in significant wave height is 0.2 m. The peak wave period remains the same for all output locations. There is a small difference in the wave angle at each location. This however, will not influence the decision, because the orientation of the terminal can be

changed accordingly when certain orientation angles pose limitations on the operability of the terminal. This is further discussed in §6.3.2.

From this table it can be concluded that a change of the output location to another location nearby does not significantly influence the wave conditions. A lower water depth in the order of tens of metres reduces the significant wave height in the order of tenths of metres. A different output location would not lead to significantly different wave parameter output values.

4.6. CONCLUSION

The goal of this chapter is to determine the near shore wave climate at the port of Willemstad. With the use of SWAN results this wave climate is estimated at location *CT2*, defined in §4.3.1 and visualised in Figure 4.1 and 4.3. From the output results the following conclusions are drawn:

- There is a large shadow zone on the southern shore of Curaçao. Waves coming from between the North and East diffract at the eastern tip of the island. This reduces the amount of wave energy that reaches location *CT2*;
- The longer swell waves generated far away are hardly present any more compared to the amount of local wind wave energy;
- Results from all scenario models do not vary considerable. The models show that variations in wave direction and peak wave period of the boundary waves lead to small mutual differences at location *CT2*. The different scenarios that show little variance are merged together, to reduce the amount of required runs for the hydrodynamic study;
- From all the SWAN results, it can be seen that the incoming wave direction at *CT2* varies between 112.7° (Scenario *S2A*) and 132° (Scenario *W3C*). A dominant wave direction of 125° is assumed for the hydrodynamic analysis.

The scenarios for both wind sea waves and swell waves that hardly differ in output from each other are merged into one scenario. Table 4.10 shows the resulting scenarios and parameters, which are used for the study on the dynamic response of a floating terminal in Chapter 7.

Table 4.10: Overview of the Scenarios that will be used to determine the dynamic behaviour of a floating cruise terminal at *CT2*. The wave parameters are the calculated results from the SWAN models. These values will be used as boundary conditions in the AQWA models.

Wind sea waves							Swell waves						
#	H_s [m]	T_p [s]	σ_θ [°]	u_{10} [m/s]	θ_{wind} [°]	P_r [%]	#	H_s [m]	T_p [s]	σ_θ [°]	u_{10} [m/s]	θ_{wind} [°]	P_r [%]
W2B	0.6	3.1	30	7.4	80	26.4	S1C	0.3	16.0	15	5.6	70	58.6
W3A	0.8	3.7	30	9.5	80	4.2	S2E	0.4	2.6	15	6.6	70	13.6
W3C	1.2	4.4	30	11.7	80	0.1	S3A	0.5	2.8	15	7.5	70	1.4
							S3C	0.7	3.5	15	9.2	70	0.1

The Figures 4.8 and 4.6 present the calculated variance energy spectra at the project output location. They confirm what is concluded above in the second and third bullet and therefore support the choice to merge scenarios with similar and hardly different wave parameters.

FLOATING STRUCTURES IN GENERAL

Before going into detail about the floating concept and the modelling of the dynamic behaviour, an introduction on floating structures itself is given first. This chapter treats multiple aspects on this topic, including basic theory on the hydrodynamics of floating structures.

Floating structures may be defined as structures destined to float on water where the full weight of the structure is supported by the force of buoyancy. Within this definition a wide range of structures exist as of today: From jetties, piers and pontoons to breakwaters and complete oil rigs. They can be found in ports, along coasts or even on deep sea for a wide range of vessels. The importance of floating structures increases with the increasing amount of restrictions from environmental conditions: Expansion of harbours is often troublesome because of little space ashore. Coastal expansions often face large water depths making bottom founded structures very costly. These are just examples of reasons why a such a structure is not an option.

General advantages and disadvantages for floating structures are treated in §5.1. This is followed up with an elaboration on a number of different types and structures that float in §5.2. Section 5.3 explains important definitions and gives a brief elaboration on motion limits and hydrodynamics in irregular waves. This information is essential to understand the various steps carried out in the hydrodynamic assessment in Chapter 7.

5.1. ADVANTAGES AND DISADVANTAGES

Floating structures sound like the perfect solution for any harbour or city wanting to increase the amount of usable area. These kind of solutions still have their own advantages and disadvantages in comparison with fixed structures. These largely depend on the conditions at the location of interest and on the application of the structure. General advantages and disadvantages of floating structures in comparison with fixed structures are listed below.

5.1.1. ADVANTAGES

General advantages for floating structures are:

- The ability to move and replace it making it possible to design it for less extreme conditions;
- the possibility to integrate multiple functions. For example: the floating breakwater in Monaco [W11];
- tidal changes are followed by the structure, as with (berthed) vessels, especially advantageous for large tidal variations;
- the less destructive impact for the environment, like bottom habitat or disturbance to water circulation;
- for increasing water depths there is a turning point where floating structures become more economic attractive in comparison with fixed-pier constructions.

5.1.2. DISADVANTAGES

The following list presents general disadvantages for structures that float:

- Susceptible to wave and wind action. Especially at waves with a frequency close to the natural frequency of the floating structure;
- higher maintenance and operation costs;
- difficulties in shore access as there is in general a horizontal and vertical distance to be crossed;
- requires additional, possibly extensive, mooring structures to keep it on its place.

5.2. STRUCTURE TYPES AND APPLICATIONS

There are many types of floating structures in use around the world with a wide range of applications. Each application has its own set of functional requirements with respect to the type of floating structure. Basic hull configurations and applications for floating structures are described in this section. It is not the intention to

compose a complete list of variants. As part of the introduction on floating structures, only the most common structure types are discussed.

In general there are three types of hull configurations used for floating structures. These three basic types are as listed in Table 5.1.

Table 5.1: Overview of three basic hull types and their main properties. Parts of this overview are obtained from the following source: [7].

Basic Hull Types	Schematic illustration [13]
Single Pontoon	
Multi-Pontoon / Catamaran	
Semi-Submersible	

5.3. DYNAMICS AND MOTION LIMITS

5.3.1. DEFINITIONS

The analysis on the dynamic behaviour of a floating structures is carried out in a right handed axis system (x, y, z) . At the centre of gravity (CoG) a floating body has six degrees of freedom consisting of and defined as:

- Three translations in the x -, y -, z -direction:

$$\text{Surge in the longitudinal } x\text{-direction [m]: } x_f = x_a \cos(\omega t + \epsilon_{x\zeta}) \quad (5.1)$$

$$\text{Sway in the lateral } y\text{-direction [m]: } y_f = y_a \cos(\omega t + \epsilon_{y\zeta}) \quad (5.2)$$

$$\text{Heave in the vertical } z\text{-direction [m]: } z_f = z_a \cos(\omega t + \epsilon_{z\zeta}) \quad (5.3)$$

- Three rotations about these axes:

$$\text{Roll about the } x\text{-axis [°]: } \phi_f = \phi_a \cos(\omega t + \epsilon_{\phi\zeta}) \quad (5.4)$$

$$\text{Pitch about the } y\text{-axis [°]: } \theta_f = \theta_a \cos(\omega t + \epsilon_{\theta\zeta}) \quad (5.5)$$

$$\text{Yaw about the } z\text{-axis [°]: } \psi_f = \psi_a \cos(\omega t + \epsilon_{\psi\zeta}) \quad (5.6)$$

In which:

ϕ_f, θ_f, ψ_f	=	rotation of floating structure about the x -, y - or z -axis [°]
x_a, y_a, z_a	=	displacement of floating structure in the x -, y - or z -direction [m]
ϕ_f, θ_f, ψ_f	=	Amplitude of the rotation about the x -, y - or z -axis [°]
x_a, y_a, z_a	=	Amplitude of the translation in the x -, y - or z -direction [m]
ϵ	=	Phase angle [rad]
ω	=	Circular wave frequency [rad/s]

The definitions of these motions are visualised in Figure 5.1. These motions are induced by wave forces acting on floating structures.

5.3.2. DYNAMICS IN IRREGULAR WAVES

The dynamics of floating structures in irregular waves are calculated in this study in the frequency domain. This means that the motion response is a function of the frequency or period of incoming waves and therefore independent of time. The response in irregular waves is determined with the following steps:

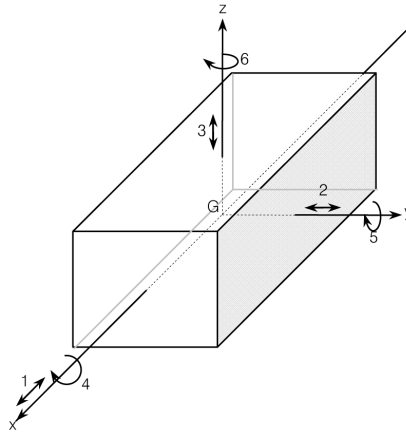


Figure 5.1: Definition of motions for a floating structure in six degrees of freedom. Source: [14].

- Determine the *Wave Spectrum*. This depends on the location at sea, the amount of exposure to deep sea waves and wind. This step is done in Chapter 4;
- Determine the *Response Amplitude Operator*. This depends a.o. on the main particulars of the floating structure. This will be discussed in Chapter 7;
- With these previous two parameters, the response spectrum of a motion (surge, heave etc.) can be found. These results are presented in §7.5.4;
- From these response spectra it is possible to calculate RMS-values for displacements and accelerations in the directions of interest. These RMS-values are then compared to motion criteria. This downtime assessment is carried out in Chapter 8.

A small theoretical elaboration on these steps is given below in the same order as in the list. These items are also visualised in Figure 5.2 to help understand these steps. In this figure the Variance Density Spectrum is indicated with $S_{\xi}(\omega)$, the transfer function as $\frac{z_a}{\xi_a}$ and the resulting Wave Spectrum as $S_z(\omega)$.

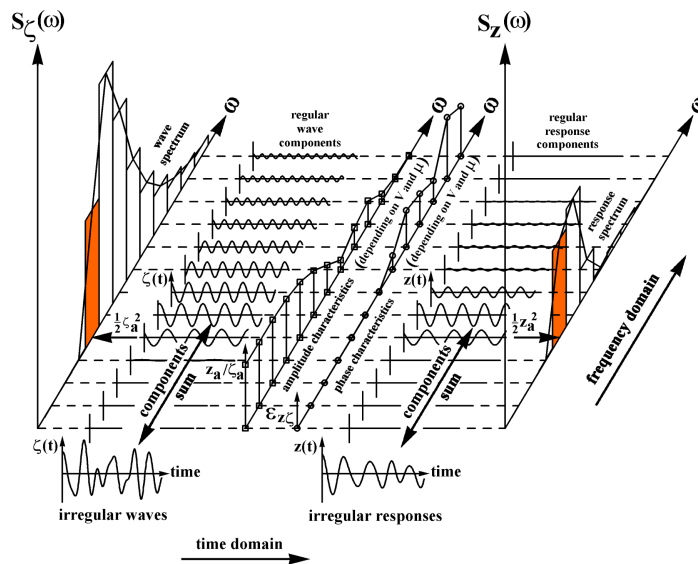


Figure 5.2: The principle of transforming a wave spectrum into a response spectrum for the heave motion. Source: [15].

AXIS TRANSFORMATION OF VARIANCE DENSITY SPECTRUM

This parameter has been introduced in §4.5.3. As previously mentioned, the variance density spectrum describes the variance of the surface elevation of water distributed over the wave period. Any irregular wave history is in fact the sum of a large number of regular wave components. These regular wave components have their own amplitude, frequency and phase shift acting with their own harmonic forcing on floating structures. From

this irregular wave history the wave energy spectrum can be deduced in the following way, which is further discussed in Appendix A.2.2:

$$S_{\zeta}(f_n)\Delta f = \frac{1}{2}\zeta_{a_n}^2(f) \quad (5.7)$$

This discretization is also visible in Figure 5.2 with the orange highlighted areas and the corresponding regular wave components.

The local wave climate has been determined in Chapter 4 with the use of SWAN. The SWAN model saves the calculated wave spectrum on specified locations. For this study the output parameters and dimensions are set to variance densities E [m^2/Hz] and absolute frequencies [Hz]. In the field of Hydromechanics the frequency is more often expressed on the ω -basis [rad/sec]. The spectral values of $E(\omega)$ and $E(f)$ are not equal and therefore have to be transformed. The relations between the two frequencies and spectra are:

$$\omega = 2\pi \cdot f \quad (5.8)$$

$$S_{\zeta}(\omega) = \frac{S_{\zeta}(f)}{2\pi} \quad (5.9)$$

The Figures 5.4 and 5.3 show an example of this transformation. The graph on the left shows the wave spectrum as a function of frequency in Herz. The Herz-based output data are transformed to values based on ω using Equations 5.8 and 5.9.

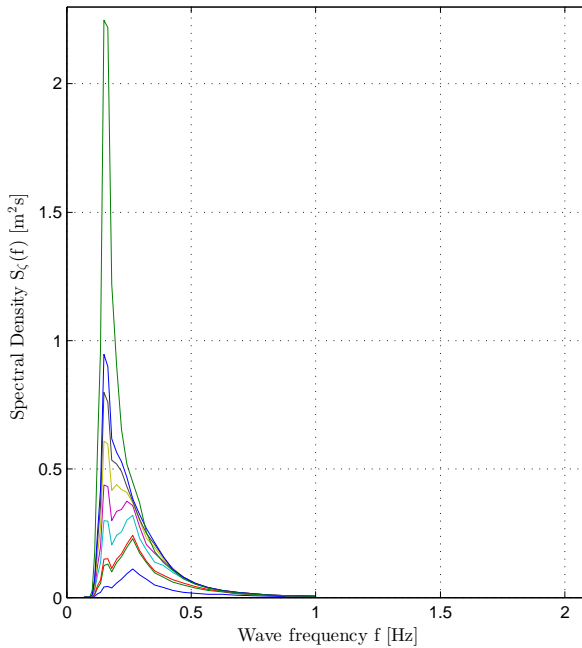


Figure 5.3: Variance density spectra plotted as a function of frequency in Hertz.

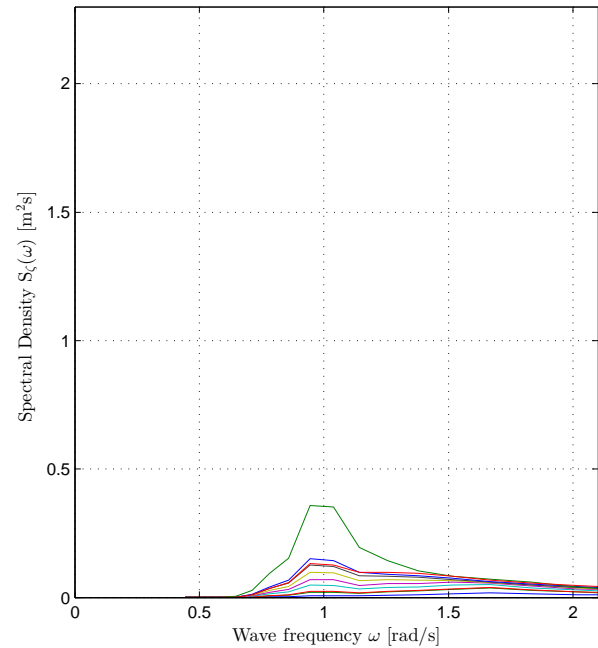


Figure 5.4: Variance density spectra plotted as a function of frequency in ω .

FREQUENCY CHARACTERISTICS OF FLOATING STRUCTURES: RESPONSE AMPLITUDE OPERATOR

The transfer function, also referred to as Response Amplitude Operator (RAO) of a floating structure needs to be determined as part of the hydrodynamic analysis. The RAO shows the frequency dependent influence of waves on the motion behaviour of floating structures and is defined as followed in the case of heave motions:

$$\text{RAO: } \hat{R}_z(\omega) = \left| \frac{z_a}{\zeta_a}(\omega) \right| \quad [-] \quad (5.10)$$

$$\text{Velocity RAO: } \hat{R}_{\dot{z}}(\omega) = \left| \frac{z_a \omega}{\zeta_a}(\omega) \right| \quad [1/s] \quad (5.11)$$

$$\text{Acceleration RAO: } \hat{R}_{\ddot{z}}(\omega) = \left| \frac{z_a \omega^2}{\zeta_a}(\omega) \right| \quad [1/s^2] \quad (5.12)$$

In which:

$$\begin{aligned} z_a &= \text{Heave amplitude} && [\text{m}] \\ \zeta_a &= \text{Wave amplitude} && [\text{m}] \end{aligned}$$

RESPONSE SPECTRA

Combining a local wave spectrum and the transfer function of a floating structure, yields the Response Spectrum (S_r) for a motion of a floating structure in this particular wave climate:

$$\text{Response Spectrum: } S_{r,z}(\omega) = |\hat{R}_z(\omega)|^2 \cdot S_\zeta(\omega) \quad [\text{m}^2/\text{s}] \quad (5.13)$$

$$\text{Velocity Response Spectrum: } S_{r,\dot{z}}(\omega) = |\hat{R}_{\dot{z}}(\omega)|^2 \cdot S_\zeta(\omega) \quad [\text{m}^2/\text{s}] \quad (5.14)$$

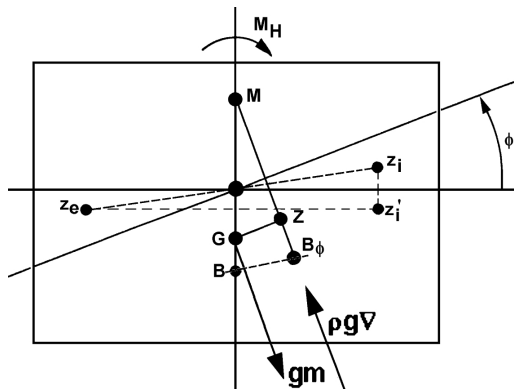
$$\text{Acceleration Response Spectrum: } S_{r,\ddot{z}}(\omega) = |\hat{R}_{\ddot{z}}(\omega)|^2 \cdot S_\zeta(\omega) \quad [\text{m}^2/\text{s}^3] \quad (5.15)$$

The principle of this transformation is visualised in Figure 5.2.

5.3.3. STABILITY OF FLOATING STRUCTURES

A floating structure moves and rotates under the influence of waves and wind action. The sensitivity for motions depends on the location of the *metacentre* (M) and the radius of gyration. Rotations result in a shift of the *Centre of Buoyancy* (CoB), which in extreme cases might result in capsizing of the entire structure. Obviously this effect should be avoided at all cost. To prevent this, the metacentre should be well above the *Centre of Gravity* (CoG). The location of M is determined with the rotational equilibrium between a stationary situation ($\phi_f = 0^\circ$) and at a small angle of heel.

Figure 5.5 shows the trigonometry of static stability of a floating barge. The metacentric height \overline{GM} in this figure is described by Equation 5.16.



$$\overline{GM}_t = \overline{KB} + \overline{BM} - \overline{KG} \quad (5.16)$$

Figure 5.5: Rectangle barge stability, showing the equilibrium at an angle of heel ϕ_f .

In which:

$$\begin{aligned} \overline{GM} &= \text{Metacentric height} && [\text{m}] \\ \overline{KB} &= \text{Distance between the bottom of the structure to the } CoB && [\text{m}] \\ \overline{BM} &= \text{Distance between the } CoG \text{ and the metacentre } M && [\text{m}] \\ M_H &= \text{Restoring heeling moment about the principal axes per degree of rotation} && [\text{Nm}] \end{aligned}$$

The goal in defining stability is to determine a value for \overline{GM} (Distance between CoG and M), where the structure is not tender (low value for \overline{GM}), but neither is overly stiff (high value for \overline{GM}). The latter results in high angular accelerations in wave conditions with a wave period close to the eigenperiod of the structure. As these values for \overline{GM} depend on the dimensions of the structure, they will be given together with the details on the main particulars in §6.2.2.

5.3.4. MOTION AND SAFETY LIMITS FOR SHIPS

For this study the focus lies on motion responses. The design requirements used in this study have been presented in §3.5.3. If the floating structure moves or accelerates much, cruise tourists will eventually have a hard time standing without any support. PIANC has determined motion criteria to help determine suitable mooring alignments and lay-outs. Table 5.2 shows the criteria as defined by PIANC for ferries. Because ferries also handle passengers, these criteria may also apply on embarking and disembarking from cruise ships.

Chapter 3 introduced the existence of motion criteria determined by PIANC and Nordforsk. The PIANC criteria define recommended maximum displacements to guarantee safe conditions. Horizontal and vertical displacements are of importance because of the use of a ramp. This ramp is often only able to cope with limited displacements. These criteria are not necessarily important for the safety cruise passengers, but limit the operability of ferries during (un)loading.

As stated before, Nordforsk [8] also determined motion criteria with respect to the human effectiveness under the influence of movements. The criteria are in this case not describing displacements, but accelerations. High accelerations might people cause to fall, which is totally undesired in the case of realising a floating cruise terminal. The criteria can be found in Table 3.2.

Table 5.2: Recommended motion criteria for safe working conditions according to PIANC [9]. These criteria will not be used in the determination of downtime because of wave loads. It is important to keep in mind that these criteria exist to guarantee safe working conditions.

Ship Type #	Cargo Handling	Surge [m]	Sway [m]	Heave [m]	Yaw [m]
Ferries, Ro-Ro	Side ramp	0.60	0.60	0.60	1.00
	Dew/storm ramp	0.80	0.60	0.80	1.00
	Linkspan	0.10	0.60	0.80	3.00
	Rail ramp	0.10	0.10	0.40	-

GENERAL DESIGN CONSIDERATIONS

6.1. INTRODUCTION

With the use of the described general design requirements in Chapter 3, the initial idea of a floating terminal will in this section be made more concrete. This will be done by giving a general description of the floating terminal in §6.2. Chapter 4 presented the output location for the SWAN-model. This was a rather large area. The exact location for the new terminal will be presented in §6.3. This section will also discuss the considerations on the alignment of the berth. After these general specifications on the concept, the studied models are presented in §6.2.2. For this study three variants are defined to investigate the relations between structural parameters and the motion dynamics i.e. the resulting downtime. After this chapter these variants will be modelled in the next chapter with the software Ansys AQWA.

6.2. GENERAL DESCRIPTION AND CHARACTERISTICS

The conceptual idea of Witteveen + Bos is a floating terminal near the shore of the southern coast of Curaçao. The floating aspect is suggested because of the steep ocean bed floor past the 5 metres water depth contour line. The idea is that this concept could save cost compared with a bottom-founded permanent structure further from the shore than the current Mega Pier Cruise Terminal.

6.2.1. STRUCTURAL DESCRIPTION

The floating structure studied is a hollow concrete prism. Concrete is chosen as material as it is a dense material what helps to keep motion responses low for shorter wind waves, but makes it more sensitive to longer waves. Accelerations will remain lower with this type of structure than with lighter prism structures. Although semi-submerged structures remain relatively motionless compared to barge-type hulls with the same displacement, their lower deck load capacity is considered as a disadvantage because of the large number of passengers and loads from the cruise ship itself and the ramp construction to the shore.

The main particulars of the floating structure will vary for each variant and therefore will be presented in next. The freeboard height of all variants will be kept the same: 2.5 m.

6.2.2. MAIN PARTICULARS OF TWO STRUCTURAL VARIANTS

The two variants differ in their dimensions. Of interest in this study is in particular what the influence of these dimensions is on the dynamic response of the floating structure at location *CT2*. These models are based on the Figure 6.5, but further simplified. These simplifications and additional details are treated in §7.2. This section describes the set-up of the structural models in an AWQA model. The following list presents the variants and the used naming. This list is presented in a graphical way in Figure 6.3.

- Model A: 30x30 m Pontoon;
- Model B: 80x30 m Pontoon;
- Model C: Design cruise ship, free floating next to Model A and Model B.
 - Model C+A: Combination of Model C and Model A with a distance of 2 meters
 - Model C+B: Combination of Model C and Model B with a distance of 2 meters

The main particulars of these three models can be found in Table 6.1.

6.2.3. STATION KEEPING: ANCHORAGE

Station keeping of the floating terminal for both variants is realised by anchors and catenaries. The schematic layout of the anchorage is presented in Figure 6.1. The properties of the anchors and catenaries can be found in Table 6.2. The small angle stability parameters for both variants are presented in Table 6.1.

Table 6.1: Main particulars of the two floating terminal structures and cruise ship.

	Length	Width	Height	Draught	Mass	Water Displacement	Mass Moment of Inertia
	L_f	W_f	D_h	D_d	m_f	V_w	I_{xx}
	[m]	[m]	[m]	[m]	[t]	[m ³]	[t · m ²]
Model A	30	30	5	2.53	2.334	$2.3 \cdot 10^3$	265021
Model B	80	30	5	2.50	6.150	$6 \cdot 10^3$	3421486
Model C	362	47	81	9.2	100.000	$97.5 \cdot 10^3$	$19.8 \cdot 10^6$

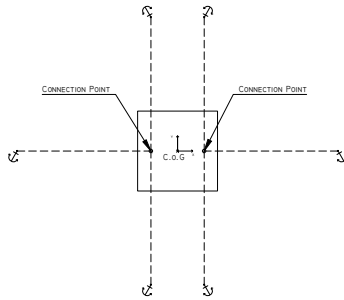


Figure 6.1: Schematic anchorage layout for both variants (0° alignment angle).

Table 6.2: Properties of the modelled catenaries.

Mass per metre	A_{eq}	EA	T_{max}	l_c
[t/m]	[m ²]	[kN]	[kN]	[m]
0.15	0.01	$9 \cdot 10^5$	750	55

6.2.4. HYDROSTATIC PROPERTIES

As described in §5.3.3 the sensitivity to motions is influenced by the hydrostatic properties of a floating structure. These properties have been determined for both structural variants and can be found in Table 6.3.

As stated before, it is important that the metacentric height is large enough for static stability.

Table 6.3: Small angle stability parameters of Models A and B

	\overline{BG}	Transverse Direction			Longitudinal Direction		
		\overline{GM}	\overline{BM}	M_H	\overline{GM}	\overline{BM}	M_H
Model A	1.25	28.75	30.0	$1.13 \cdot 10^7$	28.75		$1.13 \cdot 10^7$
Model B	1.25	28.75	30.0	$3.03 \cdot 10^7$	212.09	213.34	$2.23 \cdot 10^8$

In which:

$$\overline{BG} = \text{Distance between } CoG \text{ and } CoB \quad [m]$$

6.3. TERMINAL LOCATION AND ALIGNMENT

The local wave climate has been determined for a specific grid cell in the SWAN model. Deviations in the water depth in the order of several metres do not significantly influence the local wave climate. Still, an exact location needs to be specified for the new floating cruise terminal. At this exact location the values of a.o. the water depth and distance to the shoreline can be determined. This section presents also the berth arrangement for cruise ships and the considerations regarding the alignment of the terminal and berth.

6.3.1. LOCATION OF THE FLOATING TERMINAL

The location of the floating terminal has already been roughly indicated in §4.3.3. This indication depended on the computational grid and availability of grid data, in order to determine an as accurate as possible estimation of the local wave climate. The coordinates of this location are the grid point at 12.1025°N; -68.945°E. Recall Figure 4.3. The water depth at this location is 42.3 m according to the GEBCO'08 data set and between 67 m and 136 m according to the nautical chart.

This indicated area will not be the location of the new terminal because of the very large water depth and

the long distance to the shore. The location is chosen closer to the shore, West of the current Megapier Cruise terminal. This choice seems obvious because of the already existing facilities for cruise tourists. The area can be easily expanded with all necessary extra facilities and an extension of the boulevard. Figure 6.2 shows the chosen location for the floating cruise terminal CT2.

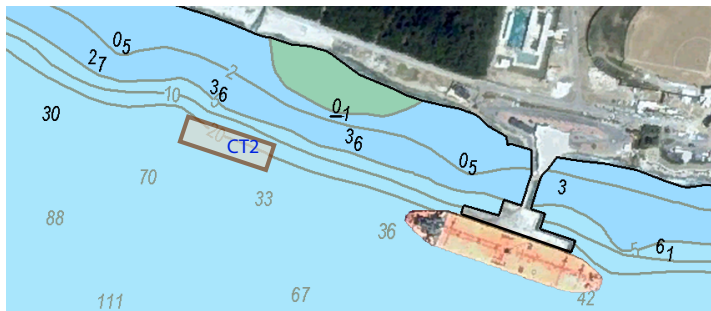


Figure 6.2: Indication of the project location CT2. The rounded off coordinates of this location are: 12.1025°N ; -68.945°E . Satellite image source: [F4]. Source of nautical chart: [S1]

The floating structure will be moored within the indicated box. As the variants differ in dimensions, the figure only shows an indication of the used area. The terminal will be placed just on the 20 m contour line. This is chosen to guarantee sufficient underkeel clearance because of the possible displacement of the floating structure due to slack on the anchor lines and external horizontal loads. The distance from the current shore line to the floating structure is about 114 metres, but because of the previously mentioned possible displacement, variations in the order of metres should be taken into account.

6.3.2. BERTH ARRANGEMENT AND ALIGNMENT

The initial intention is to align the new cruise terminal parallel to the shore, just like the current Megapier. To determine the influence of the orientation angle of the terminal on the dynamic response and downtime, three alignment angles are studied. The alignment angles are defined relative to the dominant wave angle as indicated in Figure 4.7. A 0° -alignment angle corresponds to an angle of 125° relative to the North. The additional incoming wave angles that are studied are 45° and 90° . An overview of the studied alignment angles and the corresponding wave directions is presented in Figure 6.3.

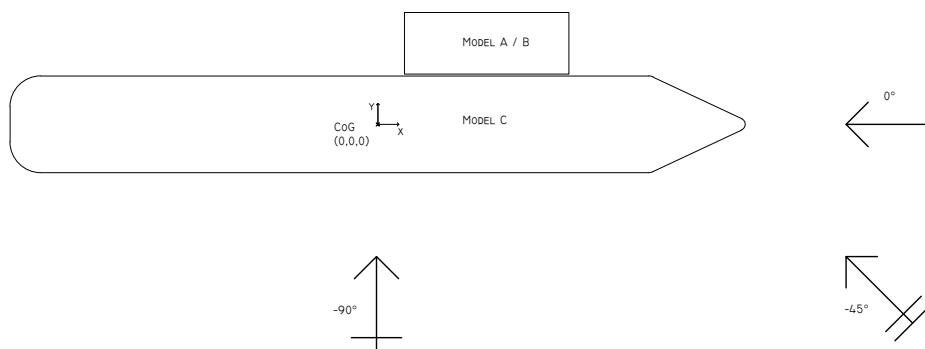


Figure 6.3: The three studied wave directions are shown relative to the floating terminal. The values of the angles are indicated in correspondence with the local coordinate system, which is shown at the centre of gravity.

The results from the study on the dynamic response in Chapter 7 will determine what the most ideal orientation for the floating cruise terminal will be. Recommendations on the ideal alignment follow from this hydrodynamic assessment.

The terminal layout and berth arrangement for the case parallel to the shoreline are sketched in the Figures 6.5 and 6.5. The sketches indicate the position and layout of the pier, ramp, anchors and buoys.

6.3.3. CONNECTION TO THE SHORE

The following solution is just a suggestion, as the design of this connection falls out of the scope of this study. It's influence and feasibility requires additional research. For the connection to shore, a solution must be chosen such, that the transport capacity of passengers is high enough to keep waiting times and queues while

(dis)embarking low.

A ramp should bridge the distance between the floating structure and a piled pier. The fixed pier reduces the bridged distance by the boarding ramp. To reduce the loads on the floating terminal from the ramp and to provide support for the ramp covering the 16 m span it may be interesting to apply semi-submerged floaters underneath the ramp. Motions of the ramp should be limited to keep passengers safe and within their comfort-zone while crossing the ramp. These floats are therefore placed well under the waterline to prevent excessive motion dynamics. In this way the ramp itself remains relatively insensitive for wave loads.

The floaters are not meant to support the full weight of the ramp. By employing fixed adjusting towers on the fixed pier the ramp can be lifted free from the floating structure. This makes it possible to move the terminal to sheltered areas under severe weather conditions.

Slotted, energy-absorbing, sliding bearings are a structural solution for the shore connection to allow longitudinal movements due to motions of the floating structure or vessel impact. Going further into the structural details of this ramp falls out of the scope of this study. To take the ramp into account, a static load will be added to the dynamic model of the floating structure. This is not realistic but the influence will be assumed to be negligible for this study. This assumption requires additional research on the actual influence of the boarding ramp.

6.3.4. STATION KEEPING OF THE FLOATING COMPONENTS

A station keeping system is required to keep both the floating terminal and the vessels at their position. Both components are described separately below. Horizontal displacements of the *cruise ship - cruise terminal* combination have to remain limited because of the limited capability of the shore connection between the pier and floating terminal to follow these displacements. Horizontal displacements towards the shore because of wind or wave loads also affect the minimal under keel clearance which is taken into account in the mooring system layout. These displacements will not be quantified in this study, but still is an important point of concern in the detailed design. The assumption is made that the horizontal displacements can be kept within reasonable limits, by paying sufficient attention in the design of the mooring system of both the floating terminal and the cruise ship.

As indicated in Chapter 3, Witteveen + Bos is interested in a station keeping system for the floating terminal concept which is economically interesting at larger water depths as can be found in exposed areas. This study focusses on the application of anchors and catenaries. Other station keeping systems are not considered in this study.

COMPONENT: FLOATING TERMINAL

The floating cruise terminal will be kept in place by means of catenaries and weighted concrete blocks placed on the ocean bed. To limit horizontal displacements, anchors are placed in both longitudinal and lateral direction of the floating structure. The station keeping system will not be designed to withstand the complete load of the cruise ship. The cruise ship will be moored with it's own station keeping system, which is discussed next.

COMPONENT: CRUISE SHIP

Because of larger water depths, not all systems are economically very attractive. A system with fixed mooring dolphins on a shallow contour line, as is the case with the current Megapier, is not possible. When a vessel uses mooring dolphins to moor against the floating terminal and tension is applied on the mooring lines, the ship is pulled towards them. This means that the ship will be pulled towards shallow water. The floating structure is anchored with catenaries and therefore not able to completely prevent this displacement without catenaries becoming fully tensioned. This increases peak loads on the whole anchor system and therefore is not ideal.

For this study anchor blocks and catenaries are also applied for the mooring of the cruise ship. Proposed are to the ocean bed floor secured weighted anchors. The dimensions and details on these anchors fall out of the scope of this study. The mooring forces follow from the dynamic analysis and these are needed for further design. The lay-out of the anchors i.e. the mooring configuration for each variant are presented in §6.2.2.

The design requirements stated that the station keeping system should be detachable from the cruise terminal in order to move it into the St Anna Bay when severe weather conditions are predicted. This is something that needs to be taken into account in the detailed design of the anchorage and floating structure.

6.3.5. PLAN VIEW IMPRESSION AND CROSS SECTION SKETCH

Details and descriptions mentioned in this section are summarised and visualised in Figure 6.4. This plan view impression shows the situation for Model A that is further described in §6.2.2.

From these figures it can be seen that approximately half of the distance between the terminal and the shore is very shallow water. Realising a permanent structure over this distance will not be very costly because of the limited water depth. The deeper part of the pier can then be realised by a piled structure. Both figures do not include a high level of detail on the pier and boarding ramp as this falls out of the scope of this study.

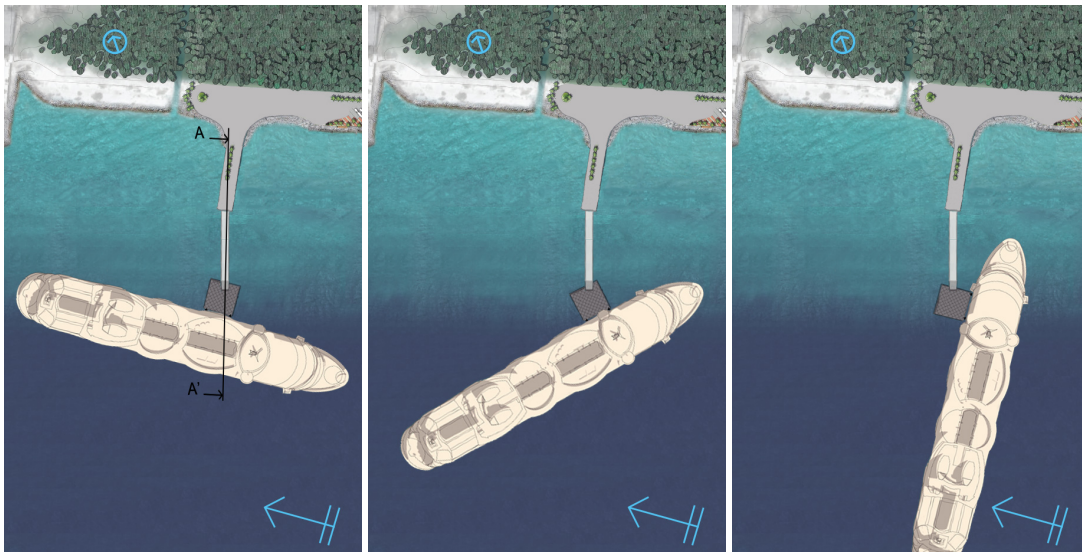


Figure 6.4

CROSS SECTION A-A': BASIC SKETCH OF BERTH ARRANGEMENT AND LAY-OUT

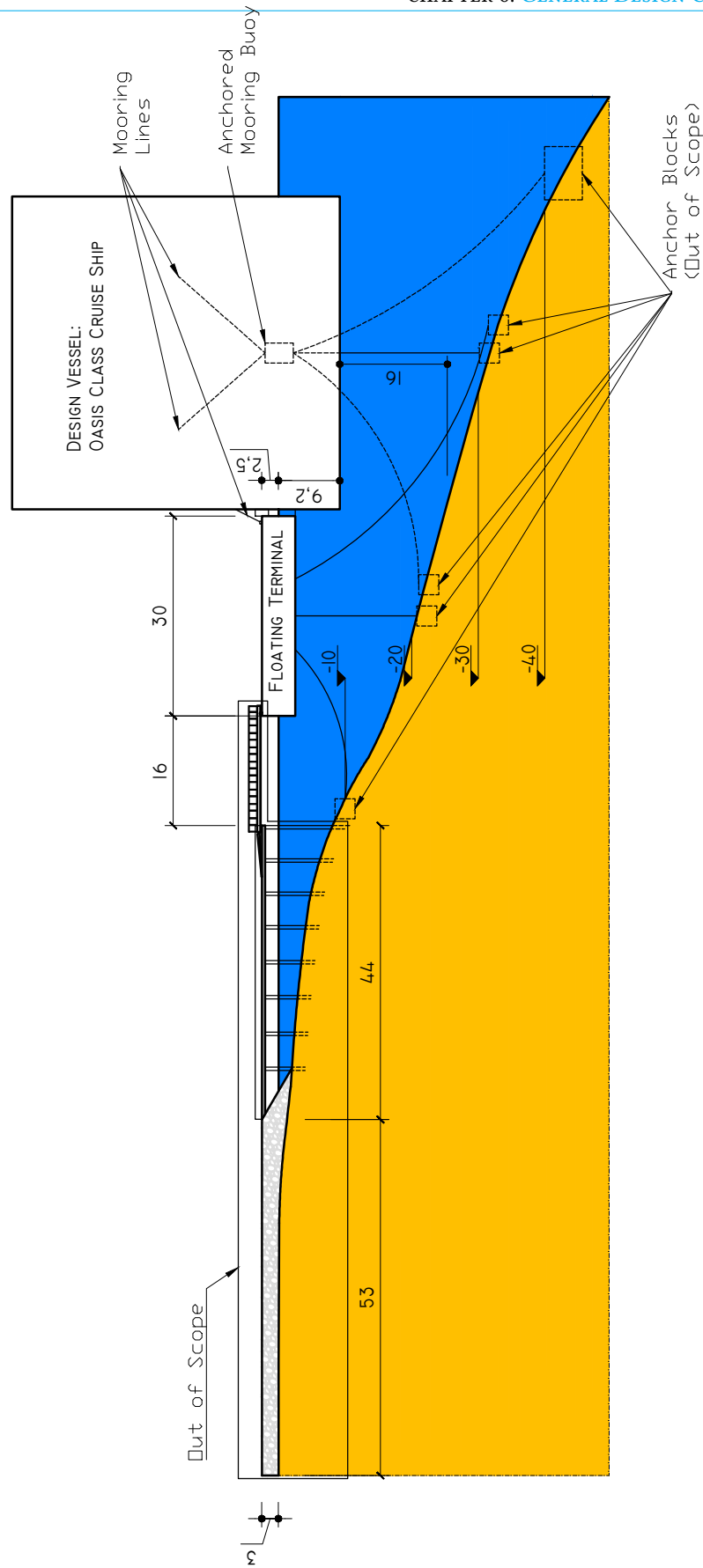


Figure 6.5: Cross sectional sketch of cruise terminal location CT2 with an alignment angle of 0° relative to the dominant wave angle, including anchorage and pier.

HYDRODYNAMIC ASSESSMENT OF VARIANTS

7.1. APPROACH

A hydrodynamic assessment is carried out with the software product Ansys AQWA. A brief introduction to this software product is given in §7.2, together with its limitations. The goal of this hydrodynamic assessment is to answer a number of research questions:

- Two structural variants are studied to determine the influence of dimensions on the motion response;
- Runs with the previously defined wave scenarios provide insight on their influence on the motion responses;
- Three incoming angles of these wave scenarios are studied to determine the ideal alignment angle, which leads to the lowest amount of motion responses;
- A rough model of the *Oasis of the Seas* is created to determine the influence of its presence on the motion response of the terminal.

The hydrodynamic analysis starts by preparing and setting up a model system, presented in §7.3. Details on the actual simulations are presented in §7.4. Section 7.5 presents the various results. The data is interpreted and discussed. Verification of the results is done by means of an analytical approximation of hydrostatic and hydrodynamic properties of both structural variants. This is briefly treated in §7.4.3. The full calculations can be found in Appendix E.

The output data obtained from the simulations are plotted in graphs for all scenarios and models. The plots are then used to determine the area under the different spectral curves ($= m_0$) which is required to determine the RMS of motions in five directions, described in §3.5.3.

Conclusions that can be drawn from the obtained results will intend to answer the relevant research questions of this study in §7.7.

7.2. THE ANSYS AQWA MODEL

7.2.1. PROGRAMS IN THE ANSYS AQWA SUITE

The ANSYS AQWA Suite is a set of programs that are able to address the majority of tasks associated with hydrodynamic assessments of floating structures. The description of the AQWA Suite is based on the reference manual and contains the following programs [16]:

AQWA-LINE	3-D diffraction & radiation analysis program for regular harmonic wave environments, which creates a hydrodynamic data base, which contains full details of the fluid loads acting on a body.
AQWA-LIBRIUM	Structure equilibrium position and force balance calculations for moored or freely floating bodies. It determines the eigen modes and dynamic stability properties.
AQWA-FER	Used to analyse the coupled or uncoupled responses of bodies in irregular wave environments in the frequency domain.
AQWA-NAUT	Program to simulate real-time motions of a body in either regular or irregular wave environments.
AQWA-DRIFT	Real-time simulation of motions of a body in irregular waves where low period oscillatory drift motions can be considered.

This study is carried out in the frequency domain, so only the top three programs of the AQWA Suite are used for this hydrodynamic assessment.

7.2.2. LIMITATIONS AND NOT CONSIDERED EFFECTS

The following simplifications or limitations affect the output results. These should be taken into consideration when interpreting the output results of AQWA. Also the not considered effects form a drawback on the accuracy of output results. Attention should be paid on these aspects, as their influence is not necessary negligible.

- AQWA-FER contains the option to define a user-defined wave spectrum. The program is able to accept only 20 entries in such a user-defined wave spectrum, therefore limiting the frequency band that can be taken into account in the simulation. This study focusses on boundary waves with the frequency band between 0.3 rad/s and 2.1 rad/s with $\Delta f = 0.1$;
- Wind force Coefficients have not been taken into account in the determination of the motion dynamics;
- As stated in §3.5.1, tides and currents have not been taken into account. Current/ drag force coefficients are therefore not taken into account, although there are limited current speeds actually present near shore;
- The ocean bed floor is modelled as horizontal. This also means that the anchors on the shallower side are also placed lower, with longer catenaries. It is assumed that these simplifications do not significantly influence the dynamic response as the water depth is still 15+m at the shallower side of the floating structure;
- Ansys AQWA is only able to create a limited amount of meshes for a structure: at most 12000 diffracting elements can be created, which leads to inaccuracy for large and/ or curved structures.

Additional study should try to include these effects and circumvent the mentioned limitations.

7.3. SET-UP OF HYDRODYNAMIC ANALYSIS SYSTEM

This section briefly presents the different steps undertaken to set up a hydrodynamic analysis in Ansys AQWA. More detailed information about these steps can be found in Appendix F.

7.3.1. GEOMETRIC MODELS OF THE VARIANTS

Models are created of the variants presented in Chapter 6. The Tables 6.1 and 6.3 provide the values that are used to define the geometry of these variants.

The suit AQWA contains its own geometry modeller called DesignModeler. It is also possible to create the model with third party software and to import the model file in AQWA. Either way, the geometry of each variant is grouped by a structure label, which groups all parts, elements and properties together. Two important aspects are part of the geometry: the definition of connection points and the point mass. They are both treated briefly below.

The software requires that the model is split at the water line into two bodies to be able to form non-diffracting (above water) elements and diffracting (below water) elements.

CONNECTION POINTS

An anchorage is required for station keeping. Modelling this anchorage is split up into two parts: connection points and connections. The actual connections are treated in §7.3.2. More detailed information regarding this topic can be found in Appendix F.2.2.

Connection points are allocated at the sea bed and on the structure. Such a point on the sea bed is a fixed point defined in global space. A connection point on a structure is allocated to a node of the structure and defined as either a fixed connection or as a winch. Figure 7.1 shows the modelled anchorage for the 30x30m-variant (Model A), including the coordinates of all connection points of the floating structure. The models in this study don't make use of winches but of fixed attachment points.

For this study, the fixed connection points on the sea bed are all defined 50 m from the connection points of the floating structure. Further research and detailed design should be considered to optimise this mooring configuration.

POINT MASS

A point mass element is included in each structure. This is important for the hydrostatic and hydrodynamic analysis, as the mass distribution and radii of gyration have a large influence on the motion response of the floating structure.

For both variants of floating terminals, the point mass element is inserted at the CoG , which is located at the local origin of the geometric bodies:

$$\begin{bmatrix} x \\ y \\ z \end{bmatrix}_{A, \text{ point mass}} = \begin{bmatrix} x \\ y \\ z \end{bmatrix}_{B, \text{ point mass}} = \begin{bmatrix} 0 \\ 0 \\ 0 \end{bmatrix} \quad (7.1)$$

7.3.2. ANCHORAGE AND CONNECTIONS

The floating terminal is kept in place by means of anchor blocks and catenaries. The anchors are modelled as a fixed points on the sea bed with coordinates in global space. They do not move with any structure. The locations and coordinates of the anchor points can be found in Figure 7.1.

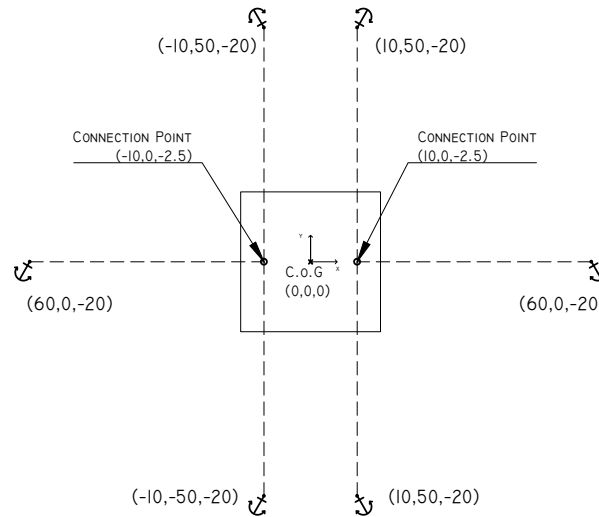


Figure 7.1: Schematic anchorage as defined in AQWA for Model A, indicating the locations of anchors and connection points.

The floating structure is connected with the anchor blocks with catenaries. In AQWA, these are modelled as non-linear catenaries. AQWA is able to model catenaries with up to ten different sections. For this study, the whole catenary exists just out of one section.

Numerous properties need to be assigned to the catenary section, including the catenary length, maximum tension etcetera. An overview of all parameters and values can be found in Appendix F.2.2. An analytical approximation of the restoring force coefficients of this anchor system can be found in Appendix E.5.

7.3.3. MESH

AQWA is able to automatically generate a mesh on bodies in the model. The density is based on the defeaturing tolerance and maximum element size parameters. The maximum element size is explicitly related to the maximum allowed wave frequency.

It is important to realise that a larger maximum element leads to less accurate results. However, an important limitation of AWQA is the support of at most 12000 diffracting elements. This restricts the ability to use very small meshes and to accurately model large and/ or curved structures.

As stated in §7.3.1 it is necessary to explicitly define the submerged part of the geometry. The application of a mesh on the submerged part of floating terminal Model A is shown in Figure 7.2. The parameters and properties that are used to create the meshes can be found in Table 7.1.

Table 7.1: Mesh details of the different models

		Model A	Model B	Cruise ship Model C
Number of Nodes	-	705	1677	9077
Number of Elements	-	660	1596	8830
Max Element Size	m	2.33	2.33	2.33
Max Allowed Frequency	rad/s	2.1	2.1	2.1

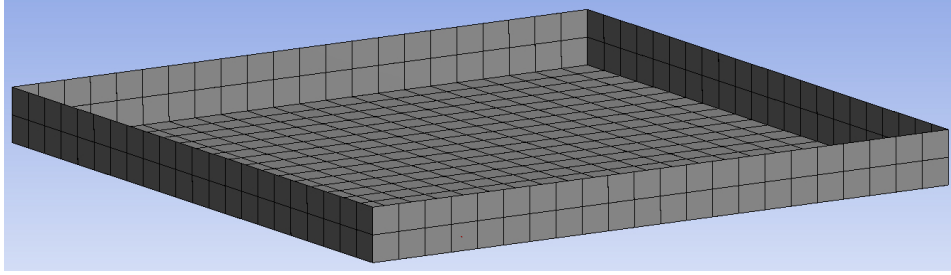


Figure 7.2: Mesh of the submerged part of Model A: the 30x30m pontoon.

7.3.4. MODEL DOMAIN AND OCEAN ENVIRONMENT

Defining the model domain and ocean environment is done by going through a number of steps. These steps are treated below.

GRAVITY

The gravitational acceleration has already been defined in §4.3.4. Its value is kept the same for this hydrodynamic assessment. The same holds for the density of water. The defined values for these parameters can be found in Table 4.2.

WAVE DIRECTIONS

It is possible to define and use a range of wave directions in the analysis. The 0° and 180° are automatically analysed. Additional intervals or intermediate directions can be specified. A defined wave spectrum will then be simulated for all defined wave directions.

Wave directions of interest that are analysed in AQWA Line are⁴: 0° , 45° and 90° .

A radiation/diffraction analysis is performed for these wave angles. This is an obligatory step in order to perform additional post-processing in the other AQWA programs. Subsequently, these wave directions are individually analysed in AQWA-LIBRIUM (static and dynamic stability analysis) and AQWA-FER (wave frequency motions).

WAVE FREQUENCIES

It is possible to define a wave frequency range to use in the analysis. This is done by defining a lowest and highest frequency. Intermediate values are added with an interval of $\Delta\omega$.

Table 7.2: Defined frequency range and interval

	Lower Limit	Interval	Upper limit
	ω_{min}	$\Delta\omega$	ω_{max}
Frequency rad/s	0.1	0.1	2.1

As with the previous section, these are the frequencies that are considered in the radiation/diffraction analysis performed in AQWA-LINE.

CURRENTS

Currents can be modelled in AQWA, but as indicated in §3.5.1 currents are not taken into account in this study. For further information on the implementation of currents in AQWA, reference is made to the AQWA Reference Manual [16].

IRREGULAR WAVE

Ansys AQWA provides the possibility to input a user-defined wave spectrum. This is used for input of non-deterministic data, which is the case for the acquired SWAN wave spectra for the different wave scenarios. This user-defined spectrum is limited to one dimension. Multiple user-defined spectra can be defined as long as the maximum number of total frequency entries of 25 has not been exceeded. For this study, only one user-defined spectrum has been defined, with the maximum amount of frequency entries.

The direction of the spectrum can be defined for this spectrum. The studied wave directions are presented in the corresponding paragraph of this section.

⁴Additional directions have been analysed. This can be seen in the codes presented in §F.3, but these additional wave directions remain unused in this study.

WIND

Although wind is taken into account with the wave simulations in SWAN, this is not taken into account in the hydrodynamic analysis. The focus of this study lies on determining the influence of different wave scenarios. Although it is expected that the influence of wind on the hydrodynamic behaviour remains limited, it will most likely lead to higher loads on the anchorage of the pontoons.

Especially cruise ships will feel the effect of higher wind speeds. Wind can therefore not be neglected to determine the feasibility of this project. This needs to be taken into account in an additional study.

7.4. AQWA SIMULATIONS

The previous section elaborated on the set-up of the AQWA models. It also presented the parameters and values that are used to set-up and define the different models. With the set-up and initialisation finished, it is now possible to start simulating. Parameters are varied to determine their influence on the operability of the floating terminal. To help verify and put the output of simulations into perspective, an analytical approximation of the hydrostatic and hydrodynamic properties is carried out. This section summarises the carried out simulations.

The following parameters are determined from the executed simulations and calculations:

- Natural Frequencies
- Free Floating RAO's
- RAO's
- Horizontal and vertical acceleration response spectra
- Roll and pitch response spectra

7.4.1. SIGN CONVENTION & DATA EXTRACTION POINTS

The output values of all parameters are determined at specific nodes. Horizontal accelerations are extracted at the *CoG*, which is Node 0. The same goes for rotations. Vertical acceleration data is extracted from a node on a corner of the terminal. This location is chosen because of the larger accelerations that occur at the extends of a floating structure. Rotations for example, lead to vertical accelerations, which add up with the accelerations due to the vertical heave motion of the whole structure. Node 1 is located at the lower left corner of both structural models. This node is used for the extraction of vertical accelerations. This is visualised in Figure 7.3.

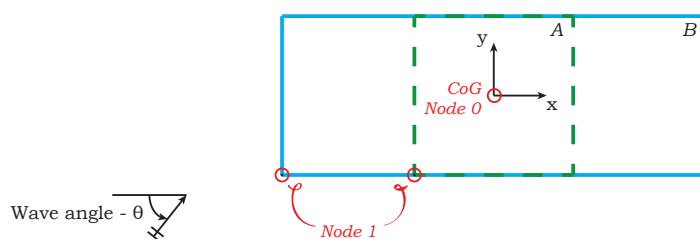


Figure 7.3: Top view of floating terminal A (green) and B (blue). Red circles indicate the location of the used nodes for extraction of the simulation results. Node 0 is used for the horizontal motions and rotations. The vertical acceleration results are extracted from node 1 on the lower left corner of both structures.

7.4.2. VARIED PARAMETERS

To be able to answer the sub questions of the main research question, it is necessary to vary more than one parameter. Simulations have been carried out with the following list of parameters that have been varied. Each varied parameter corresponds with one of the sub questions, which is indicated after the parameter within brackets.

Wave conditions: (<i>sub question 2</i>)	Incoming wave angle i.e. orientation of the terminal: (<i>sub question 3</i>)
<ul style="list-style-type: none"> - Wind wave scenarios; - Swell wave scenarios. 	<ul style="list-style-type: none"> - 0°; - 45°; - 90°.
Structural geometry: (<i>sub question 3</i>)	Operational situations: (<i>sub question 4</i>)
<ul style="list-style-type: none"> - Model A: 30x30 m; - Model B: 80x30 m. 	<ul style="list-style-type: none"> - unused situation: only the floating terminal; - used but unmoored situation: terminal and cruise ship side by side.

7.4.3. ANALYTICAL APPROXIMATION OF HYDROSTATIC AND HYDRODYNAMIC PROPERTIES

The hydrodynamic properties of both floating structures are approximated by means of basic calculations. These calculations are used to verify the results of the numerical AQWA models. Details on the derivations and calculations can be found in Appendix E.

When applicable, plots indicate the estimated natural frequencies (ω_N) of the floating structures with a vertical line. It is emphasized that the inaccuracy of these estimated natural frequencies can be as much as 10% of the calculated value.

7.5. AQWA RESULTS

The variation of the parameters presented above provides information on their influence on the hydrodynamic response. This influence is studied for five motions. Limiting criteria are defined for these motions and they are used to determine the downtime. These limiting motion criteria can be found in Appendix H. These five studied motions are:

- Accelerations in surge direction;
- Accelerations in sway direction;
- Accelerations in heave direction;
- Roll rotation;
- Pitch rotation.

The intermediate calculation results of parameters are presented to get a better understanding of the effect and influence of varying parameters. Much data is acquired from these simulations. To keep all this data comprehensible, calculation results are grouped together in plots, as much as possible in the next section.

7.5.1. NATURAL FREQUENCIES

With Ansys AQWA it is possible to calculate the natural frequencies in the six DOF. These values are compared with results from the hand calculations, as to verify the reliability of the AQWA results. Although the hand calculations have a margin of error of around 10%, they still can be used to check the simulations.

The AQWA results for the natural frequencies are presented in Table 7.3 and compared with the previously presented mathematically calculated values.

⁵The calculated natural frequency for yaw of Model B ($\omega_{55} = 1.53$) is highly inaccurate due to a limitation on the Brown& Root Vickers method to determine the added mass. A more realistic assumption is $\omega_{55} = 1.0$. This value is thus used in this table. More details can be found in §E.8.

Table 7.3: Presentation of the natural frequencies for the considered motions. These values are compared with the results of the analytical approximation.

	Model A				Model B			
	ω_n		Δ		ω_n		Δ	
	AQWA [rad/s]	Analytical [rad/s]	Δ_{abs} [rad/s]	Δ_{rel} [%]	AQWA [rad/s]	Analytical [rad/s]	Δ_{abs} [rad/s]	Δ_{rel} [%]
Surge	0.09	0.10	0.01	11	0.07	0.06	-0.01	-14
Sway	0.10	0.13	0.03	30	0.08	0.08	0.00	0
Heave	0.98	0.91	-0.07	-7	0.88	0.91	0.03	3
Roll	1.05	1.07	0.02	2	1.06	1.10	0.04	4
Yaw	1.05	1.07	0.02	2	0.95	1.00 ⁵	0.56	5

7.5.2. FREE FLOATING RAO'S

The first results that are presented consider Free Floating RAO of the structural models. This means that motion responses are determined for the situation that motions are not restricted by for example an anchorage system. Only the modelled structure is considered, which gives good insight in both the frequency dependant behaviour and the location of the undamped natural frequencies.

SIMULATION RESULTS

Free floating RAO's are presented for three displacements (x-, y-, and z-direction) in three separate plots. These plots are depicted in Figure 7.5. Each plot shows the results for solely the two variants of a floating terminal, Models A and B, subjected to incoming waves from three different angles.

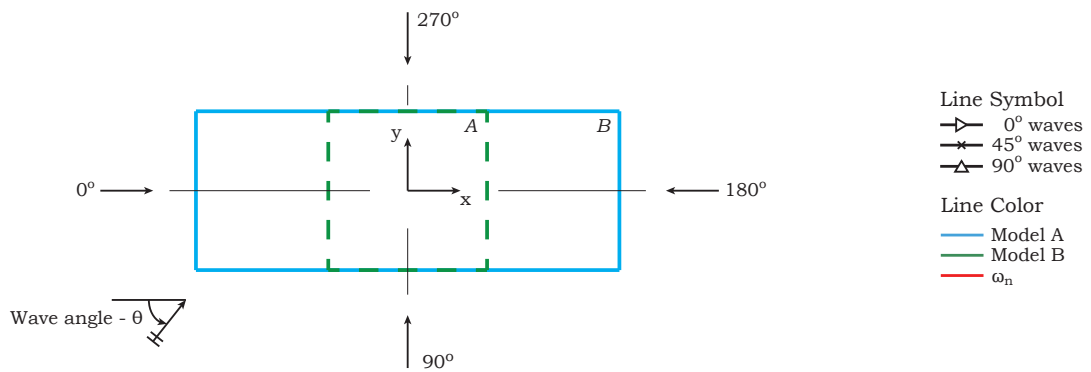


Figure 7.4: Top view of floating terminals A (green) and B (blue) including the applied sign convention.

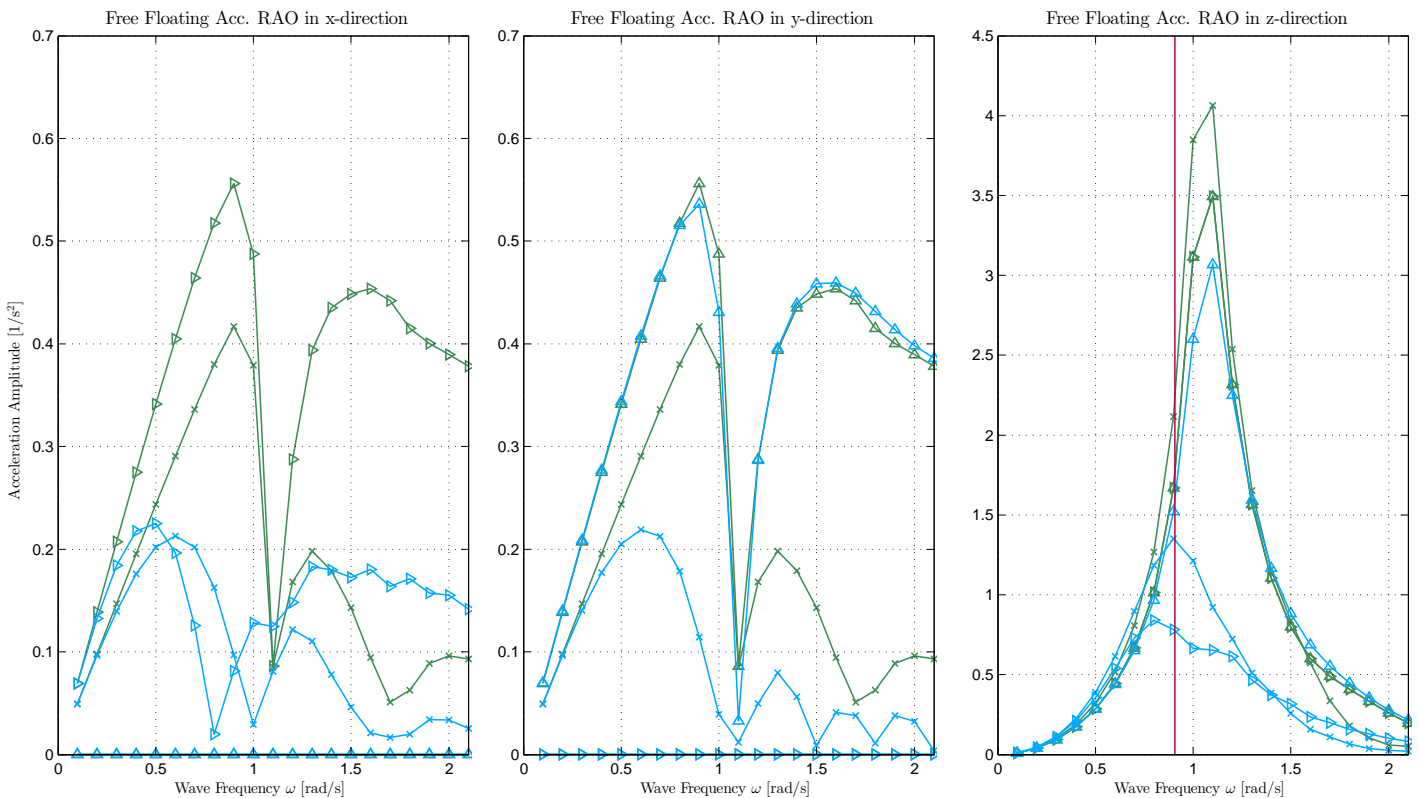


Figure 7.5: Free Floating Acceleration RAO's in x-direction (left), y-direction (middle) and z-direction (right) for the Models A and B. The simulated incoming waves have angles of 0°, 45° and 90°.

DISCUSSION

Looking at the three plots in Figure 7.5, it is possible to do some simple verifications. As this section considers free floating RAO's, it is important to understand the following.

For surge and sway:

- there is no natural frequency line plotted. Without any anchor system, there is no restoring spring term which prevents any floating structure from drifting away. Therefore, for horizontal displacements a natural frequency of a free floating structure is out of the question;
- there is no coupling between these two motions. A wave spectrum parallel with the x- or y-axis of the structure leads to no amplitude response in the direction perpendicular to the wave direction. The left and middle plots verify this for both structures;
- as Model A is symmetric, the amplitude response in both x- and y-direction should be identical, which can be confirmed;
- for a considered motion direction, the largest amplitudes occur for wave angles parallel to the considered motion direction.

For heave:

- there is a hydrostatic restoring spring term which leads to the existence of a natural frequency. The estimated values for both structures are indicated by vertical lines. In this case, the calculated values are identical, which results in only one line showing. The peak of the RAO's does lie on the vertical line for some directions, but not for all. This may be the result of the inaccuracy of the calculation method;
- again, due to the symmetry of structure A, the RAO has to be identical for wave directions parallel to the principal reference axes. From the simulation results it can be seen that this is the case.

7.5.3. RAO's

This section presents the response amplitude operators for different motions. An anchor system as previously described has been applied on the structural models, meaning that motions are now being restricted. This section now also includes simulation results of not only the modelled terminals, but also the design cruise ship. The cruise ship is modelled next to the terminal without any anchorage and with some space in between. This helps to determine the actual influence of a large cruise vessel on the motion response of the terminal models.

SIMULATION RESULTS

Again, an overview of the used sign convention is presented in Figure 7.6, including the location of the cruise vessel. The large length and depth of the cruise vessel will limit the amount of wave energy that directly reaches the cruise terminal behind the ship. Especially from the shorter waves much energy will be reflected by the cruise ship. The cruise vessel is not modelled as infinitely long, so waves coming from an angle of 45° and 135° will be able to travel past the cruise ship on both of the ends of the cruise vessel. Due to diffraction and reflection at these ends of the cruise vessel, it is possible for waves to reach the cruise terminal. These waves will have an additional influence and they will lead to a more sporadic RAO than the RAO's without the modelled cruise ship next to the terminal.

The processes and phenomena discussed here should be notable from the following plots of the RAO's. Locations of the natural frequencies are again visualised by vertical blue (Model A) and red (Model B) lines. If only one line appears in the following plots, then these two lines are on top of each other.

DISCUSSION

Like the previous section, it is possible to verify the simulation results by taking a closer look at Figure 7.7. This time the cruise terminal is anchored by an anchor system, which keeps the whole at its place. The following notes are taken into consideration for the verification of the simulation results:

For surge and sway:

- Unlike the free floating RAO's, the plots show calculated values for the natural frequencies of both structures. The mooring system has its natural frequency in the range of 60-70 seconds, which is a region with little wave energy. Resonance phenomena are therefore less likely to occur. The two natural frequencies are almost the same because the mass properties play a less significant role compared to mooring properties like catenary length and the catenary's specific weight;
- there is no coupling between these two motions. A wave spectrum parallel with the x- or y-axis of the structure leads to no amplitude response in the direction perpendicular to the wave direction. The plots on the left and middle verify this for the models without a cruise ship. The models C+A and C+B do show motion responses in this case. This is the result of diffraction and reflection phenomena at both of the ends of the cruise vessel. Because of these phenomena, it is possible that wave energy reaches the cruise terminal. This induces a motion response, despite of the wave spectrum direction being in line with the observed principal axis. Still, these motion responses remain very limited;
- as Model A is symmetric, the amplitude response in both x- and y direction should be identical for higher frequencies. The mooring stiffness is not identical, so the response in the low frequency domain will not be the completely the same: the location of the resonance peak is located at different frequencies. This symmetry is not the case for Model C+A because of the previously mentioned diffraction phenomena;
- For the models C+A and C+B, the largest motion responses occur for waves with the direction parallel to the x-axis. This is obvious because in this case the cruise ship does not act as an obstacle that protects the terminal from the incoming waves. Wave spectra with an angle of 45° and 90° show a significantly lower motion response in the y- and z-direction for both terminals, which is according to the expectations.

For heave:

- because Model A has a lower mass than Model B, Model A shows the largest accelerations in the vertical direction;
- the mooring configuration practically has no influence on the heave motion for wave directions parallel with the x- and y-direction, so the responses for model A show little difference in these cases. Model B does not show this symmetry because of the asymmetric shape. The largest motions occur as expected for waves perpendicular to the longitudinal axes of the terminal;

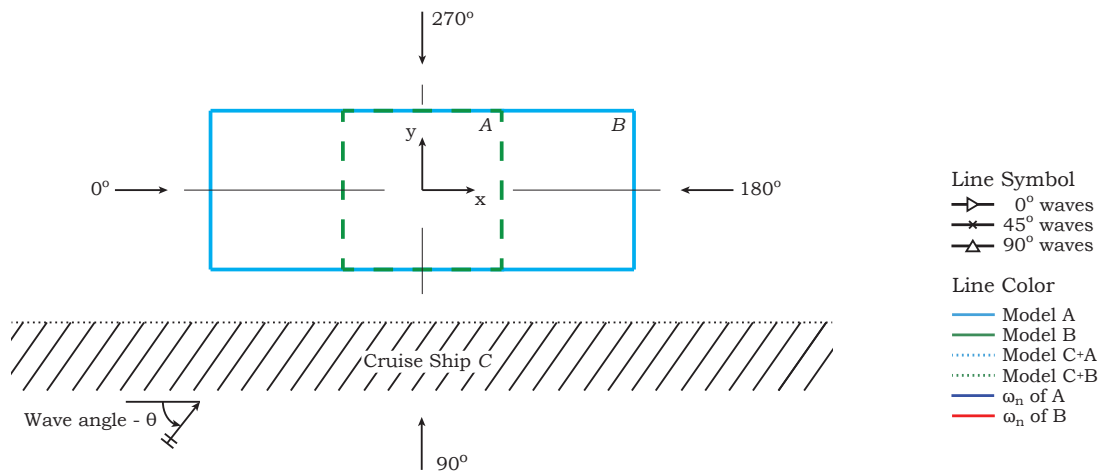


Figure 7.6: Top view of floating terminals A (green), B (blue) and cruise vessel shown together with the applied sign convention.

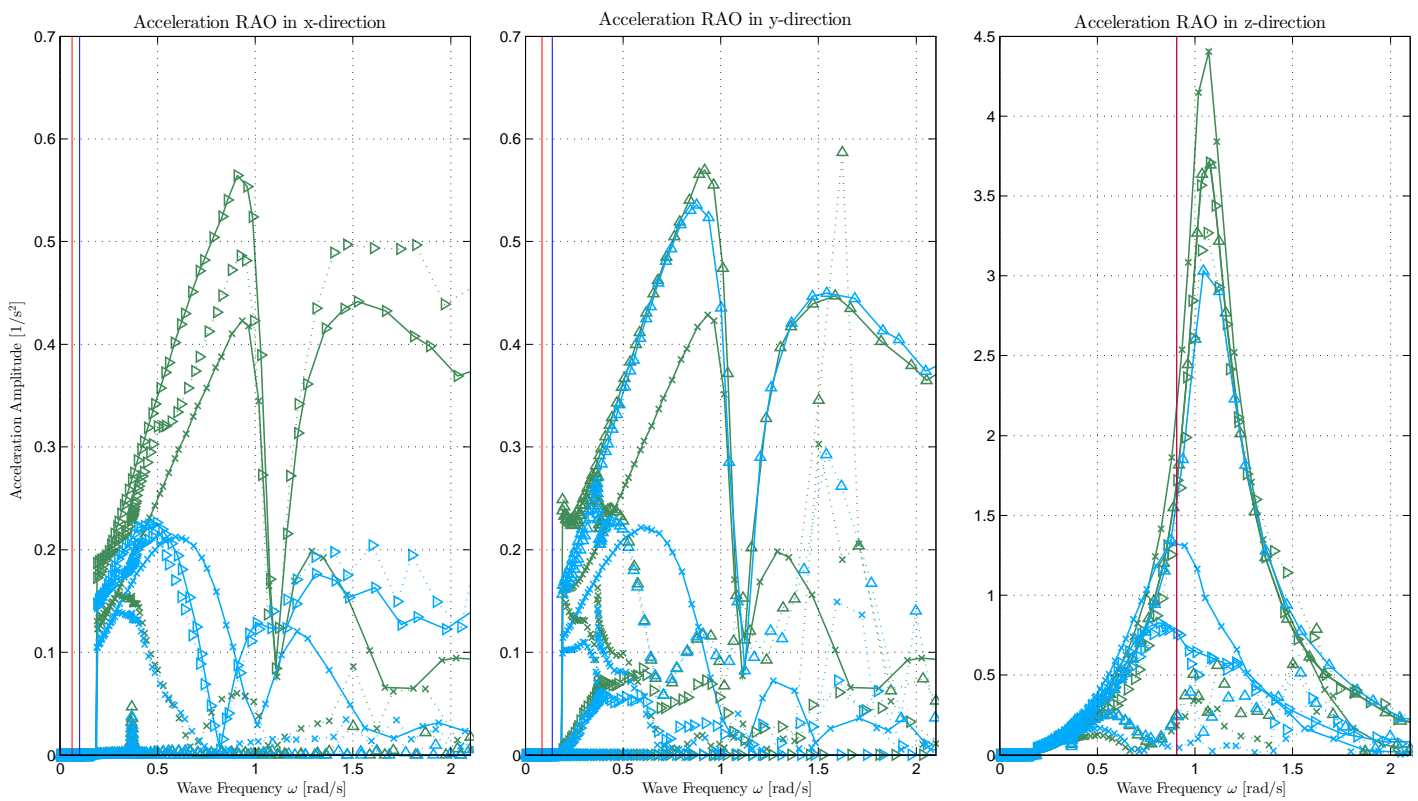


Figure 7.7: Acceleration RAO's in x-direction (left), y-direction (middle) and z-direction (right) for Models A, B, C + A and C + B. The simulated incoming waves have angles of 0°, 45° and 90°.

- In all cases, the scenarios including the cruise terminal show a lower response amplitude than the scenarios without the cruise ship. The ship functions as an obstacle for the 45° and 90° waves, which reduces the amount of energy reaching the cruise terminal. Still, not all energy from waves with an angle of 90° is reflected. Long waves are not reflected as much as short waves. For the longer waves this is visible around 0.5 rad/s. The higher frequencies show a much lower response amplitude for the vertical accelerations;
- for 0° waves the difference between model B and C+B is not as much compared with the other two wave directions. The cruise ship does not act as a real obstacle in this case. Still, the response is a bit lower due to reflective and dissipative processes when the incoming waves reach the cruise ship.

7.5.4. RESPONSE SPECTRA

This section presents and discusses only the calculated response spectra for Model *C+B*. The plots presented in this section are the result of the multiplication of the RAO's from the previous section with the wave energy spectrum of each wave scenario.

The observed motion of the response spectrum follows from the used RAO, i.e. the use of a RAO that describes the heave motion in the above equation results in a response spectrum for heave. The response spectrum of each motion is used to determine a statistical expression for the accelerations and displacements of the floating cruise terminals. This step is treated in §G.4.

Swell scenarios are indicated in four tones of green: the more wave energy the scenario contains, the darker the colour. The wind wave scenarios are indicated in three shades of red, with again the darkest shade for the worst scenario. Each plot of the response spectra in a specific direction therefore contains seven different colours. Additionally, each scenario consists of three wave direction calculations: 0°, 45° and 90°.

MODEL *C+B* SIMULATION RESULTS

The simulation results of Model *C+B* are presented together with the sign convention in Figure 7.8. The design cruise ship is placed parallel with the cruise terminal, in line with the x-axis. Waves coming from an angle of 45° and 90° are able to travel past the cruise ship. Diffraction and reflection phenomena lead to the spreading of energy, which means that even in the case of full reflection, it is possible that wave energy reaches the cruise terminal.

DISCUSSION

The discussion in this section is limited to conclusions that can be drawn from the plots presented in this section. The previous two sections already discussed and verified key aspects of the simulations. The results of the previous two sections are required to obtain the response spectra. Therefore, all the notes made in the previous sections still hold for the results presented in this section, but they will not be repeated here.

The discussion will be held in two parts: the first part considers the response spectra for displacements, followed by the response spectra for rotations. Each of these parts treats the different observed motions separately.

A summation of key aspects with regard to the displacement and rotation response spectra is given below. This summation starts with the motions surge and sway. Roll and pitch results are discussed subsequently.

Displacements - surge and sway:

- the largest acceleration response occurs in the y-direction, despite of the cruise ship acting as an obstacle. The high frequency at which these responses occur is most likely due to radiation forces induced by the cruise ship, which absorbs wave energy of the reflecting waves, which are in general the shorter wave frequencies;
- the wind wave scenarios lead in all cases to a higher amount of response. Even at the low frequencies, there is hardly any response visible from the longer swell waves. Swell waves therefore hardly influence the downtime of a floating terminal. This is not too strange, because swell waves do not lead to high accelerations, as the whole terminal has the tendency to follow the shape of the wave because of its large length;

Displacements - heave:

- the heave response remains fairly constant for all less extreme wave scenarios and wave directions. The most accelerations response occurs for the extreme wind wave scenarios along a broad frequency range. Especially the waves parallel to the x-axis lead to relatively large vertical accelerations;
- similar to the surge and sway motions, there is hardly any additional motion response in the lower frequency regions for the swell wave scenarios. The response that does occur is induced by the shorter waves created by the imposed wind in SWAN. The lower frequencies of swell waves therefore do not impose any restrictions on the operational time of the cruise terminal;
- although there is wave energy present around the natural frequencies of the floating structures in the wave scenarios, the response spectra do not show significantly larger responses around $\omega_{N,33}$. The influence of the heave natural frequency on the motion response for the different wave scenarios therefore does not lead to notably large responses compared to the wave frequencies which lie further away from the natural frequencies.

Rotations - roll and pitch:

- rotations in both directions remain fairly limited for all scenarios except for the more severe wind wave scenarios. As long as the wave height remains small, there would be hardly any angular response such that it would pose a limitation to the operability of the cruise terminal;
- the largest response for pitch occurs for waves which travel parallel to the x-axis. Similarly, the largest roll motions occur for the waves travelling parallel to the y-axis. In terms of absolute value, the largest response is found for the roll motion around its natural frequency. The lower width of the floating terminal is the reason why its response is larger than for pitch;
- values for swell wave scenarios do not come near to the values for response spectra of the wind wave scenarios. The presence of wave energy in the lower frequencies does not significantly contribute to the total response of both of the terminal models;
- full reflection is not the case for a broad band of the wave frequency. Still, diffraction phenomena and radiation forces coming from the motions of the cruise ship are able to impose roll and pitch motions, independently from the incoming wave angle.

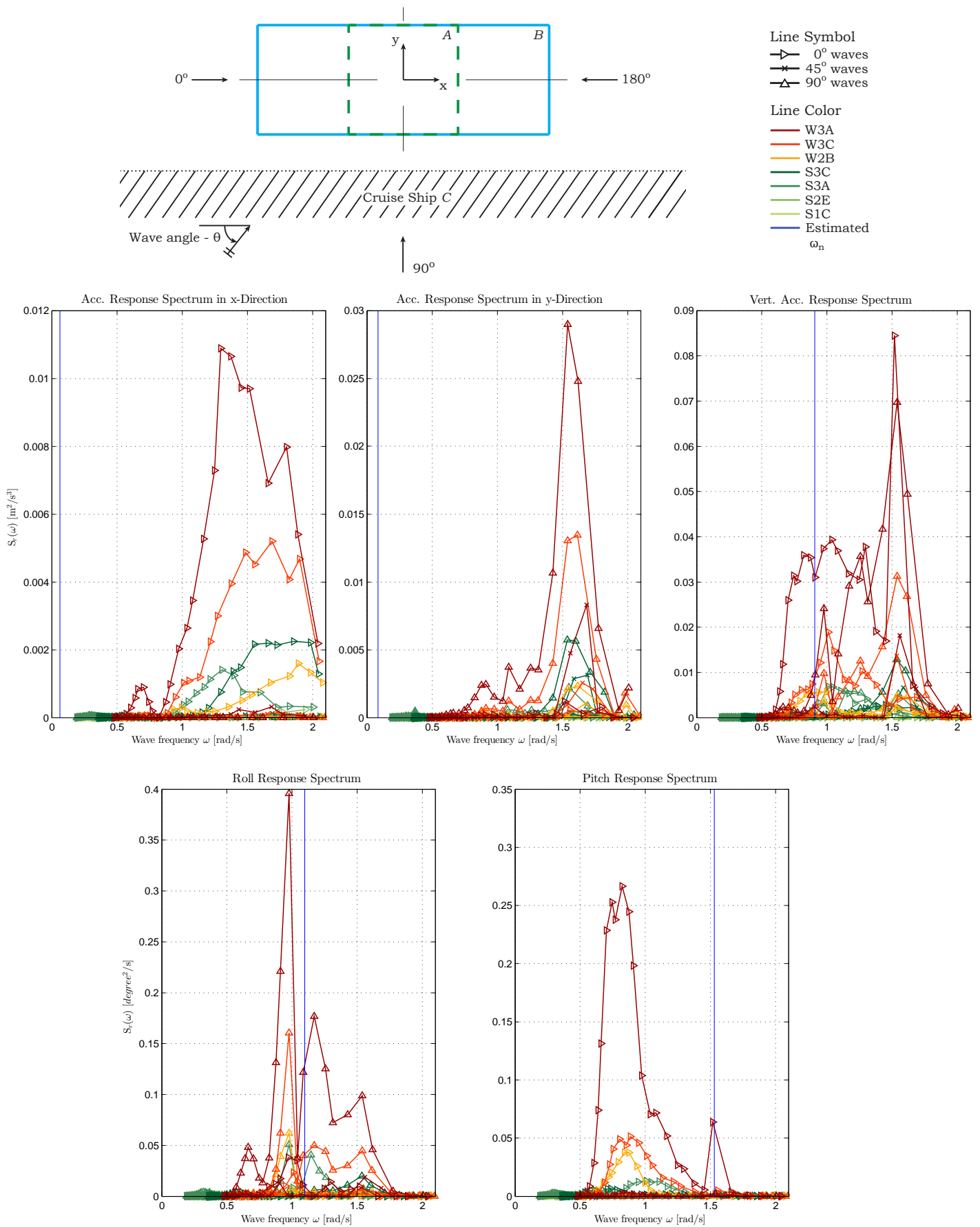


Figure 7.8: Acceleration Response spectra surge, sway and heave (top three plots) and response spectra for roll (lower left) and pitch(lower right) of model C+B for three different orientations.

7.5.5. ROOT MEAN SQUARED VALUES OF THE RESPONSE SPECTRA

The criteria as introduced by Nordforsk are defined as Root Mean Square (RMS) values. This section presents additional calculations. These calculations are carried out to end up with the same RMS parameter as the one of the Nordforsk criteria. This section begins with a brief description of the meaning of RMS and how it can be obtained. This is followed by the presentation of the calculation results in §7.5.5.

PARAMETER DESCRIPTION

The previous section presented the calculation method and the results of the response spectra of the floating terminals. Recapitulating, the response spectrum for, for example, heave ($S_z(\omega)$) is obtained by using the RAO for the heave motion (Z_a/ξ_a) and the wave spectrum $E_\xi(\omega)$. The next step that needs to be carried out is the determination of the RMS values. This is done as follows.

The calculation of a RMS value requires the zeroth moment of the response spectrum. The moments of, for example, the heave response spectrum are given by:

$$m_{n,33} = \int_0^{\infty} S_z(\omega) \cdot \omega^n \cdot d\omega \quad \text{with: } n = 0, 1, 2, \dots \quad (7.2)$$

where $n = 0$ provides the area, $n = 1$ the first moment and $n = 2$ the moment of inertia of the spectral curve. The Root Mean Square value is then determined by taking the square root of the zeroth moment of the spectral curve:

$$RMS_* = \sqrt{m_{0*}} = \sigma_* \quad (7.3)$$

In which:

- * = Subscript indicating the observed motion/ direction.
- σ = Standard deviation.

These values of the RMS, also referred to as standard deviation σ , can now be compared with the motion criteria from Nordforsk [8]. For this study, it is assumed that when parameters do not meet these criteria, it will lead to downtime of the cruise terminal. The following section will present the calculation results for the RMS values of the studied motions.

CALCULATION RESULTS

The RMS values that have been determined from the response spectra can be found in Appendix G.4. The table in this appendix also includes the downtime assessment, i.e. the comparison of calculated RMS values with the Nordforsk criteria. It presents the results for both structural models (A and B), with and without a cruise ship Model C next to the cruise terminals. Each model presents the results for different observed motions, including all combinations of wave scenarios and wave angles.

7.6. REMARKS

There are a number of important remarks that should be mentioned, when interpreting the presented simulation results, about the following aspects:

- Access bridge loading;
- Sloshing;
- Relative RAO's;
- Gap in output data;

These aspects are treated separately in the indicated order.

ACCESS BRIDGE LOADING

An access bridge is required to reach the shore from the terminal. The access bridge itself is not part of the scope of this study. Nonetheless, it will have influence on the motion responses of a floating terminal. It will lead to a load on a specific location on the pontoon, most likely near an edge.

This load is not taken into account in the hydrodynamic assessment. It is likely that the access bridge will try to damp out certain motions, thereby positively influencing the downtime. Still, additional studies are required to determine its exact influence.

Horizontal displacements of the floating terminal have not been studied. Still, it is of essence that these displacements are quantified and remain limited. Otherwise, creating a proper shore line connection will become a very daunting task: quick displacements make the access ramp very dangerous for people that want to set foot on it from the terminal, as it can move either towards or away from the tourists. Special care should be taken in the design, to limit very large and sudden displacements.

SLOSHING BETWEEN THE TERMINAL AND VESSEL

Large peaks are noticed around $\omega = 1.6$ when taking a closer look at the acceleration RAO's in the y-direction (See Figure 7.7). These peaks do not show in the simulations of only a terminal. They occur when both the terminal and cruise vessel are simulated. This leads to the suspicion that sloshing occurs. Sloshing is the splashing of water and waves on and between walls. This phenomena is well capable of increasing loads and motions on vessels and floating structures. Additional study is required to confirm that these peaks are caused by sloshing and how this effect can be limited, in order to reduce motion responses caused by it.

RELATIVE RAO'S

Not only the terminal moves and rotates. The cruise vessel moves too, and these motions are not identical. All may be okay when only the response of the terminal is considered, but the (un)boarding fase can be critical, when the cruise vessel and the terminal move a lot more relative to each other. It can become, as with the access bridge, a challenging task to make the switch from one to the other when displacements are too large.

Relative RAO's provide insight in the amount of motions of one floating structure with respect to another floating structure. These relative RAO's should be determined in an additional study, in order to quantify relative motions and accelerations. If not great care is put into these relative motions, it may result in much larger downtimes than initially calculated in this study.

GAP IN OUTPUT DATA

Certain simulation results show a gap in the output data between $\omega = 0$ and $\omega = 0.1$. The occurrence of this gap is not consistent and the specific cause of this could not be found or addressed. Despite much effort in attempts to remove this flaw, it could not be corrected. Presumably this is a bug of the software AQWA, because other simulations, created with exactly the same scripts do not show this gap.

The lack of data in this frequency band leads to an underestimation of the motion response for the horizontal accelerations. The natural frequency of these accelerations lies within this band, because of the limited hydrostatic stiffness of the mooring system in these directions.

In an additional study, these gaps should be eliminated, to correctly approximate the motion responses in the horizontal direction. The gap also occurs in the results for other directions, but the values are not as significant as with the horizontal accelerations.

7.7. CONCLUSION

The drawn conclusions are related to the research questions of this study. They are based on the above presented plots and results: free floating RAO's, RAO's and response spectra for all studied motions. Also the notable differences in RMS values between the different simulations are taken into account for the deduction of conclusions. The downtime assessment does not play a part in the formulation of the conclusions in this section.

The results presented in the previous sections will be interpreted in the context of the following relevant topics:

- significant differences in the response spectra between Model A and Model B;
- the impact of the presence of a cruise ship (Model C) next to both of the floating terminals on the response spectra;
- the location of the estimated natural frequency compared with the peaks in the response spectra of the models;
- the effect of different incoming wave angles on the response spectra of both terminal models;
- the significant differences between the swell wave scenarios and wind wave scenarios;

The drawn conclusions for each of these topics are discussed below in the following sections.

MODEL A VS MODEL B

From not only the plots of the free floating RAO, but also from the plots of the RAO and response spectra it follows that the larger mass and longer length of the pontoon of Model B, compared with Model A, result in notably lower responses for all studied motions. In this sense, the size and shape of the pontoon does have a notable influence on the motion response. Whether this also leads to lower operational downtimes will follow from the downtime assessment, when the values are compared with the Nordforsk criteria, at a later stage in this study.

MODELS A AND B VS MODELS C+A AND C+B

The presence of a cruise ship next to the floating cruise terminal does reduce the total amount of wave energy that reaches the terminal. Due to diffraction phenomena at the extremities of the cruise ship and the radiation forces induced by the motions of the cruise ship itself, spreading of wave energy in both the spatial domain as in the frequency domain occurs. This leads to generally lower responses of the cruise terminal, but it may lead to new local peaks, exceeding the amount of response that would occur without the presence of the design cruise ship. Overall, the influence of the cruise ship can be described by the presence of an obstacle which reflects and diffracts wave energy, generally lowering the amount of wave energy that is able to reach the floating terminal. This will therefore result in lower responses and smaller amplitudes. The effect it has on the operational downtime is discussed at a later stage in this study.

NATURAL FREQUENCY

The estimated values of the natural frequencies for the different motions do approach the values as calculated by Ansys AQWA. This holds that the computational model can be assumed to be reliable and accurate. The same holds for the effects and phenomena that have been taken into account for the simulation of the dynamic behaviour. With respect to the natural frequency, the models seem to give realistic results, which are verified by calculations that have been carried out.

INCOMING WAVE ANGLE

The symmetric Model A does not give interesting conclusions by itself, response is along the symmetry axes the same. But the presence of a cruise ship obviously leads to different responses for different incoming wave angles. Logically, the direction for which the pontoon is unprotected leads to the largest overall responses. Model B shows, following from the larger dimensions and mass, less response than model A for identical wave angles. Looking at the absolute values of the RAO's in Figure 7.7, it can be concluded that the 90° waves are favourable for the situation where a cruise ship lies alongside. Yet, the RMS values of these spectral curves are used to determine the resulting downtime. To give a more accurate conclusion about the influence of the incoming wave angle, a downtime assessment is made.

As the incoming wave angle is directly related to the orientation of the whole terminal, it is of importance to take the effect of the incoming wave angle on the response into consideration. The incoming wave angle does have a notable influence on the absolute amount of response on all studied motions. This is mostly the result of the cruise ship that acts as an obstacle for the waves, which reflects and spreads the energy.

SWELL WAVES VS WIND WAVES

This study took into account different wave scenarios which included scenarios for swell waves and wind waves. From the results can be concluded that the low amount of swell wave energy in the spectra of the different scenarios does not lead to significantly large motions. The amplitudes of the RAO are also not very large. This means that there should be quite a high amount of swell wave energy present in the spectrum, to become of real significance in the total amount of (acceleration) responses for the different motions.

When the anchorage is taken into account, it should be noted that the mooring system induces a large response around the natural frequency of the mooring system. The catenaries act as non-linear springs, which therefore may result in large unwanted motions when there is much energy in this low frequency band. This is a topic which requires special attention when this concept is worked out in more detail.

DOWNTIME ASSESSMENT

Response spectra have been determined for the two floating terminals. From these response spectra, RMS-values have been calculated. These RMS-values are now used to carry out the downtime assessment. The approach of this assessment is described in §8.1. An example table is added for better understanding. The complete results can be found in Table G.2.

Section 8.2 presents the determined downtimes. The varied parameters lead to different downtime values. From these differences, it is possible to draw conclusions with respect to the influence of these parameters on the downtimes. From these conclusions it is possible to formulate answers on the sub research questions 2, 3, 4 and 5, as written in §1.2.

8.1. APPROACH

To determine the downtime use is made of an example, which is a part of Table G.2. In this example, the downtime as a result of accelerations in the x-direction is discussed. Table 8.1 presents the RMS-values of this motion for both Model A and Model C+A, including different wave scenarios and alignment/ incoming wave angles. The complete table can be found in §G.4.

Table 8.1: Overview of the RMS accelerations in the x-direction for the models A and C+A. The values are compared with the Nordforsk Criteria. Cells highlighted in green indicate that these scenarios that do not exceed the *Cruise Liner* criteria of Nordforsk. Orange highlighted cells indicate scenarios that meet the *Transit Passengers*-criteria.

		Model A			Model C+A			
		0 deg	45 deg	90 deg	0 deg	45 deg	90 deg	
Acceleration in x-Direction	S1C	8,6E-03	2,8E-03	0	S1C	7,8E-03	1,8E-03	3,1E-04
	S2E	2,3E-02	7,1E-03	0	S2E	3,0E-02	3,3E-03	9,9E-04
	S3A	6,4E-02	3,3E-02	0	S3A	6,8E-02	8,0E-03	1,9E-03
	S3C	1,1E-01	3,2E-02	0	S3C	1,2E-01	1,4E-02	3,7E-03
	W2B	7,9E-02	3,8E-02	0	W2B	8,7E-02	8,7E-03	1,9E-03
	W3A	1,6E-01	6,7E-02	0	W3A	1,7E-01	1,7E-02	4,7E-03
	W3C	2,4E-01	1,1E-01	0	W3C	2,5E-01	2,6E-02	4,0E-03

All the RMS values are compared with the Nordforsk criteria for both *Cruise Liners* and *Transit Passengers* (See §3.5.3 for the criteria). The *Probability of Exceedance* P_E for the key scenarios, which have been defined in §4.4.1, are used. The downtime for each incoming wave angle can now be determined: this is the largest P_E of the scenarios that do not meet the criteria, where a differentiation is made between swell waves and wind waves.

Model A is used here as an example for the case of accelerations in the x-direction: working from the top of the scenario list downwards, it is the first scenario in each column (=incoming wave direction) that determines the downtime. In the first column (0° for Model A) of the table one can see that the first scenario that fails the criteria is in this case: scenario S3A. Of the wind-wave scenarios, none of them meet the two Nordforsk criteria.

This means that swell-wave conditions similar to scenario S3A lead to too much motion response. It is not clear where the transition between operability and downtime exactly lies, but scenario S2E does meet the criteria. The probability of exceedance for worse wave conditions than the latter swell-wave scenario is 13.6%. So the downtime due to the exceedance of the criteria in scenario S3A is at most 13.6%, assuming that it could be possible that the transition takes place at just slightly worse wave conditions.

Looking at scenario with the cruise ship next to the floating terminal (Model C+A), it can be seen that now more scenarios meet the Nordforsk Criteria. In the 0° case, the Cruise Liner criteria for accelerations in the x-direction are exceeded by worse wave conditions than scenario S1C. Scenario S2E meets the less strict Transit Passenger Criterion. Would these Transit Passenger criteria be safe enough for cruise tourist to use the

floating terminal, then the downtime due to swell waves would be at most 13.6%. Again, this is the probability that swell wave conditions exceed those of scenario S2E. Unfortunately, there are still no wind-wave scenarios that meet the two Nordforsk criteria, leading to at least 26.4% downtime.

8.2. DOWNTIMES OF THE FLOATING TERMINALS

The determined downtimes for the Cruise Line criteria are presented in Table 8.2. Table 8.3 presents the downtimes for the Transit Passenger criteria. This study focusses on the influence of the following aspects on the downtime of a concept floating cruise terminal at location CT2:

- Swell and wind waves;
- Structural dimensions;
- Alignment angle;
- a moored design vessel;
- decisiveness of the motion criteria.

Each column presents the values for the downtime by model corresponding with the indicated incoming wave angles. These values are split into the downtime for the swell wave scenarios and the wind sea wave scenarios. Recapitulating the definition of downtime as it is used in this study:

The time that the floating structure is not able to fulfil its function as a cruise terminal, because of the sea state at the terminal's location. More extreme wave conditions, exceeding the conditions of the scenarios W3C and S3C are not taken into account in this downtime assessment and study. In these cases, it is assumed that cruise ships skip port and sail to a destination with calmer weather. This leads to downtime on all off the berths in Willemstad, which is not related to the hydrodynamic response of a floating terminal.

Summarised, this means that a downtime percentage of 0% does not mean that the cruise terminal is 100% operational all year long. Instead, it indicates that there are no wave conditions limiting the operability of the floating structure, excluded these earlier mentioned storm conditions. Repeating this statement helps to understand and read the numbers from Table 8.2 correctly.

Table 8.2: Calculated downtimes sorted by model and incoming wave angle after comparing the RMS-values with the Cruise Liner criteria.

Wave Angle	Terminal Only				Terminal + Design Ship			
	Model A		Model B		Model C+A		Model C+B	
	Swell	Wind	Swell	Wind	Swell	Wind	Swell	Wind
0°	≤ 13.6%	≥ 26.4%	≤ 13.6%	≥ 26.4%	≤ 58.6%	≥ 26.4%	≤ 13.6%	≥ 26.4%
45°	≤ 13.6%	≥ 26.4%	≤ 13.6%	≥ 26.4%	≤ 13.6%	≥ 26.4%	≤ 1.4%	≥ 26.4%
90°	≤ 58.6%	≥ 26.4%	≤ 58.6%	≥ 26.4%	≤ 58.6%	≥ 26.4%	≤ 13.6%	≥ 26.4%

Table 8.3: Calculated downtimes sorted by model and incoming wave angle after comparing the RMS-values with the Transit Passenger criteria.

Wave Angle	Terminal Only				Terminal + Design Ship			
	Model A		Model B		Model C+A		Model C+B	
	Swell	Wind	Swell	Wind	Swell	Wind	Swell	Wind
0°	≤ 13.6%	≥ 26.4%	≤ 0.1%	≤ 26.4%	≤ 13.6%	≥ 26.4%	≤ 13.6%	≤ 26.4%
45°	≤ 13.6%	≥ 26.4%	≤ 13.6%	≥ 26.4%	≤ 1.4%	≤ 26.4%	≤ 0.1%	≤ 4.2%
90°	≤ 13.6%	≥ 26.4%	≤ 13.6%	≥ 26.4%	≤ 13.6%	≥ 26.4%	≤ 1.4%	≤ 26.4%

8.3. CONCLUSIONS

Based on the results presented in Tables 8.2 and 8.2 a set of statements are formulated about the downtime of both structural models for the different alignment angles.

The conclusions for the case of no moored design ship next to the floating structure, i.e. Models *A* & *B* are presented first, followed by the conclusions for the case with a cruise ship next to the terminal.

Models *A* & *B*

- The alignment angles that lead to the lowest downtimes are 0° and 45° . An incoming wave angle of 90° leads to the largest amount of downtime for both models;
- The influence of different wave conditions does not influence the downtime much until the scenarios close to storm conditions, i.e. the *W3** series. The remaining amount of swell wave energy is so low that it does not seem to limit the operability of a floating terminal;
- Because of its larger dimensions, Model *B* meets the criteria for different motions notably more than Model *A*. The dimensions or size do influence the downtime of a floating structure with the function of a cruise terminal;
- The most ideal model and alignment angle leads to a downtime of at most 13.6% of the time, not taking into account storm conditions as stated before. This is the case for both Model *A* and *B* with an incoming wave angle of both 0° and 45° . This downtime does exceed the predefined criterion for a floating cruise terminal to be feasible;
- Accelerations in the heave direction are clearly the limiting factor in the determination of the downtime. The downtime is solely determined by the exceedance of the RMS vertical accelerations. None of the other motions pose a limitation on the operability of the terminal.

Now the conclusions about a design ship next to the two floating variants remain:

Models *C+A* & *C+B*

- The presence of a design vessel next to the floating terminal does not decrease the amount of downtime as expected. It can be seen that for the less strict criteria the downtime decreases. In case of the Cruise Liner criteria, the downtime for swell wave scenarios remains the same for model *A* and decreases to 1.4% for model *B*;
- Apparently, much wave energy still manages to reach the floating terminals for the 45° and 90° alignment angles. The expectation that the wind-wave scenarios would not lead to large amounts of downtime when a cruise vessel lies next to the floating terminal is not confirmed by this study. This could be explained by diffraction at the ends of the cruise ship and by sloshing between the cruise ship and the terminal;
- Accelerations in the *z*-direction are the leading factor in the total amount of downtime. The type of waves does not make any differences. For the less strict Transit-Passengers criteria, these vertical accelerations are still the main reason of downtimes, but downtimes are much lower for 0° and 45° alignment angles when model *B* is used.

From these statements a final conclusion is drawn. This conclusion is presented, along with additional recommendations, in the next and final chapter.

CONCLUSIONS AND RECOMMENDATIONS

9.1. CONCLUSIONS

The goal of this study is to provide insight in the suitability and feasibility of a floating structure to be utilised as a cruise terminal at an exposed area near the shore of Willemstad, Curaçao. This feasibility study focuses on determining the dynamic response of two conceptual floating structures and comparing the results with motion criteria. The influences of both the alignment angle and the structural model on the downtime are studied. By looking at multiple variables, instead of only one structural model and one incoming wave angle, a more integral conclusion can be drawn on the feasibility.

Not taking into account storm-like weather conditions, the main conclusion that is drawn from this study is: According to this study, in which two floating terminal variants have been studied, it is deemed feasible to realise a floating terminal in exposed sea near the St Anna Bay. This statement is based on a study on the dynamic responses occurring due to local wave loads and with the application of the Nordforsk Passenger Line criteria.

The vertical and lateral accelerations and roll motions have been studied. According to this study, these motions remain within the above mentioned criteria for only the 80x30 metres (Model B) floating structure, with an alignment angle of the terminal of 45 degrees, relative to the dominant wave angle.

Additional conclusions that can be drawn from this study and support this main conclusion are presented below, grouped by the two main topics of this study.

LOCAL WAVE CLIMATE

In order to simulate the local wave climate just offshore near St Anna Bay, use is made of the numerical wave model SWAN. From this study on the determination of the local wave climate near Willemstad, the following conclusions are drawn:

- It is possible to simulate local wave conditions with SWAN based on the distant deep water wave data from BMT ARGOSS, which serve as an input for the dynamic analysis in AQWA;
- The amount of remaining wave energy after bending around the island of Curaçao is very limited. The local wave climate is dominated by locally generated wind sea waves, because of the blocking shadow effect that the island creates. According to the SWAN Model, hardly any swell wave energy reaches the project location near the St Anna Bay;
- Wave energy bends, due to refraction and diffraction, considerably around the island. Waves with an original deep sea wave angle relative to the North of 70° ended up with an incoming wave angle of 125-135° at the project location;
- The amount of remaining wave energy at the project location leads to small mutual differences between the defined scenarios;

DYNAMIC RESPONSE OF FLOATING TERMINAL

The conclusions based on the study into the dynamic response are presented in two parts: the first part considers solely the floating structure itself. The second part takes into account a moored design ship next to the floating structure.

Only Floating Structure

- The influence of different wave scenarios on the downtime of the floating terminal is rather high. Only in the case of more calm weather conditions, the dynamic response is guaranteed to be low enough in all motion directions;
- The swell wave scenarios do not lead to as much downtime as the wind wave scenarios do. From the hydrodynamic assessment it could be concluded that the limited swell waves hardly are of any influence on the operability of the terminals.
- With no ship next to the terminal, downtime of the two terminals exceeds in almost all cases the defined design downtime criterion of 10%, with little differences between the three alignment angles;
- The dimensions of the floating structure do have an influence on the motion responses and resulting downtimes. From this study it is concluded that the longer structure Model *B* results in lower downtimes than the square Model *A*. This is explained by the larger dimensions and mass. This results in a lower response amplitude operator of the model.

Design Cruise Ship Freely Floating Next to Floating Structure

- The influence of a moored design vessel remains rather limited. The downtime is caused by heave accelerations, and greatly reduces the amount of operational time. The downtime criterion is only met for the case of Model *C+B* when the *Transit Passenger* Criteria are applied. This leads to the conclusion that these structural models are not optimal designs regarding the dynamic behaviour at this location;
- In the case of swell waves, there are possibilities with less downtime, when a right alignment is chosen. In the case of Model *A*, the most ideal direction would be 0° or 45° . Model *B* is somewhat more flexible, leading to the lowest amount of downtime in the case of either 0° , or 45° .

Based on all of the conclusions and statements presented above, the following main conclusion can be drawn from the study on the feasibility of a floating cruise terminal:

Realising a floating cruise terminal with the structural concepts as presented in this study that remains below the maximum downtime requirement of 10% is in almost all cases not feasible. The dynamic behaviour leads to too large motion responses, particularly in the *z*-direction for both structural models and all studied incoming wave angles. The presences of a design vessel next to the floating terminal does lead to reductions of the accelerations and motions, but only limited. The reduction of downtime remains limited, despite the huge dimensions of the design vessel. Still, for specific cases in this study, the downtimes remain below the downtime requirements. This leads to the suspicion that there are possibilities. These are further elaborated in recommendations in the next section.

9.2. RECOMMENDATIONS

Numerous assumptions are made during this study. To increase the reliability and accuracy of this study it is recommended to take note of these assumptions. Additional research can help take away the uncertainties that required the author to define assumptions during this study. With use of the obtained knowledge after completing this research, the following recommendations are suggested.

LOCAL WAVE CLIMATE

Regarding the study on the local wave climate with the use of the numerical model SWAN, the following is suggested:

- The accuracy of the actual downtime remains limited, because of the limited amount of wave scenarios that have been taken into account in the hydrodynamic assessment. Large jumps in downtime values are the result, when specific scenarios do not meet one of the wave scenarios. A better approximation of the downtime could be achieved by doing a full-scale analysis of all wave conditions. From these results, a much more accurate prediction of the downtime can be made. But this requires extensive computational power to run all SWAN and AQWA scenarios.
- The SWAN wave model provides a numerical estimation of the wave climate at the project location. The dynamic analysis is based on this estimation. A much higher accuracy is obtained when actual field research is carried out to obtain the local wave conditions;
- Reflection from the shore line and diffraction from moored ships at the current Megapier is not taken into account in this study. It is recommended to include these effects in the dynamic analysis to achieve a higher accuracy and reliability of the results. The numerical model SWASH can simulate these effects accurately, which can then be included in the AQWA model as an additional wave spectrum with its own corresponding incoming wave angle;
- The resolution of the computational grid used in this study is rather rough. Either make use of the above suggested field research or increase the resolution of the computational grid. This can be done by mapping the bathymetry in a higher resolution than the GEBCO'08 data. This increases the accuracy of the simulations.

DYNAMIC RESPONSE OF FLOATING TERMINAL

The suggestions with respect to the dynamic response are split into two parts: one part describes the suggestions for the simulation of only one floating structure and the second part presents recommendations based on a multi-body simulation.

Only Floating Structure

- The mooring arrangement of the floating terminal should be further detailed. Displacements and mooring forces need to be quantified in order to design this mooring arrangement more accurately. The dynamic response can then also be modelled with a higher accuracy;
- An optimization of both the pontoon geometry and the mooring system can be very beneficial when focus is put on reducing the vertical accelerations. Heave acceleration is the limiting parameter which leads to downtime.
- The AQWA results for the response spectra are not consistent with respect to the availability of data between the 0 rad/s and 0.1 rad/s frequencies. This is the location of the eigen-frequency for the horizontal motions, induced by the mooring system. A lack of data within this interval leads to an underestimation of the total amount of response in those particular motions. This should be taken into account when interpreting the results of this study. It should be determined in an additional study what the extra response due to the mooring system is for the cases where the data is not complete. Despite much effort, it was not possible to find the reason for this gap in the data. It is assumed that this is because of a bug of the software AQWA.

Design Cruise Ship Freely Floating Next to Floating Structure

- All model results with the cruise vessel apply on the presence of the largest cruise vessel at the moment: Oasis of the Seas. This is an ideal situation. Smaller vessels are likely to provide less shelter for the terminal. With respect to the downtime values, it has to be studied, whether the influence of the size of the cruise vessel does significantly change the operability of the floating terminal;
- Displacements of the Ship-Terminal combination should be quantified and require additional study. Large displacements may result in a difficult challenge to create a safe connection to the shore, without large spans between the shoreline pier and the terminal, and safe margins with respect to the underkeel clearance of the cruise ship.
- Taking into account the total load on the floating structure, including wind, wave and drag loads, it will result in different values for motion responses compared with the calculated values in this study. It is therefore not only recommended, but necessary to do additional research on the influence of these loads on the dynamic response of the floating terminal.

MOTION CRITERIA

It should be determined whether the used Nordforsk criteria are too strict for this particular case. The Cruise Line Criteria are meant to be applied on cruise ships on which passengers stay for several days. To be able to enjoy a comfortable journey, especially when sleeping or eating, the average motions and accelerations should remain very low at all times.

Applying such criteria might be overkill for this particular cruise terminal, which is in fact nothing more than a transfer hub which makes a connection between the shore and ship.

Because of the short presence of cruise tourist on the terminal, it should be determined, whether less strict motion criteria might suffice for cruise tourists of all ages. As could be seen in this study, an increase in the operational time of the terminal is directly visible in particular cases, when the criteria are deemed less strict.

BIBLIOGRAPHY

BOOK REFERENCES

- [1] Corlett, E. *The Iron Ship: the Story of Brunel's SS Great Britain*. Conway: 5th Edition, SS Great Britain Trust, 2012.
- [2] IMO. *International Convention on Tonnage Measurement of Ships*. 1969.
- [3] McCluskie. *Anatomy of the Titanic*. London: PRC Publishing, 1998.
- [4] Brida, J. G. AND Zapata, S. *Economic Impacts of Cruise Tourism: The Case of Costa Rica*. 2008.
- [5] Curaçao Ports Authority. *Directory*. 2014.
- [6] Derksen, G. *Aruba, Curacao, Bonaire*. 7nd Edition. Haarlem: Gottmer Uitgevers Groep b.v., 2014. ISBN: 9789025758127.
- [7] Thorensen, C. A. *Port Designers Handbook*. 2nd Edition. London: 2nd Edition, Thomas Telford Limited, 2010. ISBN: 9780727740861.
- [8] NordForsk. *Seakeeping Criteria*. 1987.
- [9] PIANC Working Group no. 24. *Criteria for Movements of Moored Ships in Harbours*. 1995.
- [10] The SWAN Team. *SWAN - User Manual*. Delft University of Technology. 2014.
- [11] The SWAN Team. *SWAN - Scientific and Technical Documentation*. Delft University of Technology. 2014.
- [12] Holthuijsen, L. H. *Waves in oceanic and coastal waters*. Cambridge: Cambridge University Press, 2007.
- [13] Ali, A. *Floating Transshipment Container Terminal*. Msc Thesis. Delft: Delft University of Technology, 2005.
- [14] Fousert, M. W. *Floating Breakwaters*. Msc Thesis. Delft: Delft University of Technology, 2006.
- [15] Journee, J. M. J. AND Massie, W. W. *Offshore Hydromechanics*. Delft University of Technology, 2001.
- [16] Ansys, Inc. *AQWA Reference Manual Release 15.0*. 2013.
- [17] Bosboom, J. AND Stive, M. J. F. *Coastal Dynamics 1 - Lecture Notes CIE4305*. Delft: VSSD, 2012.
- [18] Akkermans, I. *Handout: Mechanics of catenary mooring lines*.
- [19] Ruol, ET AL. "Formula to Predict Transmission for π -Type Floating Breakwaters". In: *Journal of Waterway, Port Coastal and Ocean Engineering* 139.1 (2013), pp. 1–8.
- [20] Fjelde, S. *Stability and Motion Response Analyses of Transport With Barge*. Msc Thesis. Delft: University of Stavanger, Norway, 2006.

WEBSITES

- [W1] Zakelijk Curaçao. *Haven*. <http://www.zakelijkcuracao.com/index.asp?page=http://www.zakelijkcuracao.com/pages/1022/Haven.htm>. [Online, accessed 01-10-2014]. 2014.
- [W2] Redactie. *Tweede megapier in ministerraad*. <http://www.kkcuracao.net/?p=40895>. [Online, accessed 01-10-2014]. 2013.
- [W3] Grace, M. *A Brief History of the Cruise Ship Industry*. Retrieved from <http://cruiselinehistory.com/a-brief-history-of-the-cruise-ship-industry/>. [Online, accessed 24-09-2014]. 2008.
- [W4] Fowler, D. *Titanic Facts*. Retrieved from <http://www.titanicfacts.net/titanic-victims.html>. [Online, accessed 24-09-2014]. 2013.
- [W5] Wikipedia. *List of Cruise ships*. Retrieved from http://en.wikipedia.org/wiki/List_of_cruise_ships. [Online, accessed 02-03-2015]. 2011.

- [W6] Det Norske Veritas. *Oasis of the Seas: Dimensions*. Retrieved from <http://vesselregister.dnvgl.com/vesselregister/vesselregister.html>. [Online, Accessed 24-09-2014]. 2009.
- [W7] Cruise Market Watch. *Statistics - Growth*. Retrieved from <http://www.cruisemarketwatch.com/>. [Online, accessed 24-09-2014]. 2014.
- [W8] Cruise Lines International Association. *The Overview: 2010 CLIA Cruise Market Overview*. Retrieved from <http://www.cruising.org/sites/default/files/misc/2010FINALOV.pdf>. [Online, accessed 24-09-2014]. 2010.
- [W9] Caribbean Hurricane Network. *Climatology of Caribbean Hurricanes - Curaçao*. Retrieved from http://stormcarib.com/climatology/TNCC_all_isl.htm. [Online, accessed 24-09-2014]. 2008.
- [W10] Royal Caribbean International. *Oasis Class Vessels: Harmony of The Seas*. Retrieved from <http://www.royalcaribbean.com/findacruise/ships/class/ship/home.do?shipClassCode=OA&shipCode=HM&br=R>. [Online, accessed 25-04-2015]. 2015.
- [W11] FDN. *Multifunctional Floating Breakwater in Monaco*. Retrieved from <http://www.fdn-engineering.nl/#!floating-breakwater-in-monaco/c1w36>. [Online, accessed 09-06-2015]. 2015.

DATASETS

- [D1] European Center for Medium-Range Weather Forecast. *Wind Climate - Wind Data*. [Online, accessed 20-06-2014]. 2014.
- [D2] BMT Argoss. *Wave Climate - Wave Data*. Datasets are retrieved from <http://www.waveclimate.com/>. [Online, accessed 28-03-2014]. 2014.
- [D3] General Bathymetric Charts of the Oceans. *Gridded Bathymetry Data 2008*. [Online, accessed 26-05-2014]. 2014.

SOFTWARE PACKAGES

- [S1] TheMap ®10VR 3d for Windows (x64) with Jeppesen C-Map Max charts from 2011). Chartworx Holland. 2014.
- [S2] SWAN 41.01 for Windows (x64). The SWAN Team. <http://swanmodel.sourceforge.net> Downloaded: 25-04-2014. 2014.
- [S3] Delftdashboard v1.01.8218 for Windows (x64). Deltares. <https://publicwiki.deltares.nl/display/OET/DelftDashboard> Downloaded: 20-03-2014. 2014.
- [S4] Matlab R2013b for Windows (x64). The Mathworks Inc. 2013.
- [S5] AQWA 14.5 for Windows (x64). ANSYS Inc. 2012.

FIGURES

- [F1] GeoAtlas. *Physical map of the Caribbean Sea and Curaçao*. <http://www.geoatlas.com/en/maps/continental-maps-2/caribbean-sea-508>, [Downloaded: 24-11-2014]. 2014.
- [F2] Curaçao Ports Authorities. *Edited image from the original Rif Sea Port Masterplan*. Obtained by email, [Downloaded: 02-06-2015]. 2015.
- [F3] Caribbean Hurricane Network. *Stormtracks 1851-2010 - Curaçao*. Retrieved from http://stormcarib.com/climatology/images/TNCC_1851_2010_isl.png. [Online, accessed 24-09-2014]. 2008.
- [F4] Google Maps. *Curaçao - Willemstad*. <https://www.google.nl/maps/place/Curacao/>, [Downloaded: 02-05-2015]. 2015.

LIST OF FIGURES

2.1	Picture of the first purpose-built cruise ship "Prinzessin Victoria Luise".	7
2.2	Scatter plot of the increase of the gross tonnage of passenger vessels in time.	8
2.3	Graph of the growth of worldwide passengers carried by cruise liners	9
2.4	Geographic map of the Caribbean Sea and the island Curaçao.	10
2.5	Picture of the port of Willemstad.	11
2.6	Picture of the Megapier Cruise Facility	12
2.7	Windrose indicating the probability of wind speeds and directions.	14
2.8	The long term distribution of the wind speeds near Curaçao.	14
2.9	Storm tracks of all storms with a category of tropical storm or worse from 1851 - 2010.	15
2.10	Nautical chart from C-Map of the area near port of Willemstad.	15
3.1	Sketch of the areas to be developed to realise the non-floating part of the new cruise terminal.	18
4.1	Presentation of the SWAN model domain and boundaries.	24
4.2	Depth-contours near the Island Curaçao, using data from the GEBCO'08 database.	24
4.3	Project area with the water depths and geographical coordinates shown for all grid cells.	24
4.4	Scenario <i>W2A</i> : Plot showing both wave directions and significant wave heights H_s as calculated by the SWAN Model	28
4.5	Scenario <i>W2A</i> : Plot showing the results for the peak wave period T_p	28
4.6	The variance density spectra plotted against the wave frequency in the case of wind waves at location <i>CT2</i>	28
4.7	The dominant wave angle at <i>CT2</i> is considered to be 125° relative to the North.	29
4.8	Wave spectrum of swell waves at location <i>CT2</i>	30
5.1	Definition of motions for a floating structure in six degrees of freedom.	35
5.2	The principle of transforming a wave spectrum into a response spectrum for the heave motion	35
5.3	Variance density spectra plotted as a function of frequency in Hertz.	36
5.4	Variance density spectra plotted as a function of frequency in ω	36
5.5	Rectangle barge stability, showing the equilibrium at an angle of heel ϕ_f	37
6.1	Schematic anchorage layout for both variants (0° alignment angle).	40
6.2	Indication of the project location <i>CT2</i>	41
6.3	The orientation of the cruise terminal relative to the three wave directions that are studied.	41
6.4	43
6.5	Cross sectional sketch of cruise terminal location <i>CT2</i> with an alignment angle of 0° relative to the dominant wave angle, including anchorage and pier.	44
7.1	Schematic anchorage as defined in AQWA for Model <i>A</i> , indicating the locations of anchors and connection points.	47
7.2	Mesh of the submerged part of Model <i>A</i> : the 30x30m pontoon.	48
7.3	Top view of floating terminal <i>A</i> (green) and <i>B</i> (blue) showing the applied sign convention and locations of specific nodes.	49
7.5	Free Floating Acceleration RAO's in x-direction (left), y-direction (middle) and z-direction (right) for the Models <i>A</i> and <i>B</i> . The simulated incoming waves have angles of 0° , 45° and 90°	52
7.7	Acceleration RAO's of the different simulation models for three incoming wave angles.	55
7.8	Response spectra of the different simulation models for three incoming wave angles.	58
A.1	Definition of parameters for a propagating harmonic wave.	81
A.2	Linearised basic equations and boundary conditions for the linear wave theory, in terms of the velocity potential.	82

A.3	The orbital motion of water particles under a propagating harmonic wave.	83
A.4	Left: two-dimensional variance density spectrum of an irregular ocean-surface with swell and wind-sea. Right: one-dimensional variance density spectrum for all/one direction(s).	84
A.5	Diffraction of waves around an island.	84
B.1	Available grid cells at BMT ARGOSS that contain wave data.	85
B.2	Wind rose indicating the dominant wind direction.	90
B.3	Cumulative distribution plot of the wind speeds at Curaçao according to data from ECMWF.	90
B.4	The wind speed plotted in a bar chart. From this plot it can easily be concluded that the governing wind speeds is between 7-9 m/s.	91
C.1	Computational grid as used by the software SWAN	93
C.2	Defined boundaries of the computational grid for the model.	93
C.3	Differences in significant wave height H_s for Scenario <i>W2A</i> without (left) and with wind (right). $u_{10} = 7.7\text{m/s}$, $\theta_{wind} = 80^\circ$	94
D.49	The change of wave energy is clearly visible for different locations perpendicular to the depth contour lines.	114
D.50	The variance density plotted against the wave frequency in the case of swell waves at location <i>CT2</i>	115
D.51	The variance density plotted against the wave frequency in the case of wind sea waves at location <i>CT2</i>	115
E.1	Schematic representation of a mass damper spring system.	118
E.2	Schematic representation of a mass damper spring system for heave.	118
E.3	Overview of the different types of fluid forces, related to the equation of motions.	118
E.4	Basic geometry of the catenary mooring.	120
E.5	Simplification of the catenary mooring system into a mass-spring system.	120
E.6	Plot of the restoring force as a function of the displacement.	121
E.7	Approximation of the amount of added mass for the heave motion.	122
E.8	Method of Brown & Root Vicker to determine the hydrodynamic mass of a floating structure.	123
F.1	Definition of the Fixed Reference Axes and Local System Axes in AQWA.	125
F.2	Mesh of the submerged part of Model <i>A</i> : the 30x30m pontoon.	126
F.3	Mesh of the submerged part of Model <i>B</i> : the 80x30m pontoon.	126
F.4	Close-up detail of Mesh of the bow of the cruise vessel.	127
F.5	Mesh of the submerged part of the cruise vessel.	127
F.6	Schematic anchorage as applied in AQWA for Model <i>A</i> indicating the locations of the anchors and connection points.	128
G.1	Overview of the applied sign convention in the model domain.	135
G.2	Free Floating RAO and RAO simulation results for two models and three incoming wave angles.	135

LIST OF TABLES

2.1	Comparison of properties between the Titanic and Oasis of the Seas.	8
2.2	Ports of Curaçao and their maximum particulars	11
2.3	Properties of the datasets for swell and wind waves used in this study.	13
2.4	Wave climate scatter diagram of wind waves of the past 20 years at deep water, North of Curaçao.	13
2.5	Wave Climate Scatter Diagram of swell waves of the past 20 years at deep water, North of Curaçao.	13
3.1	Main Particulars of the Design Cruise Ship: Oasis Class Ships from Royal Caribbean International	17
3.2	Limiting criteria with regard to accelerations (vertical and lateral) and roll motions	20
4.1	Preparation steps for the simulation of local wave data, indicating data sources and software.	21
4.2	General parameters values to start-up the SWAN Wave Model.	25
4.3	Deep water wind wave scatter diagram: Wave height vs. wave direction.	25
4.4	Overview of scenarios used as boundary conditions in SWAN.	26
4.5	Wind sea wave scatter diagram showing the wave parameters that each wave scenario represents.	27
4.7	Wind sea wave scatter diagram showing the covered area with respect to the peak wave period of the different scenarios.	27
4.8	Difference between imposed boundary wind waves and the waves at the project location <i>CT2</i>	29
4.9	Wave parameter sensitivity for three different wave data output locations.	30
4.10	Overview of the scenarios with corresponding wave parameters that will be used for the hydrodynamic assessment.	31
5.1	Overview of three basic hull types and their main properties.	34
5.2	Recommended motion criteria for safe working conditions.	38
6.1	Main particulars of the two floating terminal structures and cruise ship.	40
6.2	Properties of the modelled catenaries.	40
6.3	Small angle stability parameters of Models <i>A</i> and <i>B</i>	40
7.1	Mesh details of the different models	47
7.2	Defined frequency range and interval	48
7.3	Presentation of the natural frequencies for the considered motions. These values are compared with the results of the analytical approximation.	51
8.1	Overview of the RMS accelerations in the x-direction for both Model <i>A</i> and Model <i>C+A</i>	63
8.2	Calculated downtimes sorted by model and incoming wave angle after comparing the RMS-values with the Cruise Liner criteria.	64
8.3	Calculated downtimes sorted by model and incoming wave angle after comparing the RMS-values with the Transit Passenger criteria.	64
B.1	Details about the BMT ARGOS data sets.	85
B.2	General details about the ECMWF data sets.	86
B.3	Scatter diagram of the wind: direction vs speed.	89
C.1	Different scenarios for boundary wave conditions run in SWAN-model.	95
C.2	Swell wave scatter diagram of the significant wave height related to the wave direction. It visualises the covered areas of the defined swell wave scenarios.	95
C.3	Swell wave scatter diagram showing the covered area with respect to the peak wave period of the defined scenarios.	95
C.4	Wind sea wave scatter diagram showing the wave parameters that each wave scenario represents for this model.	96

C.5	Wind sea wave scatter diagram showing the covered area with respect to the peak wave period of the different scenarios.	96
D.1	Results and difference between the swell waves imposed on the boundaries and the waves near the project location.	99
D.2	Results and difference between the wind sea waves imposed on the boundaries and the waves near the project location.	100
E.1	Overview of the used parameters for the calculations carried out in the following sections. . . .	119
E.2	Overview of the calculated values for the hydrostatic stiffness.	121
E.3	Calculated values of the undamped natural frequency without hydrodynamic mass in five directions.	122
E.4	Overview of all the calculations values of the hydrodynamic mass.	123
E.5	Overview of all important parameters for the calculations carried out in this appendix.	123
E.6	Summary of the calculated hydrostatical and hydrodynamical parameters by means of basic calculations.	124
F.1	Mesh details	126
F.2	Properties of the catenaries applied in AQWA	127
G.1	Summary of the hydrostatic and hydrodynamic parameters as calculated by AQWA	133
G.2	Overview of RMS calculation results. The comparison with the Nordforsk Criteria is visualised by means of coloured cells. The green highlighted cells indicate the scenarios that do not exceed the <i>Cruise Liner</i> criteria. Orange cells meet the <i>Transit Passengers</i> criteria from Nordforsk. . . .	145

APPENDICES

A	Introduction on Physics of Waves	79
B	Wave and Wind Data	85
C	SWAN Model Set-Up	93
D	SWAN Model Results	99
E	Analytic Approximation of Hydrodynamic Properties	117
F	AQWA Model Set-Up	125
G	AQWA Simulation Results	133
H	Seakeeping Criteria by Nordforsk	147

INTRODUCTION ON PHYSICS OF WAVES

This chapter deals with physics of waves. It gives a brief introduction on the description and definition of waves in §A.1. With this information the *Linear Wave Theory* is derived in §A.2. In this section both regular and irregular waves are treated. With the knowledge of linear wave theory an explanation is given on wave transformation, whereby the energy balance plays an important role. This is treated in §A.3.

A.1. DESCRIPTION OF WAVES

This section deals with ocean waves. Ocean waves have an irregular pattern, because they are a sum of countless oscillations generated in the ocean. The source of these oscillations are either wind- or tidal forces. The oldest skills in describing waves are all about observing the ocean waves from the shore or from a ship.

A.1.1. OBSERVING WAVES

Whenever people look at the ocean, one of the first thoughts concern the state of the sea: "what a high waves", or "what is the sea calm today". Human beings always try to estimate the height of waves whenever they see waves. From this the significant wave height H_s or $H_{1/3}$ has been derived. It is called the significant wave height because it was an approximate mathematical expression of the wave height as estimated by experienced observers at sea. The mathematical definition is as follows:

$$H_{1/3} = \frac{1}{N/3} \sum_{j=1}^{N/3} H_j \quad (\text{A.1})$$

A variant on this significant wave height is the root-mean-square wave height H_{rms} , which is the square root of the mean wave heights squared:

$$H_{rms} = \sqrt{\frac{1}{N} \sum_{i=1}^N H_i^2} \quad (\text{A.2})$$

For the observation of waves it is desired to formulate the wave characteristics in short-term wave statistics. To do this, an observation record should be long enough to get reliable averages, in the order of 20 minutes. This observation record is in practice repeated every three hours and it is assumed that this record is representative for these three hours. It is then assumed that the statistical properties are constant during this time frame.

A.1.2. MEASUREMENT OF SEA-STATE

Visual observation is just one of several methods to do measurements: in-situ with wave buoys or poles and with remote-sensing techniques like for example radar with an accuracy of around 10 % or better [17].

The measurements of sea-states result in wave records which can be characterised by means of time-series or through a spectral analysis. Data obtained from the latter method is used for this study. More information on this can be found in the next Appendix.

A.2. LINEAR WAVE THEORY

Understanding random waves starts with knowledge on harmonic waves. Key knowledge on harmonic waves is given here by explaining the linear wave theory. The explanation is intended to be only a short summary of the entire theory and all its derivations. More detailed explanations and derivations from the information below can be found in the book *Ocean Waves* by Holthuijsen ([12], pages 28-47 and 109-121).

The linear wave theory describes in detail surface gravity waves and is based on two fundamental equations. After linearising a mass balance equation and a momentum balance equation, freely propagating, harmonic

waves are the solution to these two equations. Several assumptions are made to be able to apply the linear wave theory:

- Water is an ideal fluid;
 - Non-viscous;
 - Incompressible;
 - Constant density;
 - Motion of water particles is irrotational.
- The amplitude of the waves is small, to the wave length and to the water depth;
In this case non-linear effects of waves are negligible.

These assumptions are used below to explain and derive the continuity equation and the momentum balance equation.

CONTINUITY EQUATION

The continuity equation can be derived from the mass balance equation by assuming a constant mass density ($\frac{\partial \rho}{\partial t} = 0$) and no production of water (i.e. $S = 0$):

$$\text{Mass balance equation} \quad \frac{\partial \rho}{\partial t} + \frac{\partial \rho u_x}{\partial x} + \frac{\partial \rho u_y}{\partial y} + \frac{\partial \rho u_z}{\partial z} = S \quad (\text{A.3})$$

$$\text{Continuity equation} \quad \frac{\partial u_x}{\partial x} + \frac{\partial u_y}{\partial y} + \frac{\partial u_z}{\partial z} = 0 \quad (\text{A.4})$$

In which:

- ρ = mass density of fluid ($\approx 1025 \text{ kg/m}^3$ for sea water)
- u = velocity
- x, y, z = indication of direction in a 3-dimensional reference frame

The continuity equation is very important in fluid mechanics. It describes the transport of a conserved quantity, like for example the mass of water. The velocity potential function $\phi = \phi(x, y, z, t)$ is then used to solve the continuity equation (Requires irrotational water particles). The function states that the spatial derivatives are equal to the velocity of the water particles (Eq. A.5). When the velocity potential function is substituted into the continuity equation, the result is the Laplace equation (see Eq. A.6).

$$\text{Velocity Potential function:} \quad u_x = \frac{\partial \phi}{\partial x}, \quad u_y = \frac{\partial \phi}{\partial y}, \quad u_z = \frac{\partial \phi}{\partial z} \quad (\text{A.5})$$

$$\text{Laplace Equation:} \quad \frac{\partial^2 \phi}{\partial x^2} + \frac{\partial^2 \phi}{\partial y^2} + \frac{\partial^2 \phi}{\partial z^2} = 0 \quad (\text{A.6})$$

With the introduction of kinematic boundary conditions, a solution to the Laplace equation can then be obtained. These boundary conditions are required at the surface and bottom of the model domain. Water particles on the free-surface ($z = 0$) should follow the vertical motions of the wave profile. At the bottom ($z = -d$), water particles do not move through the bed floor. Expressed in terms of the velocity potential function this leads to the following conditions:

$$\text{Kinematic boundary conditions} \quad \begin{cases} \frac{\partial \phi}{\partial z} = \frac{\partial \zeta}{\partial t} & \text{at } z=0 \\ \frac{\partial \phi}{\partial z} = 0 & \text{at } z=-d \end{cases} \quad (\text{A.7})$$

The solution of the Laplace Equation (Equation A.8) is a long-crested harmonic wave, propagating in the positive x-direction. Figure A.1 presents the solution of the Laplace Equation and the definitions of parameters in a graphical way.

$$\zeta(x, t) = \zeta_a \sin(\omega t - kx) \quad (\text{A.8})$$

In which:

a	=	wave amplitude [m]
ω	=	radian frequency [rad/s]
t	=	time [s]
k	=	wave number [rad/m]

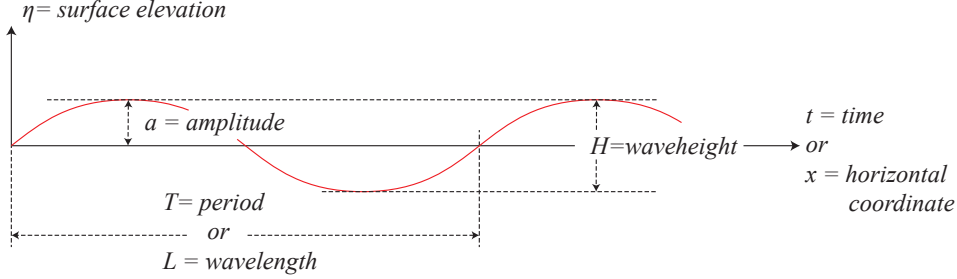


Figure A.1: Definition of parameters for a propagating harmonic wave [12].

MOMENTUM BALANCE EQUATION

The second part of the linear wave theory is the momentum balance equation. This equation is derived from the second law of Newton: a net force on an object equals the rate of change of momentum:

$$F = \frac{\partial mv}{\partial t} \quad (\text{A.9})$$

To obtain the momentum balance equation, the mass density of water is multiplied with the velocity of water particles. The velocity is in this case a vector quantity meaning that the equation is a vector equation with three components (x, y, z). For the x -component, the momentum balance equation is as follows:

$$\frac{\partial(\rho u_x)}{\partial t} + \frac{\partial u_x(\rho u_x)}{\partial x} + \frac{\partial u_y(\rho u_x)}{\partial y} + \frac{\partial u_z(\rho u_x)}{\partial z} = F_x \quad (\text{A.10})$$

F_x is in this case the body force in the x -direction per unit volume. The first component on the left side is the rate of change of momentum in time. The second, third and fourth terms are advective terms, making the equation non-linear. For this equation to be usable in the linear wave theory, these terms should be removed. It then reduces to the linearised momentum balance equation:

$$\frac{\rho u_x}{\partial t} = F_x \quad (\text{A.11})$$

In the case of a sea, the deeper the water, the higher the pressure at the bottom. This pressure is the result of gravitation and would be the only external force on the water, which is also the case in Eq. A.11. With some derivation ([12], pages 114-116) the linearised Bernoulli equation for unsteady flow is found:

$$\frac{\partial \phi}{\partial t} + \frac{p}{\rho} + gz = 0 \quad (\text{A.12})$$

Using the velocity potential function again on the dynamic boundary condition on the water surface with $z = \zeta$, and $p = 0$, this results in:

$$\frac{\partial \zeta}{\partial t} + g\zeta = 0 \quad (\text{A.13})$$

All these explained and derived equations above are summarised in Figure A.2, including the boundary conditions. So both parts of the linearised wave theory are depicted here with both the derived equations from the mass balance equation and momentum balance equation.

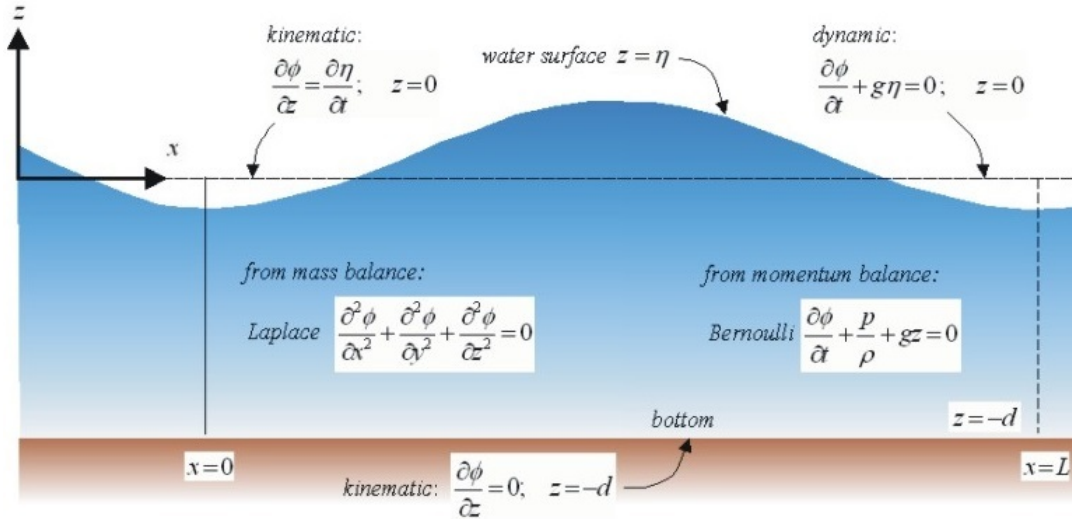


Figure A.2: Linearised basic equations and boundary conditions for the linear wave theory, in terms of the velocity potential [12].

A.2.1. PROPAGATING HARMONIC WAVES, DERIVED FROM LINEAR WAVE THEORY

The propagating harmonic wave is a solution to the previously mentioned Laplace equation. It has a constant height and propagates in the positive x -direction. A sine wave represents this regular wave in the following way:

$$\zeta(x, t) = \frac{H}{2} \sin\left(\frac{2\pi}{T}t - \frac{2\pi}{L}x\right) \quad (\text{A.14})$$

The middle part of the above equation turns out to be in the same shape as the earlier presented Equation A.8. A distinct property of this equation is that there is a certain propagation speed c while the phase ($\omega t - kx$) remains constant. Therefore the phase speed is defined as follows:

$$c = \frac{\omega}{k} = \frac{L}{T} \quad (\text{A.15})$$

Of big influence in this study is the motion of water particles under a harmonic wave. These particles move with a so called 'orbital velocity', since the motion of the particles in deep water is a closed and circular orbit. These particle velocities can be derived from the velocity potential function. For further detailed information on this, reference is made to Holthuijsen [12].

From Figure A.3 it can be seen that the wave-induced velocities decrease exponentially with the distance to the surface. This is of direct influence on the dynamic response of floating structures and their draught.

A.2.2. DESCRIBING IRREGULAR WAVES

Looking at the sea, one conclusion that can be made is that there are no single regular waves visible. The sea surface is irregular, random and never the same. Still, it is important to describe this irregular surface in a mathematical way to be able to apply any statistical analyses. Two ways to characterise a wave record are:

1. Wave-by-wave analysis;
2. Spectral analysis.

The significant wave height, as presented in §A.1.1, is in fact a wave-by-wave approach, as it shows the value of the average height of the highest one third of the occurring waves. This section gives more information on the spectral analysis in particular, as it is important for the use and understanding of the used wave model SWAN.

If multiple regular waves with different amplitudes and frequencies are added up, the result is not a regular wave any more. Now we do this the other way around: finding individual regular wave properties from an irregular wave record to reproduce this wave record. This is called a Fourier analysis: any random signal can be decomposed into multiple harmonic components, called Fourier series (see Eq. A.16)

For one stationary three-hour wave record, the amplitude and phase of the individual harmonic waves are assumed constant.

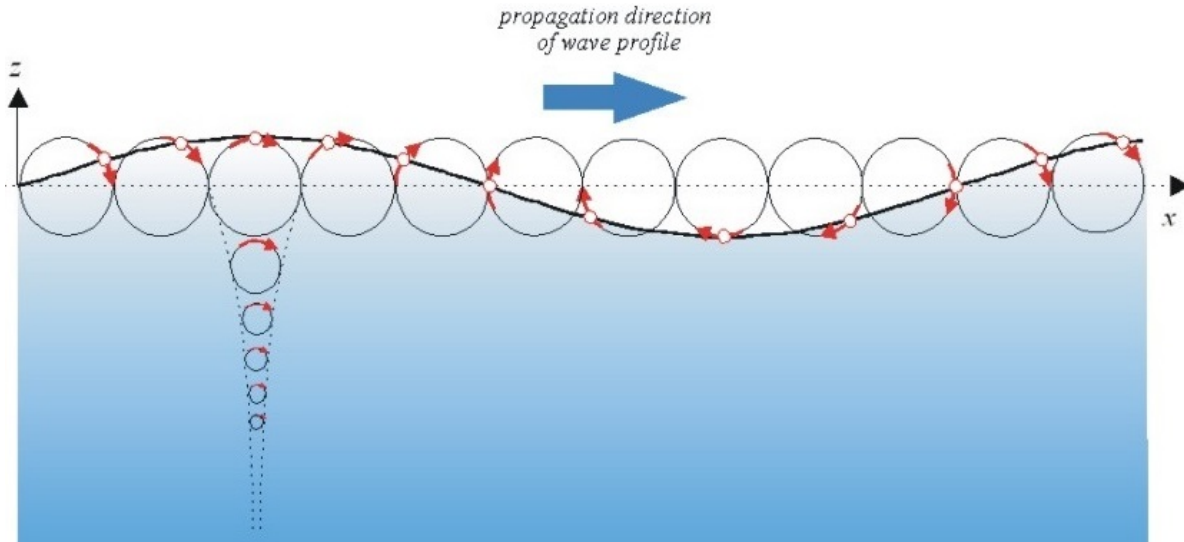


Figure A.3: The orbital motion of water particles under a propagating harmonic wave. Source [12].

$$\zeta = \sum_{n=1}^N a_n \cos(2\pi f_n t + \alpha_n) \quad (\text{A.16})$$

Where:

- $f_n = \frac{n}{T_r}$ for $n = 1, 2, \dots$
- N = Number of frequencies
- α_i = phase of individual regular wave
- a_i = amplitude of individual regular wave
- f_i = wave frequency of individual regular wave
- T_r = Wave record duration

Each wave with a certain amplitude contains energy. So all the energy in an irregular wave field is spread throughout a range of frequencies and directions. If only the frequency of waves is taken into account, a one-dimensional variance density spectrum can be created by determining the wave amplitude variance $E_{var}\{\frac{1}{2}a_i^2\}$ for all the components of the Fourier series. The variance is then distributed over the frequency interval Δf_i , whereby $\Delta f_i \rightarrow 0$, to obtain the continuous variance density spectrum:

$$E_{var}(f) = \lim_{\Delta f \rightarrow 0} \frac{1}{\Delta f} E_{var}\{\frac{1}{2}a_i^2\} \quad (\text{A.17})$$

This equation does not include information about the distribution of variance over the direction of waves. Including this information, this equation becomes as follows:

$$E_{var}(f, \theta) = \lim_{\Delta f \rightarrow 0} \lim_{\Delta \theta \rightarrow 0} \frac{1}{\Delta f \Delta \theta} E_{var}\{\frac{1}{2}a_i^2\} \quad (\text{A.18})$$

From this 2-d variance density spectrum a 1-d spectrum can be extracted based on frequency f or wave direction θ .

Multiplying the variance density spectrum of a particular motion with ρg leads to the energy density spectrum of that motion:

$$E_e(f) = \rho g E_{var}(f) \quad (\text{A.19})$$

This equation is very important for the next section, as it lies at the base of the reason why waves are able to transform as they continuously propagate through a changing environment.

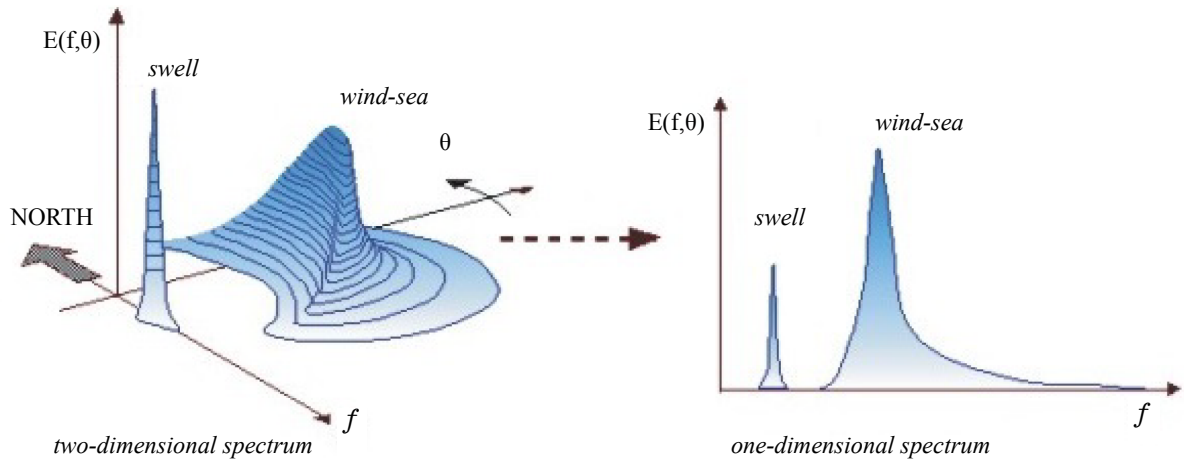


Figure A.4: Left: two-dimensional variance density spectrum of an irregular ocean-surface with swell and wind-sea. Right: one-dimensional variance density spectrum for all/one direction(s) θ [12].

A.3. WAVE TRANSFORMATION

Waves transform during the propagation from deep water ($\frac{h}{L} > 0.5$) to areas with a decreasing water level. This transformation is the result of the waves being affected by the seabed. Numerical models are able to take into account these wave transformations simultaneously. This section discusses two processes briefly as they are of importance for the wave model: wave reflection is discussed in §A.3.1 and §A.3.2 treats the phenomena of wave diffraction.

A.3.1. WAVE REFLECTION

Whenever there is an obstruction, either man-made or natural, on the path of a propagating wave, this wave will show reflection. The slope and angle of the structure and the incoming wave angle determine the wave height (H_r). If the reflected wave height is divided by the incoming wave height (H_i), it gives us the reflection coefficient:

$$C_r = \frac{H_r}{H_i} \quad (\text{A.20})$$

This coefficient will be 1 if there occurs no energy loss during reflection. This happens normally with non-porous high walls with no overtopping. Laboratory model tests are used to determine C_r for all kinds of other structures and situations.

A.3.2. DIFFRACTION

Diffraction is the bending of waves around obstacles and thus these waves penetrate into the shadow zone of an obstacle. Figure A.5 shows normal incident waves directed towards an island. The waves passing the island bend around it showing concentric circular arcs with lower wave amplitudes compared to the incident waves.

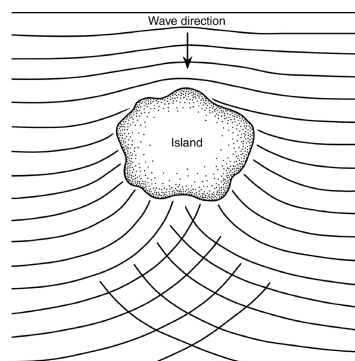


Figure A.5: Diffraction of waves around an island.

APPENDIX B

WAVE AND WIND DATA

B.1. DEEP SEA WAVE DATA

This section presents the wave data that is used as input for the SWAN model. The source of the raw data is the numerical model of BMT ARGOSS, a company specialised in metocean consultancy and weather forecasting. The following tables are created for a better presentation of the raw data.

B.1.1. GENERAL INFORMATION ABOUT THE DATASET

The service of BMT ARGOSS that distributes wave- and wind data is called *Wave Climate* [D2]. The data set was created on march 28th of 2014 and was extracted from the company's wave model. Further details are given in Table B.1.

These data sets are numerical approximations of real sea states at a grid point with an exact geographical location. This location represents the wave climate for the entire grid cell.

Table B.1: Details about the BMT ARGOSS data sets [D2].

www.waveclimate.com	Created: 28-03-2014
Begin of Dataset	1-1-1992 0:00
End of Dataset	31-12-2012 21:00
Time steps [hours]	3
Grid Cell Centre [°N]	12.50
Grid Cell Centre [°E]	-68.75
Size of Cell [km]	200x200
No. of Data Records	61368

The data is extracted at the location indicated in Table B.1. Figure B.1 shows the geographical location of the used cell which is dashed with black stripes.

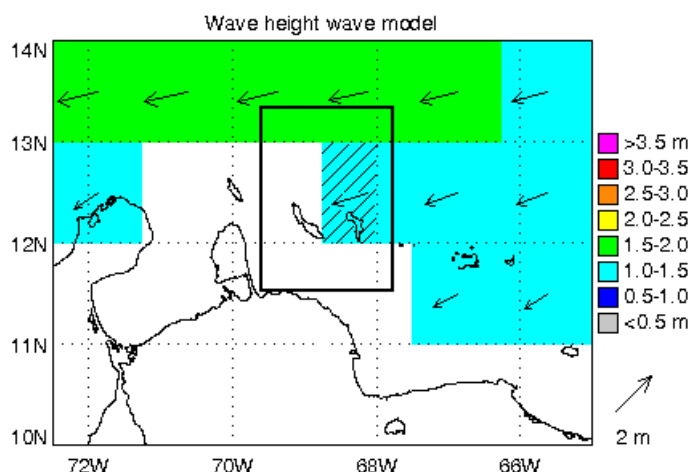


Figure B.1: The available grid cells in the Waveclimate data set indicating the average significant wave height for each cell. The black dashed cell is the one used for this study. From this image it can be confirmed that there is no wave data available on the south side of the island of Curaçao [D2].

B.2. WIND DATA

This section presents the wind data that is used for this thesis. The source of the raw data is the numerical model of the European Centre for Medium-Range Weather Forecasts (ECMWF), an independent intergovernmental organisation specialised in global numerical weather forecasting. The wind data is used to determine the wind climate at Curaçao. From this data plots are made to visualise the predominant wind direction and wind speed distribution. Also a wind scatter diagram is made from this data.

B.2.1. GENERAL INFORMATION ABOUT THE DATASET

Table B.2: General details about the ECMWF data sets [D2].

Corporate License	Created: 28-05-2014
<i>Latitude [°N]</i>	12.00
<i>Longitude [°E]</i>	-69.00

B.2.2. WIND SCATTER DIAGRAM

From the ECMWF Dataset a wind scatter diagram is created. This diagram is presented in Table B.3 and shows the distribution of the wind speed over the wind directions. The cells that are green indicate the most frequent wind conditions. From the scatter diagram it can be concluded that the predominant wind direction is from the East with a wind speed between 6 and 10 m/s.

An interesting conclusion that can be drawn from this wind scatter diagram is that the wind hardly blows from other directions than between the North-East and South-East. Also the wind speed is hardly lower than 5 m/s which corresponds to 3 on the scale of Beaufort.

B.1.2. WIND SEA WAVE DATA

WAVE HEIGHT VS. WAVE PEAK PERIOD

Significant Wave Height [m]	Wave Peak Period [s]																#	%		
	3.2	3.6	3.9	4.3	4.7	5.2	5.7	6.3	6.9	7.6	8.4	9.2	10.2	11.2	12.2	13.2				
0 - 0.3	326	195	96	39	7	5	-	-	-	-	-	-	-	-	-	-	0	- 0.3	668	1.1
0.3 - 0.6	1060	1480	1220	756	359	128	37	7	-	-	-	-	-	-	-	-	0.3 - 0.6	5054	8.7	
0.6 - 0.9	38	377	1412	3302	3042	1586	516	110	49	18	4	-	-	-	-	-	0.6 - 0.9	10454	17.9	
0.9 - 1.2	-	64	785	3513	5372	3106	774	165	62	12	1	-	-	-	-	-	0.9 - 1.2	13854	23.7	
1.2 - 1.5	-	-	6	414	3421	5177	2694	574	122	34	5	-	-	-	-	-	1.2 - 1.5	12447	21.3	
1.5 - 1.8	-	-	-	-	2	320	3110	3726	1210	172	26	6	-	-	-	-	1.5 - 1.8	8572	14.7	
1.8 - 2.1	-	-	-	-	-	1	316	2486	1589	332	34	7	-	-	-	-	1.8 - 2.1	4765	8.2	
2.1 - 2.4	-	-	-	-	-	-	349	1179	366	34	3	1	-	-	-	-	2.1 - 2.4	1932	3.3	
2.4 - 2.7	-	-	-	-	-	-	7	240	208	36	2	-	-	-	-	-	2.4 - 2.7	493	0.8	
2.7 - 3.0	-	-	-	-	-	-	-	10	75	26	1	-	-	-	-	-	2.7 - 3.0	112	0.2	
3 - 3.3	-	-	-	-	-	-	-	-	6	16	-	-	-	-	-	-	3 - 3.3	-	-	
3.3 - 3.6	-	-	-	-	-	-	-	-	-	2	-	-	-	-	-	-	3.3 - 3.6	-	-	
3.6 - 3.9	-	-	-	-	-	-	-	-	-	-	1	-	-	-	-	-	3.6 - 3.9	-	-	
	3.2	3.6	3.9	4.3	4.7	5.2	5.7	6.3	6.9	7.6	8.4	9.2	10.2	11.2	12.2	13.2				
#	1424	2052	2792	4888	7337	10833	12262	10153	5023	1355	206	25	1	0	0	0	58351			
%	2.4	3.5	4.8	8.4	12.6	18.6	21.0	17.4	8.6	2.3	0.4	0.0	0.0	0.0	0.0	0.0	100			

WAVE HEIGHT VS. WAVE DIRECTION

Hs - Significant Wave Height [m]	Wave Direction [deg]																																				#	%					
	0	10	20	30	40	50	60	70	80	90	100	110	120	130	140	150	160	170	180	190	200	210	220	230	240	250	260	270	280	290	300	310	320	330	340	350			360				
0 - 0.3	9	32	50	97	111	180	254	421	486	314	169	67	43	15	9	11	5	7	4	3	1	1	3	2	1	1	3	2	1	1	4	6	5	17	14	18	15	24	22	0	- 0.3	2434	4.0
0.3 - 0.6	5	19	15	43	103	205	504	1064	1697	1114	427	131	37	20	9	4	5	4	1	3	3	2	1	1	1	1	1	1	4	1	2	5	4	4	6	13	15	10	8	0.3 - 0.6	5489	9.1	
0.6 - 0.9	2	7	21	44	240	732	2166	4265	2247	532	115	32	16	2	-	-	-	-	-	-	-	-	-	-	-	-	-	-	-	-	-	-	-	-	-	-	-	-	-	-	0.6 - 0.9	10449	17.3
0.9 - 1.2	-	1	14	44	225	827	2963	6744	2749	232	41	3	-	-	-	-	-	-	-	-	-	-	-	-	-	-	-	-	-	-	-	-	-	-	-	-	-	-	-	-	0.9 - 1.2	13854	22.9
1.2 - 1.5	-	7	18	26	139	682	2570	6641	2234	116	4	1	-	-	-	-	-	-	-	-	-	-	-	-	-	-	-	-	-	-	-	-	-	-	-	-	-	-	-	-	1.2 - 1.5	12447	20.5
1.5 - 1.8	-	-	-	20	74	446	1834	4690	1482	21	-	-	-	-	-	-	-	-	-	-	-	-	-	-	-	-	-	-	-	-	-	-	-	-	-	-	-	-	-	-	1.5 - 1.8	8572	14.2
1.8 - 2.1	-	-	-	5	40	179	1035	2671	823	11	-	-	-	-	-	-	-	-	-	-	-	-	-	-	-	-	-	-	-	-	-	-	-	-	-	-	-	-	-	-	1.8 - 2.1	4765	7.9
2.1 - 2.4	-	1	1	4	14	70	436	1108	296	2	-	-	-	-	-	-	-	-	-	-	-	-	-	-	-	-	-	-	-	-	-	-	-	-	-	-	-	-	-	-	2.1 - 2.4	1932	3.2
2.4 - 2.7	-	-	-	-	1	31	103	292	65	1	-	-	-	-	-	-	-	-	-	-	-	-	-	-	-	-	-	-	-	-	-	-	-	-	-	-	-	-	-	-	2.4 - 2.7	493	0.8
2.7 - 3.0	-	-	-	-	1	3	9	37	56	6	-	-	-	-	-	-	-	-	-	-	-	-	-	-	-	-	-	-	-	-	-	-	-	-	-	-	-	-	-	-	2.7 - 3.0	112	0.2
3.0 - 3.3	-	-	-	-	-	-	2	15	2	3	-	-	-	-	-	-	-	-	-	-	-	-	-	-	-	-	-	-	-	-	-	-	-	-	-	-	-	-	-	-	3.0 - 3.3	22	0.0
3.3 - 3.6	-	-	-	-	-	-	1	1	1	-	-	-	-	-	-	-	-	-	-	-	-	-	-	-	-	-	-	-	-	-	-	-	-	-	-	-	-	-	-	-	3.3 - 3.6	3	0.0
	0	10	20	30	40	50	60	70	80	90	100	110	120	130	140	150	160	170	180	190	200	210	220	230	240	250	260	270	280	290	300	310	320	330	340	350	360						
#	16	54	80	195	357	1121	3737	12645	28652	11333	1511	358	116	51	20	15	11	12	6	6	5	4	4	3	5	10	13	7	6	13	11	28	20	33	41	42	31	60572	100				
%	0	0	0	0.3	0.6	1.9	6.2	20.9	47.3	18.7	2.5	0.6	0.2	0.1	0	0	0	0	0	0	0	0	0	0	0	0	0	0	0	0	0	0	0	0	0	0	0	0	0				

B.1.3. SWELL WAVE DATA

WAVE HEIGHT VS. WAVE PEAK PERIOD

Significant Wave Height [m]	Wave Peak Period [s]																											#	%
	3.2	3.6	3.9	4.3	4.7	5.2	5.7	6.3	6.9	7.6	8.4	9.2	10.2	11.2	12.3	13.5	14.9	16.3	18.0	19.8	21.8								
0 - 0.3	-	1	-	1	2	27	94	183	267	624	1041	1468	1751	1975	1863	1076	497	149	34	10	1	0	-	0.3	11064	18.4			
0.3 - 0.6	-	3	1	15	89	224	510	845	1303	2440	2702	1862	1339	930	768	517	191	40	5	3	1	0.3	-	0.6	13788	22.9			
0.6 - 0.9	1	2	1	41	174	447	1182	2158	2207	2664	2485	1642	1045	831	566	350	159	38	4	-	-	0.6	-	0.9	15997	26.6			
0.9 - 1.2	-	-	1	-	30	173	690	1690	2343	1933	1427	965	655	488	401	191	83	20	4	-	-	0.9	-	1.2	11094	18.4			
1.2 - 1.5	-	-	-	-	7	121	516	1191	1295	828	483	372	238	179	107	59	8	3	-	-	-	1.2	-	1.5	5407	9.0			
1.5 - 1.8	-	-	-	-	-	5	62	324	563	435	242	173	84	31	34	28	5	3	3	-	-	1.5	-	1.8	1992	3.3			
1.8 - 2.1	-	-	-	-	-	-	3	37	153	215	123	52	24	10	5	7	5	1	-	-	-	1.8	-	2.1	635	1.1			
2.1 - 2.4	-	-	-	-	-	-	-	4	26	64	62	19	3	5	2	1	-	-	-	-	-	2.1	-	2.4	186	0.3			
2.4 - 2.7	-	-	-	-	-	-	-	1	4	14	16	4	-	3	-	-	-	-	-	-	-	2.4	-	2.7	42	0.1			
2.7 - 3.0	-	-	-	-	-	-	-	-	-	2	2	6	-	1	-	-	-	-	-	-	-	2.7	-	3.0	11	0.0			
	3.2	3.6	3.9	4.3	4.7	5.2	5.7	6.3	6.9	7.6	8.4	9.2	10.2	11.2	12.3	13.5	14.9	16.3	18.0	19.8	21.8				60216	100			

WAVE HEIGHT VS. WAVE DIRECTION

Hs - Significant Wave Height [m]	Wave Direction [deg]																																				#	%			
	0	5	10	20	30	35	40	45	50	55	60	65	70	75	80	85	90	95	100	105	110	115	120	125	130	135	140	145	150	155	160	165	170	175	180						
0 - 0.3	6	207	444	1763	1177	1086	1755	2836	1524	204	35	-	-	-	-	-	-	-	-	-	-	-	-	-	-	-	-	1	1	-	-	-	-	-	-	0	-	0.3	11050	18.5	
0.3 - 0.6	19	255	502	1039	1260	1674	2942	4265	1655	67	6	-	-	-	-	-	-	-	-	-	-	-	-	-	-	-	-	1	-	-	-	-	-	-	-	0.3	-	0.6	13696	22.9	
0.6 - 0.9	3	110	360	855	1235	2103	3854	5497	1833	70	2	-	-	-	-	-	-	-	-	-	-	-	-	-	-	-	-	-	-	-	-	-	-	-	-	0.6	-	0.9	15929	26.6	
0.9 - 1.2	5	54	186	566	1043	1481	2716	3629	1254	59	2	-	-	-	-	-	-	-	-	-	-	-	-	-	-	-	-	-	-	-	-	-	-	-	-	0.9	-	1.2	11008	18.4	
1.2 - 1.5	3	38	82	313	557	864	1304	1683	483	18	-	-	-	-	-	-	-	-	-	-	-	-	-	-	-	-	-	-	-	-	-	-	-	-	-	1.2	-	1.5	5347	8.9	
1.5 - 1.8	-	8	47	124	229	375	454	605	112	12	-	-	-	-	-	-	-	-	-	-	-	-	-	-	-	-	-	-	-	-	-	-	-	-	-	1.5	-	1.8	1968	3.3	
1.8 - 2.1	-	-	5	50	70	99	182	193	27	1	-	-	-	-	-	-	-	-	-	-	-	-	-	-	-	-	-	-	-	-	-	-	-	-	-	1.8	-	2.1	629	1.1	
2.1 - 2.4	-	-	2	17	44	32	61	24	5	-	-	-	-	-	-	-	-	-	-	-	-	-	-	-	-	-	-	-	-	-	-	-	-	-	-	2.1	-	2.4	185	0.3	
2.4 - 2.7	-	-	-	3	8	2	23	5	1	-	-	-	-	-	-	-	-	-	-	-	-	-	-	-	-	-	-	-	-	-	-	-	-	-	-	2.4	-	2.7	42	0.1	
2.7 - 3.0	-	-	-	-	1	-	2	7	1	-	-	-	-	-	-	-	-	-	-	-	-	-	-	-	-	-	-	-	-	-	-	-	-	-	-	2.7	-	3.0	11	0.0	
	0	5	10	20	35	30	35	40	45	50	55	60	65	70	75	80	85	90	95	100	105	110	115	120	125	130	135	140	145	150	155	160	165	170	175	180				59865	100

Table B.3: Scatter diagram of the wind: direction vs speed. Source: [D1].

		Wind direction (\circ N)														
		-15,00	15,00	45,00	75,00	105,00	135,00	165,00	195,00	225,00	255,00	285,00	315,00			
lower	upper	15,00	45,00	75,00	105,00	135,00	165,00	195,00	225,00	255,00	285,00	315,00	345,00	sum	cum sum	
Wind speed U_{10} (m/s)	0	1	0,02	0,03	0,05	0,04	0,05	0,03	0,02	0,03	0,04	0,02	0,01	0,03	0,37	0,37
	1	2	0,05	0,08	0,13	0,16	0,11	0,09	0,05	0,03	0,04	0,02	0,05	0,05	0,87	1,24
	2	3	0,07	0,11	0,30	0,43	0,28	0,11	0,05	0,03	0,05	0,04	0,06	0,05	1,56	2,79
	3	4	0,06	0,12	0,45	1,06	0,61	0,10	0,02	0,02	0,03	0,03	0,06	0,05	2,60	5,40
	4	5	0,01	0,08	0,70	2,44	1,08	0,06	0,01	0,00	0,02	0,02	0,04	0,02	4,48	9,88
	5	6	0,01	0,03	1,05	5,69	1,92	0,03	0,00	-	0,00	0,01	0,03	0,00	8,80	18,68
	6	7	-	0,03	1,42	11,69	3,23	0,03	0,00	-	0,00	0,01	0,01	0,01	16,45	35,13
	7	8	0,00	0,03	1,25	18,45	4,03	0,01	-	-	0,00	0,02	0,00	-	23,81	58,94
	8	9	-	0,01	0,85	19,28	3,37	0,01	-	-	0,00	0,01	0,00	-	23,54	82,48
	9	10	-	0,00	0,32	11,58	1,58	0,00	-	0,00	0,00	-	-	-	13,48	95,96
	10	11	-	-	0,09	3,15	0,34	0,00	-	-	-	0,01	-	-	3,58	99,54
	11	12	-	-	0,00	0,39	0,03	-	-	-	-	0,00	-	-	0,43	99,98
	12	13	-	-	0,00	0,02	0,00	-	-	-	-	-	-	-	0,02	100,00
	13	14	-	-	-	-	-	-	-	-	-	-	-	-	-	100,00
	14	15	-	-	-	-	-	-	-	-	-	-	-	-	-	100,00
	15	16	-	-	-	-	-	-	-	-	-	-	-	-	-	100,00
	16	17	-	-	-	-	-	-	-	-	-	-	-	-	-	100,00
	17	18	-	-	-	-	-	-	-	-	-	-	-	-	-	100,00
	18	19	-	-	-	-	-	-	-	-	-	-	-	-	-	100,00
	19	20	-	-	-	-	-	-	-	-	-	-	-	-	-	100,00
	20	21	-	-	-	-	-	-	-	-	-	-	-	-	-	100,00
	21	22	-	-	-	-	-	-	-	-	-	-	-	-	-	100,00
	22	23	-	-	-	-	-	-	-	-	-	-	-	-	-	100,00
	23	24	-	-	-	-	-	-	-	-	-	-	-	-	-	100,00
	24	25	-	-	-	-	-	-	-	-	-	-	-	-	-	100,00
sum		0,22	0,52	6,62	74,36	16,65	0,48	0,15	0,11	0,19	0,22	0,26	0,22	100,00		

WIND DIRECTION

To better visualise the predominant wind direction at Curaçao a wind rose has been plotted in Figure B.2. It confirms the dominant wind direction.

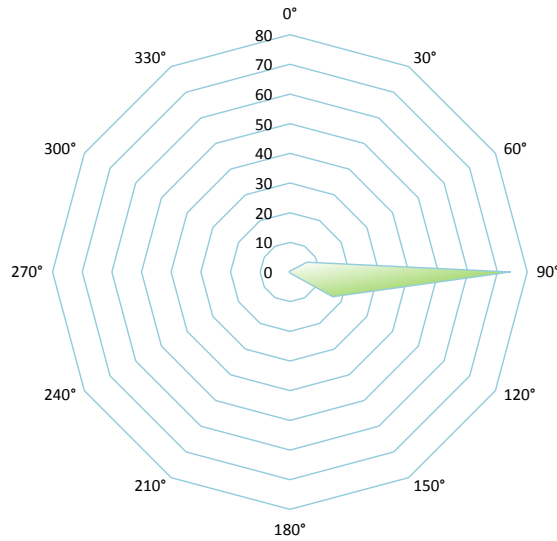


Figure B.2: Distribution of the wind over the directions it is blowing from according to the data from ECMWF [D1].

CUMULATIVE DISTRIBUTION OF WIND SPEED

The next plot shows the cumulative distribution of the wind speeds at Curaçao.

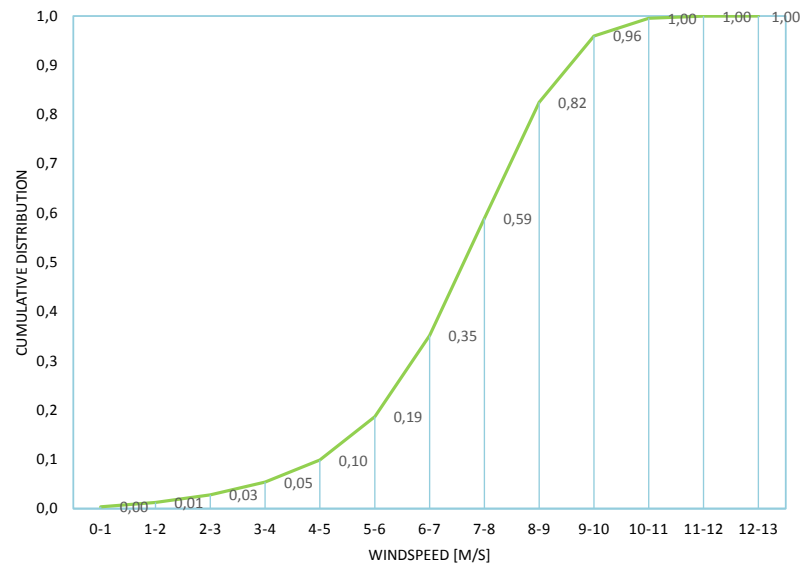


Figure B.3: Cumulative distribution plot of the wind speeds at Curaçao according to data from ECMWF [D1].

WIND VELOCITY

Visualising the probability of occurrence of the blowing wind speeds helps to show the small bandwidth of wind speeds that predominantly blow at Curaçao.

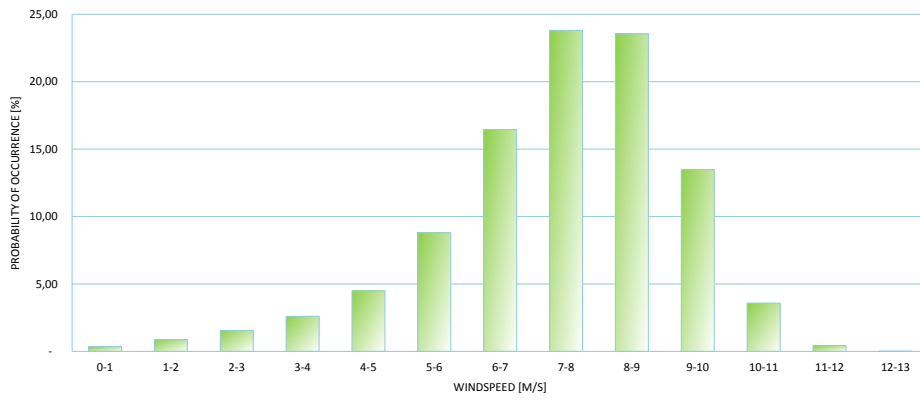


Figure B.4: The wind speed plotted in a bar chart. From this plot it can easily be concluded that the governing wind speeds is between 7-9 m/s.

SWAN MODEL SET-UP

This appendix discusses important aspects in further detail with respect to the SWAN Model initialisation. In §C.1 the importance of wind on the wave model is shown. The second section presents the used command file for this study.

C.1. SET-UP OF MODEL DOMAIN WITH BOUNDARIES

A model needs to be bounded because only a limited space can be taken into account to reduce time and cost. The SWAN Model uses a computational grid to define the model domain. On the boundaries of this grid, boundary conditions are imposed that influence this model domain. In this case, boundary conditions are waves from the northern and eastern boundaries. Wind is imposed on the entire model space.

The definition of the computational grid and its boundaries is shown visually in Figure C.2.

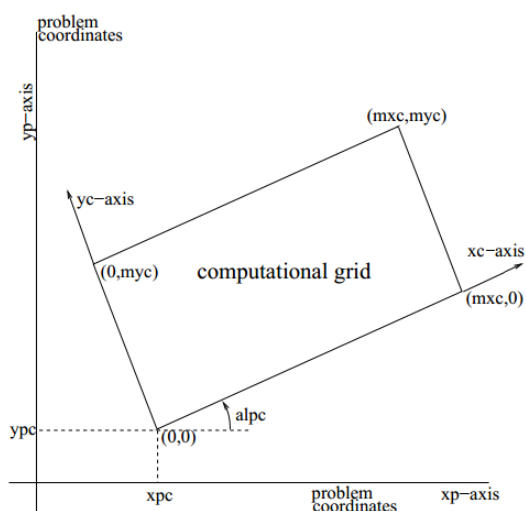


Figure C.1: Computational grid as used by the software SWAN [10].

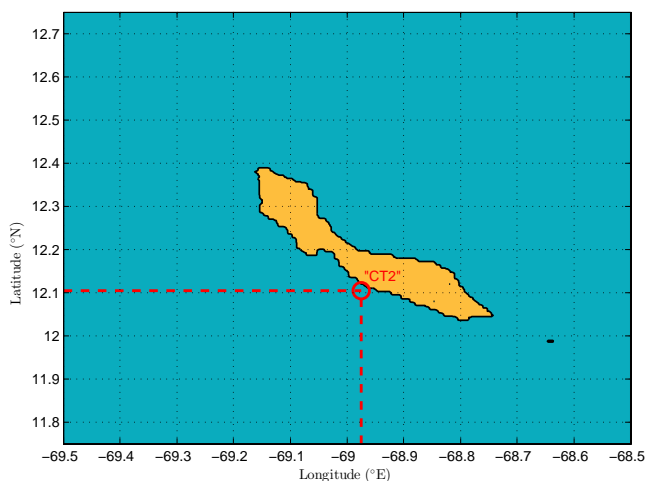


Figure C.2: Defined boundaries of the computational grid for the model.

IMPOSED BOUNDARY WAVES

To impose boundary waves propagating into the model domain, SWAN requires a number of parameters. Firstly, the boundary is defined with two coordinates. The boundary wave spectra are constant along the side. They are defined by means of the spectral parameters: significant wave height, peak wave period, peak wave direction and the coefficient of directional spreading.

These parameters are implemented in the SWAN command file in the following way. Note that lines beginning with an exclamation mark are comments.

```
!Eastern Boundary [Boundary Coordinates ]
BOUNDSPEC SEGMENT XY -68.5 11.75 -68.5 12.75 CONSTANT PAR [Hs] [Tp] [θ] [σθ]
!Northern Boundary [Boundary Coordinates ]
BOUNDSPEC SEGMENT XY -69.5 12.75 -68.5 12.75 CONSTANT PAR [Hs] [Tp] [θ] [σθ]
```

In which:

- [H_s] = Significant wave height [m]
- [T_p] = Peak wave period [s]
- [θ] = Wave direction [$^\circ$]
- [σ_θ] = Directional spreading of waves [$^\circ$]

C.2. THE IMPORTANCE AND INFLUENCE OF WIND ON THE WAVE MODEL

Wind is added to the SWAN model by placing the following line in de SWAN command file:

```
WIND [u10] [θwind]
```

In which:

[u₁₀] = wind velocity at 10 m elevation [m/s]
 [θ_{wind}] = wind direction at 10m elevation [°]

To show the influence of wind on the model, two runs have been executed with the parameters of Table C.1. The first run (left in Figure C.3) has been executed without any wind added to the model. The second run (Figure 4.4) shows the model with wind added to the model. The two figures clearly shows a significant difference in the significant wave height close to the island. It can be concluded that the wave height, defined at the eastern and northern boundary decay very fast without wind.

The goal of the preliminary run is to determine the wind speed for a particular scenario at which the waves maintain their wave height as specified on the boundaries. Accurate results can only be obtained when the waves maintain their wave height while propagating through the model domain.

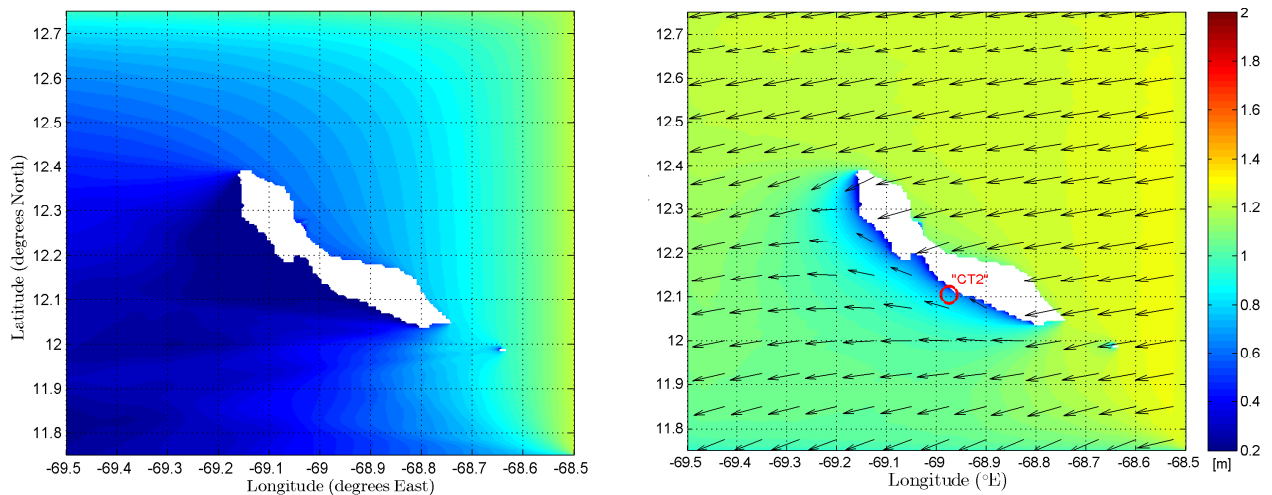


Figure C.3: Differences in significant wave height H_s for Scenario W2A without (left) and with wind (right). $u_{10} = 7.7\text{m/s}$, $\theta_{wind} = 80^\circ$

C.3. OVERVIEW OF DEFINED SCENARIOS

Key scenarios are defined to determine the local wave climate with the limited computational capacity available for this study. In a extensive wave climate study, runs are made for every cell in a wave scatter diagram. The required capacity can be limited by defining scenarios, which represent a combination of range of wave parameters.

The defined scenarios that will be simulated in SWAN and AQWA are defined in the table below. This table shows the characteristic parameters of all scenarios. The probability of exceedance indicates how often the conditions of a particular scenario are exceeded. More severe the conditions, occur less often.

Scatter diagrams have been created from the BMT ARGUSS data set. A distinction is made between swell waves and wind sea waves. These scatter diagrams visualise the range of values that each scenario represents. Not all parts of the scatter diagram are considered. These areas are market in grey. The wave period in these areas are too low to be of significance in the hydrodynamic study.

C.3.1. SWELL WAVE SCENARIOS VISUALISED IN SCATTER DIAGRAMS

The following two tables show the wave scatter diagrams for swell: the first table relates the significant wave height to the wave direction; the second table relates the significant wave height with the peak wave period.

Table C.1: Different scenarios for boundary wave conditions run in SWAN-model. These are determined from the wave scatter diagrams in §B.1.

Wind sea waves								Swell waves							
#	H_s	T_p	θ_{wave}	σ_θ	u_{10}	θ_{wind}	P_E	#	H_s	T_p	θ_{wave}	σ_θ	u_{10}	θ_{wind}	P_E
[-]	[m]	[s]	[°]	[°]	[m/s]	[°]	[-]	[-]	[m]	[s]	[°]	[°]	[m/s]	[°]	[%]
W1A	0.6	5.2	80	30	5.8	80	70.3	S1A	0.3	8.4	70	15	4.9	70	
								S1B	0.3	11.2	70	15	5.2	70	58.6
								S1C	0.3	16.3	70	15	5.6	70	
W2A	1.2	5.2	80	30	7.7	80		S2A	0.9	8.4	70	15	6.6	70	
W2B	1.2	6.9	80	30	7.4	80	26.4	S2B	0.9	8.4	50	15	6.6	50	13.6
W2D	1.2	5.2	70	30	7.8	70		S2C	0.9	8.4	80	15	6.6	80	
W2E	1.2	5.2	90	30	7.8	90		S2E	0.9	11.2	70	15	6.6	70	
W3A	1.8	6.3	80	30	9.5	80	4.2	S3A	1.5	11.2	70	15	7.5	70	1.4
W3C	2.7	6.9	80	30	11.7	80	0.1	S3C	2.1	8.4	70	15	9.2	70	0.1

Table C.2: Swell wave scatter diagram of the significant wave height related to the wave direction. It visualises the covered areas of the defined swell wave scenarios.

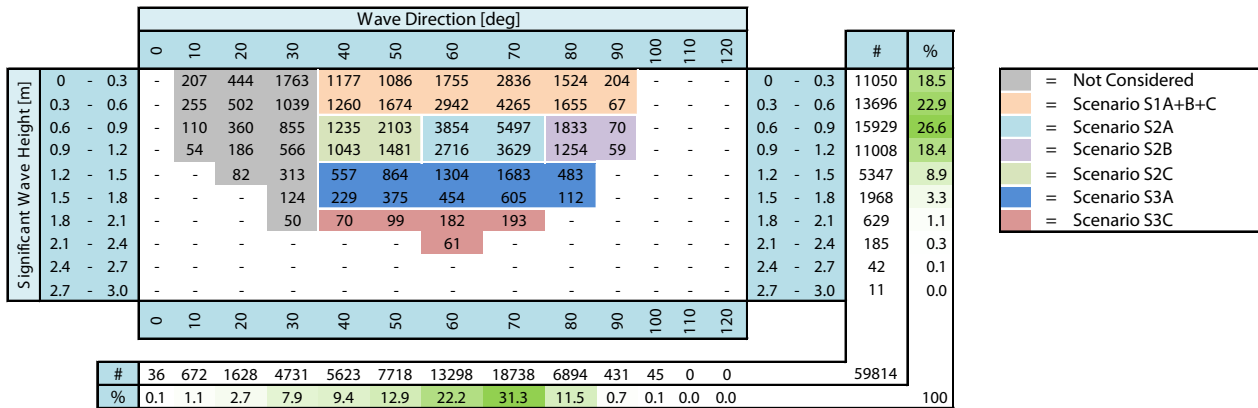
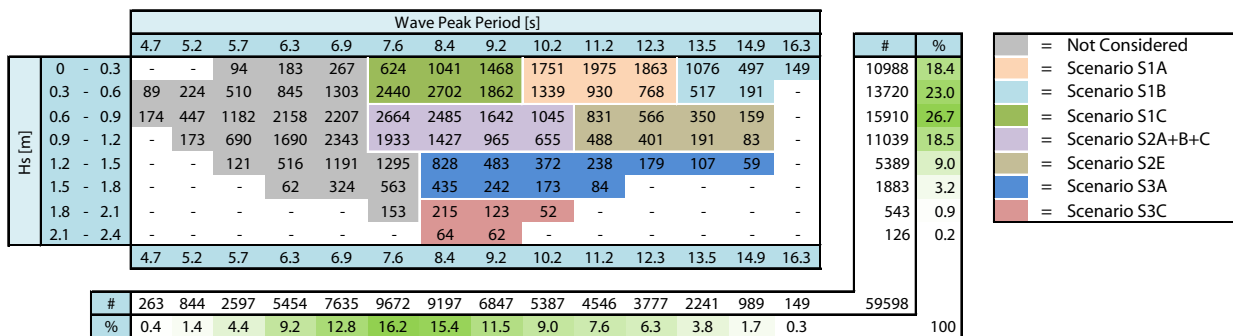


Table C.3: Swell wave scatter diagram showing the covered area with respect to the peak wave period of the defined scenarios.



C.3.2. WIND SEA WAVE SCENARIOS VISUALISED IN SCATTER DIAGRAMS

Just like above, wind wave scatter diagrams are created to visualise the range of parameters for each scenario. Parts of the scatter diagrams that are not considered because of their very short wave periods are marked in grey.

Table C.4: Wind sea wave scatter diagram showing the wave parameters that each wave scenario represents for this model.

		Wave Direction [deg]													#	%			
		0	10	20	30	40	50	60	70	80	90	100	110	120					
Significant Wave Height [m]	0 - 0.3	-	-	50	97	111	180	254	421	486	314	169	67	-	0 - 0.3	2149	3.6		
	0.3 - 0.6	-	-	-	-	103	205	504	1064	1697	1114	427	131	-	0.3 - 0.6	5245	8.8		
	0.6 - 0.9	-	-	-	-	-	240	732	2166	4265	2247	532	115	-	0.6 - 0.9	10297	17.3		
	0.9 - 1.2	-	-	-	-	-	-	225	827	2963	6744	2749	232	-	0.9 - 1.2	13740	23.1		
	1.2 - 1.5	-	-	-	-	-	-	-	139	682	2570	6641	2234	116	-	1.2 - 1.5	12382	20.8	
	1.5 - 1.8	-	-	-	-	-	-	-	-	74	446	1834	4690	1482	-	1.5 - 1.8	8526	14.3	
	1.8 - 2.1	-	-	-	-	-	-	-	-	-	179	1035	2671	823	-	1.8 - 2.1	4708	7.9	
	2.1 - 2.4	-	-	-	-	-	-	-	-	-	-	70	436	1108	296	-	2.1 - 2.4	1910	3.2
	2.4 - 2.7	-	-	-	-	-	-	-	-	-	-	-	103	292	65	-	2.4 - 2.7	460	0.8
	2.7 - 3.0	-	-	-	-	-	-	-	-	-	-	-	-	56	-	-	2.7 - 3.0	56	0.1
		0	10	20	30	40	50	60	70	80	90	100	110	120					
		#	0	0	50	97	214	1063	3694	12592	28650	11324	1476	313	0		59473		
		%	0	0	0	0	0	2	6	21	48	19	2	1	0			100	

Grey	=	Not Considered
Orange	=	Scenario W1A
Light Blue	=	Scenario W2A
Purple	=	Scenario W2D
Light Green	=	Scenario W2E
Dark Blue	=	Scenario W3A
Red	=	Scenario W3C

Table C.5: Wind sea wave scatter diagram showing the covered area with respect to the peak wave period of the different scenarios.

		Wave Peak Period [s]										#	%	
		3.2	3.6	3.9	4.3	4.7	5.2	5.7	6.3	6.9	7.6			
Significant Wave Height [m]	0 - 0.3	326	195	96	-	-	-	-	-	-	-	617	1.1	
	0.3 - 0.6	1060	1480	1220	756	359	128	-	-	-	-	5003	8.6	
	0.6 - 0.9	-	377	1412	3302	3042	1586	516	110	-	-	10345	17.9	
	0.9 - 1.2	-	-	64	785	3513	5372	3106	774	165	62	13841	23.9	
	1.2 - 1.5	-	-	-	-	414	3421	5177	2694	574	122	12402	21.4	
	1.5 - 1.8	-	-	-	-	-	320	3110	3726	1210	172	8538	14.7	
	1.8 - 2.1	-	-	-	-	-	-	316	2486	1589	332	4723	8.2	
	2.1 - 2.4	-	-	-	-	-	-	-	349	1179	366	1894	3.3	
	2.4 - 2.7	-	-	-	-	-	-	-	-	240	208	448	0.8	
	2.7 - 3.0	-	-	-	-	-	-	-	-	-	75	75	0.1	
		3.2	3.6	3.9	4.3	4.7	5.2	5.7	6.3	6.9	7.6			
		#	1386	2052	2792	4843	7328	10827	12225	10139	4957	1337		57886
		%	2.4	3.5	4.8	8.4	12.7	18.7	21.1	17.5	8.6	2.3		100

C.4. SWAN COMMAND FILE

This section presents the used command file as input to run the SWAN model. SWAN is one single computer program which requires this command file and additional input files before it can be run successfully. This command file contains all important commands, parameters and paths to other input files needed. For the sake of completeness and any desired additional research, this command file is given below.

Listing C.1: SWAN Command File for Simulation of Local Wave Climate

```

!***** HEADING *****
! Witteveen+Bos, 2015 *
! Wave transformation from deep-water to near-shore *
! X. Groenenberg *
! *
PROJECT 'Model' '[**_**]' *
! 'MSc Thesis' *
! 'Scenarios with different periods and angles' *
!*****

!***** GENERAL SETTINGS *****
SET DEPMIN = 0.05 MAXMES = 1000 MAXERR = 2 _
GRAV = 9.81 RHO = 1025.00 INRHOG = 0 NAUT
SET LEVEL 0
MODE STATIONARY TWOD

!***** MODEL SETUP *****
COORD SPHE CCM
! READ GRID
CGRID CURV 400 400 EXCEPT 0.0 0.0 CIR 120 0.03 1.00
READGRID COOR 1. './Input/Model.grd' IDLA=3 NHEDF=3 FORMAT '(10X,5E26.17)'
! READ BATH
INPGRID BOTTOM CURV 0. 0. 400 400
READINP BOTTOM 1.0 './Input/Model.dep' 3 0 FREE
! READ WIND
WIND [Wind speed] [Wind direction]

!***** BOUNDARY CONDITIONS *****
BOUND SHAPE JONSWAP 3.3 PEAK DEGREES
! Eastern Boundary
BOUNDSPC SEGMENT XY -68.5 11.75 -68.5 12.75 CONSTANT PAR [Hsig] [Tp] [Dir.] [Dir. deviation]
! Northern Boundary
BOUNDSPC SEGMENT XY -69.5 12.75 -68.5 12.75 CONSTANT PAR [Hsig] [Tp] [Dir.] [Dir. deviation]

!***** PHYSICS *****
GEN3 WESTH
WCAP KOM
BREA CON alpha=1
FRIC JONSWAP cfjon=0.038000
TRIAD
DIFFRAC
LIMITER ursell=10.0000 qb=1.00000

!***** NUMERICS *****
NUM STOPC 0.00 0.02 0.01 98.0 STAT 30

!***** OUTPUT REQUESTS *****
QUANT Hswell fswell = 0.1
OUTPUT OPTIONS TABLE 16 BLOCK 9 12 SPEC 8

BLOCK 'COMPGRID' NOHEAD 'Out_[**_**].mat' XP YP HSIGN TMM10 TPS DIR STEEPNESS &
HSWELL PDIR TM01 TM02 RTP QB DEPTH BOTLEV &
TDIR WLEN WIND FORCE DISSIP DISWCAP DISSURF QB GENERAT GENWIND

POIN 'output' FILE './Input/I_XY_check.pnt'
TABLE 'output' HEADER 'Out_[**_**].tbl' XP YP HSIGN TMM10 TPS DIR&
DEP HSWELL TM02 PDIR WLEN WIND TM01 RTP
SPECOUT 'output' SPEC1D ABSOLUTE './output/41/SpecOut_[**_**].spe'
COMPUTE STATIONARY
STOP
!***** End of File *****

```


APPENDIX **D**

SWAN MODEL RESULTS

This appendix presents the results of the SWAN model. All scenarios have been simulated, resulting in much data. From this data the local wave climate is estimated and the data describing this will be used as input for the motion dynamics model. To be able to do this, all the output data is processed and parameters are visualised in plots. The goal of the model is to transform the deep-sea wave climate data to near-shore wave climate data at project location *CT2*. The processed and plotted data helps determining what happens with these deep water waves while propagating into the model domain, towards the project location.

D.1. PARAMETER COMPARISON BETWEEN INITIAL SCENARIOS AND SIMULATED LOCAL WAVE CLIMATE RESULTS

To get a picture of the local wave climate, scenarios have been determined. These scenarios are imposed as boundary conditions in the SWAN model. The output of each scenario has been organised in Tables D.2 and D.1. These tables include the parameters H_s , T_p and θ , but the calculated data is not limited to only these parameters.

A distinction has been made between wind sea waves and swell waves. This is because both types of waves have a different influence on the dynamic response of a floating structure. Table D.1 shows the results of the different scenarios for wind sea waves. The results of the simulations for swell waves are given in Table D.2.

The first column of the tables show the initial parameter values, corresponding with the different scenarios. The column with the header '*CT2*' shows the simulated wave parameters at the project location. The third column with the header ' Δ ' shows the difference between the first and the second column.

Table D.1: Results and difference between the swell waves imposed on the boundaries and the waves near the project location.

Swell waves									
#	Input			CT2			Δ		
	H_s	T_p	θ	H_s	T_p	θ	H_s	T_p	θ
[–]	[m]	[s]	[°]	[m]	[s]	[°]	[m]	[s]	[°]
S1A	0.3	8.4	70	0.34	8.3	69.6	+0.04	–0.1	–0.4
S1B	0.3	11.2	70	0.33	11.1	69.6	+0.03	–0.1	–0.4
S1C	0.3	16.3	70	0.29	16.0	69.6	–0.01	–0.3	–0.4
S2A	0.9	8.4	70	0.38	2.8	112.7	–0.52	–5.6	+52.7
S2B	0.9	8.4	50	0.31	2.5	113.8	–0.59	–5.9	+63.8
S2C	0.9	8.4	80	0.42	2.8	125.3	–0.48	–5.6	+45.3
S2E	0.9	11.2	70	0.37	2.6	121.0	–0.53	–8.6	+51.0
S3A	1.5	11.2	70	0.48	2.8	122.8	–1.02	–8.4	+52.8
S3C	2.1	8.4	70	0.73	3.5	127.5	–1.37	–4.9	+58.0

Table D.2: Results and difference between the wind sea waves imposed on the boundaries and the waves near the project location.

Wind sea waves

#	Input			CT2			Δ		
	H_s [m]	T_p [s]	θ [°]	H_s [m]	T_p [s]	θ [°]	H_s [m]	T_p [s]	θ [°]
W1A	0.60	5.2	80.0	0.62	5.2	76.8	+0.00	+0.0	-3.2
W2A	1.20	5.2	80.0	0.61	3.2	129.3	-0.59	-2.0	+49.3
W2B	1.20	6.9	80.0	0.56	3.1	127.4	-0.64	-3.8	+47.4
W2D	1.20	5.2	70.0	0.59	3.2	127.3	-0.61	-2.0	+57.3
W2E	1.20	5.2	90.0	0.71	3.5	133.3	-0.49	-1.7	+43.3
W3A	1.80	6.3	80.0	0.84	3.7	130.1	-0.94	-2.6	+50.1
W3C	2.70	6.9	80.0	1.20	4.4	132.0	-1.50	-2.5	+52.0

D.2. PLOTS OF SCENARIO RESULTS

All described scenarios have been modelled with SWAN. This is required to estimate the local wave climate. Additionally, it is easier to understand what happens with the propagating waves while bending around the island. Because modelling all these scenarios leads to large amounts of data, plots have been made of key parameters. These parameters are in this case the significant wave height, peak wave period and the dominant wave direction. The plots of these parameters help to visualise the model results. From these plots it is possible to get a better understanding of the situation. Additional plots are made in the next section that go further into the details of the results.

The results presented in this section are sorted by parameter. For each parameter, the plots are grouped together by wave type: Swell waves, or Wind waves. Section [D.2.1](#) presents the results for the significant wave height. The plots of the peak wave period are given in [§D.2.2](#). Finally, the dominant wave propagation direction is given for swell and wind waves in [§D.2.3](#).

The scales of the plots are generally the same for each wave type. Keep in mind that the scale limits for the more extreme scenarios *S3* and *W3* can be different from the other scenarios.

D.2.1. SIGNIFICANT WAVE HEIGHT IN THE CASE OF WIND SEA WAVES ON THE BOUNDARIES

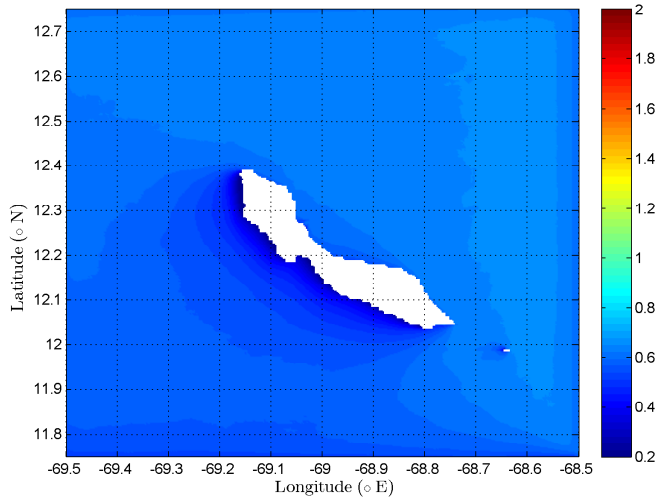


Figure D.1: Scenario W1A: Significant wave height

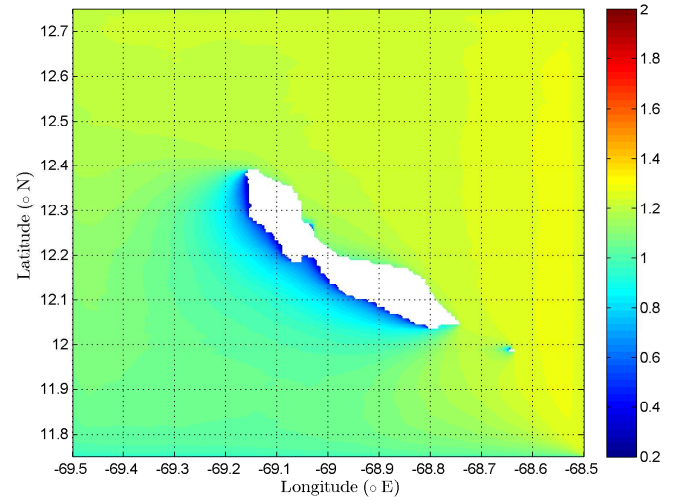


Figure D.2: Scenario W2A: Significant wave height

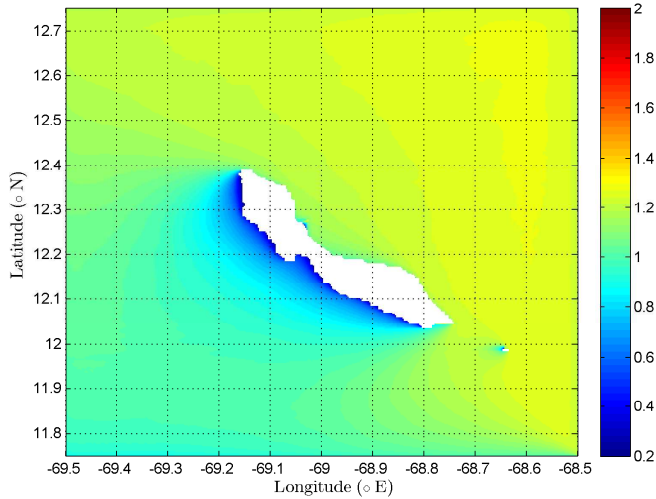


Figure D.3: Scenario W2B: Significant wave height

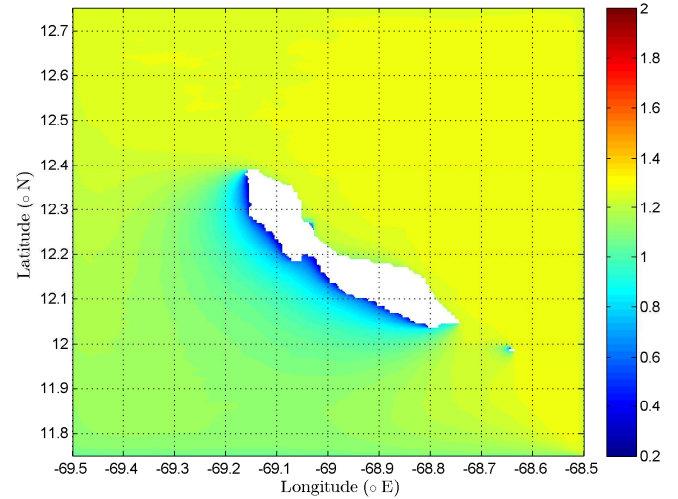


Figure D.4: Scenario W2D: Significant wave height

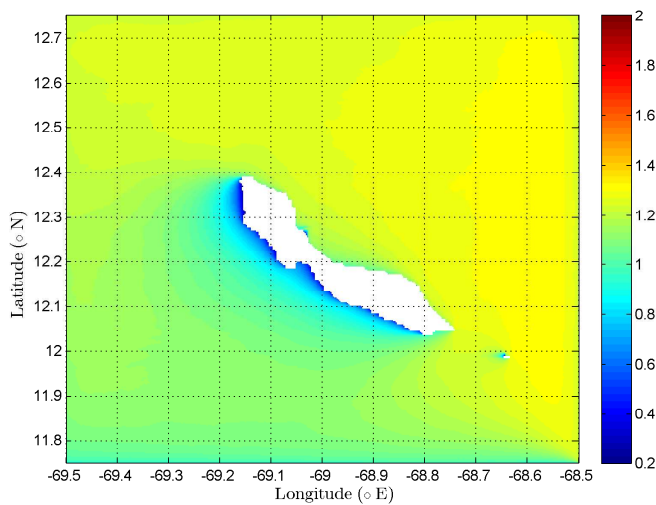


Figure D.5: Scenario W2E: Significant wave height

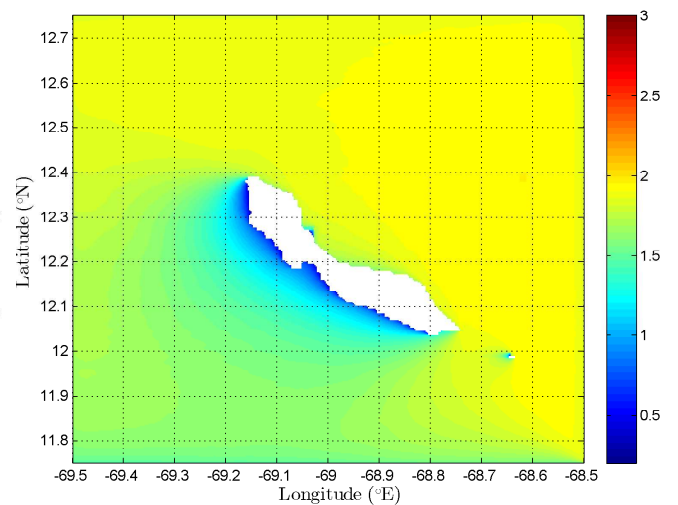


Figure D.6: Scenario W3A: Significant wave height

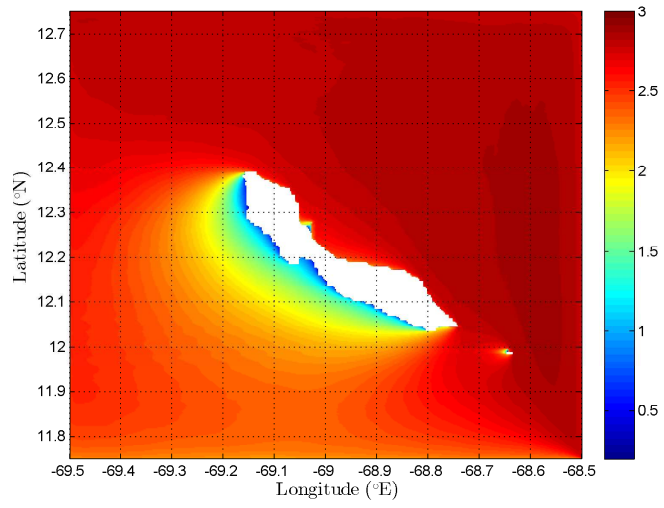


Figure D.7: Scenario W3C: Peak wave period

IN THE CASE OF SWELL WAVES ON THE BOUNDARIES

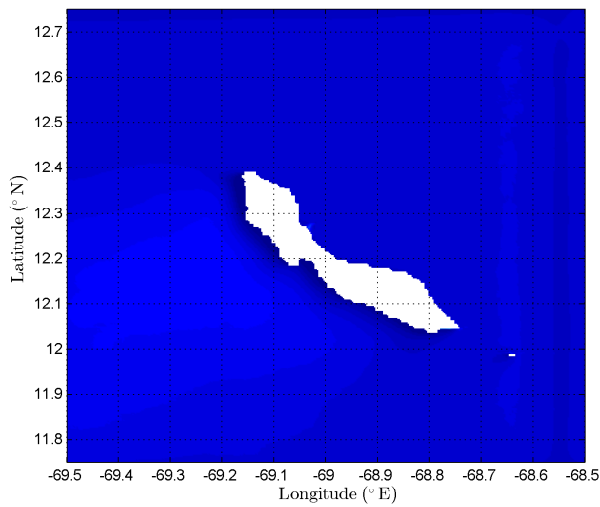


Figure D.8: Scenario S1A: Significant wave height

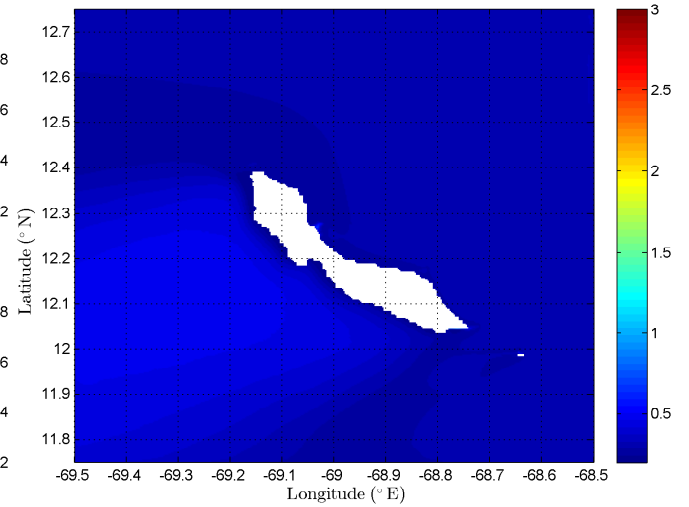


Figure D.9: Scenario S1B: Significant wave height

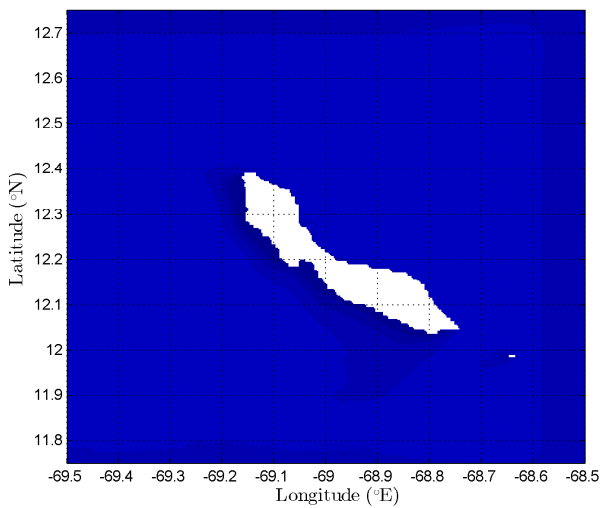


Figure D.10: Scenario S1C: Significant wave height

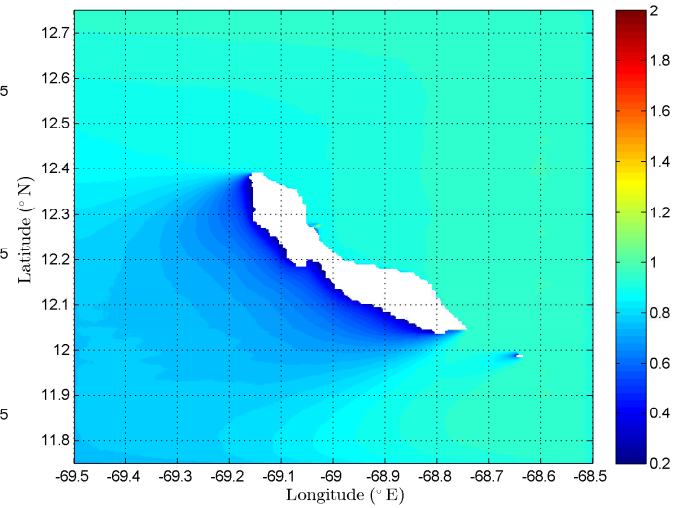


Figure D.11: Scenario S2A: Significant wave height

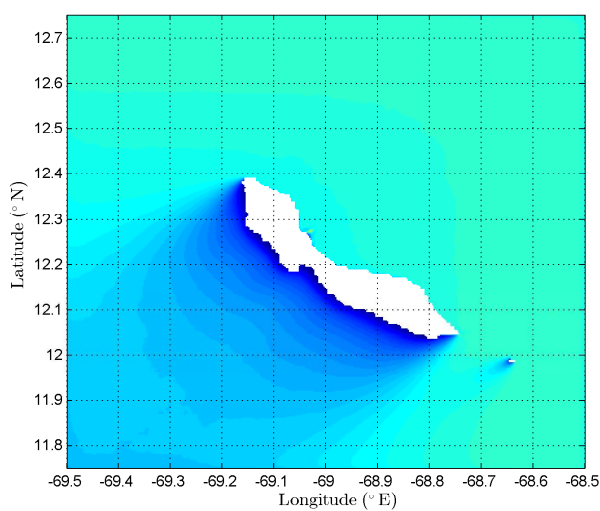


Figure D.12: Scenario S2B: Significant wave height

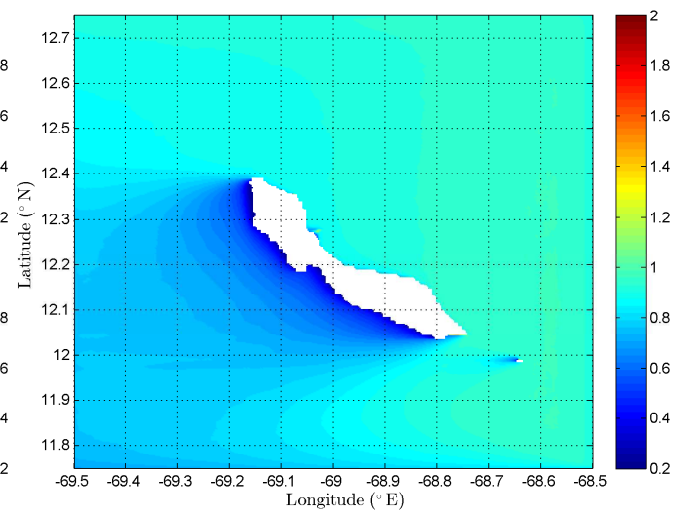


Figure D.13: Scenario S2C: Significant wave height

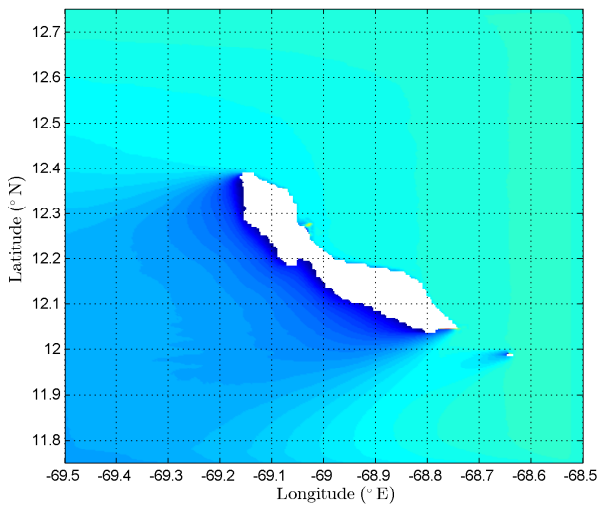


Figure D.14: Scenario S2E: Significant wave height

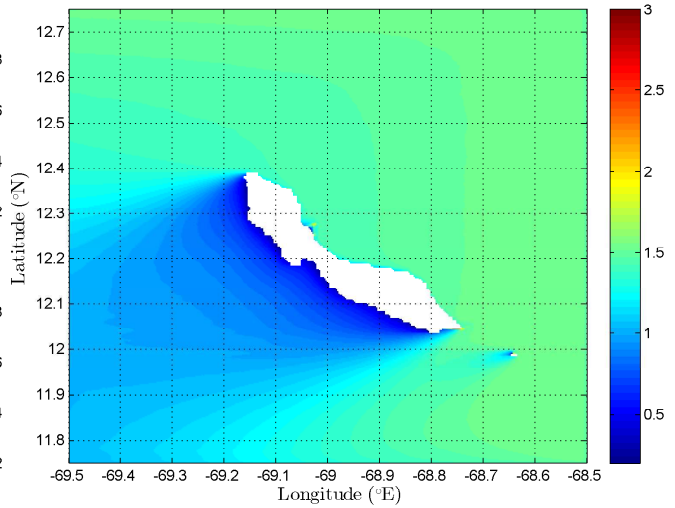


Figure D.15: Scenario S3A: Significant wave height

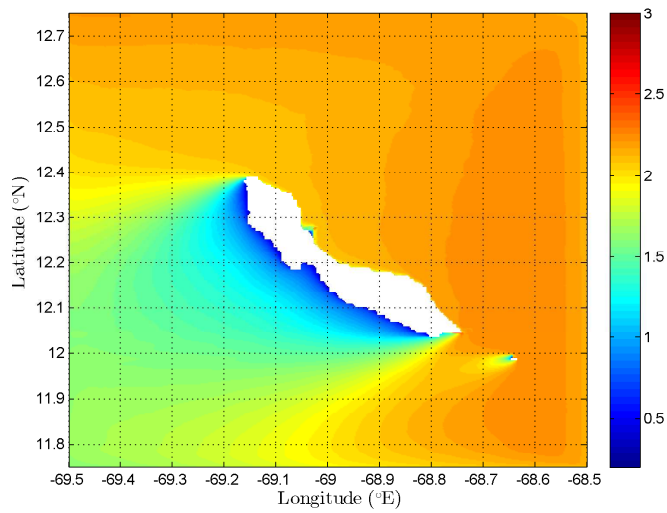


Figure D.16: Scenario S3C: Significant wave height

D.2.2. PEAK WAVE PERIOD

IN THE CASE OF WIND SEA WAVES ON THE BOUNDARIES

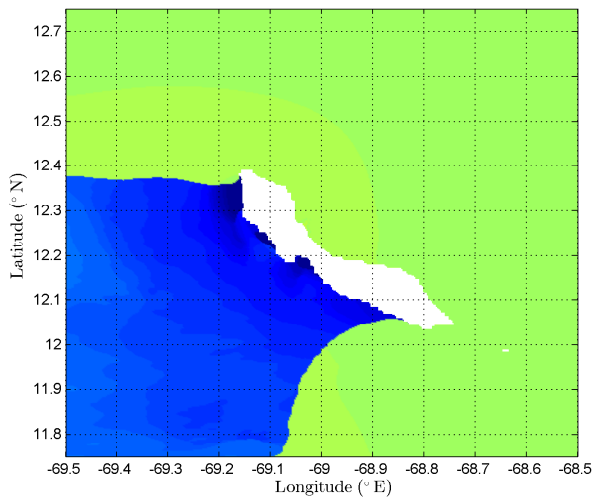


Figure D.17: Scenario W1A: Peak wave period

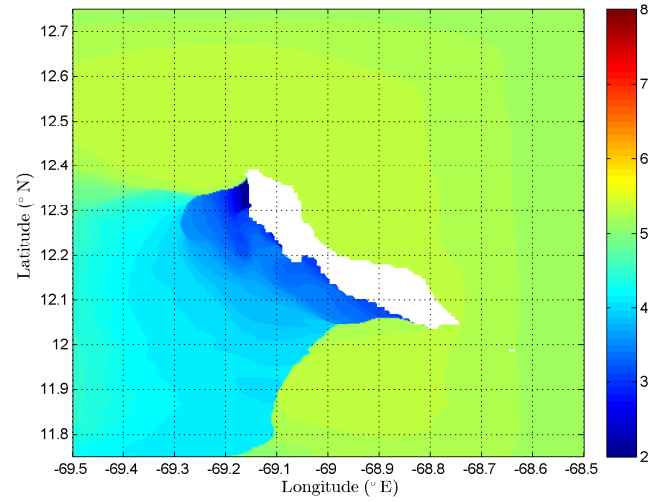


Figure D.18: Scenario W2A: Peak wave period

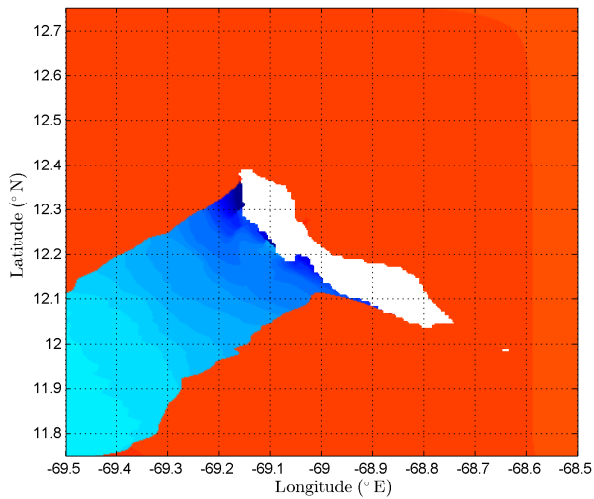


Figure D.19: Scenario W2B: Peak wave period

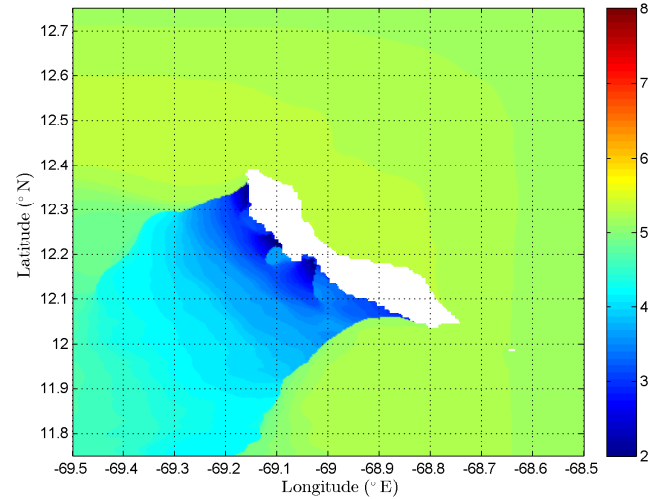


Figure D.20: Scenario W2D: Peak wave period

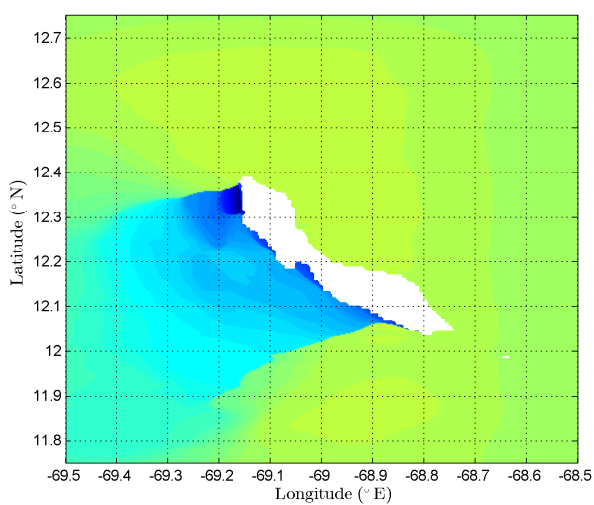


Figure D.21: Scenario W2E: Peak wave period

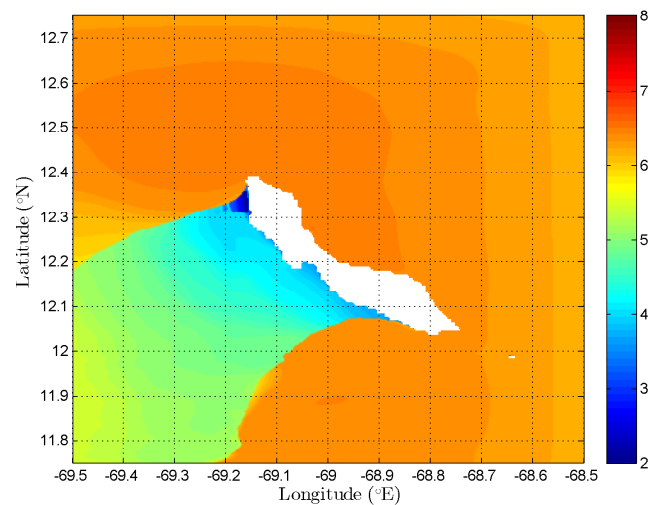


Figure D.22: Scenario W3A: Peak wave period

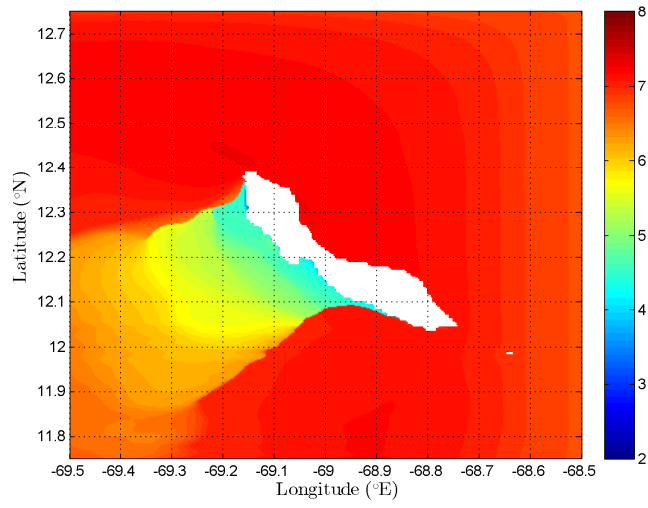


Figure D.23: Scenario W3C: Peak wave period

IN THE CASE OF SWELL WAVES ON THE BOUNDARIES

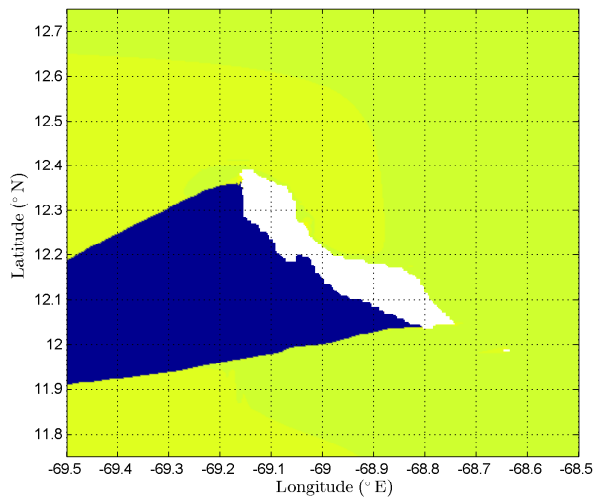


Figure D.24: Scenario S1A: Peak wave period

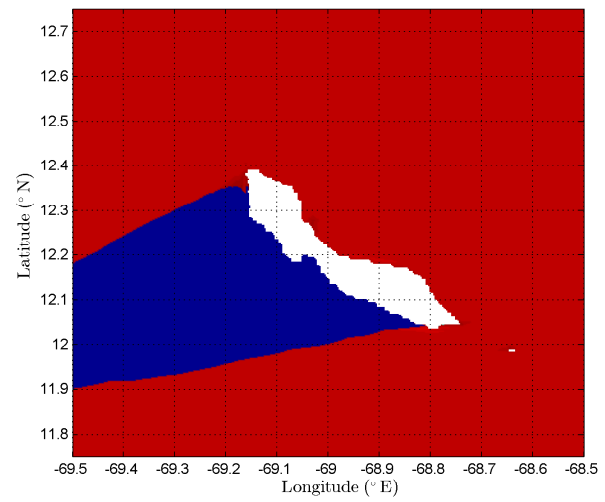


Figure D.25: Scenario S1B: Peak wave period

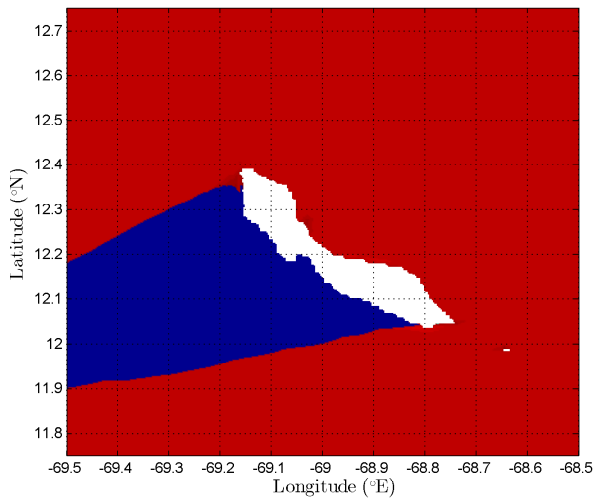


Figure D.26: Scenario S1C: Peak wave period

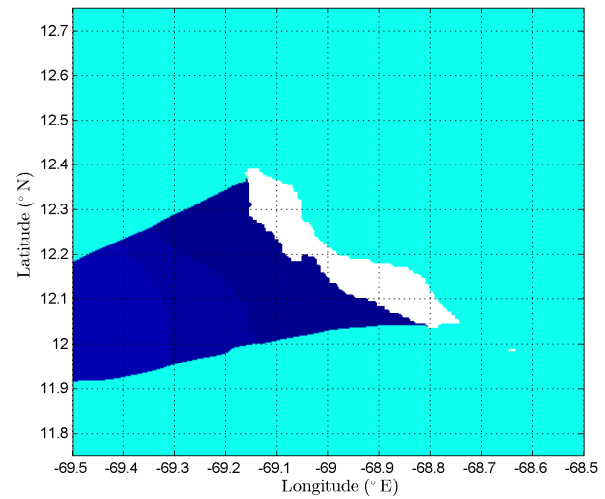


Figure D.27: Scenario S2A: Peak wave period

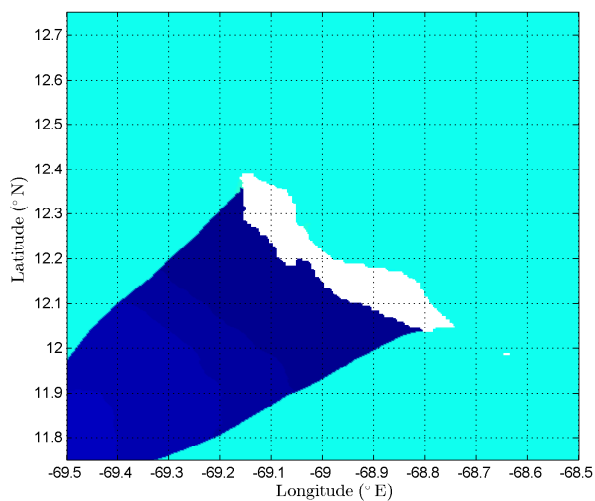


Figure D.28: Scenario S2B: Peak wave period

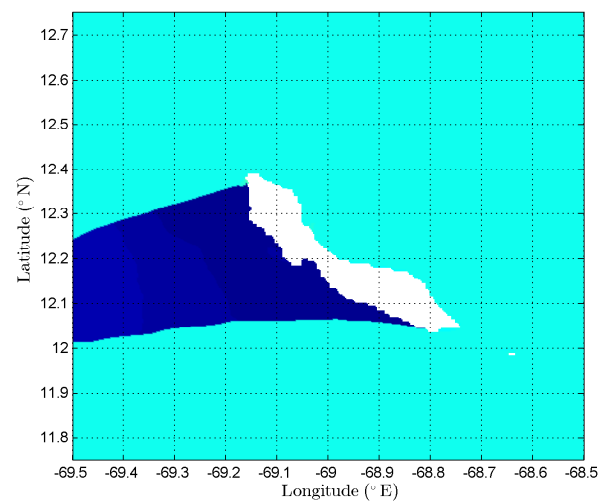


Figure D.29: Scenario S2C: Peak wave period

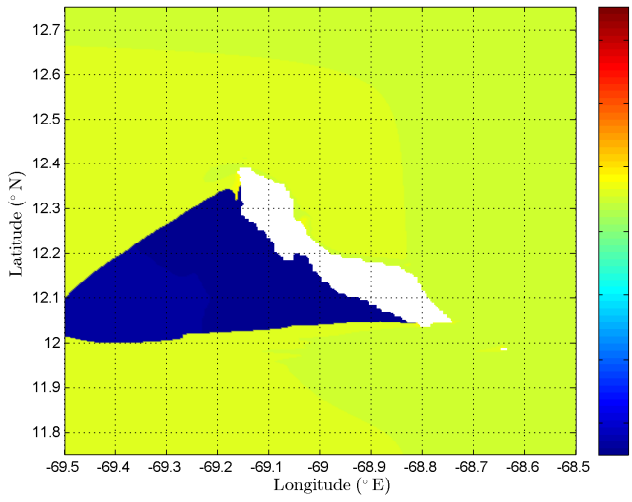


Figure D.30: Scenario S2E: Peak wave period

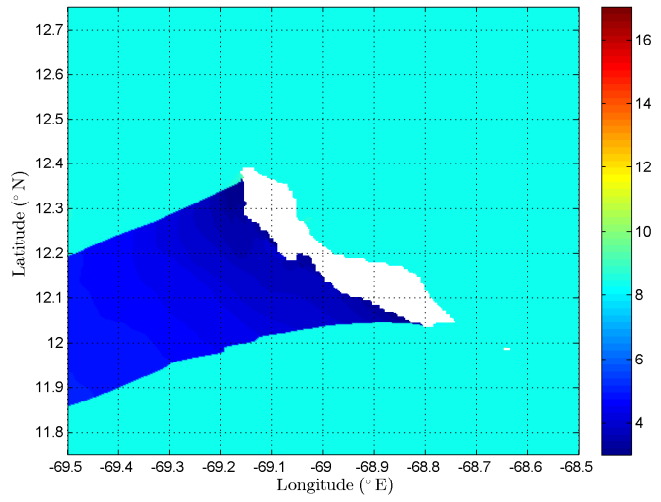


Figure D.31: Scenario S3A: Peak wave period

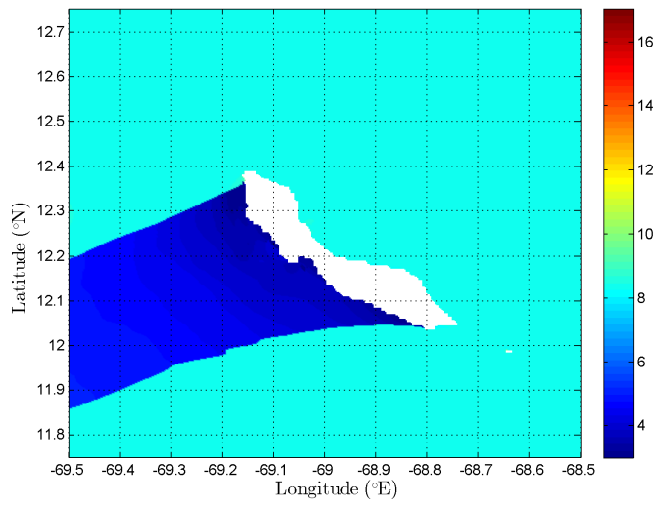


Figure D.32: Scenario S3C: Peak wave period

D.2.3. DIRECTION OF WAVE PROPAGATION IN THE CASE OF WIND SEA WAVES ON THE BOUNDARIES

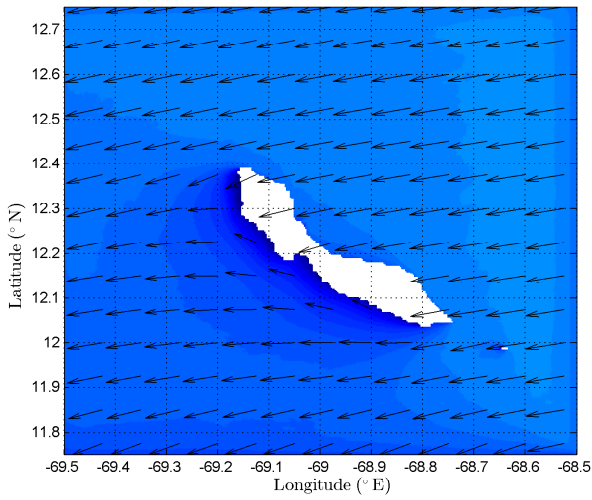


Figure D.33: Scenario W1A: Wave Direction

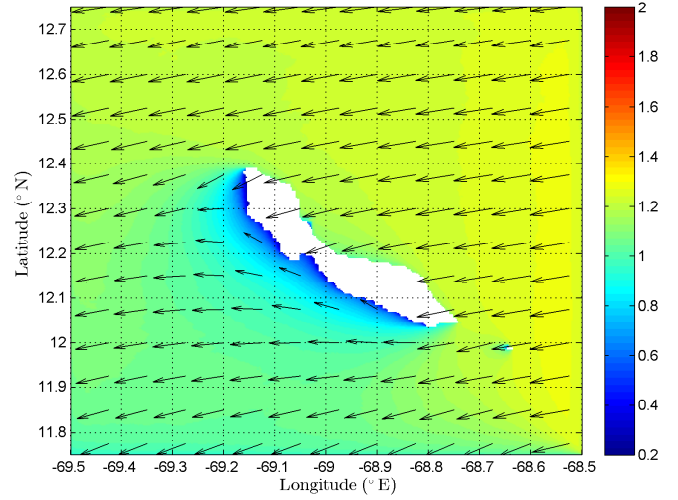


Figure D.34: Scenario W2A: Wave Direction

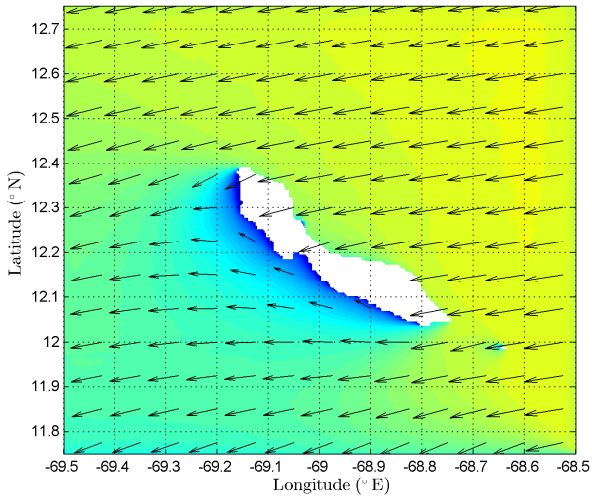


Figure D.35: Scenario W2B: Wave Direction

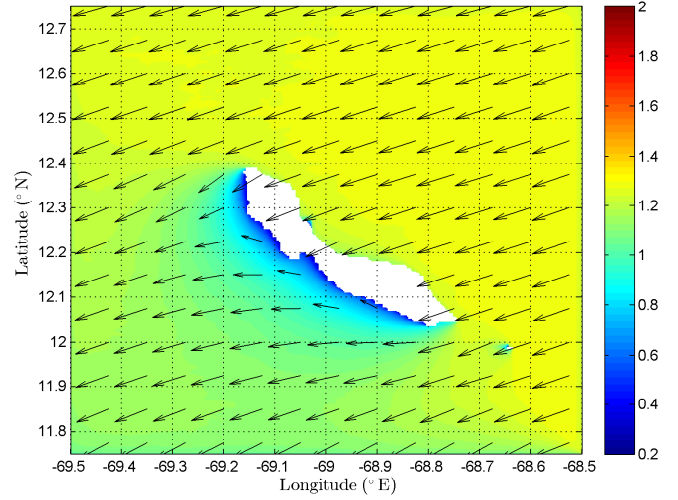


Figure D.36: Scenario W2D: Wave Direction

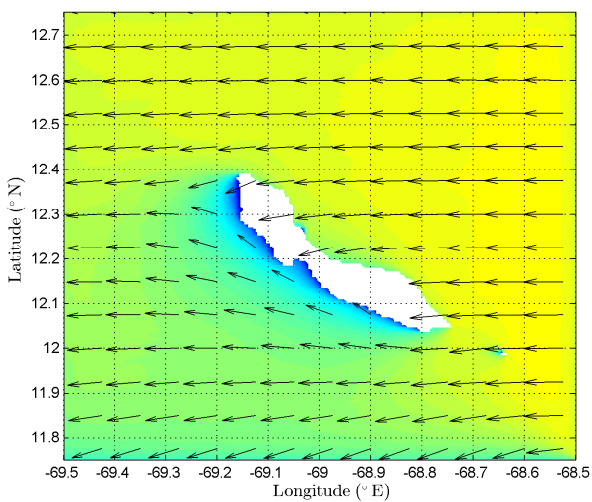


Figure D.37: Scenario W2E: Wave Direction

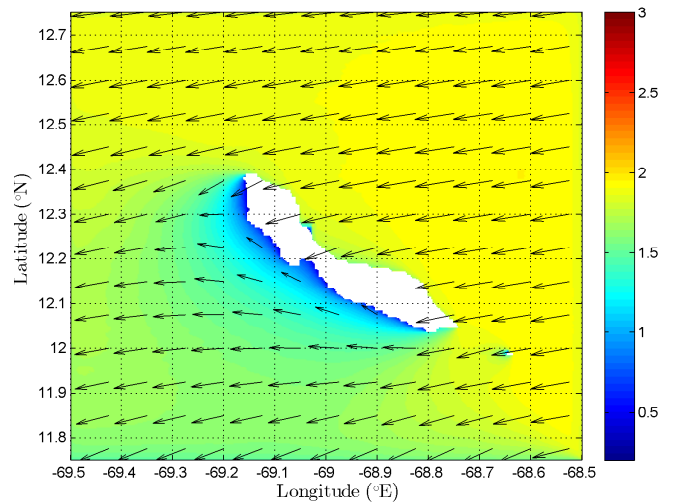


Figure D.38: Scenario W3A: Wave Direction

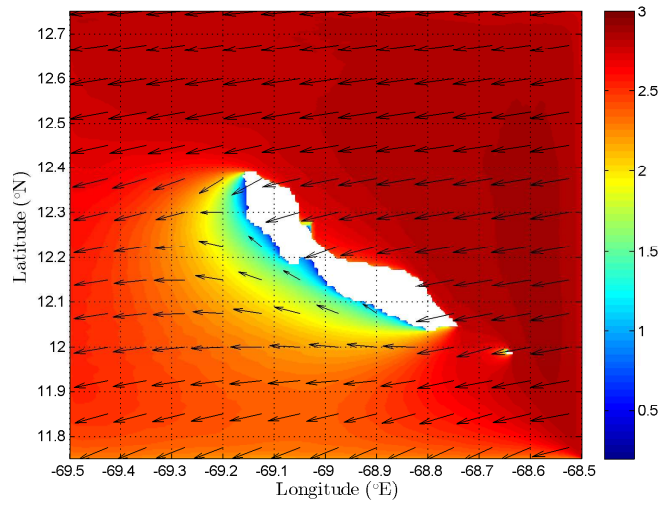


Figure D.39: Scenario W3C: Peak wave period

IN THE CASE OF SWELL WAVES ON THE BOUNDARIES

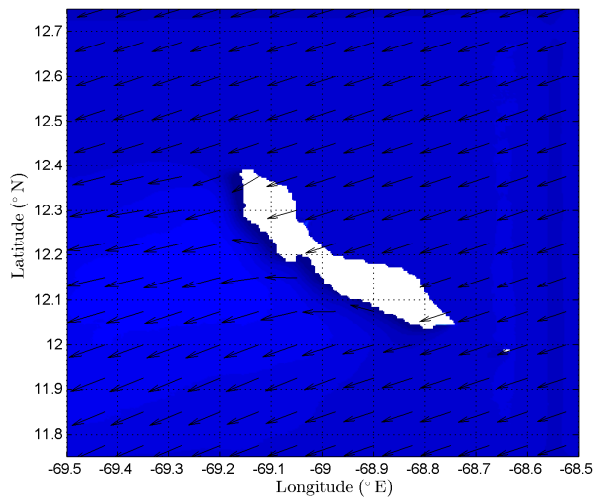


Figure D.40: Scenario S1A: Wave Direction

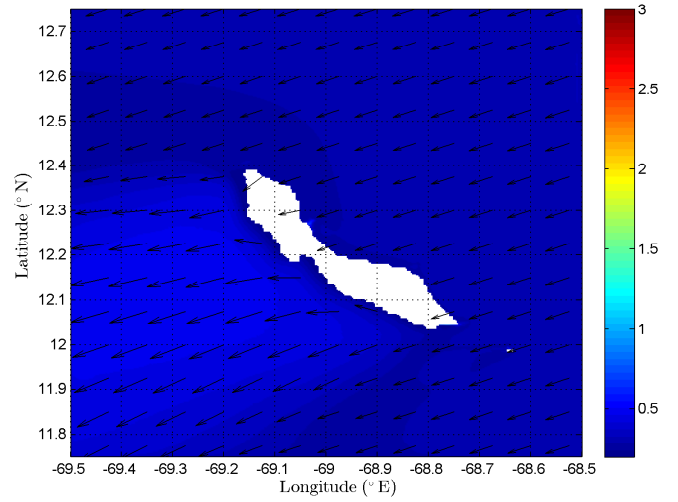


Figure D.41: Scenario S1B: Wave Direction

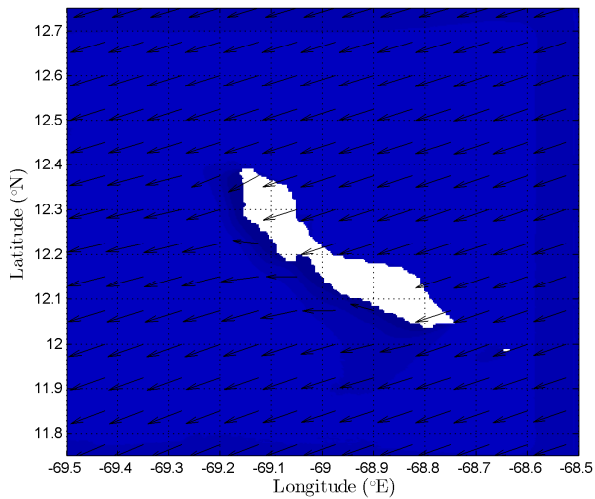


Figure D.42: Scenario S1C: Wave Direction

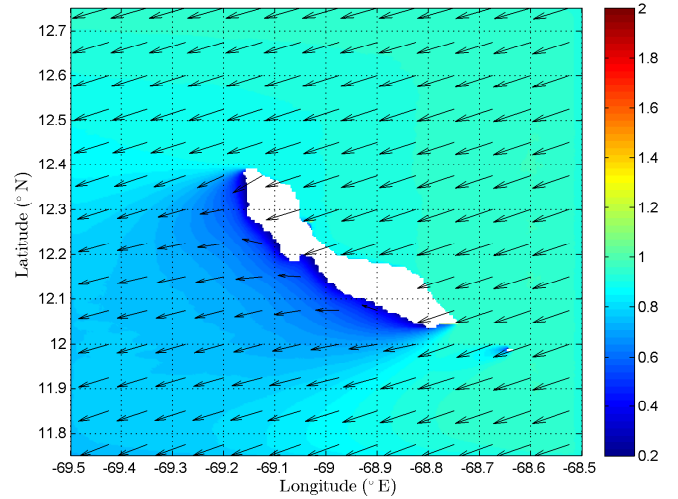


Figure D.43: Scenario S2A: Wave Direction

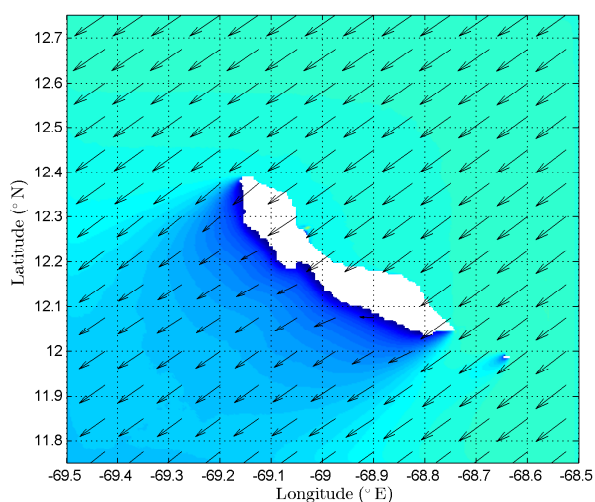


Figure D.44: Scenario S2B: Wave Direction

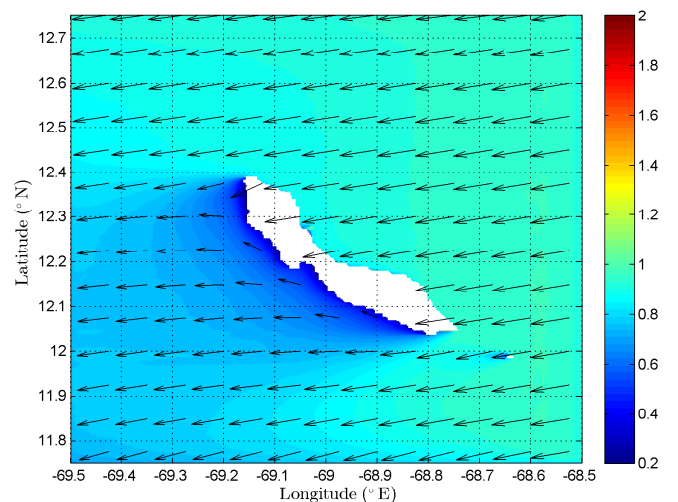


Figure D.45: Scenario S2C: Wave Direction

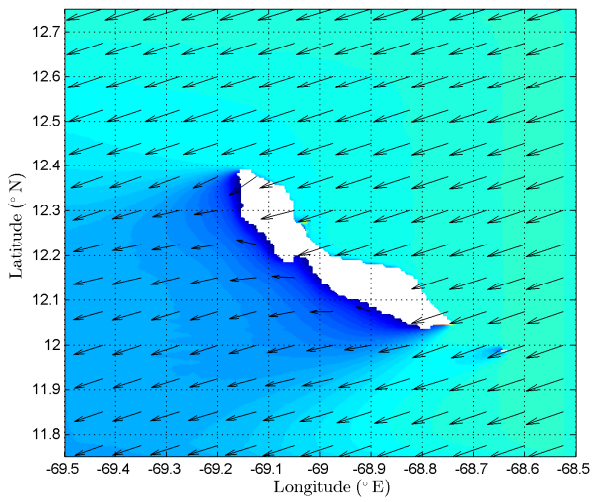


Figure D.46: Scenario S2E: Wave Direction

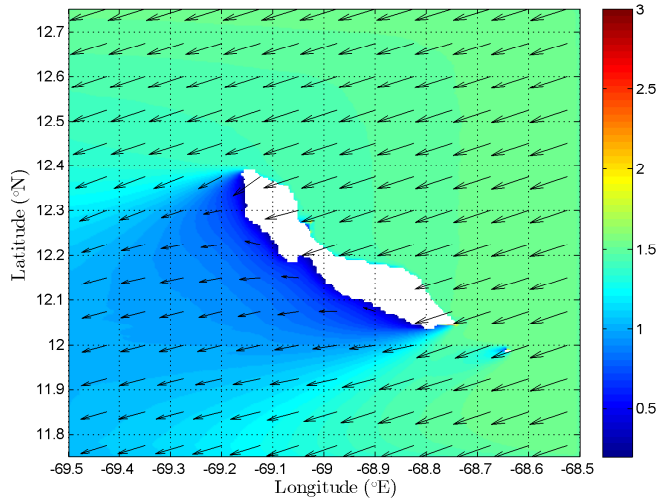


Figure D.47: Scenario S3A: Wave Direction

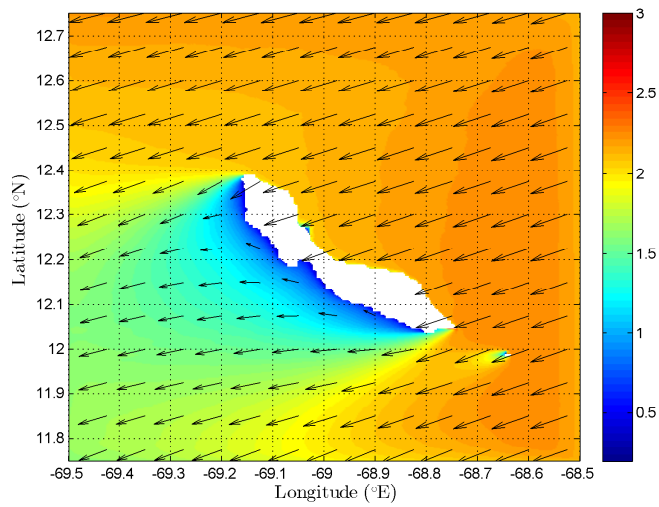


Figure D.48: Scenario S3C: Wave Direction

D.3. LOCAL SWELL- AND WIND WAVE SPECTRA

SWAN makes use of the energy balance to determine the propagation of wave energy through the model domain. With an optional command, the 1D or 2D variance density spectra $E(f)$ at predefined locations can be obtained and saved to a file. The variance density spectrum shows how the variance of the sea-surface is distributed over the frequencies. The transportation of wave energy through the model domain along a series of locations is presented in the next section. Section D.3.2 elaborates on the simulated variance densities for the different scenarios.

D.3.1. PROPAGATION OF WAVE ENERGY

To see how and how much of the wave energy is transported from deep water to the project location, a predefined series of output locations has been added to one scenario. Particularly the swell waves may have significant influence on the dynamics. Therefore, a scenario with a rather long swell wave, with not too low significant waves has been examined. This particular scenario is *S2E*, in which $H_s = 0.9m$, $T_p = 11.2s$ and $\theta = 70^\circ$. Figure D.49 shows the change in the variance density for different locations.

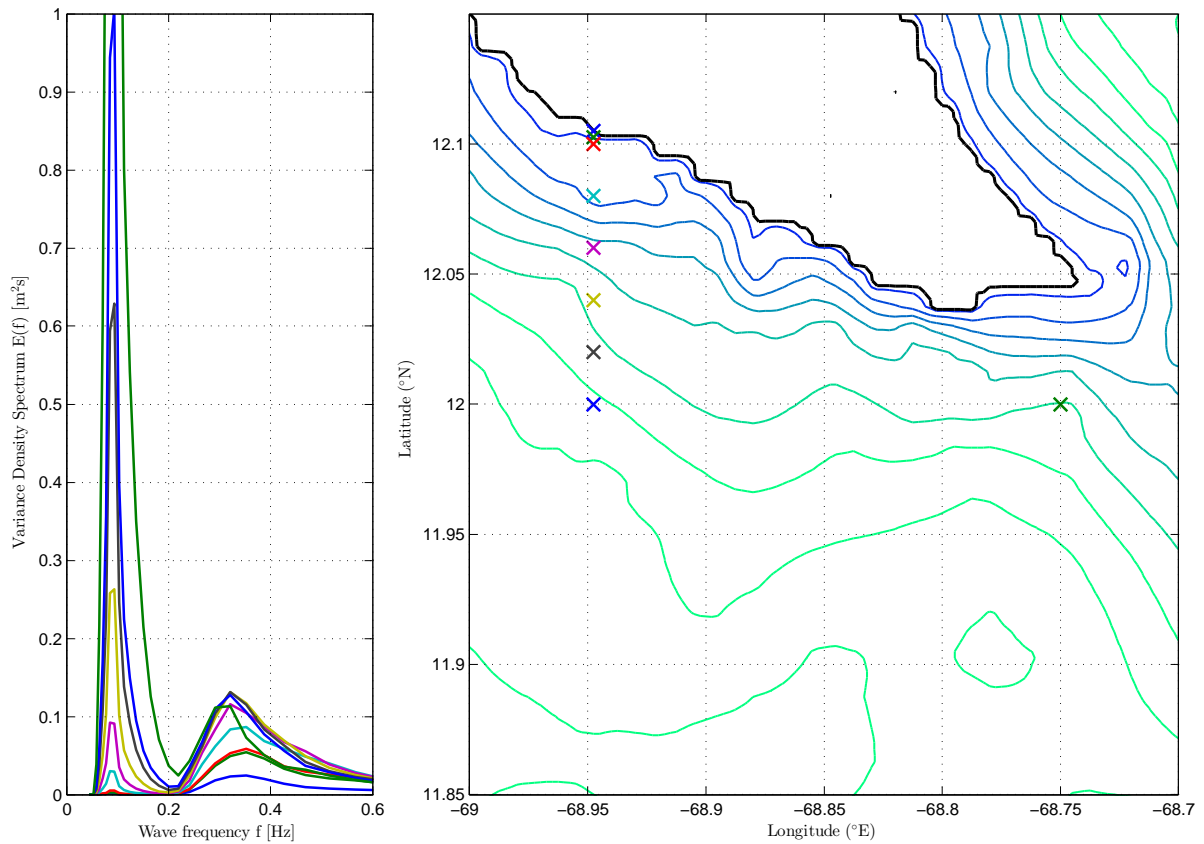


Figure D.49: The change in the variance density for scenario *S2E* is shown in the plot on the left. The locations of each lines are shown in the plot on the right. The colour of the lines correspond with the colours of the marks.

From the figure it can be concluded that a significant amount of swell energy is dissipated while propagating to the southern shore of Curaçao. As the location gets closer to the shore, the energy in the frequency band of wind sea waves slowly gets larger, eventually surpassing the amount of swell wave energy. This explains the abrupt change of and the shadow effect in the peak wave period T_p plots in §D.2.2. The long swell waves seem to be unable to diffract around the South-Eastern corner of the island without losing much wave energy.

D.3.2. VARIANCE DENSITY SPECTRA FOR THE SWELL AND WIND SEA SCENARIOS

Figure D.50 shows the variance density as a function of wave frequency for swell waves. Similarly, Figure D.51 shows the results for wind sea waves. From these two figures, it can be seen that the variance density for the mild to regular scenarios (*1* and *2* series) are of the order $0.2 \text{ m}^2/\text{Hz}$. The frequency in these cases is between 0.25 Hz and 0.4 Hz. Waves within this frequency range are in general called wind waves. The

extreme scenarios *W3A* and *S3A* show both a larger peak compared to the other scenarios. This is because of the higher wind speeds, in order to maintain these larger wave heights.

A small peak for all swell scenarios is visible around the 0.1 Hz frequency. These are the swell waves, which seem to have a much lower variance density compared to the waves locally generated by wind. This indicates that swell waves are not dominantly present, but still can not be neglected. As swell waves are the type of waves most likely to give problems with motion criteria, these small peaks can be of significant influence in the stage of modelling motion dynamics.

The variance density spectra will be used as input data for the modelling of motion dynamics with the software package Ansys AQWA [S5].

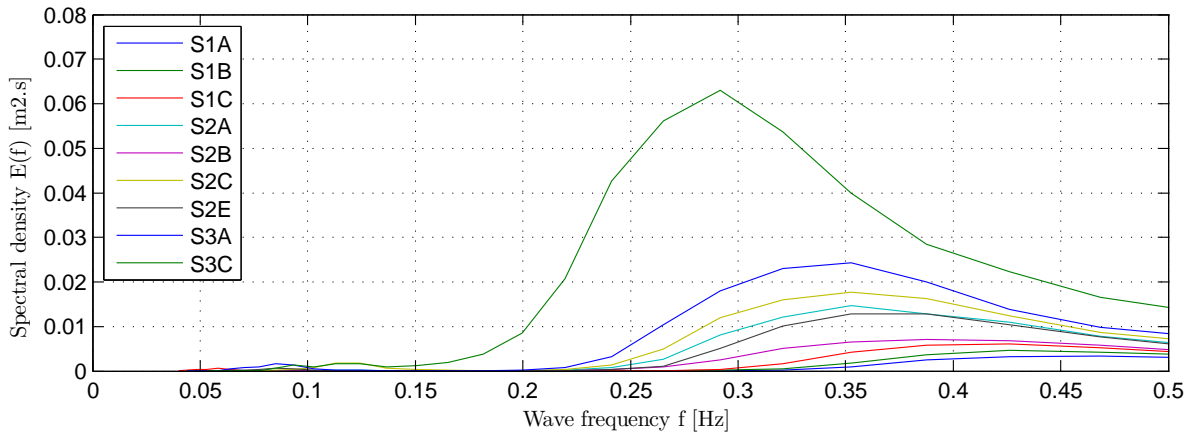


Figure D.50: The variance density plotted against the wave frequency in the case of swell waves at location CT2.

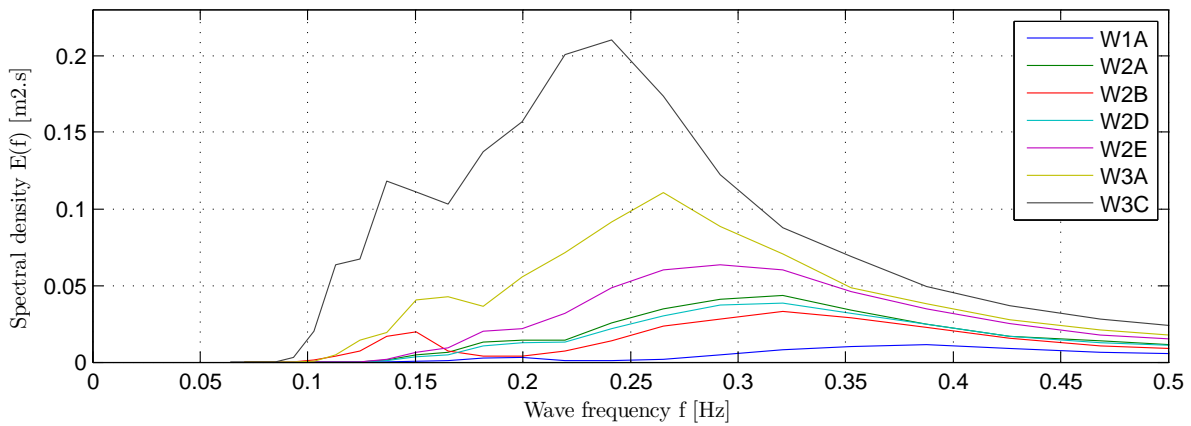


Figure D.51: The variance density plotted against the wave frequency in the case of wind sea waves at location CT2.

ANALYTIC APPROXIMATION OF HYDRODYNAMIC PROPERTIES

The hydrodynamic properties of both floating structures are approximated by means of basic calculations. These calculations are used to verify the results of the numerical models, which are presented in Appendix G. The first section presents a short derivation and the equations of motion in one direction. This is then further expanded into the five directions of interest in §E.2. With this theoretical background given, the general parameters required for these calculations are presented in §E.3. First, the calculation of the hydrostatic terms of both structural models is discussed in §E.4. With these terms it is possible to determine the undamped natural frequencies. This is done in §E.7. Section E.8 then elaborates on the approximation of the hydrodynamic terms. The last calculated property is the undamped natural frequency including the added mass. These results, together with all the previously calculated parameters are presented in §E.9.

E.1. EQUATIONS OF MOTION

In general, the motions of a free floating structure show a linear behaviour. The hydrodynamic properties of such a floating structure are therefore derived from a single linear mass damper spring system. This means that motion can be described by linear equations. Equation E.3 describes the motion of a mass damper spring system in dry conditions. The next equation describes the same system, but now located in water. Applying Newton's second law and Archimedes' law shows that motions are influenced by the mass m of a structure and the hydromechanical loads on this floating structure:

$$\text{Newton's second law: } \vec{F} = \frac{d}{dt}(m \cdot \vec{v}) = \frac{d}{dt}(\rho \nabla \cdot \vec{v}) \quad (\text{E.1})$$

$$\text{Archimedes's law: } P = \rho g \nabla \quad (\text{E.2})$$

After combining these two equations, the general linear equation of motion of a floating body becomes as shown in Equation E.3. Rewriting this equation for two separate bodies and for all forces acting on these floating structure leads to Equation E.4.

$$m\ddot{x} + b\dot{x} + cx = F(t) \quad (\text{E.3})$$

$$(m + a_{ij})\ddot{\underline{x}} + (b_s + b_{ij})\dot{\underline{x}} + (c_s + c_{ij})\underline{x} = \underline{F}_1(t) + \underline{F}_2(t, z, \dot{z}, \ddot{z}) \quad (\text{E.4})$$

Equation E.4 shows that the equation of motion consists of first and second order excitation forces. The second order forces F_2 are coupled and describe non-linear vibrations, but are not taken in account in this study, as they only start to play a significant role for large amplitudes. There are several sources of forces that may act on a floating body:

- Irregular waves;
- Wind;
- Currents.

Focussing on fluid forces, it is possible to relate these forces to the previously introduced equation of motion. This is shown in Figure E.3.

E.2. EQUATION OF MOTION IN MULTIPLE DEGREES OF FREEDOM

The motions of a rigid body in water can be described by equations of motion for six Degrees of Freedom (DOF). This study does not focus on the yaw motion, so the equations of motions of the remaining five DOF

In which:

- \vec{F} = external harmonic wave force acting in the centre of gravity [N]
- m = mass of floating structure [kg]
- \vec{v} = instantaneous velocity of centre of gravity [m/s]
- \underline{x} = vectorial notation of the displacements of 2 bodies in a particular direction [m]
- ∇ = displaced volume [m³]
- P = mass force downwards [N]
- a_{ij} = hydrodynamic mass in direction i due to a motion in direction j [kg]
- b_s = structural hydrodynamic damping, which is neglected in this study [kg/s]
- b_{ij} = hydrodynamic damping in direction i due to a motion in direction j [kg/s]
- c_s = structural hydrostatic stiffness, which is neglected in this study [kg/s²]
- c_{ij} = hydrostatic stiffness in direction i due to a motion in direction j [kg/s²]
- \underline{F}_1 = first order external harmonic wave forces for two bodies [N]
- \underline{F}_2 = second order external harmonic wave forces for two bodies [N]

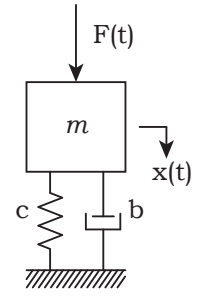


Figure E.1: Schematic representation of a mass damper spring system.

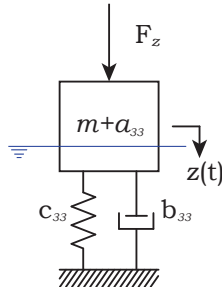


Figure E.2: Schematic representation of a mass damper spring system for heave.

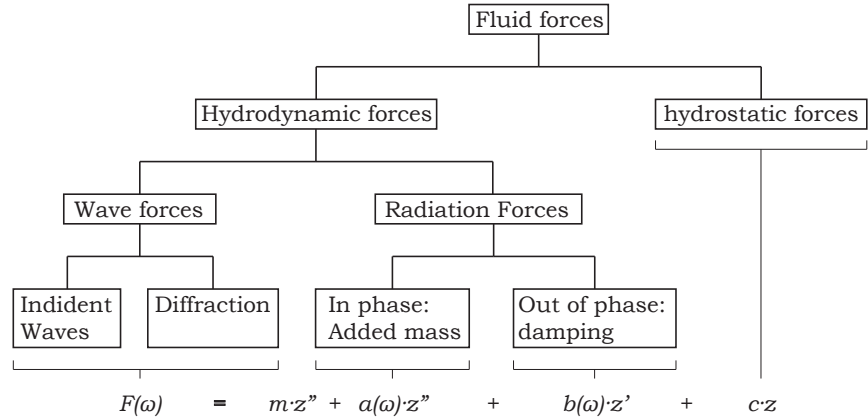


Figure E.3: Overview of the different types of fluid forces, related to the equation of motions [16].

are presented in Equation E.5. These equations are referenced to the local system of axes, located at the centre of the floating structure.

Compared with Equation E.4, this set of equations does only include the directional hydrodynamic mass a_{ij} and damping b_{ij} coefficients, leading to the assumption of an infinitely stiff floating structure without structural damping.

$$\begin{bmatrix} m + a_{11} & & & & \\ & m + a_{22} & & & \\ & & m + a_{33} & & \\ & & & I_{44} + a_{44} & \\ & & & & I_{55} + a_{55} \end{bmatrix} \cdot \begin{bmatrix} \ddot{x}(t) \\ \ddot{y}(t) \\ \ddot{z}(t) \\ \ddot{\phi}(t) \\ \ddot{\theta}(t) \end{bmatrix} + \begin{bmatrix} c_{11} & & & & \\ & c_{22} & & & \\ & & \ddots & & \\ & & & c_{55} & \end{bmatrix} \cdot \begin{bmatrix} x(t) \\ y(t) \\ z(t) \\ \phi(t) \\ \theta(t) \end{bmatrix} = \begin{bmatrix} F_{11}(t) \\ F_{22}(t) \\ F_{33}(t) \\ M_{44}(t) \\ M_{55}(t) \end{bmatrix} \quad (\text{E.5})$$

In which:

x	=	surge direction, also denoted with subscript 11 [m]
y	=	sway direction, also denoted with subscript 22 [m]
z	=	heave direction, also denoted with subscript 33 [m]
ϕ	=	roll direction, also denoted with subscript 44 [rad]
θ	=	pitch direction, also denoted with subscript 55 [rad]
I_{ij}	=	mass moment of inertia in direction i due to a motion in direction j [kg m^2]
M_{ij}	=	exciting moment in direction i due to a motion in direction j [Nm]

The undamped natural frequency ω_0 is defined by Equations E.6 and E.7. From this equation can be seen that the hydrodynamic mass a and hydrostatic stiffness c in each direction need to be determined in order to calculate the undamped natural frequency ω_0 in each direction.

$$\text{Translation: } \omega_{0,T} = \sqrt{\frac{c}{m+a}} \quad (\text{E.6})$$

$$\text{Rotation : } \omega_{0,R} = \sqrt{\frac{c}{I+a}} \quad (\text{E.7})$$

The calculations of the directional hydrodynamic terms are described in the following sections, followed by the determination of the undamped natural frequencies for each motion.

E.3. OVERVIEW OF GENERAL PARAMETERS

Calculations are carried out for both structural models (Model A and B). A number of parameters are required to calculate the different terms in all the directions of interest. An overview of the general parameters and their values is given in Table E.1.

Table E.1: Overview of the used parameters for the calculations carried out in the following sections.

		Model A	Model B
m	t	2306.25	6150
L	m	30	80
W	m	30	30
D	m	2.5	2.5
\overline{GM}_T	m	28.75	28.75
\overline{GM}_L	m	28.75	212.09
I_{44}	t m^2	$2.65 \cdot 10^5$	$6.39 \cdot 10^5$
I_{55}	t m^2	$2.65 \cdot 10^5$	$34.21 \cdot 10^5$

E.4. HYDROSTATIC TERMS: HEAVE, ROLL AND PITCH

The hydrostatic term in Equation E.3 is the *hydrostatic stiffness* c , also called *restoring spring term*. In case of free floating bodies, this stiffness only exists in the heave, roll and pitch motion, because of the buoyancy force, which prevents submergence of a floating body. The restoring spring terms for each of these motions can be calculated with the following formulae:

$$\text{Heave: } c_{33} = \rho g \cdot A_{WL} \quad (\text{E.8})$$

$$\text{Roll : } c_{44} = \rho g \cdot \overline{GM}_T \quad (\text{E.9})$$

$$\text{Pitch : } c_{55} = \rho g \cdot \overline{GM}_L \quad (\text{E.10})$$

In which:

A_{WL}	=	horizontal cross-sectional area at the waterline [m^2]
\overline{GM}_T	=	metacentric height in transverse direction [m]
\overline{GM}_L	=	metacentric height in longitudinal direction [m]

E.5. HYDROSTATIC TERMS: SURGE AND SWAY

In order to find the natural frequency in the surge and sway motion, the restoring force coefficient of the mooring system needs to be determined. In this case the mooring system consists of anchor blocks and catenaries, which is a non-linear mooring. For the following calculations, use has been made of a brief handout of Ido Akkermans [18] on the mechanics of catenaries.

E.5.1. GEOMETRY AND PARAMETER DEFINITION

The restoring force coefficient is found for the geometry as shown in Figure E.4. The geometry and the catenaries are simplified into a mass-spring system as indicated in Figure E.5. The parameter c is the spring coefficient derived from the restoring force of the catenaries caused by displacements of the anchored floating structure.

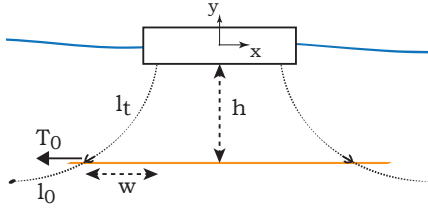


Figure E.4: Basic geometry of the catenary mooring.

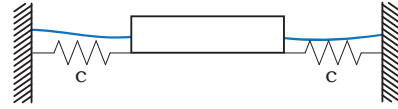


Figure E.5: Simplification of the catenary mooring system into a mass-spring system.

Where:

l_t	= 56	length of the catenary [m]
l_0	= TBD	length of the imaginary line between the imaginary touchdown point and anchor point [m]
h	= 17.5	underkeel clearance [m]
w_i	= 50	initial distance (displacement) relative to the anchor point [m]
T_0	= TBD	horizontal force resulting from the pulling pontoon [N]
c	= TBD	restoring force coefficient of one catenary [N/m]

As can be seen from the figure indicating the geometry of the catenary mooring, a semi-taut case is considered: there is no touchdown point. Instead the catenary terminates at an angle at the anchor point.

E.5.2. PARAMETRIC RELATIONS

The considered mooring is non-linear: the restoring force will increase exponentially with an increasing displacement. The relation between force and displacement will need to be determined in order to calculate the restoring force coefficient. Ido Akkermans derived the parametric relations at the hookup point of the floating structure, which can be found below. The derivation of the parametric relation can be found in his handout [18].

$$x(l_0 + l_t) = w = a \operatorname{arcsinh}\left(\frac{l_0 + l_t}{a}\right) - a \operatorname{arcsinh}\left(\frac{l_0}{a}\right) \quad (\text{E.11})$$

$$y(l_0 + l_t) = h = \sqrt{a^2 + (l_0 + l_t)^2} - \sqrt{a^2 + l_0^2} \quad (\text{E.12})$$

Where a is given by:

$$a = \frac{T_0}{\lambda g}, \quad \lambda = \text{specific mass of the chain} \quad [\text{kg/m}] \quad (\text{E.13})$$

E.5.3. RESTORING FORCE COEFFICIENT

The *Restoring Force Coefficient* is the derivative of the relation between the horizontal force and the displacement:

$$c_x = \frac{dT_0}{dx} = \frac{\lambda g}{\frac{dw}{da}} \quad (\text{E.14})$$

Using the above two parametric relations, the restoring force coefficient can be determined. First the specified force T_0 needs to be converted to a . With a calculated, it is now possible to determine l_0 using Equation E.12, with a root finding algorithm. Afterwards w can be found using Equation E.11. With this relation it is possible to calculate and plot the relation between T_0 and w . This plot is presented in Figure E.6. It is now possible to calculate the derivative of the curve at a given displacement, which is the restoring force coefficient for a single catenary as defined by Equation E.14.

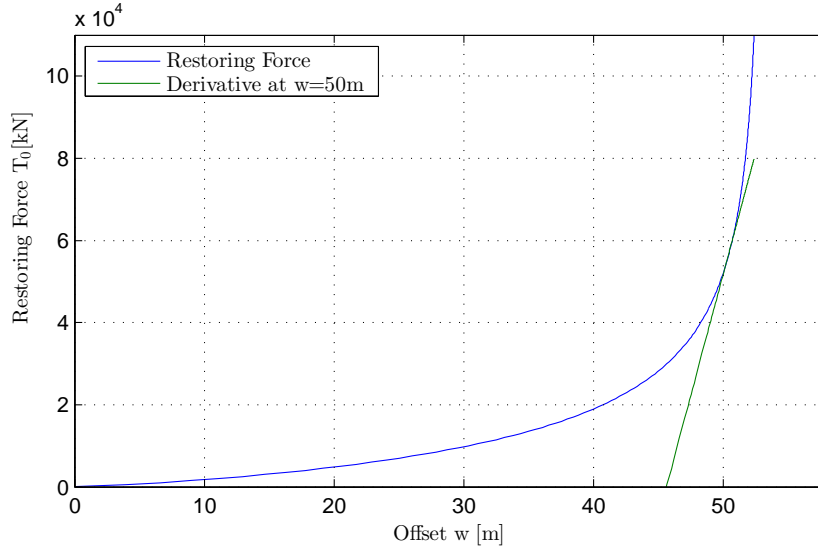


Figure E.6: Plot of the restoring force as a function of the displacement.

The determined value for the restoring force coefficient for a single catenary is 11 834 kN/m. Although limited, the catenary also introduces a restoring force when the pontoon is displaced perpendicular to the direction of the catenary. This addition c_{\perp} is assumed to be 1% of c . In the case of a surge motion, this means that the total value of the restoring force coefficient becomes:

$$N_0 \cdot c + N_0 \cdot c_{\perp} = c_{11}$$

$$2 \cdot 13507 + 4 \cdot 135.07 = 29715$$

E.6. OVERVIEW OF CALCULATED HYDROSTATIC VALUES

This section presented the different calculation methods to determine the hydrostatic stiffness in the directions of interest. The results of the calculations made in this section are briefly summarised in Table E.2. The results in this table include the previously mentioned additional perpendicular hydrostatic stiffness from catenaries.

Table E.2: Overview of the calculated values for the hydrostatic stiffness.

	c_{11} N/m	c_{22} N/m	c_{33} N/m	c_{44} Nm/rad	c_{55} Nm/rad
Model A	$2.97 \cdot 10^4$	$5.54 \cdot 10^4$	$9.05 \cdot 10^6$	$9.04 \cdot 10^8$	$6.50 \cdot 10^8$
Model B	$2.97 \cdot 10^4$	$5.54 \cdot 10^4$	$2.41 \cdot 10^7$	$2.41 \cdot 10^9$	$1.28 \cdot 10^{10}$

E.7. UNDAMPED NATURAL FREQUENCY WITHOUT HYDRODYNAMIC MASS

With the calculation results in Table E.2 it is possible to calculate the undamped natural frequencies of the floating structures without the hydrodynamic mass. This means that for now $a = 0$. Using the Equations E.6 and E.7 leads to the following results:

Table E.3: Calculated values of the undamped natural frequency without hydrodynamic mass in five directions.

	$\omega_{0,11}$ [rad/s]	$\omega_{0,22}$ [rad/s]	$\omega_{0,33}$ [rad/s]	$\omega_{0,44}$ [rad/s]	$\omega_{0,55}$ [rad/s]
Model A	0.10	0.14	1.98	1.57	1.57
Model B	0.06	0.09	1.98	1.65	1.93

E.8. HYDRODYNAMIC TERMS

The equations of motion have already been presented in §E.1 and show the influence of the hydrostatic and dynamic terms. The hydrodynamic coefficients in the equation of motion are the hydrodynamic damping and mass. These basic calculations describe the determination of the *undamped natural frequencies* of the floating structures in 5 DOF. This means that the hydrodynamic damping is not taken into account. The damped natural frequencies will not defer significantly, because of the limited influence of damping on the studied pontoons.

From Equation E.5, it can be seen that there is a value of the hydrodynamic added mass in each degree of freedom. The calculation of this parameter in each direction is given below.

E.8.1. ADDED MASS FOR THE SURGE AND SWAY MOTION

For this study the added mass in the surge and sway direction is assumed to be 25% of the total mass of the floating structure:

$$a_{11} = a_{22} = 0.25 \cdot m \quad (\text{E.15})$$

The calculation results of this approximation are presented in Table E.5.

E.8.2. ADDED MASS FOR THE HEAVE MOTION

The heave motion leads to accelerations of fluid underneath the structure. The volume of water that is set in motion during heaving is approximated by Ruol et al. [19]. This approximation is given by Equation E.16 and visualised in Figure E.7.

Ruol et al. estimated the volume of the accelerated fluid by a semicircle with a radius of about half the width of the structure per unit length, taking into account a correction factor for the precise radius of the semi-circle. Experimental research concluded that the term for the area calculation ($\frac{\pi}{8} - \gamma$) has a value of 0.35. With this

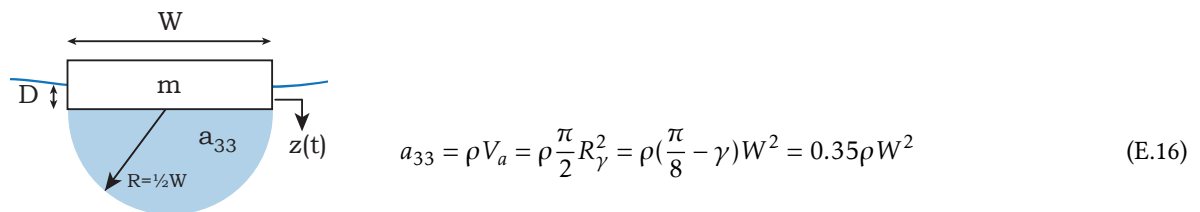


Figure E.7: Approximation of the amount of added mass for the heave motion.

approximation it is possible to estimate the added mass for heaving for both structural models. The calculated values of a_{33} are presented in Table E.5.

E.8.3. ADDED MASS MOMENT OF INERTIA FOR THE ROLL AND PITCH MOTION

Brown & Root Vickers developed a method to determine the hydrodynamic mass moment of inertia of a floating structure in 1991 (cited in [20]). This method consists of a number of steps which will be explained next.

Brown & Root Vicker introduced the following parameters H and λ :

$$H = \frac{W}{2D} \tag{E.17}$$

$$\lambda = \frac{gT_0^2}{2\pi} = \frac{2\pi g}{\omega_0^2} \tag{E.18}$$

Table E.4 shows the values of the different parameters that are needed to determine the added mass moment of inertia due to roll and pitch. The final calculated values of the latter are presented in Table E.5. Intersecting the calculated value for the expression $\frac{\pi W_f}{\lambda}$ with the calculated value for H makes it possible to read a value from the y-axis. Rearranging the terms leads to a value for the hydrodynamic mass in the direction considered. These steps have been visualised in Figure E.8.

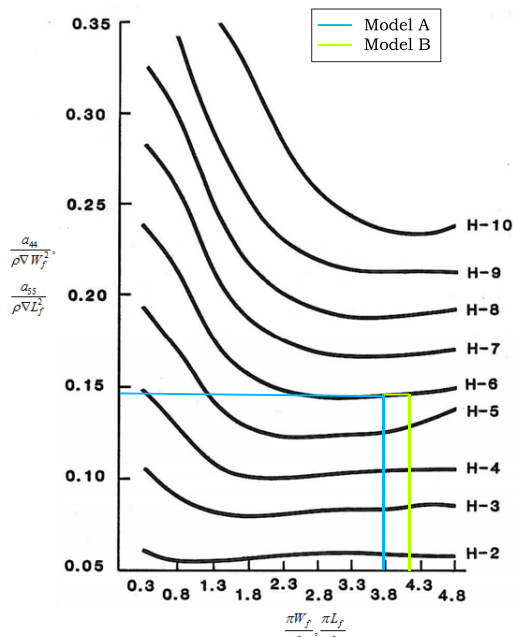


Figure E.8: Method of Brown & Root Vicker to determine the hydrodynamic mass of a floating structure in a roll motion [20].

Table E.4: Overview of all the calculations values of the hydrodynamic mass.

Model	H	Roll		Pitch	
		$\frac{\pi W_f}{\lambda}$	$\frac{a_{44}}{\rho V W_f^2}$	$\frac{\pi L_f}{\lambda}$	$\frac{a_{55}}{\rho V L_f^2}$
A	6	3.75	0.145	3.75	0.145
B	6	4.15	0.145	15.25	0.37

E.8.4. OVERVIEW OF CALCULATED VALUES

The results of the calculations made in this section are briefly summarised in Table E.5.

Table E.5: Overview of all important parameters for the calculations carried out in this appendix.

	a ₁₁ kg	a ₂₂ kg	a ₃₃ kg	a ₄₄ kg m ²	a ₅₅ kg m ²
Model A	5.77 · 10 ⁵	5.77 · 10 ⁵	8.72 · 10 ⁶	3.01 · 10 ⁸	3.01 · 10 ⁸
Model B	1.54 · 10 ⁶	1.54 · 10 ⁶	2.32 · 10 ⁷	8.03 · 10 ⁸	2.05 · 10 ⁹

E.9. CONCLUSION

This final section presents the results of all the basic calculations of the hydraulic parameters of the two structural models A and B. All the parameters and values are put together into one table. The results of these basic calculations are used to verify the output from the Ansys AQWA simulations. The set-up and simulation of the AQWA Models is discussed in the following two appendices.

Table E.6: Summary of the calculated hydrostatical and hydrodynamical parameters by means of basic calculations.

Surge (11)				
	c	a	ω_0	ω_n
	[N/m]	[kg]	[rad/s]	[rad/s]
Model A	$2.97 \cdot 10^4$	$5.77 \cdot 10^5$	0.10	0.10
Model B	$2.97 \cdot 10^4$	$1.54 \cdot 10^6$	0.06	0.06

Sway (22)				
	c	a	ω_0	ω_n
	[N/m]	[kg]	[rad/s]	[rad/s]
Model A	$5.53 \cdot 10^4$	$5.77 \cdot 10^5$	0.14	0.13
Model B	$5.53 \cdot 10^4$	$1.54 \cdot 10^6$	0.09	0.08

Heave (33)				
	c	a	ω_0	ω_n
	[N/m]	[kg]	[rad/s]	[rad/s]
Model A	$9.05 \cdot 10^6$	$8.72 \cdot 10^6$	1.98	0.91
Model B	$2.41 \cdot 10^7$	$2.32 \cdot 10^7$	1.98	0.91

Roll (44)				
	c	a	ω_0	ω_n
	[N/m]	[kg]	[rad/s]	[rad/s]
Model A	$6.50 \cdot 10^8$	$3.01 \cdot 10^8$	1.57	1.07
Model B	$1.73 \cdot 10^9$	$8.03 \cdot 10^8$	1.64	1.10

Pitch (55)				
	c	a	ω_0	ω_n
	[N/m]	[kg]	[rad/s]	[rad/s]
Model A	$6.50 \cdot 10^8$	$3.01 \cdot 10^8$	1.57	1.07
Model B	$1.28 \cdot 10^{10}$	$2.05 \cdot 10^9$	1.93	1.53

REMARKS

A number of remarks are mentioned considering the results that follow from the carried out analytic approximation.

- For the calculation of the added mass for the surge and sway motion, an assumption has been made. Additional study should confirm the percentage of 25% (see §E.8.1).
- Due to the specific dimensions of Model B, the parameter H , as introduced by Brown & Root Vickers, is much larger than initially studied (see Figure E.8). This leads to a large overestimation of the natural frequency for pitch. Additional study is required to be able to calculate the natural frequency with this specific method. Or, a more appropriate method should be applied to determine the natural frequency for this particular case.
- All calculations carried out in this appendix are analytic approximations. Results just give a first indication of the order of the parameter values. A margin of error of approximately 10% should be expected. More accurate approximations, taking into account second order effects become much more labor intensive, to be carried out by means of hand calculations. Another method to verify the simulation results could be to carry out tests with physical models.

APPENDIX F

AQWA MODEL SET-UP

This appendix discusses important aspects of the AQWA Model set up in further detail. In §C.1 the importance of wind on the wave model is shown. The second section presents the command files used for this study.

F.1. CONVENTIONS FOR SIGNS AND DIRECTIONS

The conventions as used by the AQWA programs are explained in the following sections. It is of importance for the readers to take note of these conventions to read and interpret the input data and simulation results correctly.

F.1.1. AXES SYSTEM

The AQWA programs make use of two different sets of axes:

- Fixed Reference Axes (FRA), with the origin placed on the mean water surface and with the z-axis pointing upwards.
- Local System Axes (LSA), with the origin at the *CoG* of a modelled structure and parallel to the FRA.

The floating terminal structures are modelled in the conventional way, meaning that the x-axis is placed in line with the length of the pontoon (considering Model B). This conventional definition is visualised in Figure F.1.

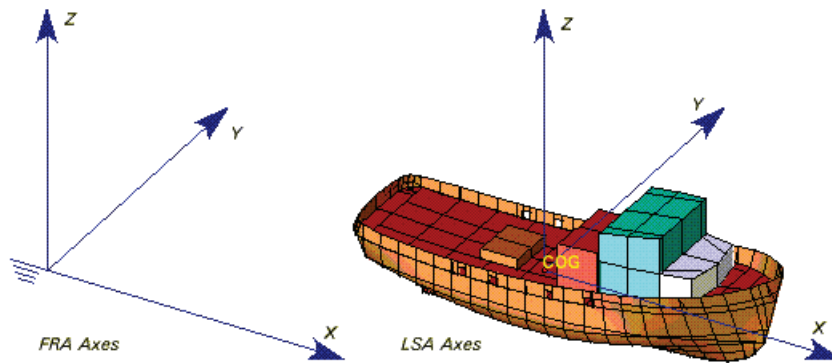


Figure F.1: Left figure: FRA definition in the AQWA programs. Right figure: LSA definition in the AQWA programs. Source: [16]

F.1.2. WAVE DIRECTION

The AQWA Reference Manual [16] defines the wave direction as follows. The wave direction is defined as the angle from the positive global x-axis to the direction in which the wave is travelling, measured anti-clockwise when seen from above. Therefore waves travelling along the X axis (from -x to +x) have a 0° wave direction, and waves travelling along the y-axis (from -y to +y) have a 90° wave direction.

F.2. SET-UP OF AND INPUT FOR THE ANSYS AQWA PROGRAMS

In order to acquire correct simulation results, it is essential to set-up the simulation model accurately. All relevant information about the set-up of the simulation models is presented in this section. Figures and tables indicate used parameter values and lay-outs.

F.2.1. MESH AND GEOMETRY DETAILS

The submerged part of all structures have been created in Workbench. To mesh the structures it is required to impose boundaries on the elements/ panels and wave length. The required resolution of the mesh depends

on the maximum frequency. For this study only the longer wind- and swell waves are of interest. Table F.1 shows the mesh details of all three models. Meshed submerged parts of the different models are visualised in the following sections.

Table F.1: Mesh details

		Model A	Model B	Cruise vessel C
Number of Nodes	-	705	1677	9077
Number of Elements	-	660	1596	8830
Max Element Size	m	2.33	2.33	2.33
Max Allowed Frequency	rad/s	2.1	2.1	2.1

MODEL A - 30x30M

A mesh is automatically created for the 30x30m pontoon. The details of this mesh can be found in Table F.1. Only the submerged part of the pontoon is modelled and meshed. This is visualised in Figure F.2.

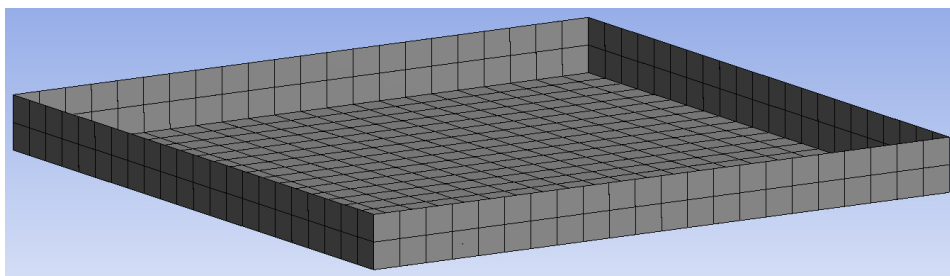


Figure F.2: Mesh of the submerged part of Model A: the 30x30m pontoon.

MODEL B - 80x30M

Just like with Model A, a mesh has been generated for the submerged part of the structure. As this structure is much longer, a larger amount of nodes and elements are necessary for the mesh. Figure F.3 shows the applied mesh for this structure.

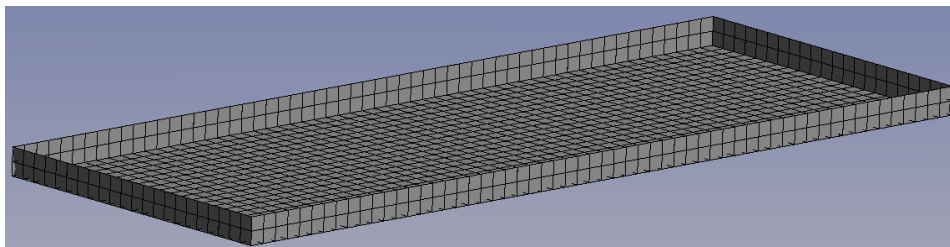


Figure F.3: Mesh of the submerged part of Model B: the 80x30m pontoon.

MODEL C - CRUISE VESSEL

A rough model of the largest cruise ship - Oasis of the Seas - has been created. The hull of a ship consists of many curves. The generated mesh of this structure therefore contains much more elements than the two simple pontoon structures. As the AQWA-suite is bound to a maximum amount of elements (maximum = 12.000), the geometry is simplified. This leads to a less accurate geometric model, but a lower amount of nodes and elements. The influence of a less accurate geometry on the motion response of the floating terminal is deemed minimal due to the huge dimensions of the cruise vessel.

Visualisations of the applied mesh on the cruise vessel model can be found in Figures F.4 and F.5, where the first figure shows the meshed bow and the second figure presents a side-view.

F.2.2. ANCHORAGE & CONNECTIONS

To keep the floating structure and the cruise ship on their position a station keeping system is necessary. In this study use is made of anchors. These anchors are modelled in AQWA by means of defining anchor points

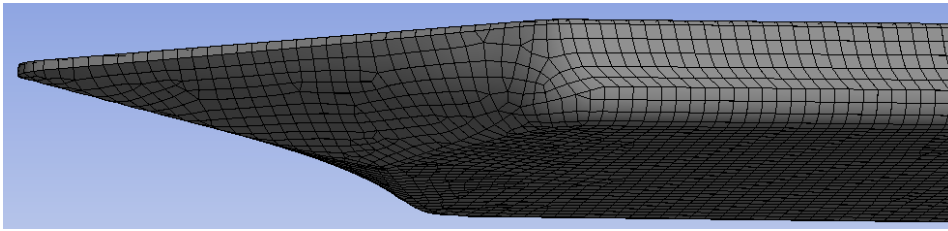


Figure F.4: Close-up detail of Mesh of the bow of the cruise vessel.

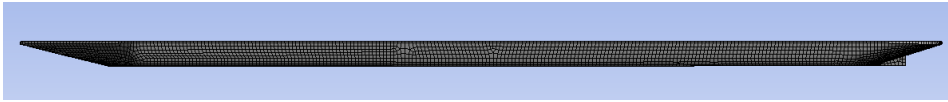


Figure F.5: Mesh of the submerged part of the cruise vessel.

and connection points. Between these two points runs a cable. This cable is defined by a list of parameters to define its properties in the model. The parameters used in and required by AQWA are presented in the next section.

RELEVANT PARAMETERS

To model catenaries in AQWA, it is required to define values for a number of parameters. These parameters and their values can be found in Table F.2.

Table F.2: Properties of the catenaries applied in AQWA

	Unit	Cable Properties
Type of Cable		Non-Linear Catenary
Number of Elements		100
Section Length	m	55
Positive dZ Range	m	10 m
Mass / Unit Length	t/m	0.15
Stiffness, EA	kN	900000
Maximum Tension	kN	750
Equivalent Diameter	m	0.2
Longitudal Drag Coeff.	-	0.025

LAY-OUT

The lay-out of the anchorage is not different for both models. The distances and angles between the anchors and the connection points on the pontoon are the same. The distance between the two connection points is the only parameter that is different, because of the larger length of Model B. This has all been visualised in Figure F.6.

CABLE DYNAMICS

The lay-out of the anchorage of both modelled floating structures is shown in the previous section. The anchorage itself is modelled by non-linear composite catenary lines. The software AQWA is able to include the dynamics of these cables in the analysis of cable motions and takes the effects of the cable mass and drag forces into account. Although this study only focusses on calculations in the frequency domain, the calculation in this frequency domain are fully coupled with the solution during a time history.

Using the option of AQWA to include cable dynamics leads to limitations and implications [16]:

- The cables are modelled as semi-taut and therefore have a minimum tension;
- The sea bed is considered horizontal at the anchor;
- The cable is modelled with a fixed number of elements;
- In-line dynamics is included;
- Seabed friction is ignored;

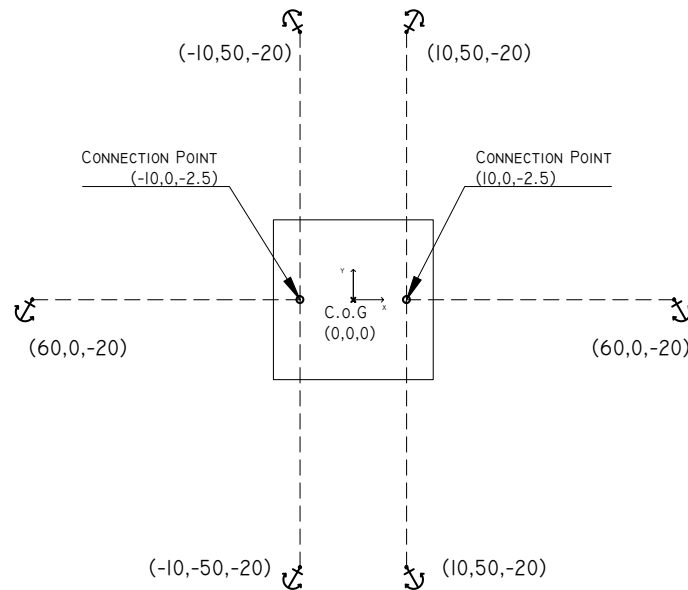


Figure F.6: Schematic anchorage as applied in AQWA for Model A indicating the locations of the anchors and connection points. Model B only differs in the distance between the two connection points because of the larger length; the connected catenaries and anchors shift with the displacement of the connection point.

In this report, use is made of figures, which indicate the position and location of the modelled catenaries. It should be stated that all these visualisations are based on the quasi-static configuration and tension for the static equilibrium position.

FENDERS

Fenders are to be applied between the floating structure and moored vessels. In this study the hydrodynamic response is studied for two scenarios: one without any ships next to it, and a second with a design cruise vessel next to the floating terminal, without being moored and a distance of two meters between the two. This is done to solely determine the influence of the cruise vessel on the hydrodynamic response of the floating terminal. The application and design of fenders is not taken into account in this study and is to be considered in an additional study.

F.3. AQWA COMMAND FILES

This section presents the used command file as input to run the AQWA models. AQWA is one single computer program which requires this command file and additional input files before it can be run successfully. This command file contains all important commands, parameters, settings and paths to other input files needed. For the sake of completeness and any desired additional research in the future, this command file is given below.

F.3.1. AQWA-LINE

Listing F.1: AQWA-LINE Command File

```

*****
* Project name           : MSc Thesis Floating Cruise Terminal Curacao
* Project title         : Model A
* Project author        : X.Groenberg
* Project description    : 30x30x5 + 56m catenaries + 20m depth
* Model name            : ModelA
*****
JOB AQWA LINE
***** DECK 0 *****
TITLE
      MSc Thesis - ModelA
OPTIONS REST END
RESTART 1 3
***** DECK 1 *****
      COOR
      NOD5
      STRC          1
      1 1          -15.    -15.    0.
      ...
      1 705        -13.636364 13.636364 -2.5
* FAIRLEAD POINTS FOR MOORING LINES (will be shifted by Z=-ZLWL)
      199000         0.      0.      0.
      199700        -60.     0.     -20.
      199701        -10.     0.     -2.5
      199712         60.     0.     -20.
* ANCHOR POINTS FOR MOORING LINES (fixed points)
      199708         10.     50.    -20.
      199709         10.     0.     -2.5
      199704        -10.     50.    -20.
      199716        -10.    -50.    -20.
      199720         10.    -50.    -20.
END
***** DECK 2 *****
      ELM1
      ZLWL          (      0.)
      1 ILID AUTO 950
      1QPPL DIFF 31(1)( 1)( 2)( 4)( 3)
      1QPPL DIFF 31(1)( 3)( 4)( 6)( 5)
      ...
      1PMAS          32(1)(99000)(99000)(99000)
      Aqwa Elem No: 1
      Aqwa Elem No: 2
END
FINI
***** DECK 3 *****
      MATE
      1 99000 2332800.
END
***** DECK 4 *****
      GEOM
      1PMAS 99000 2.65021e8 0. 0. 2.65021e8 0. 5.13619e8
END
***** DECK 5 *****
      GLOB
      DPTH 20.
      DENS 1025.
      ACCG 9.80665
END
***** DECK 6 *****
      FDR1
      1FREQ 1 6 0.1 0.2 0.3 0.4 0.5 0.6
      1FREQ 7 12 0.7 0.8 0.9 1.0 1.1 1.2
      1FREQ 13 18 1.3 1.4 1.5 1.6 1.7 1.8
      1FREQ 19 21 1.9 2.0 2.1
      1DIRN 1 6 -180.00 -90.0 -45 0.00 90 135
      1DIRN 7 7 180.00
END
***** DECK 7 *****
      6 NONE
***** DECK 8 *****
      7 NONE
!***** End of File *****

```

F.3.2. AQWA-LIBRIUM

Listing F.2: AQWA LIBRIUM Command File

```

JOB MScT  LIBR
TITLE                               MSc Thesis - Model A
OPTIONS REST PBIS END
RESTART  4 5  01-LINE
  09  NONE
  10  NONE
*234567890123456789012345678901234567890123456789012345678901234567890
  11  NONE
  12  NONE
  13  SPEC
  13SPGR
  13SGNM          SWAN SPECTRUM Scenario S1C
  13HRTZ
  13SPDN          180
  13NAME          Spectrum 1: S1C --> Energy Density Spectrum
  13UDEF          0.03000
  ...
  13UDEF          0.35260.0424
END
  14  MOOR
* Anchorline Y
  COMP  15  40          1  17.5  22.5  0.
  ECAT          130.  1.e-2  9.e8  7.500E6  56.
  COMP  15  40          1  17.5  22.5  0.
  ECAT          130.  1.e-2  9.e8  7.500E6  56.
  COMP  15  40          1  17.5  22.5  0.
  ECAT          130.  1.e-2  9.e8  7.500E6  56.
  COMP  15  40          1  17.5  22.5  0.
  ECAT          130.  1.e-2  9.e8  7.500E6  56.
* Anchorline X
  COMP  15  40          1  17.5  22.5  0.
  ECAT          130.  1.e-2  9.e8  7.500E6  56.
  COMP  15  40          1  17.5  22.5  0.
  ECAT          130.  1.e-2  9.e8  7.500E6  56.
  ECAB          0.
  ECAH          1.          1.          0.2  2.5e-2
  NCEL  100
  NLID  199701  099704
  NLID  199701  099716
  NLID  199709  099708
  NLID  199709  099720
* Anchorline X
  NLID  199701  099700
  NLID  199709  099712
END
  15  NONE
  16  LMST
END16MXNI  200
  17  NONE
  18  PROP
  PTEN  1
END
  19  NONE
  20  NONE
!***** End of File *****

```

F.3.3. AQWA-FER

The program Ansys AQWA FER (Frequency-domain Evaluation of Response) is a program which is a simple and fast program that can indicate a floating structure's response in the frequency domain. It is capable to include the influence of mooring configurations and different environmental states. As this study focusses on both frequency-domain and responses with an applied mooring configuration, simulations are carried out in AQWA-FER.

Running AQWA-FER simulations is the third and final step in the hydrodynamic assessment with the computer program Ansys AQWA. The goal with these simulations is to obtain RAO's and Response Spectra of the models *A* and *B*. These simulations are also carried out in the case of a design cruise ship located next to the terminal (unmoored).

The code used to run the simulation in AQWA-FER is given below for the sake of completeness.

Listing F.3: AQWA FER Command File

```

JOB MScT FER
TITLE ModelA-S1C-0Deg
OPTIONS REST PBIS RDEP PRRS NOLL CRAO PRRP END
RESTART 4 5 ..\PreRun\Ship3-02\S1C-0
09 NONE
10 NONE
*234567890123456789012345678901234567890123456789012345678901234567890
11 NONE
12 NONE
13 SPEC
13SPGR
13SGNM SWAN SPECTRUM Scenario S1C
13HRTZ
13SPDN 180.0
13NAME Spectrum 1: S1C --> Energy Density Spectrum
13UDEF 0.03000
...
13UDEF 0.35260.0424
END
14 MOOR
* Anchorline Y
COMP 15 40 1 17.5 22.5 0.
ECAT 130. 1.e-2 9.e8 7.500E6 56.
COMP 15 40 1 17.5 22.5 0.
ECAT 130. 1.e-2 9.e8 7.500E6 56.
COMP 15 40 1 17.5 22.5 0.
ECAT 130. 1.e-2 9.e8 7.500E6 56.
COMP 15 40 1 17.5 22.5 0.
ECAT 130. 1.e-2 9.e8 7.500E6 56.
* Anchorline X
COMP 15 40 1 17.5 22.5 0.
ECAT 130. 1.e-2 9.e8 7.500E6 56.
COMP 15 40 1 17.5 22.5 0.
ECAT 130. 1.e-2 9.e8 7.500E6 56.
ECAB 0.
ECAH 1. 0.2 2.5e-2
NCEL 100
NLID 199701 099704
NLID 199701 099716
NLID 199709 099708
NLID 199709 099720
* Anchorline X
NLID 199701 099700
NLID 199709 099712
END
15 NONE
16 NONE
17 NONE
18 PROP
PTEN 1
NODE 1 1
ALLM
END
19 NONE
20 NONE
!***** End of File *****

```


APPENDIX G

AQWA SIMULATION RESULTS

This appendix presents the results of all the simulations that have been carried out with the software package Ansys AQWA.

G.1. HYDROSTATIC & HYDRODYNAMIC PROPERTIES

This section presents the output results for hydraulic parameters of the two structural models *A* and *B*. All the parameters and values are put together into one table. This table can be used to interpret the simulation results and its differences with the analytic approximation.

Table G.1: Summary of the hydrostatic and hydrodynamic parameters as calculated by AQWA, in which c = total stiffness, a = added mass, ω_n = damped natural frequency.

Surge (11)			
	c	a	ω_n
	[N/m]	[kg]	[rad/s]
Model A	$2.55 \cdot 10^4$	$5.44 \cdot 10^5$	0.09
Model B	$3.00 \cdot 10^4$	$6.35 \cdot 10^5$	0.07
Sway (22)			
	c	a	ω_n
	[N/m]	[kg]	[rad/s]
Model A	$4.75 \cdot 10^4$	$5.44 \cdot 10^5$	0.10
Model B	$5.59 \cdot 10^4$	$1.76 \cdot 10^6$	0.08
Heave (33)			
	c	a	ω_n
	[N/m]	[kg]	[rad/s]
Model A	$9.07 \cdot 10^6$	6.57	0.98
Model B	$2.42 \cdot 10^7$	$2.22 \cdot 10^7$	0.88
Roll (44)			
	c	a	ω_n
	[N/m]	[kg]	[rad/s]
Model A	$6.51 \cdot 10^8$	$3.10 \cdot 10^8$	1.05
Model B	$1.73 \cdot 10^9$	$8.65 \cdot 10^8$	1.06
Pitch (55)			
	c	a	ω_n
	[N/m]	[kg]	[rad/s]
Model A	$6.51 \cdot 10^8$	$3.10 \cdot 10^8$	1.05
Model B	$1.29 \cdot 10^{10}$	$9.90 \cdot 10^9$	0.95

G.2. FREE FLOATING RAO'S AND RAO'S

This section presents an overview of the results of the following parameters and simulations:

Free Floating RAO's

- Model *A*
- Model *B*

RAO's

- Model *A*
- Model *B*
- Model *C + A*
- Model *C + B*

The free floating RAO's and RAO's are presented in Figure G.2. The plots of the RAO's for each motion include all four simulations: *A*, *B*, *C+A* and *C+B*. The sign convention, indicating the orientation of the axis and the direction of the different wave angles, is shown in Figure G.1.

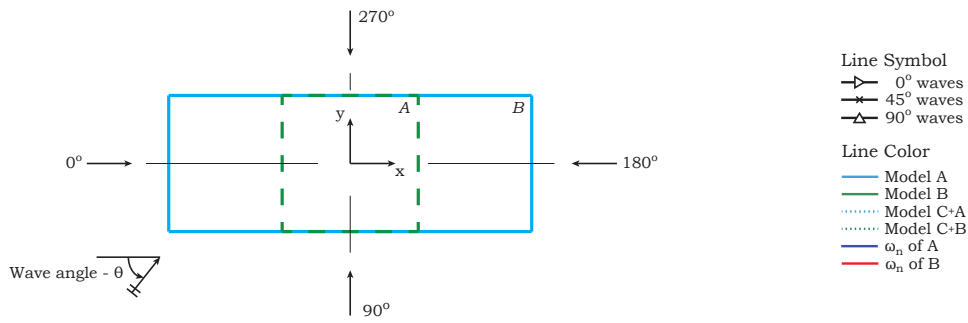


Figure G.1: Left: top view of floating terminals A (Green), B (Blue) and cruise vessel. Right: the applied sign convention.

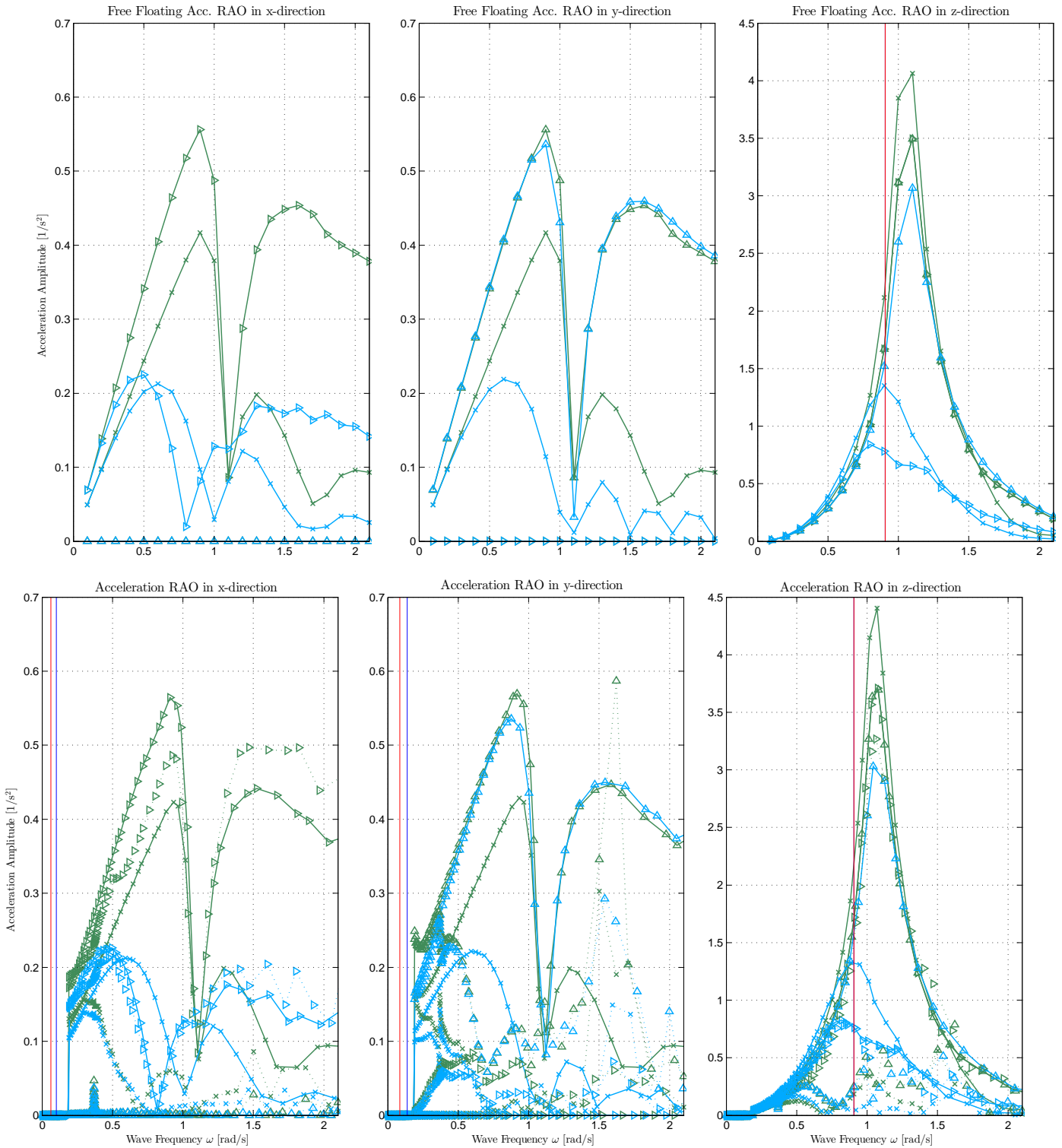


Figure G.2: Results for the models A and B and three incoming wave angles: 0°, 45° and 90°. Top row: Free floating RAO's in x-direction (left), y-direction (middle) and z-direction (right). Bottom row: RAO's in x-direction (left), y-direction (middle) and z-direction (right).

G.3. RESPONSE SPECTRA

The response spectrum is a result of a multiplication between the wave energy spectrum and the response amplitude operator:

$$S_r(\omega) = |\hat{R}(\omega)|^2 \cdot E_\zeta(\omega) \quad (\text{G.1})$$

The response energy is used to determine the accelerations and displacements of floating structures. This parameter shows the influence of sea loads and structural model characteristics on the behaviour and operability of in this case the floating cruise terminal.

Variants are modelled in AQWA. The software can then calculate the response spectrum. Results are plotted for each scenario and three model variants. From these plots it is possible to deduct how the response spectra is influenced by wave angles over the wave frequency. This section contains the simulation results of the following models:

- Model A
- Model B
- Model C + A
- Model C + B

They are treated separately on the following pages.

G.3.1. MODEL A

The following parameters are calculated with AQWA and plotted below in the same order:

- Vertical Acceleration Response;
- Horizontal Acceleration Response in X- and Y-direction;
- Roll Response
- Pitch Response

The plots show the spectra for all seven scenarios and three different incoming wave angles. Swell wave scenarios are plotted in four different tones of green: the milder conditions are light, and with each more severe scenario the colour is darker. Wind wave scenarios are presented in different types of red. Again, the mild scenarios are plotted in brighter tones of red, and more severe scenarios in darker red.

Each scenario consists out of three lines with the same colour, but with different icons, which refer to the incoming wave angle: scenarios with an incoming wave angle of 0° are indicated with a triangle pointing to the left. 45° angle waves are indicated with a 'x' and waves coming with an angle of 90° are indicated with a triangle pointing upwards.

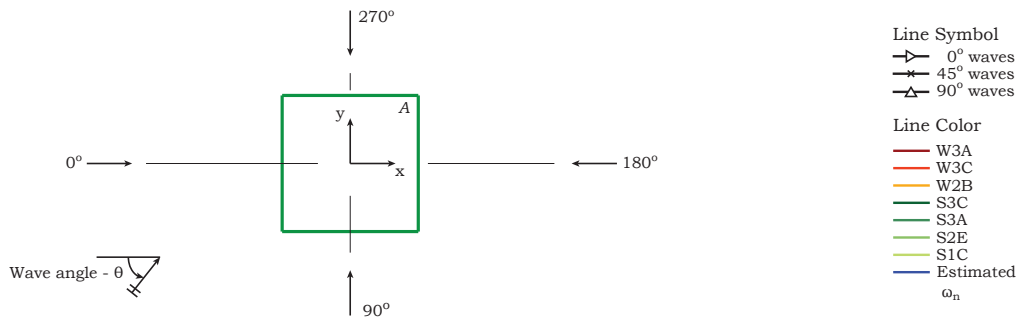


Figure G.3: Left: top view of floating terminal A, right: the applied sign convention.

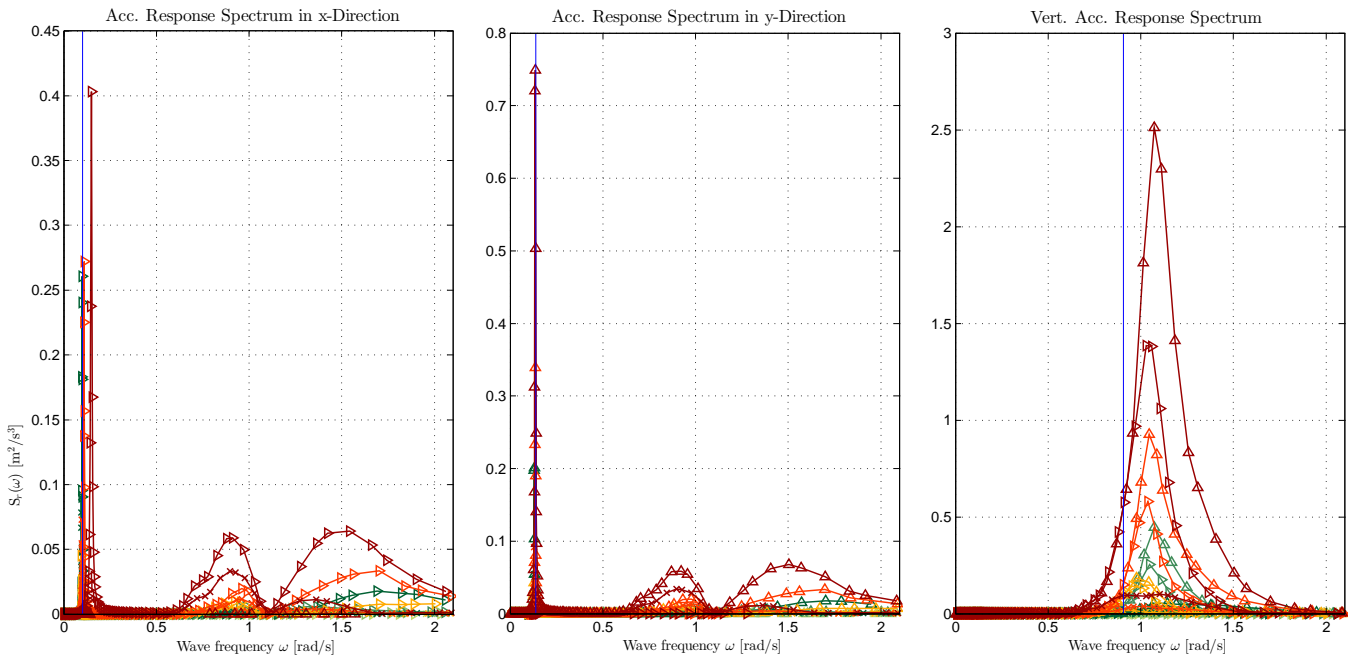


Figure G.4: Acceleration response spectra for three incoming wave angles: 0°, 45° and 90°. From left to right: in x-, y and z-direction.

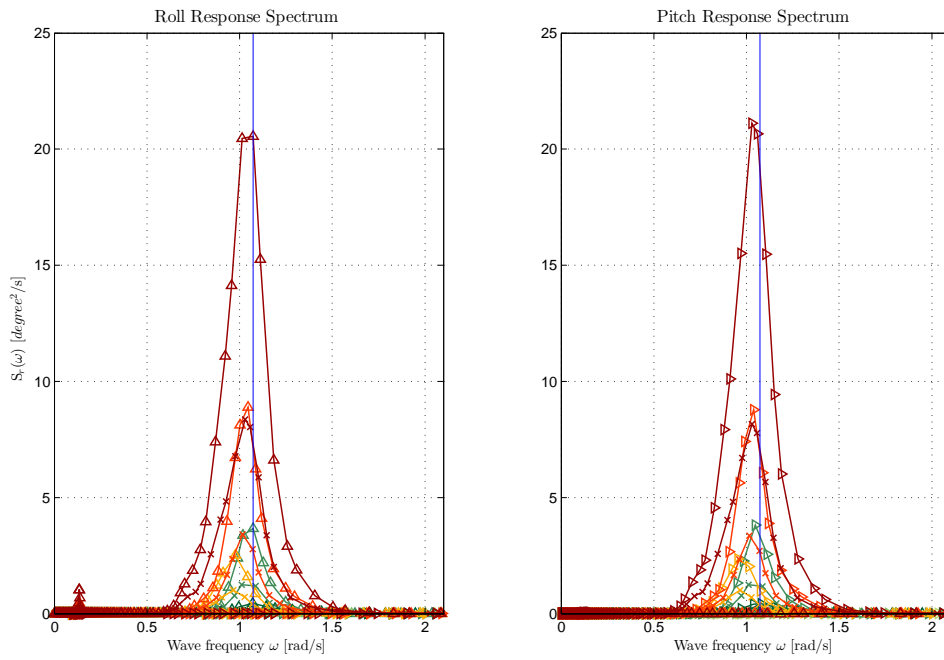


Figure G.5: Response spectra for roll (left) and pitch (right) for three incoming wave angles: 0°, 45° and 90°.

G.3.2. MODEL B

The following parameters are calculated with AQWA and plotted below in the same order:

- Vertical Acceleration Response;
- Horizontal Acceleration Response in X- and Y-direction;
- Roll Response
- Pitch Response

The plots show the spectra for all seven scenarios and three different incoming wave angles. Swell wave scenarios are plotted in four different tones of green: the milder conditions are light, and with each more severe scenario the colour is darker. Wind wave scenarios are presented in different types of red. Again, the mild scenarios are plotted in brighter tones of red, and more severe scenarios in darker red.

Each scenario consists out of three lines with the same colour, but with different icons, which refer to the incoming wave angle: scenarios with an incoming wave angle of 0° are indicated with a triangle pointing to the left. 45° angle waves are indicated with a 'x' and waves coming with an angle of 90° are indicated with a triangle pointing upwards.

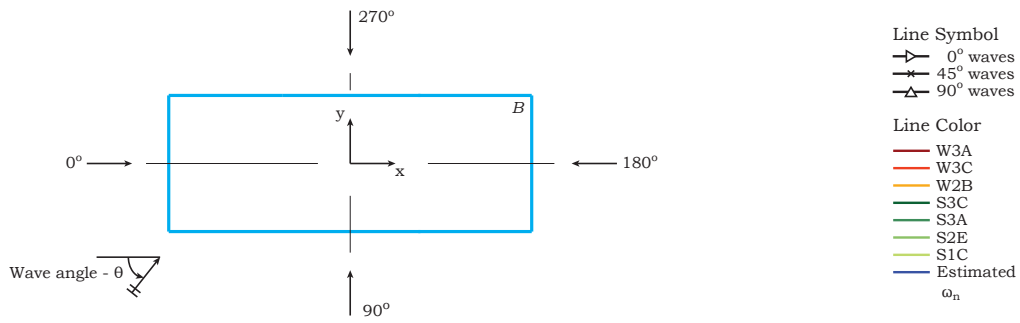


Figure G.6: Left: top view of floating terminal B, right: the applied sign convention.

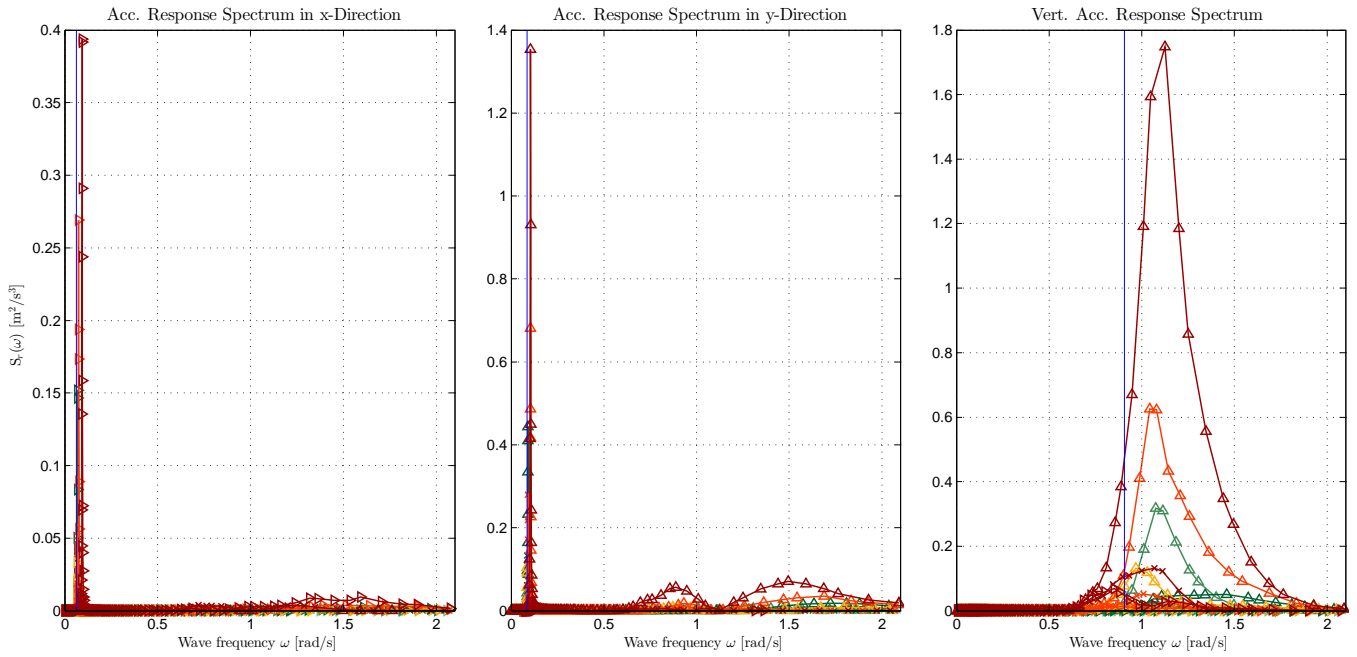


Figure G.7: Acceleration response spectra for three incoming wave angles: 0°, 45° and 90°. From left to right: in x-, y and z-direction.

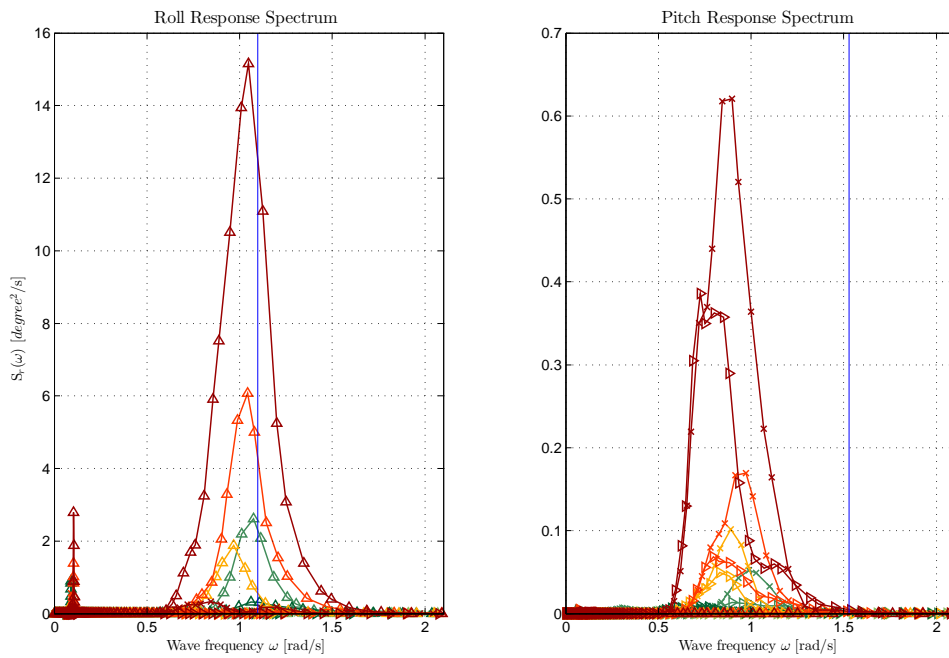


Figure G.8: Response spectra for roll (left) and pitch(right). The plots include the results for three incoming wave angles: 0°, 45° and 90°.

G.3.3. MODEL C+A

The following parameters are calculated with AQWA and plotted below in the same order:

- Vertical Acceleration Response;
- Horizontal Acceleration Response in x- and y-direction;
- Roll Response
- Pitch Response

The plots show the spectra for all seven scenarios and three different incoming wave angles. Swell wave scenarios are plotted in four different tones of green: the milder conditions are light, and with each more severe scenario the colour is darker. Wind wave scenarios are presented in different types of red. Again, the mild scenarios are plotted in brighter tones of red, and more severe scenarios in darker red.

Each scenario consists out of three lines with the same colour, but with different icons, which refer to the incoming wave angle: scenarios with an incoming wave angle of 0° are indicated with a triangle pointing to the left. 45° angle waves are indicated with a 'x' and waves coming with an angle of 90° are indicated with a triangle pointing upwards.

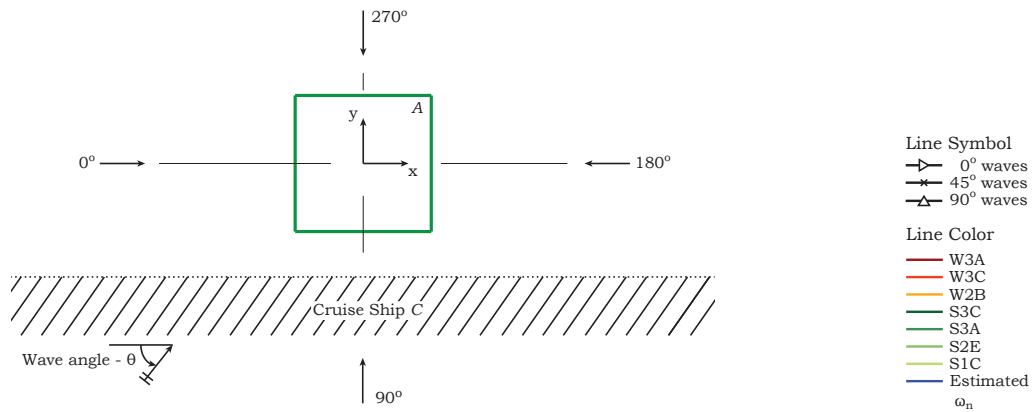


Figure G.9: Left: top view of floating terminal and cruise vessel (Model C+A), right: the applied sign convention.

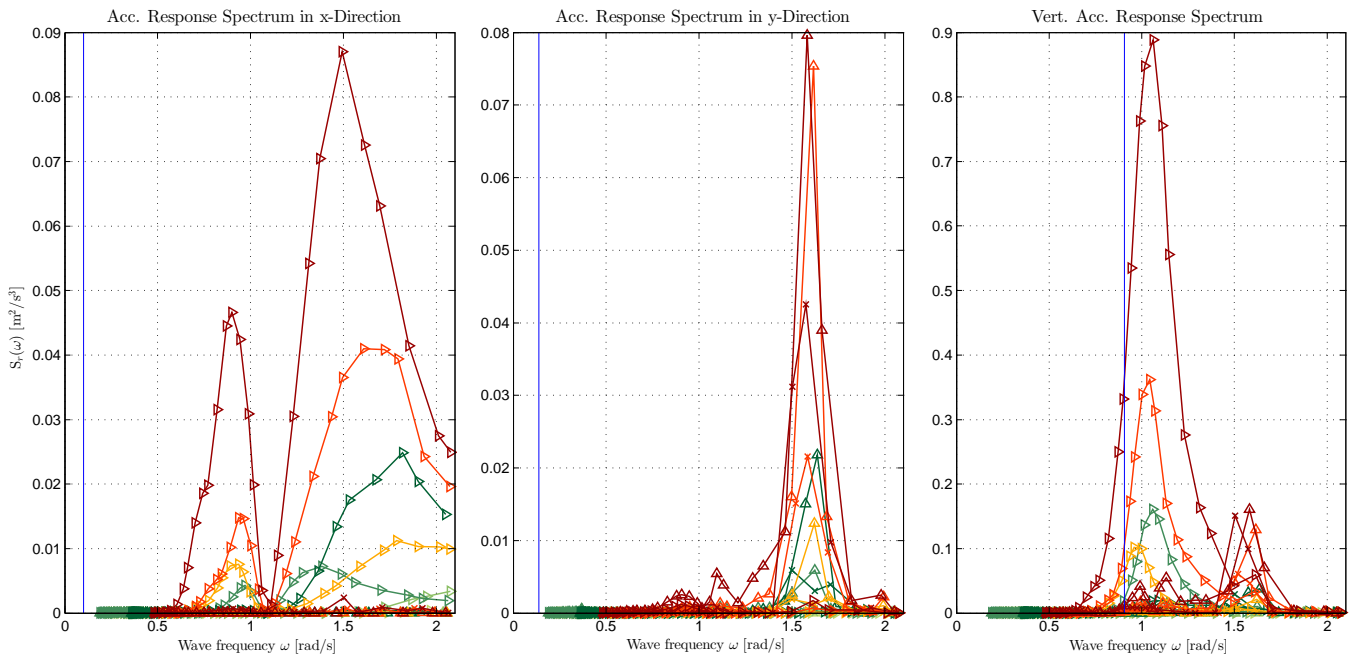


Figure G.10: Acceleration response spectra for three incoming wave angles: 0°, 45° and 90°. From left to right: in x-, y and z-direction.

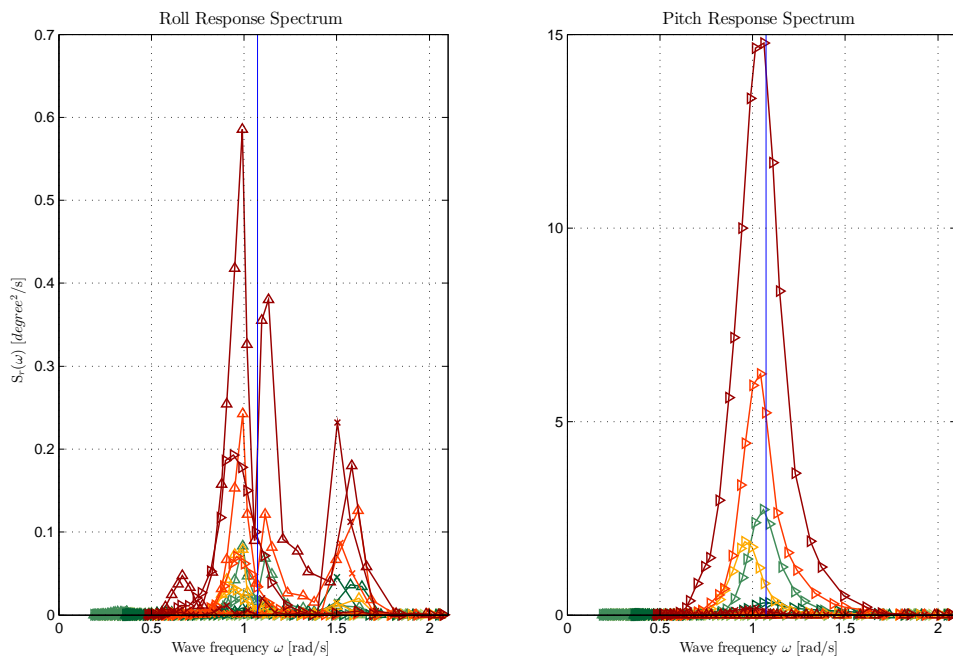


Figure G.11: Response spectra for roll (left) and pitch (right). The plots include results for three incoming wave angles: 0°, 45° and 90°.

G.3.4. MODEL C+B

The following parameters are calculated with AQWA and plotted below in the same order:

- Vertical Acceleration Response;
- Horizontal Acceleration Response in x- and y-direction;
- Roll Response
- Pitch Response

The plots show the spectra for all seven scenarios and three different incoming wave angles. Swell wave scenarios are plotted in four different tones of green: the milder conditions are light, and with each more severe scenario the colour is darker. Wind wave scenarios are presented in different types of red. Again, the mild scenarios are plotted in brighter tones of red, and more severe scenarios in darker red.

Each scenario consists out of three lines with the same colour, but with different icons, which refer to the incoming wave angle: scenarios with an incoming wave angle of 0° are indicated with a triangle pointing to the left. 45° angle waves are indicated with a 'x' and waves coming with an angle of 90° are indicated with a triangle pointing upwards.

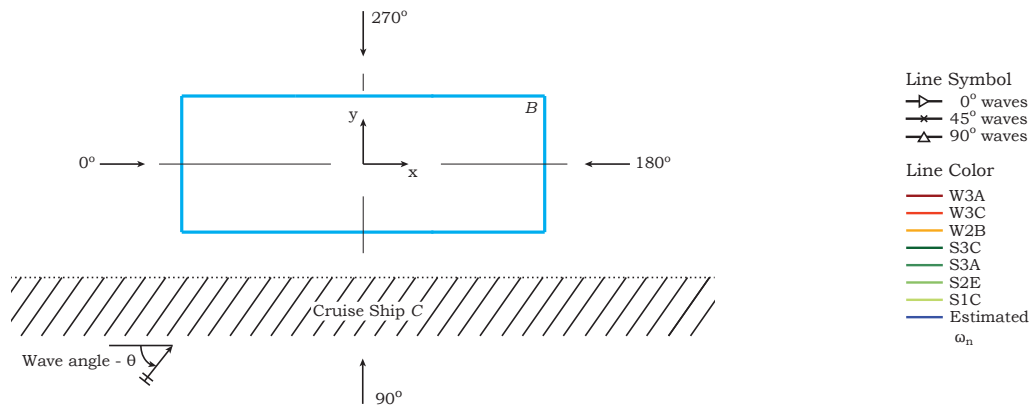


Figure G.12: Left: top view of floating terminal and cruise vessel (Model C+B), right: the applied sign convention.

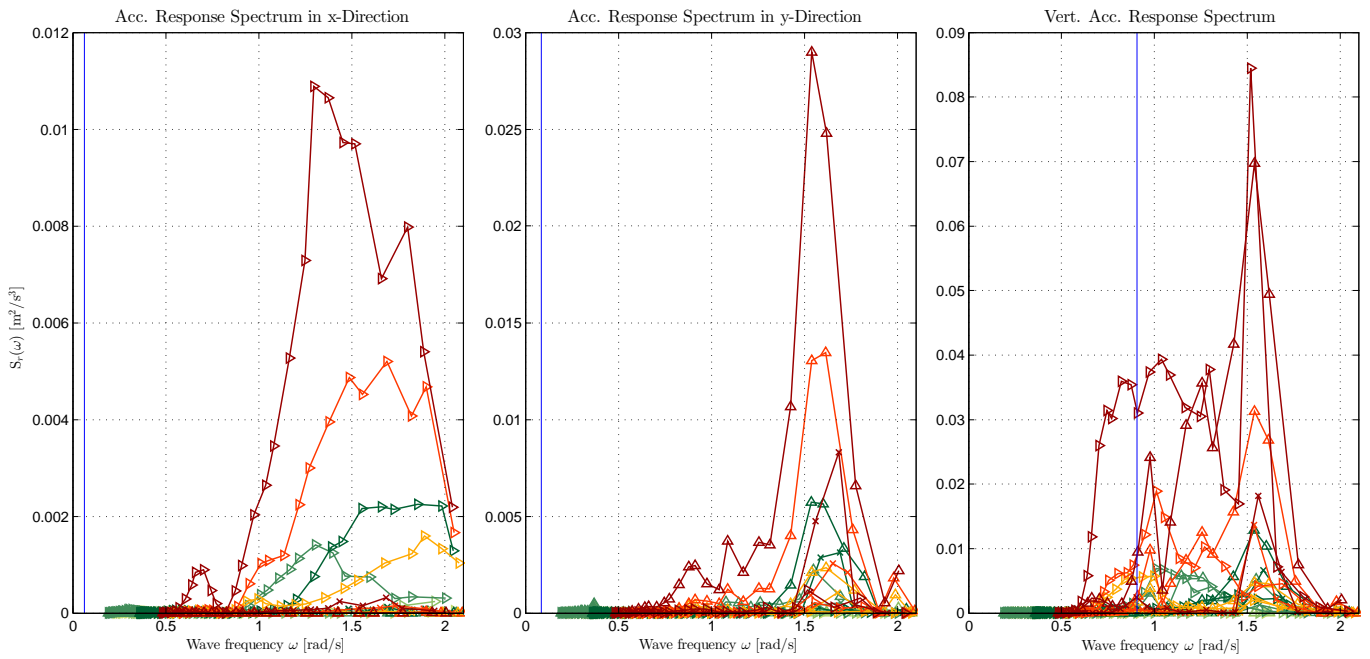


Figure G.13: Acceleration response spectra for three incoming wave angles: 0°, 45° and 90°. From left to right: in x-, y and z-direction. The plots include the results

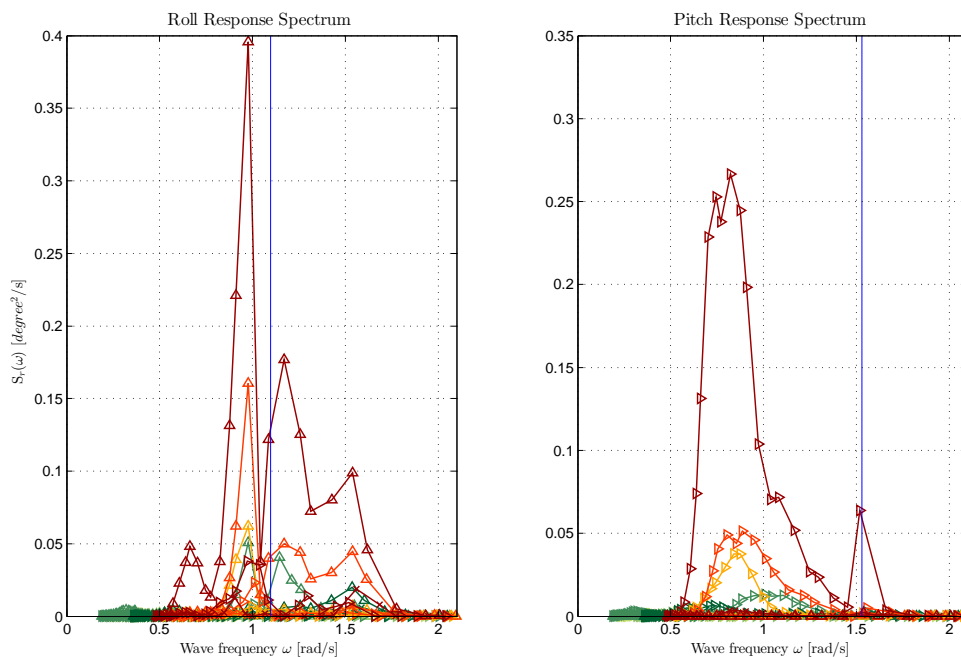


Figure G.14: Response spectra for three incoming wave angles: 0°, 45° and 90°. From left to right: roll motion and pitch motion.

G.4. RMS VALUES

The criteria as introduced by Nordforsk are defined as RMS values of motions. This section presents the calculation steps to make the transition from AQWA output data to values comparable with the Nordforsk criteria. An important step in the process of determining the right parameters for the comparison with the Nordforsk criteria is the determination of the area underneath the spectral curves:

$$m_{0*} = \int_0^{\infty} S_*(\omega) \cdot \omega^n \cdot d\omega \quad (\text{G.2})$$

After this calculation step it is possible to calculate the RMS value in the direction that belongs to the corresponding spectral curve:

$$RMS_* = \sqrt{m_{0*}} \quad (\text{G.3})$$

In which:

* = Either a_x , a_y , a_z , z_x , ϕ or θ .

Table G.2 presents the calculation results for both models. The tables are grouped by the type of motions. Each cell value is compared with the corresponding criterium of Nordforsk. The green cells indicate that for that particular scenario and incoming wave angle the calculated motion response remains below the criterium. Chapter 8 elaborates on this comparison and presents the results in terms of operational downtime.

Table G.2: Overview of RMS calculation results. The comparison with the Nordforsk Criteria is visualised by means of coloured cells. The green highlighted cells indicate the scenarios that do not exceed the *Cruise Liner* criteria. Orange cells meet the *Transit Passengers* criteria from Nordforsk.

		Model A			Model C+A			Model B			Model C+B					
		0 deg	45 deg	90 deg	0 deg	45 deg	90 deg	0 deg	45 deg	90 deg	0 deg	45 deg	90 deg			
Acceleration in X-Direction	S1C	8,6E-03	2,8E-03	0	S1C	7,8E-03	1,8E-03	3,1E-04	S1C	3,1E-03	1,9E-03	0	S1C	3,8E-03	1,4E-03	1,7E-04
	S2E	2,3E-02	7,1E-03	0	S2E	3,0E-02	3,3E-03	9,9E-04	S2E	9,2E-03	3,4E-03	0	S2E	7,6E-03	1,4E-03	3,5E-04
	S3A	6,4E-02	3,3E-02	0	S3A	6,8E-02	8,0E-03	1,9E-03	S3A	2,5E-02	1,3E-02	0	S3A	2,7E-02	3,9E-03	6,8E-04
	S3C	1,1E-01	3,2E-02	0	S3C	1,2E-01	1,4E-02	3,7E-03	S3C	3,7E-02	1,3E-02	0	S3C	3,9E-02	6,6E-03	1,4E-03
	W2B	7,9E-02	3,8E-02	0	W2B	8,7E-02	8,7E-03	1,9E-03	W2B	2,4E-02	1,2E-02	0	W2B	2,9E-02	3,9E-03	8,4E-04
	W3A	1,6E-01	6,7E-02	0	W3A	1,7E-01	1,7E-02	4,7E-03	W3A	5,8E-02	2,5E-02	0	W3A	6,1E-02	8,3E-03	1,7E-03
	W3C	2,4E-01	1,1E-01	0	W3C	2,5E-01	2,6E-02	4,0E-03	W3C	8,8E-02	4,5E-02	0	W3C	8,7E-02	1,1E-02	1,8E-03
Acceleration in Y-Direction	S1C	0	2,9E-03	9,0E-03	S1C	8,9E-04	1,9E-03	4,0E-03	S1C	0	2,0E-03	9,1E-03	S1C	7,6E-04	1,4E-03	3,8E-03
	S2E	0	7,1E-03	2,7E-02	S2E	2,9E-03	5,6E-03	9,0E-03	S2E	0	4,0E-03	2,7E-02	S2E	1,9E-03	4,0E-03	7,7E-03
	S3A	0	3,3E-02	6,5E-02	S3A	6,1E-03	2,0E-02	3,6E-02	S3A	0	1,0E-02	6,3E-02	S3A	5,6E-03	1,1E-02	2,6E-02
	S3C	0	3,3E-02	1,0E-01	S3C	1,1E-02	4,0E-02	6,0E-02	S3C	0	2,0E-02	1,1E-01	S3C	8,4E-03	2,5E-02	4,2E-02
	W2B	0	3,9E-02	8,3E-02	W2B	9,8E-03	2,4E-02	4,5E-02	W2B	0	1,5E-02	8,1E-02	W2B	6,1E-03	1,3E-02	3,0E-02
	W3A	0	6,9E-02	1,6E-01	W3A	1,6E-02	6,5E-02	1,1E-01	W3A	0	3,4E-02	1,6E-01	W3A	1,3E-02	2,5E-02	6,7E-02
	W3C	0	1,2E-01	2,5E-01	W3C	2,4E-02	9,3E-02	1,3E-01	W3C	0	4,0E-02	2,5E-01	W3C	1,9E-02	3,9E-02	9,8E-02
Acceleration in Z-Direction	S1C	3,0E-03	1,7E-03	6,9E-03	S1C	2,9E-03	1,3E-03	3,6E-03	S1C	2,3E-03	1,8E-03	7,4E-03	S1C	2,2E-03	1,1E-03	3,2E-03
	S2E	1,1E-02	5,3E-03	2,3E-02	S2E	1,1E-02	5,9E-03	1,2E-02	S2E	7,4E-03	5,7E-03	2,5E-02	S2E	6,7E-03	4,1E-03	9,2E-03
	S3A	2,3E-01	7,8E-02	3,2E-01	S3A	1,9E-01	4,1E-02	6,5E-02	S3A	4,4E-02	7,7E-02	3,0E-01	S3A	5,2E-02	1,6E-02	5,3E-02
	S3C	1,0E-01	4,6E-02	1,9E-01	S3C	9,9E-02	6,4E-02	8,5E-02	S3C	3,4E-02	3,7E-02	1,9E-01	S3C	4,2E-02	3,2E-02	6,2E-02
	W2B	1,8E-01	6,6E-02	2,2E-01	W2B	1,5E-01	4,0E-02	6,8E-02	W2B	4,9E-02	6,9E-02	2,0E-01	W2B	5,0E-02	2,1E-02	4,6E-02
	W3A	3,6E-01	1,3E-01	5,1E-01	W3A	3,1E-01	1,0E-01	1,6E-01	W3A	8,1E-02	1,3E-01	4,7E-01	W3A	9,1E-02	4,5E-02	1,1E-01
	W3C	6,1E-01	2,3E-01	8,6E-01	W3C	5,3E-01	1,6E-01	2,1E-01	W3C	1,6E-01	2,3E-01	8,0E-01	W3C	1,9E-01	5,8E-02	1,7E-01
Rotation about X-axis	S1C	0	1,2E-02	1,8E-02	S1C	4,0E-03	7,3E-03	1,5E-02	S1C	0	1,1E-02	1,8E-02	S1C	3,5E-03	6,8E-03	1,5E-02
	S2E	0	3,1E-02	4,8E-02	S2E	7,8E-03	1,1E-02	2,3E-02	S2E	0	1,9E-02	4,7E-02	S2E	5,5E-03	8,1E-03	2,2E-02
	S3A	0	5,3E-01	8,8E-01	S3A	7,3E-02	4,9E-02	1,4E-01	S3A	0	9,6E-02	7,8E-01	S3A	3,4E-02	2,1E-02	1,2E-01
	S3C	0	2,3E-01	3,8E-01	S3C	3,2E-02	8,0E-02	1,0E-01	S3C	0	6,7E-02	3,6E-01	S3C	2,2E-02	3,3E-02	8,5E-02
	W2B	0	4,6E-01	7,3E-01	W2B	7,5E-02	4,8E-02	1,3E-01	W2B	0	1,0E-01	6,5E-01	W2B	3,3E-02	2,1E-02	1,0E-01
	W3A	0	8,6E-01	1,4E+00	W3A	1,2E-01	1,1E-01	2,5E-01	W3A	0	1,7E-01	1,2E+00	W3A	6,2E-02	4,0E-02	2,0E-01
	W3C	0	1,5E+00	2,4E+00	W3C	2,2E-01	1,9E-01	4,0E-01	W3C	0	3,5E-01	2,2E+00	W3C	1,0E-01	6,8E-02	3,4E-01
Rotation about Y-axis	S1C	1,8E-02	1,3E-02	0	S1C	1,6E-02	8,9E-03	7,1E-04	S1C	1,5E-02	1,1E-02	0	S1C	1,3E-02	1,6E-02	8,8E-04
	S2E	4,7E-02	3,1E-02	0	S2E	4,3E-02	8,7E-03	1,3E-03	S2E	2,5E-02	2,1E-02	0	S2E	2,1E-02	4,1E-02	2,4E-03
	S3A	8,7E-01	5,2E-01	0	S3A	7,8E-01	7,6E-02	8,2E-03	S3A	7,7E-02	1,2E-01	0	S3A	7,5E-02	1,4E-01	7,8E-03
	S3C	3,8E-01	2,3E-01	0	S3C	3,6E-01	4,5E-02	7,3E-03	S3C	6,0E-02	6,3E-02	0	S3C	5,2E-02	1,0E-01	1,8E-02
	W2B	7,2E-01	4,6E-01	0	W2B	6,4E-01	7,3E-02	6,1E-03	W2B	1,1E-01	1,5E-01	0	W2B	9,3E-02	2,3E-01	7,7E-03
	W3A	1,4E+00	8,5E-01	0	W3A	1,2E+00	1,3E-01	1,4E-02	W3A	1,5E-01	2,2E-01	0	W3A	1,4E-01	3,0E-01	1,7E-02
	W3C	2,4E+00	1,5E+00	0	W3C	2,1E+00	2,2E-01	2,3E-02	W3C	3,5E-01	4,5E-01	0	W3C	2,8E-01	6,8E-01	3,1E-02

APPENDIX **H**

SEAKEEPING CRITERIA BY NORDFORSK

General Operability Limiting Criteria for Ships (NORDFORSK, 1987)			
Description	Merchant Ships	Navy Vessels	Fast Small Craft
RMS of vertical acceleration at FP	0.275 g ($L \leq 100$ m) 0.050 g ($L \geq 330$ m)	0.275 g	0.65 g
RMS of vertical acceleration at Bridge	0.15 g	0.20 g	0.275 g
RMS of lateral acceleration at Bridge	0.12 g	0.10 g	0.10 g
RMS of Roll	6.0 deg	4.0 deg	4.0 deg
Probability of Slamming	0.03 ($L \leq 100$ m) 0.01 ($L \geq 300$ m)	0.03	0.03
Probability of Deck Wetness	0.05	0.05	0.05

General Operability Limiting Criteria for Ships (NORDFORSK, 1987).

Criteria for Accelerations and Roll (NORDFORSK, 1987)			
Description	RMS Vertical Acceleration	RMS Lateral Acceleration	RMS Roll Motion
Light Manual Work	0.20 g	0.10 g	6.0°
Heavy Manual Work	0.15 g	0.07 g	4.0°
Intellectual Work	0.10 g	0.05 g	3.0°
Transit Passengers	0.05 g	0.04 g	2.5°
Cruise Liner	0.02 g	0.03 g	2.0°

Seakeeping performance criteria for human effectiveness - Limiting Criteria with regard to accelerations (vertical and lateral) and roll motion (NORDFORSK, 1987).